DOKUZ EYLÜL UNIVERSITY
GRADUATE SCHOOL OF NATURAL AND APPLIED SCIENCES

THE ASSESSMENT OF PYROLYSIS AS A THERMAL TECHNOLOGY FOR THE UTILIZATION OF BIODEGRADABLE MUNICIPAL SOLID WASTE TO OBTAIN VALUABLE PRODUCTS

by
Ayşenur ÖZUYSAL

October, 2023
İZMİR

THE ASSESSMENT OF PYROLYSIS AS A THERMAL TECHNOLOGY FOR THE UTILIZATION OF BIODEGRADABLE MUNICIPAL SOLID WASTE TO OBTAIN VALUABLE PRODUCTS

A Thesis Submitted to the
Graduate School of Natural and Applied Sciences of Dokuz Eylül University
In Partial Fulfillment of the Requirements for the Degree of Doctor of Philosophy in Department of Environmental Engineering, Environmental Engineering Program

by
Ayşenur ÖZUYSAL

October, 2023
İZMİR

Ph.D. THESIS EXAMINATION RESULT FORM

We have read the thesis entitled **"THE ASSESSMENT OF PYROLYSIS AS A THERMAL TECHNOLOGY FOR THE UTILIZATION OF BIODEGRADABLE MUNICIPAL SOLID WASTE TO OBTAIN VALUABLE PRODUCTS"** completed by **AYŞENUR ÖZUYSAL** under supervision of **PROF. DR. GÖRKEM AKINCI** and we certify that in our opinion it is fully adequate, in scope and in quality, as a thesis for the degree of Doctor of Philosophy.

Prof. Dr. Görkem AKINCI

Supervisor

Prof. Dr. Müfide BANAR

Thesis Committee Member

Prof. Dr. Mustafa ODABAŞI

Thesis Committee Member

Assoc. Prof. Dr. Oğuzhan GÖK

Examining Committee Member

Prof. Dr. Osman Nuri AĞDAĞ

Examining Committee Member

Prof. Dr. Okan FISTIKOĞLU

Director

Graduate School of Natural and Applied Sciences

ACKNOWLEDGMENT

I would like to thank my supervisor Prof. Dr. Görkem AKINCI for her advices and support throughout this study. I would like to thank my thesis committee members Prof. Dr. Müfide BANAR and Prof. Dr. Mustafa ODABAŞI for their valuable contributions on my thesis research.

I am thankful to Assoc. Prof. Dr. Mustafa EROL and R. A. Yasin Özgür KESKİN for their valuable helps during laboratory studies. I would like to thank also Assoc.Prof. Dr. E. Duyuşen GÜVEN and Assoc. Prof. Dr. Serpil ÖZMIHÇI for their supports and helps.

This study was supported in part by the Scientific Research Foundation of Dokuz Eylül University (Project No: 2021. KB.FEN.034). I would like to thank this Foundation for its financial support.

I wish to thank all my friends, especially Meltem Nihan KILINÇ, Betül DİLER KILIÇ, Melody SHOARGHAFFARİ, Gülten GÖKAYAZ and Serenay Ceren TÜZÜN for their friendships, encouragement and moral support.

I am grateful to my families, BÖLÜKBAŞ and ÖZUYSAL, especially to my mother Yılay BÖLÜKBAŞ and father Mustafa Nevzat BÖLÜKBAŞ, they are always supporting me and encouraging me with their best wishes. I am also thankful to my nephews, Alp BÖLÜKBAŞ and Arda BÖLÜKBAŞ, for that make me smile and their endless love.

Finally, I am thankful to my husband Mustafa ÖZUYSAL and daughter Başak ÖZUYSAL for their moral support, encouragement, patience, understanding and endless love.

I am dedicating this Ph.D. thesis to my beloved daughter Başak ÖZUYSAL and mother Yılay BÖLÜKBAŞ. I thank them for making me who I am.

Ayşenur ÖZUYSAL

THE ASSESSMENT OF PYROLYSIS AS A THERMAL TECHNOLOGY FOR THE UTILIZATION OF BIODEGRADABLE MUNICIPAL SOLID WASTE TO OBTAIN VALUABLE PRODUCTS

ABSTRACT

This research aimed to assess the utilization of municipal biodegradable and local biomass wastes through pyrolysis, focusing on waste quality and water content. In order to minimize the standard deviation due to heterogeneity, dry dog/cat food, whose detailed contents were analyzed, was used to identify the ideal conditions for pyrolysis of biodegradable waste.

Primary devolatilization after water release occurred between 200-500°C and exothermic combustion at about 280°C. Preliminary experiments showed decreasing biochar yield and elevated biochar surface area (up to 213.11 m^2/g) with higher final temperatures. FT-IR confirmed functional groups removal and carbondioxide, methane, and hydrogen generation during char production. The experiments conducted at 700°C, 10°C/min heating rate, and 40 minutes of retention time yielded with optimal results regarding the final products of the pyrolysis process. Any significant impact of initial water content (25, 40 and 55%) of wastes or their particle size (5-10, 10-15, 15-20 mm) was not observed. Co-pyrolysis of biodegradable municipal waste with waste biomasses enhanced biochar surface area (170.18 m^2/g) and the amount of liquid product (34.6%), rich in n-alkanes.

Regression analysis verified that increasing final temperatures results with higher BET surface areas in biochars (r:0.490, $p \leq 0.01$). Waste humidity had no impact on biochar quality, but enhanced liquid product formation. Principal Component Analysis revealed that waste characteristics (28.95%) and operating conditions (26.68%) were the major factors on biochar quality. Pyrolysis technique can be preferred for the management of biodegradable and biomass wastes against global climate change and the biochar obtained can be used for carbon sequestration.

Keywords: Pyrolysis, municipal solid waste, biomass, biochar, bio-oil, co-pyrolysis, water content

BİYOBOZUNUR KENTSEL ATIKLARDAN DEĞERLİ ÜRÜNLERİN ELDESİ İÇİN BİR TERMAL TEKNOLOJİ OLARAK PİROLİZİN DEĞERLENDİRİLMESİ

ÖZ

Bu araştırma, atık kalitesi ve su içeriğine odaklanarak, kentsel biyolojik olarak parçalanabilir ve yerel biyokütle atıklarının piroliz yoluyla kullanımını değerlendirmeyi amaçlamıştır. Heterojenlikten kaynaklanan standart sapmayı en aza indirmek amacıyla, biyolojik olarak parçalanabilir atıkların pirolizi için ideal koşulları belirlemek üzere ayrıntılı içerikleri analiz edilen kuru köpek/kedi maması kullanılmıştır. Su salınımından sonra birincil devolatilizasyon 200-500°C arasında ve ekzotermik yanma yaklaşık 280°C'de gerçekleşmiştir. Ön deneyler, daha yüksek nihai sıcaklıklarla biyokömür üretim veriminin azaldığını ve biyokömür yüzey alanının arttığını (213,11 m^2/g'a kadar) göstermiştir. FT-IR, biyokömür üretimi sırasında bazı fonksiyonel grupların uzaklaştırıldığını ve karbondioksit, metan ve hidrojen oluşumunu doğrulamıştır. 700°C'de, 10°C/dk ısıtma hızında ve 40 dakikalık alıkoyma süresiyle gerçekleştirilen deneyler, piroliz sürecinin nihai ürün miktarlarına göre en uygun sonuçları vermiştir. Atıkların başlangıçtaki su içeriğinin (% 25, 40 ve 55) veya partikül boyutunun (5-10, 10-15, 15-20 mm) önemli bir etkisi gözlenmemiştir. Biyolojik olarak parçalanabilir belediye atıklarının atık biyokütlelerle birlikte pirolizi biyokömür yüzey alanını (170,18 m2/g) ve n-alkanlar bakımından zengin sıvı ürün miktarını (%34,6) arttırmıştır. Regresyon analizi, artan nihai sıcaklıkların biyokömürlerde daha yüksek BET yüzey alanlarını sağladığını doğrulamıştır (r:0.490, $p \leq 0.01$). Atık neminin biyokömür kalitesi üzerinde bir etkisi olmamış, ancak sıvı ürün oluşumunu arttırmıştır. Temel Bileşen Analizi, atık özelliklerinin (%28,95) ve işletme koşullarının (%26,68) biyokömür kalitesi üzerinde etkili başlıca faktörler olduğunu ortaya koymuştur. Piroliz tekniği, küresel iklim değişikliğine karşı biyobozunur ve biyokütle atıklarının yönetimi için tercih edilebilir ve elde edilen biyokömür karbon tutumu için kullanılabilir.

Anahtar kelimeler: Piroliz, kentsel katı atık, biyokütle, biyokömür, piroliz yağı, kopiroliz, nem içeriği

CONTENTS

Page

Ph.D. THESIS EXAMINATION RESULT FORM ii
ACKNOWLEDGMENT iii
ABSTRACT iv
ÖZ v
CONTENTS vi
LIST OF FIGURES ix
LIST OF TABLES xiii

CHAPTER ONE - INTRODUCTION 1

1.1 Municipal Solid Waste 3
1.2 Waste Processing Technologies 5
1.2.1 Physical Solid Waste Processing Technologies 7
1.2.2 Biochemical Solid Waste Processing Technologies 9
1.2.3 Thermal Solid Waste Processing Technologies 10
1.3 Bio-drying 11
1.4 Pyrolysis 13
1.4.1 Studies in The World 14
1.4.2 Studies in Türkiye 33

CHAPTER TWO - AIM OF THE STUDY 37

CHAPTER THREE - MATERIAL & METHODS 38

3.1 Sampling 38
3.1.1 Sampling of Biodegradable Solid Wastes 38
3.1.2 Selection of Dried Dog and Cat Foods for Experiments 41
3.2 Experimental Setup 45
3.2.1 Bio-Drying Experiments 45
3.2.2 Preliminary Experiments for Pyrolysis 45
3.2.2.1 System 45
3.2.2.2 Experimental Conditions 46

3.2.3 Pyrolysis of Biomass 47
3.2.3.1 System 47
3.2.3.2 Experimental Conditions 48
3.3 Analytical Method 53
3.3.1 Proximate Analysis 53
3.3.1.1 Water Content Analysis 53
3.3.1.2 Organic Matter Content 54
3.3.1.3 Calorific Value 54
3.3.1.4 Volatile Matter 54
3.3.1.5 Ash 55
3.3.1.6 Fixed Carbon 55
3.3.2 Ultimate Analysis 55
3.3.3 Lipid, Cellulose, Total Protein and Total Sugar Analyses 55
3.3.4 Thermogravimetric Analysis - Differential Thermal Analysis (TGA - DTA) 56
3.3.5 Fourier Transform Infrared Spectroscopy (FT-IR) 56
3.3.6 Brunauer, Emmett and Teller (BET) 56
3.3.7 Scanning Electron Microscope - Energy-Dispersive X-Ray Spectroscopy (SEM-EDS) 56
3.3.8 In-Situ Gas Analysis 56
3.3.9 Gas Chromatography-Mass Spectrometry (GC-MS) 57
3.4 Statistical Analysis 57

CHAPTER FOUR - RESULTS AND DISCUSSION 59

4.1 Characteristics of Raw Materials 59
4.1.1 Proximate Analysis 59
4.1.2 Ultimate Analysis 61
4.1.3 Lipid, Cellulose, Total Protein and Total Sugar Analyses 62
4.1.4 Thermogravimetric Analysis - Differential Thermal Analysis (TGA - DTA) 63
4.2 Results of Bio-drying Experiments 69
4.3 Results of Preliminary Experiments of Pyrolysis 70

4.3.1 Yields of Biochars 70
4.3.2 FT-IR Results of Biochars 71
4.3.3 BET Results of Biochars 83
4.3.4 SEM-EDS Results of Biochars 86
4.3.4.1 SEM Results of Biochars 86
4.3.4.2 EDS Results of Biochars 93
4.4 Results of Pyrolysis Experiments 96
4.4.1 Yields of Products 96
4.4.2 FT-IR Results of Biochars 102
4.4.3 BET Results of Biochars 107
4.4.4 SEM-EDS Results of Biochars 109
4.4.4.1 SEM Results of Biochars 110
4.4.4.2 EDS Results of Biochars 120
4.4.5 In-situ gas analysis 121
4.4.6 GC-MS Results of Bio-oils 122
4.4.7 GC-MS Results of Non-Condensable Gases 137
4.5 Results of Statistical Analysis 138
4.5.1 Results of statistical analysis for characteristics of raw materials 138
4.5.2 Results of statistical analysis for biochar properties 142

CHAPTER FIVE - CONCLUSION 150

REFERENCES 155

APPENDICES 176

LIST OF FIGURES

Page

Figure 3.1 The composition of the waste samples 40

Figure 3.2 Composting machine used for bio-drying 45

Figure 3.3 Preliminary experimental setup 46

Figure 3.4 Experimental setup of pyrolysis system 47

Figure 3.5 The cylindrical reactor cross sectional view and outer view 48

Figure 4.1 TGA-DTA graphs of W1.1-W1.2 66

Figure 4.2 TGA-DTA graphs of W2.1-W2.2 66

Figure 4.3 TGA-DTA graphs of W3.1-W3.2 66

Figure 4.4 TGA-DTA graphs of W4.1-W4.2 67

Figure 4.5 TGA-DTA graphs of W5.1-W5.2 67

Figure 4.6 TGA-DTA graphs of W6.1-W6.2 67

Figure 4.7 TGA-DTA graphs of W7.1-W7.2 68

Figure 4.8 TGA-DTA graphs of W8.1-W8.2 68

Figure 4.9 TGA-DTA graphs of CM, PM, YW, CS and SS 68

Figure 4.10 TGA-DTA graphs of M18, M21, M27 and M28 69

Figure 4.11 FT-IR graph of W1.1 80

Figure 4.12 FT-IR graph of W7.1 80

Figure 4.13 FT-IR graph of W8.1 81

Figure 4.14 FT-IR graph of CM 81

Figure 4.15 FT-IR graph of SS 82

Figure 4.16 FT-IR graph of CS 82

Figure 4.17 SEM figure of W1.1 88

Figure 4.18 SEM figure of W7.1 89

Figure 4.19 SEM figure of W8.1 90

Figure 4.20 SEM figure of CM 91

Figure 4.21 SEM figure of SS 92

Figure 4.22 SEM figure of CS 93

Figure 4.23 SEM-EDS results of W1.1-700 94

Figure 4.24 SEM-EDS results of W7.1-700 94

Figure 4.25 SEM-EDS results of W8.1-700 94

Figure 4.26 SEM-EDS results of CM-700 95

Figure 4.27 SEM-EDS results of SS-700 95

Figure 4.28 SEM-EDS results of CS-700 95

Figure 4.29 Yields of products regarding water content 99

Figure 4.30 Yields of products regarding particle size 99

Figure 4.31 Yields of products regarding final temperature, heating rate and residence time 100

Figure 4.32 Yields of products regarding waste type 101

Figure 4.33 FT-IR results of biochars for water content comparison 103

Figure 4.34 FT-IR results of biochars for particle size comparison 103

Figure 4.35 FT-IR results of biochars for comparing final temperature and heating rate 104

Figure 4.36 FT-IR results of biochars for comparing final temperature and retention time with 5^{o}C/min heating rate..... 104

Figure 4.37 FT-IR results of biochars for comparing final temperature and retention time with 10^{o}C/min heating rate..... 105

Figure 4.38 FT-IR results of biochars for comparing one stage and two stage heating 105

Figure 4.39 FT-IR results of biochars of waste and other biomass samples (Wet trial) 106

Figure 4.40 FT-IR results of biochars of waste and other biomass samples (Dry trial) 106

Figure 4.41 SEM figure of feedstock..... 110

Figure 4.42 SEM figures of biochars with different water contents..... 111

Figure 4.43 SEM figures of biochars with different particle sizes 112

Figure 4.44 SEM figures of biochars with one stage heating condition 113

Figure 4.45 SEM figures of biochars with one stage heating (5 ^{o}C/min) and retention time conditions..... 114

Figure 4.46 SEM figures of biochars with one stage heating (10 ^{o}C/min) and retention time conditions..... 115

Figure 4.47 SEM figures of biochars with two stage heating and retention time conditions..... 116

Figure 4.48 SEM figures of biochars produced from two different biodegradable wastes by pyrolysis at optimum conditions..... 117

Figure 4.49 SEM figures of biochars produced by co-pyrolysis of biodegradable wastes and other biomasses at optimum conditions 118

Figure 4.50 SEM figures of biochars produced by pyrolysis of dry biomasses 119

Figure 4.51 SEM figures of biochars produced by pyrolysis of dry biodegradable wastes and bio-dried biodegradable waste at optimum conditions 120

Figure 4.52 GC-MS result of gas sample from experiment 28 137

Figure 4.53 GC-MS result of gas sample from experiment 31 137

LIST OF TABLES

Page

Table 1.1 Pyrolysis studies in the World 16

Table 1.2 Pyrolysis studies in Türkiye 35

Table 3.1 The information of cities in the study 39

Table 3.2 The samples 41

Table 3.3 The properties of dry cat and dog foods 42

Table 3.4 The components of some solid waste types 43

Table 3.5 The components of some solid waste types (Continued) 44

Table 3.6 Conditions of pyrolysis experiments 50

Table 3.7 Conditions of pyrolysis experiments (continued) 51

Table 3.8 Conditions of pyrolysis experiments with biodegradable wastes and other biomasses 52

Table 3.9 Analyses of raw materials and products 53

Table 4.1 The proximate analysis results, water contents, organic matter contents and calorific values of samples 59

Table 4.2 The results of ultimate analysis 61

Table 4.3 The cellulose, total protein and total sugar results of four selected dried cat and dog foods 62

Table 4.4 The results of lipid analysis 62

Table 4.5 The summarized results of TGA and DTA 64

Table 4.6 The results of bio-drying experiment 69

Table 4.7 Yields of biochars 70

Table 4.8 The FT-IR results 74

Table 4.9 BET results of biochars produced at 350, 500 and 700 °C 84

Table 4.10 Yields of products 97

Table 4.11 BET results of biochars 108

Table 4.12 Methane (CH_4) results of pyrolysis gases 121

Table 4.13 GC-MS results of liquid samples of BO21 & BO32 124

Table 4.14 GC-MS results of liquid samples of BO22 & BO21 126

Table 4.15 GC-MS results of liquid samples of BO23 & BO24 128

Table 4.16 GC-MS results of liquid samples of BO25 & BO29 130

Table 4.17 GC-MS results of liquid samples of BO28 & BO34 131

Table 4.18 GC-MS results of liquid samples of BO26 & BO30 132

Table 4.19 GC-MS results of liquid samples of BO27 & BO31 133

Table 4.20 GC-MS results of liquid samples of BO33 & BO35 134

Table 4.21 GC-MS results of liquid samples of BO18 & BO21 135

Table 4.22 Correlations among the analysis results of raw materials 139

Table 4.23 Total variance explained with PCA 141

Table 4.24 KMO and Bartlett's Test 142

Table 4.25 Rotated Component Matrix[a] 142

Table 4.26 Correlations among the initial conditions, raw material properties and biochar characteristics 146

Table 4.27 Total variance explained with PCA for biochar..... 148

Table 4.28 KMO and Bartlett's Test for biochar..... 149

Table 4.29 Rotated Component Matrix[a] for biochar..... 149

CHAPTER ONE
INTRODUCTION

The population of Türkiye is increasing day by day, and accordingly the amount of municipal solid waste generated is increasing. According to the data published in 2018, the amount of solid waste production per capita in Türkiye is 1.16 kg/day and a total of 32 million solid waste is generated annually. 67.46% of these wastes were sent to landfill and 20% to open dumping. 12% of the waste went to recycling facilities. Less than 1% of waste is composted (TurkStat, 2018).

European Union directives encourage other methods instead of landfilling. According to the Waste Framework Directive (2008/98/EC), landfill is at the bottom of the waste hierarchy, since the main purpose is to prevent waste generation, recycling is preferred more than landfilling for the processing of the waste produced (European Union, 2008). If the generation of wastes could not be prevented and recovery could not be made, the Waste Directive recommends obtaining energy from waste (European Union, 2008). The Landfill Directive (1999/31/EC) also aimed to reduce the amount of waste disposed in landfills (European Union, 2018). The directive issued in 1999 was renewed in 2018 and waste recovery targets were redefined. In the directive, it is stated that until 2030, member states should not send their wastes to landfill, if wastes, especially municipal wastes, are suitable for recycling or recovery (European Union, 2018). The U.S. Environmental Protection Agency (EPA) regulates various aspects of waste management, including thermal solid waste processing technologies, to ensure they are environmentally sound and protective of public health with Resource Conservation and Recovery Act (RCRA) encouraging source reduction and reducing the amount sent to landfills. The details about thermal technologies are given in Guidelines for The Thermal Processing of Solid Wastes (Environmental Protection Agency (EPA), 2023).

The application of thermal technologies in Waste Management is included in the National Waste Management and Action Plan. Within the framework of this plan, it is aimed to recover 35% of the waste generated in 2023 and send 65% of the waste to landfill. It is aimed to increase the recovery of municipal wastes with thermal methods, which was 0.3% in 2014, to 8% in 2023. The Communiqué on Refuse Derived Fuel,

Additional Fuel and Alternative Raw Material, Compost Communiqué and Mechanical Separation, Biodrying and Biomethanization Plants with Fermented Product Management Communiqué give priority to material recovery and energy recovery and encourages studies within the scope of the circular economy approach (The Ministry of Environment and Urbanization, 2016).

However, studies and new investments in our country have mostly focused on composting and anaerobic digestion. According to TurkStat data, some of the waste was sent to composting in 2018 (TUIK, 2018). The existing facilities are insufficient for the processing of waste, whose amount is increasing, in terms of capacity and number and these technologies also create a significant amount of process residues. Anaerobic digestion, or in other words, biomethanization method, results in effective methane production at low retention times only if the waste is rich in easily soluble substances. In other cases, the initial investment and operating costs increase due to long retention times, thus this technology loses its applicability (Jenkins et al., 2008; Global Methane Initiative, 2016).

The similarity of thermal technologies with biochemical processes such as composting and bio-methanization is that they result in the production of gas, liquid and / or solid products, the difference is that the waste entering the thermal process is reduced in volume and mass at a very high rate and especially in thermal technologies that take place in an oxygen-free environment, gas, liquid and solid waste formation is very low or no formation (Stantec, 2011). For this reason, studies on thermal methods should be widespread in our country and the right investments should definitely be made. Thermal technologies consist of a wide range of methods from oxygenated to oxygen-free environments, and there are new integrated methods.

Pyrolysis is one of the most important thermal technologies in recent years. Studies on pyrolysis are limited in our country (Tozlu, Özahi & Abuşoğlu, 2016) and studies on the treatment of municipal solid wastes with pyrolysis technology have not been conducted. In our country, only thermal methods such as refuse derived fuel production, incineration, gasification are applied to a small extent in metropolitan cities such as Istanbul and Ankara (ITC, n.d.; İSTAÇ, n.d.).

Although technologies such as pyrolysis and gasification have higher capital costs, their products are more valuable than those of methods such as anaerobic digestion. The incineration has more important negative sides. One of the problems with incineration is the generation of 10-30 wt% fly and bottom ashes. Extra air pollution equipment is required to hold fly ashes, so capital costs increase. Moreover, the treatment and disposal of bottom ashes increase capital costs (Gopu, Gao, Volpe, Fiori, & Goldfarb, 2018). On the other hand, products of pyrolysis have economical value.

However, the disposal of solid wastes generated in Türkiye by thermal methods should also be economically feasible. The initial investment costs of thermal technologies are higher than the initial investment costs of biochemical technologies (Saleem, Zulfiqar, Tahir, Asif, & Yaqub, 2016). However, while biochemical technologies have operating expenses such as the use of chemicals that will support the development of bacterial culture during the process, ventilation or heating, thermal technologies do not need such expenses (Saleem et al., 2016; Tozlu, Özahi, & Abuşoılu, 2016). While thermal technologies have advantages such as very few process residues and low operating costs, the main handicaps in their applicability for Türkiye and countries in similar geography are the high moisture content of the waste and the inert components it contains as a result of the mixed collection of wastes.

Therefore, in this study, we investigated how to obtain valuable products from the biodegradable fraction of municipal solid waste having high water content by thermal methods. In addition, the thermal processing of other biomass resources in the region was investigated and their contribution to the products to be obtained from municipal solid waste was examined.

1.1 Municipal Solid Waste

Municipal solid waste (MSW) refers to the waste generated by households, commercial establishments, institutions, and other non-industrial sources within a municipality or urban area. It includes a wide range of materials discarded by individuals and businesses daily (Worrell & Vesilind, 2012).

The composition of MSW can vary depending on factors such as geography, culture, lifestyle, and waste management practices. However, typical components of MSW include (Sipra, Gao, & Sarwar, 2018; Worrell & Vesilind, 2012):

1. Biodegradable Waste: Food scraps, yard waste, paper products, and other biodegradable materials.

2. Recyclables: Paper, cardboard, plastics, glass, metals, and certain types of packaging materials that can be recycled.

3. Hazardous Waste: Batteries, electronic waste (e-waste), fluorescent bulbs, paint, chemicals, and other potentially harmful substances.

4. Bulky Waste: Large items such as furniture, appliances, mattresses, and other oversized objects.

5. Other Waste: Non-recyclable plastics, ceramics, rubber, leather, textiles, diapers, and other non-biodegradable materials.

MSW management involves various processes aimed at minimizing environmental impacts and promoting resource recovery. Some common methods of MSW management include (Sipra et al., 2018; Worrell & Vesilind, 2012):

1. Source Separation and Recycling: Encouraging to separate recyclable materials from the rest of the waste stream to facilitate recycling and resource conservation.

2. Composting: Biodegradable waste can be composted, allowing it to decompose and produce nutrient-rich compost that can be used for soil enrichment in agriculture and landscaping.

3. Waste-to-Energy (WtE): Some MSW can be processed through thermal treatments such as incineration, pyrolysis or gasification to generate electricity, heat and other valuable products. This approach helps reduce the volume of waste and recover energy.

4. Landfilling: Disposal of non-recyclable and non-compostable waste in engineered landfills. Proper landfill design and management practices are necessary to minimize environmental impacts.

Managing municipal solid waste poses several challenges to be handled carefully, including waste volume, environmental impact of waste, resource depletion, public awareness and participation and policy and infrastructure problems (Worrell & Vesilind, 2012). In detail, urbanization and population growth contribute to the increasing volume of MSW, forcing waste management infrastructure and resources. Moreover, insufficient waste management practices can lead to pollution, greenhouse gas emissions, soil and water contamination, and other environmental problems. MSW often contains valuable resources that, if not recovered through recycling or other means, are lost and contribute to the depletion of natural resources. Furthermore, encouraging public participation, awareness, and behavior change regarding waste reduction, recycling, and responsible consumption are essential for effective MSW management. Finally, adequate waste management policies, regulations, and infrastructure are necessary to support efficient and sustainable MSW management systems (Worrell & Vesilind, 2012).

Efficient management of municipal solid waste is crucial for environmental sustainability and resource conservation. By implementing effective waste reduction, recycling, and resource recovery practices, communities can minimize the environmental impact of MSW and move towards a more circular and sustainable waste management approach.

1.2 Waste Processing Technologies

Solid waste processing technologies are methods used to manage and treat solid waste, which includes various types of waste materials generated from domestic, commercial, industrial, and agricultural sources. The aim of these technologies is to minimize the environmental impact of waste disposal, reduce the volume of waste, and recover valuable resources. Here are some common solid waste processing technologies (Stantec, 2011; Worrell & Vesilind, 2012):

Landfilling: Landfills are engineered areas where waste is deposited and covered with soil. Modern landfills are designed to minimize the environmental impact, including groundwater pollution and emissions of harmful gases. However, landfills are often associated with environmental concerns (Stantec, 2011; Worrell & Vesilind, 2012).

Incineration: Waste incineration involves burning solid waste at high temperatures to convert it into ash, flue gas, and heat. Energy recovery from incineration is possible and can be used for electricity generation or heating. Proper air pollution control is necessary to manage emissions (Stantec, 2011; Worrell & Vesilind, 2012).

Composting: Composting involves the decomposition of biodegradable waste (e.g., food waste, yard waste) by microorganisms into nutrient-rich compost. Compost can be used to improve soil quality and enhance plant growth (Stantec, 2011; Worrell & Vesilind, 2012).

Anaerobic Digestion: Anaerobic digestion is a biological process that breaks down biodegradable waste in the absence of oxygen. It produces biogas (a mixture of methane and carbon dioxide) that can be used as a renewable energy source (Stantec, 2011; Worrell & Vesilind, 2012).

Recycling: Recycling involves the collection, processing, and reusing of materials from waste. It helps conserve natural resources, reduce energy consumption, and decrease waste sent to landfill (Stantec, 2011; Worrell & Vesilind, 2012).

Waste-to-Energy (WTE): Waste-to-energy technologies convert waste into electricity, heat, or fuel through processes like incineration, gasification, and pyrolysis. WTE facilities can contribute to energy generation while reducing the volume of waste (Stantec, 2011; Worrell & Vesilind, 2012).

Mechanical-Biological Treatment (MBT): MBT combines mechanical and biological processes to sort, separate, and treat waste. It can produce materials for recycling and recover biogas for energy (Stantec, 2011; Worrell & Vesilind, 2012).

The choice of technology depends on factors such as waste composition, local regulations, environmental concerns, energy needs, and available resources. Many waste management systems employ a combination of these technologies to achieve effective waste reduction and resource recovery. Detailed information on waste treatment is given in the following sections.

1.2.1 Physical Solid Waste Processing Technologies

Physical solid waste processing technologies involve the mechanical manipulation of waste materials to separate, sort, or alter their physical characteristics. These technologies are designed to improve waste management practices by recovering valuable materials, reducing waste volume, and preparing waste for further processing. Here are some key physical waste processing technologies (Worrell & Vesilind, 2012):

1. **Mechanical Sorting**: This involves using conveyors, screens, and mechanical devices to separate waste materials based on size, shape, and weight. It's commonly used to separate larger items like furniture and appliances from the rest of the waste stream (Lahtela & Kärki, 2018; Tanguay-Rioux, Spreutels, Héroux, & Legros, 2022; Worrell & Vesilind, 2012).

2. **Magnetic Separation**: Magnetic separators use magnets to attract and separate ferrous metals from the waste stream. These metals can be recycled and reused (Lahtela & Kärki, 2018; Tanguay-Rioux et al., 2022; Worrell & Vesilind, 2012).

3. **Eddy Current Separation**: This technology uses a magnetic field to induce an electric current in non-ferrous metals, causing them to be repelled and separated from the waste stream. It's effective for separating aluminum and other non-ferrous metals (Lahtela & Kärki, 2018; Tanguay-Rioux et al., 2022; Worrell & Vesilind, 2012).

4. **Air Classification**: This method uses air to separate lighter materials (like paper and plastics) from heavier materials (like glass and metals) based on their density (Lahtela & Kärki, 2018; Tanguay-Rioux et al., 2022; Worrell & Vesilind, 2012).

5. **Screening and Shredding**: Screening involves passing waste materials through a series of screens with different hole sizes to separate materials by size. Shredding reduces the size of waste items, making them easier to handle and process (Lahtela & Kärki, 2018; Tanguay-Rioux et al., 2022; Worrell & Vesilind, 2012).

6. **Ballistic Separation**: This technology uses a combination of screens and air currents to separate waste materials based on their size and shape. It's effective for separating materials like plastics, paper, and cardboard (Lahtela & Kärki, 2018; Tanguay-Rioux et al., 2022; Worrell & Vesilind, 2012).

7. **Density Separation**: Density separation technologies use air or water to separate materials based on their density. For instance, heavy items like metals sink in water, while lighter materials like plastics float (Lahtela & Kärki, 2018; Tanguay-Rioux et al., 2022; Worrell & Vesilind, 2012).

Physical solid waste processing has a lot of benefits (Das et al., 2019). It efficiently separates recyclable and valuable materials from the waste stream, reduces the volume of waste going to landfills, prepares waste for further processing or disposal, recovers materials that can be reused or recycled, helps in source reduction by compacting and shredding waste (Das et al., 2019).

But physical solid waste processing has some challenges to be handled carefully. It requires proper maintenance of equipment to ensure efficient operation. Moreover, it can be energy-intensive depending on the technology. Some materials may be difficult to separate accurately, leading to contamination. Proper disposal of non-recyclable residues or byproducts is necessary (Das et al., 2019).

Physical solid waste processing technologies play a crucial role in waste management by increasing resource recovery, reducing landfill waste, and promoting sustainable practices. However, it's important to integrate these technologies with other waste management strategies and consider their environmental and economic impacts.

1.2.2 Biochemical Solid Waste Processing Technologies

Biochemical solid waste processing technologies involve the use of biological processes to break down organic waste materials into useful products. These technologies focus on harnessing the natural capabilities of microorganisms to degrade organic matter and produce valuable end products. Here are some key biochemical waste processing technologies (Bhoi, Ouedraogo, Soloiu, & Quirino, 2020a; Worrell & Vesilind, 2012):

1. **Composting**: Composting is a widely used biochemical process that converts biodegradable waste, such as food waste, yard waste, and agricultural residues, into nutrient-rich compost. Microorganisms like bacteria, fungi, and earthworms decompose the organic matter in the presence of air. The resulting compost can be used as a soil conditioner, improving soil structure and nutrient content (Ayilara, Olanrewaju, Babalola, & Odeyemi, 2020; Azim et al., 2018).

2. **Anaerobic Digestion**: Anaerobic digestion is a process that breaks down biodegradable waste in the absence of oxygen. Microorganisms break down the organic matter into biogas (methane and carbon dioxide) and digestate. Biogas can be used for energy production, while digestate is a nutrient-rich residue that can be used as a soil amendment (Meegoda, Li, Patel, & Wang, 2018).

3. **Bio-drying:** Bio-drying is an innovative waste management technique that employs microorganisms to eliminate moisture from biodegradable waste substances like food waste, agricultural residues, and sewage sludge. This approach combines controlled aeration with biological processes to expedite the dehydration of the waste, leading to the stabilization of the material and a notable reduction in its volume (Mohammed, Ozbay, & Durmusoglu, 2017).

Biochemical Solid Waste Processing has some positive effects. It can reduce the volume of organic waste going to landfills, produces valuable end products like compost, biogas, and nutrient-rich soil amendments, decreases greenhouse gas emissions compared to landfilling, provides opportunities for decentralized waste

management, especially in rural areas and finally reduces odors and potential pest problems associated with organic waste (Saravanan et al., 2022).

These methods also include some challenges. They requires proper management and control to ensure optimal conditions for microorganisms, may not be suitable for certain waste types like plastics or hazardous waste and can be affected by factors such as temperature, moisture, pH, and waste composition (Saravanan et al., 2022).

Biochemical solid waste processing technologies play a significant role in sustainable waste management by converting organic waste into useful resources and reducing the environmental impact of waste disposal.

1.2.3 Thermal Solid Waste Processing Technologies

Thermal solid waste processing technologies involve the use of heat to treat and convert waste materials into energy, heat, or other valuable products. These technologies are particularly effective for non-recyclable waste and can help reduce the volume of waste going to landfills while recovering energy. Here are some key thermal waste processing technologies (Bhoi, Ouedraogo, Soloiu, & Quirino, 2020b; Stantec, 2011; Worrell & Vesilind, 2012):

1. **Incineration**: Incineration involves the controlled combustion of waste materials at high temperatures. It reduces the waste volume significantly and generates heat energy. The heat can be used to produce steam, which in turn can drive turbines and generate electricity. Modern incinerators are equipped with pollution control technologies to minimize emissions (Lisk, 1988).

2. **Pyrolysis**: Pyrolysis is a process that involves heating waste materials in the absence of oxygen, causing them to break down into gases, liquids (pyrolysis oil), and char. Pyrolysis can be used to convert biodegradable waste, plastics, and tires into valuable products like biochar and bio-oil. The biochar can be used as a soil amendment, while bio-oil can be used as fuel or feedstock for chemical processes and syngas for heat or electricity (Bridgwater & Bridge, 1991).

3. **Gasification**: Gasification converts carbonaceous materials into a mixture of gases, known as syngas, by exposing them to high temperatures and controlled amounts of oxygen or steam. Syngas can be used as fuel for electricity generation or as a feedstock for chemical processes (Kirubakaran et al., 2009).

4. **Plasma Gasification**: Plasma gasification uses an electrically conductive gas (plasma) to convert waste materials into syngas at extremely high temperatures. This technology can handle a wide range of waste types, including hazardous waste and medical waste (Sanlisoy & Carpinlioglu, 2017).

Thermal Solid Waste Processing has two important benefits, first it reduces the volume of waste going to landfills and generates energy in the form of heat and electricity. Moreover, it can handle mixed waste streams and non-recyclable materials. Therefore, it reduces greenhouse gas emissions compared to landfilling and can recover valuable resources like metals from the ash (Yassin, Lettieri, Simons, & Germanà, 2005).

Besides its benefits, it has some challenges. Thermal methods require careful management to control emissions and minimize environmental impacts. Moreover, certain waste types, like plastics, can release harmful gases during thermal processing. High capital and operational costs for building and maintaining facilities are needed. Proper waste segregation is also crucial to prevent harmful emissions and maintain efficiency (Yassin et al., 2005).

Thermal solid waste processing technologies are an important component of integrated waste management systems, as they can help divert waste from landfills, recover energy, and contribute to sustainable waste management practices. However, careful consideration of environmental and health impacts, as well as the choice of appropriate waste streams, is essential for their successful implementation.

1.3 Bio-drying

Bio-drying is a waste treatment method that involves the use of microorganisms to remove moisture from biodegradable waste materials, such as food waste, agricultural residues, and sewage sludge. The process combines biological activity and controlled

aeration to accelerate the drying of the waste, resulting in a stabilized and reduced volume of material (Worrell & Vesilind, 2012; J. Yuan et al., 2018).

There are some key points about bio-drying to provide efficient process. The waste should be pretreated. The waste is typically shredded or mechanically processed to achieve a homogenous particle size and increase the surface area for microbial activity. Moreover, controlled aeration should be applied. The waste is placed in a bio-drying facility or composting bed, where it undergoes aerobic decomposition. The material is regularly turned or mixed to ensure proper aeration and prevent compaction. Biological activity is one of the main issues during bio-drying. Naturally occurring microorganisms, such as bacteria and fungi, consume organic matter and produce heat during the decomposition process. The heat generated helps evaporate moisture from the waste, facilitating drying. The bio-drying process is carefully managed to maintain optimal conditions for microbial activity. This typically involves monitoring and controlling temperature, moisture content, and airflow within the bio-drying facility (Mohammed et al., 2017; J. Yuan et al., 2018).

There are important benefits of bio-drying. For example, by removing moisture, bio-drying can significantly reduce the volume and weight of biodegradable waste materials. This can lead to cost savings in waste transportation and disposal (Mohammed et al., 2017). Moreover, the elevated temperatures reached during bio-drying contribute to the elimination of pathogens, reducing the potential health risks associated with the waste. Bio-drying can also improve the characteristics of organic waste, making it more suitable for further processing or utilization. The resulting material may have improved stability, reduced odor, and enhanced composting properties. The high moisture content in organic waste makes it less suitable for energy recovery processes. Bio-drying can increase the calorific value of the waste, making it more viable for energy conversion methods like incineration or anaerobic digestion (Mohammed et al., 2017; Rada et al., 2007; J. Yuan et al., 2018) .

Bio-drying is most effective for organic waste materials with high moisture content, such as food waste and sludge. Dry waste materials may not benefit significantly from this process (Rada et al., 2007; Rada, Ragazzi, & Badea, 2012). Proper facility design, including insulation, ventilation, and leachate management, is crucial to ensure

efficient and controlled bio-drying. Regular monitoring and maintenance are required to optimize process conditions (Rada et al., 2007, 2012). Furthermore, bio-drying facilities should implement measures to control and mitigate any potential environmental impacts, such as odor emissions and leachate management (Rada et al., 2012).

Bio-drying offers an effective means of reducing moisture content in biodegradable waste, facilitating further processing and utilization. It can be a valuable component of integrated waste management systems, contributing to waste reduction, resource recovery, and environmental sustainability.

1.4 Pyrolysis

Pyrolysis is the decomposition of raw materials in an oxygen-free environment at a temperature range of 400-800^{o}C (Kumar & Samadder, 2017). The products obtained as a result of pyrolysis are i) carbon black (biochar - solid), ii) pyrolysis oil (liquid) and iii) pyrolysis gas consisting of a mixture of carbon dioxide, carbon monoxide, methane and hydrogen (Demirbaş & Arin, 2002; Stantec, 2011). Pyrolysis oil and pyrolysis gas are widely used as fuels, chemicals and/or adhesives. The solid part consists of non-combustible inorganic materials and fixed carbon. Since oxygen is not given directly into the reactor, pyrolysis requires another thermal energy. This energy is transmitted to the system from the outside through the reactor walls (Charis, Danha, & Muzenda, 2020; Stantec, 2011).

The mass distribution of the products at the end of pyrolysis depends on the process temperature, process rate and heat transfer rate. For example, pyrolysis oil is mostly produced at low temperatures, while pyrolysis gas is produced at high temperatures (Amalina, Krishnan, Zularisam, & Nasrullah, 2023; Balat, Balat, Kirtay, & Balat, 2009; Charis et al., 2020; Demirbaş & Arin, 2002; Stantec, 2011; Worrell & Vesilind, 2012). The types of pyrolysis can be classified according to time and temperature as follows: i) Fast Pyrolysis: In fast pyrolysis, biomass is rapidly heated to temperatures between 400-600°C in the absence of oxygen. The biomass is typically in contact with hot gases or heated surfaces for a short duration, usually a few seconds. This process produces a higher yield of liquid bio-oil along with smaller amounts of char and gas

(Balat et al., 2009). ii) Slow Pyrolysis: Slow pyrolysis involves heating biomass at lower temperatures, typically between 300-500°C, for a longer duration, ranging from several minutes to hours. This process produces a higher proportion of char and a lower yield of liquid bio-oil compared to fast pyrolysis (Balat et al., 2009). iii) Intermediate Pyrolysis: Intermediate pyrolysis occurs at temperatures between those used in fast and slow pyrolysis, typically around 350-500°C. The residence time is longer than fast pyrolysis but shorter than slow pyrolysis. It results in a moderate yield of liquid bio-oil, along with char and gas (Balat et al., 2009). iv) Vacuum Pyrolysis: Vacuum pyrolysis involves carrying out the pyrolysis process under reduced pressure or in a vacuum. This helps to lower the boiling point of the pyrolysis products and improve the quality of the bio-oil produced (Wentrup, 2014, 2017).

Each type of pyrolysis has its advantages and disadvantages, and the choice of pyrolysis method depends on factors such as the desired product composition, process efficiency, and specific application requirements.

Studies on pyrolysis continue to be carried out with an increasing interest in the world and in our country. The raw material used, pyrolysis type, temperature and other parameters vary according to the region (economy, geography, population etc.) and purpose. For this purpose, important pyrolysis studies carried out in the world and in our country have been examined and summarized in tables.

1.4.1 Studies in The World

In the world, pyrolysis experiments have been started firstly with other types of waste and pyrolysis experiments with municipal solid waste have been started in recent years. However, in these studies, the high moisture content of the waste was a problem that researchers had to overcome. In the studies, mostly biodegradable wastes were dried before pyrolysis and the effect of water was not investigated. In order to reduce the moisture content of municipal solid waste, Gopu et al. kept the waste at 80 ^{o}C overnight and then homogenized it. The dried sample was subjected to pyrolysis at final temperatures varying between 400 and 650 ^{o}C and at a heating rate of 5 and 10^{o}C/min, depending on the desired product (Gopu et al., 2018).

In another study, the moisture content of municipal solid waste was reduced in a vacuum drying oven, and the dried sample was pyrolyzed at final temperatures between 400 and 700 ^{o}C and with a heating rate of 20 ^{o}C/min by adding additional substances (Q. Song et al., 2018).

Yang et al., on the other hand, conducted pyrolysis experiments in the organic fraction of municipal solid waste with high moisture content to observe the effect of moisture content on pyrolysis. Organic waste with four different moisture content levels (45.8, 34.6, 22.8 and 12.7 %) was tested at four different pyrolysis temperatures (450, 550, 700 and 850 °C) and the results were evaluated. As a result, it has been observed that the moisture content has no effect on the product amounts, and the organic liquid content reaches the highest value at 550 °C in samples with 45.8% and 34.6% moisture content, and at 700 °C in samples with 22.8% and 12.7% moisture content. It has been determined that the amount of liquid product decreases as the amount of water decreases. It has been determined that the moisture content has a low effect on the energy capacity of the product, as well as the processing temperature is an important factor (Yang, Heaven, Venetsaneas, Banks, & Bridgwater, 2018).

Table 1.1 summarizes the pyrolysis studies with biomass and it is seen that these studies are generally more valuable biomass sources such as energy crops. In the studies with municipal waste, valuable fractions or mixed municipal waste were used. This positively affects the product quantities and quality. There are one or two studies that have worked with biodegradable municipal waste, but these have not addressed the problems that the waste has as a whole. High water content is one of the most important problems for biodegradable municipal waste. There are almost no studies on pyrolysis of these wastes. The effect of water content on solid, liquid and gaseous products has not been sufficiently investigated.

Table 1.1 Pyrolysis studies in the World

Raw Material	Particle Size	Sample weight	Furnace Type	Final Temperature, ^{o}C	Heating Rate, ^{o}C/min	Sweeping Gas	Condenser	Aim	Comments	Reference
Mix MSW	0.5-1 mm	5 g	2” MTI tube furnace	408 (peak DTG temperature), 900	10	N_2 (50 ml/min)	5 ml dichloromethane in a cold trap	• To investigate managing municipal solid waste through the utilization of pyrolysis for energy and biochar production by transforming into activated carbon, which finds application in water treatment processes	-Held at final temperature for 60 min -Also obtained activated carbons from biochar with N_2 and CO_2	(Gopu et al., 2018)
Mix MSW (except inorganic components)	<0.075 mm	30 g	Fixed-bed reactor (Vertical tube reactor)	400 to 700 in steps of 50	20	N_2 20 ml/min (Before pyrolysis for 30 min) 40 ml/min (during pyrolysis)	Cooling tar (#3)	• to explore how additives impact the composition and quality of pyrolysis tar derived from municipal solid waste (MSW)	-Additives (Pine, CaO & MSW char) were experienced. -Residence time:30 min	(Q. Song et al., 2018)

Table 1.1 Pyrolysis studies in the World (continued)

Raw Material	Particle Size	Sample weight	Furnace Type	Final Temperature, ^{o}C	Heating Rate, ^{o}C/min	Sweeping Gas	Condenser	Aim	Comments	Reference
Organic fraction of MSW	<10 mm	350 g/hour	Continuous auger pyrolysis reactor	450,550,700,850	-	N_2	-A Cold-water condenser (5 ^{o}C) -Two dry ice condenser (-70 ^{o}C)	• To provide the outcomes of processing the organic fraction of municipal solid waste (OFMSW) in a slow pyrolysis system under a comprehensive range of processing conditions such as moisture content.	-Before experiment purged with N_2 -Solid residence time is the travel time of feedstock through the reactor (6 min) -Four different moisture contents (45.8, 34.6, 22.8 and 12.7 wt% wet basis) were tried. -Continued until ontained at least 100 mL aqueous product.	(Yang, Heaven, et al., 2018)
Cocoa husk (CH) Waste frying oil (FO) Sunflower seed dust (DS) Waste fatty water (FW) Waste cellulose (WC)	8 x 8 mm	80	Tube furnace	800	15	N_2	Ice with sodium chloride (-10^{o}C)	• the catalytic cracking process of biomass waste oil fractions derived from food waste leachate, employing microporous catalysts	CH, 90%CH-10%FO, DS, 90%DS-10%FW, WC, 90%WC-10%FW	(Grycová, Koutník, Pryszcz, & Kaloč, 2016)

Table 1.1 Pyrolysis studies in the World (continued)

Raw Material	Particle Size	Sample weight	Furnace Type	Final Temperature, °C	Heating Rate, °C/min	Sweeping Gas	Condenser	Aim	Comments	Reference
MSW (woody fraction	1 mm	-	Spoon pyrolysis reactor	400, 600	-	N_2 (300 ml/min)	Cooling water	• to examine the properties of biochar produced from different fractions of municipal waste. • to identify feedstocks that produce favorable characteristics and can be utilized for valuable products, as well as those with properties that might hinder their use. • to investigate techniques for removing trace metals and to identify the possible presence of soluble organic pollutants and compounds containing chlorine, nitrogen, and sulfur, as these are relevant to air quality concerns.	-Residence time:30 min	(Ayiania, Terrell, Dunsmoor, Carbajal-Gamarra, & Garcia-Perez, 2019)
Sugarcane bagasse	-	15	Hastelloy-type horizontal cylindrical device of steel	390- 980 (Slow) 380-780 (Fast)	45-50	He (1 L/min)	Four condensers with aqueous solution of 20% ethylene glycol (0 °C)	• to compare the experimental outcomes of slow pyrolysis and fast pyrolysis of bagasse, with the goal of converting biomass into syngas fuel. • Investigation of the temperature effect on yields	-Residence time: 1 hour -Conventional (Slow) Pyrolysis or carbonization -Fast Pyrolysis	(Arni, 2018)

Table 1.1 Pyrolysis studies in the World (continued)

Raw Material	Particle Size	Sample weight	Furnace Type	Final Temperature, ^{o}C	Heating Rate, $^{o}C/min$	Sweeping Gas	Condenser	Aim	Comments	Reference
Rice Straw (Agricultural waste)	100 nm	-	Moderate temperature autoclave	200, 250 and 300	3	-	-	• This research paper focuses on a novel approach to solid waste pyrolysis, where the production of liquid fractions is omitted, and efforts are made to decrease the amount of carbonaceous species generated. Additionally, the investigation aims to shift the direction of the produced gases towards hydrocarbon gases, as opposed to a gas mixture containing CO, CO2, H2, and CH4.	Residence time: 2 hours	(Moneim et al., 2018)
Maize stalk	1–2 mm	2 kg/h	Bubbling fluidized bed reactor	360–540	-	N_2 (7-13 m^3/h)	Water and dry ice condensers	• There is limited research on the influence of temperature, feed particle size, and carrier gas flow rate on the pyrolysis of maize stalk in a bubbling fluidized bed reactor. This study aims: • to identify the optimal temperature, feed particle size, and carrier gas flow rate to achieve the highest bio-oil yield and characterize its properties.	Residence time: depends on flow rate	(Ali, Saleem, Shahzad, Hussain, & Chughtai, 2016)

Table 1.1 Pyrolysis studies in the World (continued)

Raw Material	Particle Size	Sample weight	Furnace Type	Final Temperature, °C	Heating Rate, °C/min	Sweeping Gas	Condenser	Aim	Comments	Reference
Cupuassu fruit shell	150 μm	10 mg	TGA-FTIR system	Up to 602	5, 10, 20, 30 and 40	N_2 (50 ml/min)	-	• The potential of cupuassu fruit shells for bioenergy production through pyrolysis has not been extensively studied in existing literature. This research's primary novelty lies in exploring the physicochemical properties of cupuassu fruit shells and analyzing the kinetic triplet, thermodynamic activation parameters, and volatile products evolved during pyrolysis using a coupled TGA-FTIR system.	-	(Alves et al., 2022a)
Rice Straw, Cotton Stalk, and Pine Sawdust	-	-	Fixed-Bed Reactor	850	-	N_2	Condenser I (hot water) and condenser II (mixed ice/water).	• to understand the pyrolysis behavior of particular biomass varieties. • to explore the impact of biomass ash on weight loss behavior under pyrolysis conditions	-	(G. Chen & Leung, 2003)
Corn straw	<0.45 mm 0.45-2.0 mm	-	Bench-scale Fluidized Bed Reactor	450, 475, 500, 525 and 550	-	lean oxygen air	-	• to research the influence of pyrolysis temperature, biomass particle size, vapors residence time, and their interactions on the product distribution • the optimization of the operational parameters to achieve the highest possible bio-oil yield	vapors residence time: 0.8 s	(Liu et al., 2009)

Table 1.1 Pyrolysis studies in the World (continued)

Raw Material	Particle Size	Sample weight	Furnace Type	Final Temperature, °C	Heating Rate, °C/min	Sweeping Gas	Condenser	Aim	Comments	Reference
S. japonica algae	300–500 μm	15 g	Tubular fixed-bed reactor	350, 400, 450, 500 or 550	-	N_2 (100, 300 and 500 ml/min)	tap water in water bath and ethylene glycol-cooled condenser (-20°C)	• to investigate the fast pyrolysis of S. japonica in a fixed-bed reactor under various reaction conditions. • to research the effects of the pyrolysis temperature and sweeping-gas flow rate on the product distributions and compositions	-Residence time: 1 hour	(Vu, Kim, Hyung, Chul, & Kim, 2016)
Waste Merbau wood (Intsia bijuga) sawdust	0.595 mm, 0.707 mm and 2 mm	200 g	Laboratory-scale tubular fixed-bed reactor	500	5-12	-	condenser with heat pipes and a condenser without heat pipes	• To investigate the impact of particle size and vapor heater on the liquid yield using L-shaped heat pipe fin condensers	-	(Abdullah, Tila, Hakim, & Koestoer, n.d.)
Organic fraction of MSW	10 mm	1.6 kg/h	Horizontal cylindrical reactor	500	-	N_2	shell and tube water-cooled condenser	• To provide the mass balance for pilot-scale intermediate pyrolysis of the organic fraction of municipal solid waste (OFMSW) and focuses on the characterization of pyrolysis oil, specifically examining its aging and rheological properties.	-Residence time: 30 min	(Yang, Zhang, et al., 2018)

Table 1.1 Pyrolysis studies in the World (continued)

Raw Material	Particle Size	Sample weight	Furnace Type	Final Temperature, ^{o}C	Heating Rate, ^{o}C/min	Sweeping Gas	Condenser	Aim	Comments	Reference
Rice bran, rice straw, dairy manure and chicken manure	0.154 mm	10 mg	TGA	800	2.5, 5, 10, 15, 20	N_2 (120 mL/min)	-	• to quantitatively analyze the thermal conversion behavior of biomass components (cellulose, hemicellulose, and lignin) into biochar	-	(Xu & Chen, 2013)
Mix biomass	<250 µm	10- 25 g	Tubular pyrolysis reactor	500	-	N_2 (500 mL/min)	-	• to conduct a thorough investigation of the pyrolysis characteristics and product distribution of different types of biomass and their individual components using both thermogravimetric analysis (t.g.a.) and pyrolysis bench-scale pilot (PBP) experiments. • to create a mathematical model that can accurately predict the pyrolysis characteristics and product distribution of biomass based on the characteristics of its individual components. • To observe the effect of ash during pyrolysis	-	(Raveendran, Ganesh, & Khilar, 1996)

Table 1.1 Pyrolysis studies in the World (continued)

Raw Material	Particle Size	Sample weight	Furnace Type	Final Temperature, ^{o}C	Heating Rate, ^{o}C/min	Sweeping Gas	Condenser	Aim	Comments	Reference
Bamboo and oak wood polypropylene [PP] and polystyrene [PS]	-	3 g	Fixed-bed reactor	450, 475, 500, 525	-	N_2 (20 mL/min)	Cooling solvent (-10^{o}C)	• to investigate the co-pyrolysis of biomass/plastic blends using bamboo and oak wood as lignocellulosic biomass feedstocks, along with two thermoplastics (polypropylene [PP] and polystyrene [PS]) focusing on analyzing the kinetic triplet, product yield, and characteristics (such as gas, oil, char, and wax) resulting from the co-pyrolysis process	-90/10–90 wt% biomass and 10 wt% plastic or 80/ 20–80 wt% biomass and 20 wt% plastic -Residence time: 1 hour -The residence time of the volatiles: 5.13 min	(Anh et al., 2022)
Sewage sludge	289 μm	3 g/min	Fluidized bed reactor	300-800	-	N_2	Two ice condensers	• to develop an empirical model for the devolatilization stage of high-ash sewage sludge during pyrolysis	-	(Jaramillo-Arango, Fonts, Chejne, & Arauzo, 2016)
Waste wood of endospermum	-	-	Batch reactor	400	5 & 20	-	Water condenser	• to suggest a multi-stage process to enhance the charcoal production procedure. • to investigate the heating rate and the target temperature for the different stages in charcoal production	-	(Oyedun, Lam, & Hui, 2012)

Table 1.1 Pyrolysis studies in the World (continued)

Raw Material	Particle Size	Sample weight	Furnace Type	Final Temperature, ^{o}C	Heating Rate, ^{o}C/min	Sweeping Gas	Condenser	Aim	Comments	Reference
Sugarcane	-	30 g	Fixed-bed reactor	700		He (1 L/min)	Four condensers with aqueous solution of 20% ethylene glycol (0 ^{o}C)	• to study an integration of the pyrolysis process with a Molten Carbonate Fuel Cell (MCFC) system for the production of electrical energy • to observe the effect of humidity on sugarcane biomass gas production	-	(Al Arni, Bosio, & Arato, 2010)
Municipal plastic wastes (MPW)	10 mm	750 g	Stirred reactor	500	-	N_2	Water cooler (20 ^{o}C)	• In this study, actual municipal plastic wastes (MPW) were subjected to pyrolysis, and the resulting heavy oil (HO) product was utilized for co-pyrolysis along with MPW in varying ratios of raw materials. • To investigate the influence of the heavy oil/municipal plastic waste ratio on the properties of the resulting products.	-Zeolite type catalysts were used. -MPW/HO: 100/0, 70/30 and 30/70	(Miskolczi & Ateş, 2016)

Table 1.1 Pyrolysis studies in the World (continued)

Raw Material	Particle Size	Sample weight	Furnace Type	Final Temperature, ^{o}C	Heating Rate, ^{o}C/min	Sweeping Gas	Condenser	Aim	Comments	Reference
Municipal solid waste (MSW) in refuse derived fuel (RDF) form	Ø8 mm	15 g	Fixed bed reactor	400, 500, 600, 700	10	N_2	Dry-ice cooled condensers	• To investigate the effects of process conditions and particle size of RDF on the product yield and composition	-RDF pellets -Residence time: 1 h	(Buah, Cunliffe, & Williams, 2007)
Sewage sludge and organic fraction of municipal solid waste (OFMSW)	0.254 mm	20 g	Fixed bed quartz reactor	350, 550 or 750	10	N_2 (100 mL/min)	-	• to confirm the combined effects of different organic fraction of municipal solid waste (OFMSW) additions on biochar properties • to investigate the changes in chemical speciation and immobilization of heavy metals (HMs) in the biochars before and after the addition of various OFMSW • to evaluate the phytotoxicity and potential environmental risk of HMs in the biochars.	-SS/various OFMSW, 4:1, w/w -Residence time: 1 h	(X. Wang, Chang, Li, Chen, & Wang, 2021)

Table 1.1 Pyrolysis studies in the World (continued)

Raw Material	Particle Size	Sample weight	Furnace Type	Final Temperature, °C	Heating Rate, °C/min	Sweeping Gas	Condenser	Aim	Comments	Reference
MSW (Paper, plastic, wood, composite material)	-	5-10mg	TGA instrument	500 or 600	10	N_2 (150 mL/min)	-	• to collect data and acquire knowledge that can be valuable for modeling, designing, and operating thermal conversion processes (pyrolysis, gasification and combustion) specifically for Municipal Solid Waste (MSW)	-	(Sørum, Grønli, & Hustad, 2001)
Mixed MSW (Yard waste, food waste, textile, paper, rubber, plastics)	-	10 mg	TGA instrument	To 900	10	N_2 (100 mL/min)	-	• to investigate and correlate the interaction effect and kinetics of the heterogeneous Municipal Solid Waste (MSW) by thermogravimetric approach	-	(Chhabra, Bhattacharya, & Shastri, 2019)
OFMSW and its digestate	<5 mm	40 g	Bench-scale reactor	450, 550, and 650	15	N_2 (200 mL/min)	Cooling condenser and two cooling bath (-20 °C)	• to investigate the pyrolysis performances of Organic Fraction of Municipal Solid Waste (OFMSW) and its digestate • to understand the impact of Anaerobic Digestion (AD) on the pyrolysis performance of OFMSW.	-Residence time: 1 h	(Wen et al., 2021)

Table 1.1 Pyrolysis studies in the World (continued)

Raw Material	Particle Size	Sample weight	Furnace Type	Final Temperature, ^{o}C	Heating Rate, ^{o}C/min	Sweeping Gas	Condenser	Aim	Comments	Reference
MSW (Paper waste)	0-10 mm 10-20 mm and as received	-	Fixed bed reactor	300-500	-	N_2	liquid condenser and ice-cooled liquid collector	• to investigate the characterization of products obtained from wastepaper by pyrolysis	-	(Islam, Islam, Beg, & Islam, 2005)
MSW (Combustible fractions, not biodegradable)	2 mm	70 g	Semi-batch reactor	Up to 550 (Slow) 450, 480, 510 and 550 (Fast)	4 (Slow)	N_2 (70 mL/min)	-	• To explore the impact of reactor temperature and heating rate on the composition and yield/distribution of pyrolysis products. • To examine the behavior of metals present in MSW during the pyrolysis process and their interaction with the pyrolysis products. • To assess the potential usability of the obtained products as fuel sources for energy production or as raw materials for chemical feedstock.	-Slow pyrolysis -Fast pyrolysis	(Velghe, Carleer, Yperman, & Schreurs, 2011)

Table 1.1 Pyrolysis studies in the World (continued)

Raw Material	Particle Size	Sample weight	Furnace Type	Final Temperature, ^{o}C	Heating Rate, ^{o}C/min	Sweeping Gas	Condenser	Aim	Comments	Reference
Cattle manure	0.508-0.635 mm	10 mg	TGA system	Up to 800	20, 40, 60, 80	N_2 (20 mL/min)	-	• To investigate the kinetic triplet for the pyrolysis and combustion processes of a blend of locally sourced cattle manure based on TGA data.	-The same procedure as with pyrolysis was carried out with oxygen to find the combustion characteristics	(Ashraf, Ramzan, Khan, & Durrani, 2021)
Chicken manure	Powdered	1 mg	TGA system	Up to 900	10-30	N_2 (50 mL/min)	-	• To examine both non-catalytic and catalytic pyrolysis of chicken manure (CM) using a combination of thermogravimetric analysis (TGA) and pyrolyzer-gas chromatography/mass spectrometry (Py-GC/MS).	-	(Shim et al., 2022)
Cattle manure	0.63 mm	-	TGA system	Up to 800	10, 20, 30, 40, 60 and 80	N_2 (100 mL/min)	-	• to precisely determine the thermal conversion behaviors of cattle manure based on TGA	-	(X. Yuan, He, Cao, & Yuan, 2017)

Table 1.1 Pyrolysis studies in the World (continued)

Raw Material	Particle Size	Sample weight	Furnace Type	Final Temperature, °C	Heating Rate, °C/min	Sweeping Gas	Condenser	Aim	Comments	Reference
Digested sewage sludge (SS) and digested manure (DM)	<50 µm	300-600 g	Stirred batch reactor	525	8	N_2 (250 mL/min)	Two ice-cooled condensers	• to assess and compare the key characteristics of pyrolysis products derived from digested sewage sludge (SS) and digested manure (DM), aiming to uncover potential synergistic and antagonistic effects during their co-pyrolysis.	- 50:50% blend -Residence time: 30 min	(Ruiz-Gómez et al., 2017)
Chicken, swine and dairy manure	1.27 mm	-	Tube furnace	200-700	10	N_2 (250 mL/min)	-	• To analyze the influence of temperature on dissolved organic carbon (DOC) content. • To identify the strength and order of changes in groups/functional groups within dissolved organic matter (DOM) resulting from various temperatures. • To assess the evolution of components within DOM across different pyrolysis temperatures. • To distinguish the differences in DOM derived from various manure feedstocks.	-Residence time: 2 h	(Gui, Liu, Li, & Wang, 2020)
Manure (Dairy, poultry, swine etc.)	2 mm	0.5-1.5 kg	Electric box furnace	350, 700	2.5 (350°C) 8.33 (700°C)	N_2 (1 L/min)	-	• To provide a comprehensive understanding of biochar properties across diverse manure feedstocks under controlled conditions	-60 min at 200°C -to final temperature within 60 min -120 min at final temperature	(Cantrell, Hunt, Uchimiya, Novak, & Ro, 2012)

Table 1.1 Pyrolysis studies in the World (continued)

Raw Material	Particle Size	Sample weight	Furnace Type	Final Temperature, °C	Heating Rate, °C/min	Sweeping Gas	Condenser	Aim	Comments	Reference
Digested dairy cattle manure	-	400 g	Fixed-bed reactor	600	10	N_2 (5.3 L/min)	-	• to enhance the understanding of slow pyrolysis applied to dairy cattle manure, encompassing both one-step and multi-step pyrolysis processes • to observe the effects of temperature on the characteristics of the resulting solid product, including variables such as ash content, elemental composition, higher heating value, pH, electrical conductivity, cation exchange capacity, water holding capacity, and surface functional groups	-Multi-step pyrolysis -one step pyrolysis	(Atienza-Martínez, Ábrego, Gea, & Marías, 2020)
Sewage sludge	-	30 or 40 g	Muffle furnace	300, 400, 500	17	N_2 (200 mL/min)	-	• to explore the viability of generating biochar from sewage sludge by assessing the characteristics of the resulting biochar, ensuring it possesses the necessary qualities to be utilized as soil improvement and soil remediation • to examine the augmentation of surface area by treating certain samples of raw sewage sludge with K_2CO_3 and H_3PO_4 through impregnation. • To evaluate the viability of using biochar in soils, the leaching tests were conducted to examine the release of heavy metals from the biochar under standardized conditions. • to investigate the ability of biochar to adsorb As(V) and Cr(III).	-Residence time: 30, 60, 90 min	(Agrafioti, Bouras, Kalderis, & Diamadopoulos, 2013)

Table 1.1 Pyrolysis studies in the World (continued)

Raw Material	Particle Size	Sample weight	Furnace Type	Final Temperature, °C	Heating Rate, °C/min	Sweeping Gas	Condenser	Aim	Comments	Reference
Sewage sludge	-	-	Vacuum tubular furnace	150, 250, 350, 450, 500	10	N_2 (100 mL/min)	-	• to examine the impact of pyrolysis on reducing microplastics in sewage sludge under varying temperatures, • to investigate the changes in microplastics characteristics as the pyrolysis temperature changes	-Residence time: 30 min	(Ni et al., 2020)
Sewage sludge and rice husk	<0.075 mm	10 mg	TGA system	Up to 1000	20	N_2 (20 mL/min)	-	• to simultaneously examine the influence of rice husk (RH) on the thermal decomposition process and the release of gaseous products during the pyrolysis of sewage sludge (SS). • To explore the impact of interactions between SS and RH on the characteristics of the resulting multiphase products, including gases and biochar	-Moreover, biochar was produced with a vacuum tube furnace.	(T. Wang et al., 2020)
Sewage sludge and rice husk	-	10 mg	TGA system	800	20 (to 100°C) Then 10, 20, 30 (100 to 800°C)	N_2 (100 mL/min)	-	• to examine the co-pyrolysis of sewage sludge (SS) and rice husk (RH) using TG-FTIR-MS to understand the thermal behavior of the blend and to characterize the properties of both condensable and non-condensable gases produced during the process. • To investigate the interaction between the two feedstocks in the blend based on data related to mass loss and the characteristics of condensable/non-condensable gases	-	(C. Wang, Bi, Lin, Jiang, & Jiang, 2020)

Table 1.1 Pyrolysis studies in the World (continued)

Raw Material	Particle Size	Sample weight	Furnace Type	Final Temperature, °C	Heating Rate, °C/min	Sweeping Gas	Condenser	Aim	Comments	Reference
Digested sewage sludge	250–500 µm	4.5 g/min	Fluidized bed reactor	550	-	N_2 (4.5 L/min)	Two condensers	• to confirm whether the type of sewage sludge has an impact on the pyrolysis process, particularly on the distribution of products and the characteristics of the resulting liquids • to discuss how the composition of sewage sludge samples influences these outcomes.	-	(Fonts, Azuara, Gea, & Murillo, 2009)
Anaerobic sewage sludge	1-3 mm	20 g	Horizontal quartz reactor	450, 650 and 850	5, 60	He (100 mL/min)	Ice and water condensers	• to enhance our understanding of how various pyrolysis conditions (such as temperature and heating rate) affect the primary attributes of the gas, liquid, and solid fractions generated during the conversion of sewage sludge obtained from an urban wastewater treatment plant	-	(Inguanzo, Domı´nguez, Mene´ndez, Blanco, & Pis, 2002)

1.4.2 Studies in Türkiye

Studies on pyrolysis in Türkiye are limited and as can be seen in Table 1.2, waste tires, lignite or other biomass sources have generally been studied.

Banar et al. carried out pyrolysis trials of Tire Derived Fuel (TDF) at 350, 400, 450, 500, 550 and 600 ^{o}C and at heating rates of 5 and 25 ^{o}C/min (Banar, Akyildiz, Özkan, Çokaygil, & Onay, 2012)

Another study is about pyrolysis trials of high-density polyethylene and low-density polyethylene at 300, 400, 500, 600 and 700 ^{o}C temperatures and at a heating rate of 5 ^{o}C per minute (Sogancioglu, Yel, & Ahmetli, 2017). In another study, pyrolysis studies were carried out with a heating rate of 300 ^{o}C/min at 500 ^{o}C of lignite and waste tire (Onay & Koca, 2015).

In another study, canola plant was subjected to pyrolysis and the effect of heating rate on the amount of pyrolysis products was investigated. In this study, the sample was kept at 140 ^{o}C for 10 minutes for complete evaporation, then the final temperature was increased to 1000 ^{o}C and kept for 30 minutes (Haykiri-Acma, Yaman, & Kucukbayrak, 2006).

In a study with cotton straw, different final pyrolysis temperatures and heating rates were tried. In addition, the effect of stripping gas on pyrolysis was investigated (Pütün, 2002).

In addition to these studies, there is no study on the pyrolysis of municipal solid waste to date. As a country with solid waste generation with high water content, this study will be enlightening and guiding for future waste management studies.

If we look at the studies on pyrolysis in the world and in Türkiye, there are not many studies on the pyrolysis of biodegradable municipal waste and especially their co-pyrolysis with other biomasses. Properties of the waste such as water and organic matter content have not been investigated in detail. One of the main objectives of this study is to investigate the quality and quantity of the products resulting from the pyrolysis of biodegradable municipal waste with very high water content. In addition,

the effect of factors such as temperature, heating rate, retention time, gradual heating will also be investigated. The main objective is to determine an optimum condition for pyrolysis of this waste.

In addition to pyrolysis of these wastes, the effect of bio-drying, a low-cost method to bring the water content of the waste to a specified level, has been investigated.

In summary, this study investigated an alternative method for biodegradable municipal waste considering its high water content.

Table 1.2 Pyrolysis studies in Türkiye

Raw Material	Particle Size	Sample weight	Furnace Type	Final Temperature, °C	Heating Rate, °C/min	Sweeping Gas	Condenser	Aim	Comments	Reference
Cotton straw and stalk	0.85-1.8 mm	3 g	Tubular reactor	400, 500, 550, and 700	700	N_2 (100 mL/min) 50, 100, 200, 400, 800 mL/min	Cold trap (0°C)	• to identify the optimal pyrolysis conditions that yield high quantities of oils with low oxygen content for cotton • to determine the effect of pyrolysis temperature, heating rate, and sweeping gas flow rates on the pyrolysis yields	-Fast pyrolysis	(Pütün, 2002)
Tire Derived Fuel (TDF)	-	10 g	Fixed bed reactor	350, 400, 450, 500, 550 and 600	5, 35	-	Cold trap (0°C)	• to generate pyrolytic oils from tire-derived materials and to examine for their potential as fuel and their compositions in relation to pyrolysis heating rate, specifically focusing on alkanes, alkenes, and PAHs	-Residence time: 1 h	(Banar et al., 2012)
Waste tyre and lignite	0.65-0.85 mm	-	Heinze reactor (HR) and fixed bed reactor (FB)	400, 500, 600 or 700	7 (HR) 300 (FB)	N_2 (100 mL/min)		• to identify the collaborative effects that arise from the co-pyrolysis of lignite and waste tires, aiming to enhance the yield of pyrolysis oil • To examine the impact of factors such as reactor type, pyrolysis temperature, and the proportion of waste tire to lignite in the blend, on the resulting products from co-pyrolysis	-Residence time: 30 min	(Onay & Koca, 2015)

Table 1.2 Pyrolysis studies in Türkiye (continued)

Raw Material	Particle Size	Sample weight	Furnace Type	Final Temperature, °C	Heating Rate, °C/min	Sweeping Gas	Condenser	Aim	Comments	Reference
Lignite	4.75, 3.35 and 1.18 mm	-	Tubular furnace	400, 500, 600, 700, 800	3	N_2 (200 mL/min)	-	• To investigate the effect of coal enrichment on carbonization/pyrolysis product yields	-Residence time: 15, 30, 45 and 60 min	(Aksoğan Korkmaz & Bentli, 2019)
Sawdust	0.850-1.60 mm	50 g	Fixed-bed reactor	400, 500, 600	5	N_2 (30 mL/min)	Cold trap	• To investigate the impact of pyrolysis parameters such as temperature and catalyst type on liquid product yields and composition during liquefaction by pyrolysis method	-Residence time: 1 h	(Özçifçi & Özbay, 2013)
Walnut shell, hazelnut shell and cotton waste	-	-	TGA system	Up to 1000	20	N_2 (30 mL/min) Air (100 mL/min)	-	• to assess the energy potential of three distinct biomass sources: walnut shell, hazelnut shell, and cotton waste through both pyrolysis and combustion processes	-	(Kanca, 2019)
Rapeseed	<0.250 mm	40 mg	TGA system	Up to 1000	5, 10, 20, 30, 40 and 50	N_2 (40 mL/min)	-	• to examine the impact of heating rate on the slow pyrolysis of rapeseed	-Residence time: 30 min	(Haykiri-Acma et al., 2006)

CHAPTER TWO
AIM OF THE STUDY

This study aimed to investigate a thermal processing method for utilization of municipal biodegradable waste and other regionally available and valuable waste biomass. For this purpose, the study has focused on the gaps on waste quality (such as proximate and ultimate analysis, and water content), which are decisive for the applicability of pyrolysis technology in the management of municipal waste in Türkiye It will also provide guidance for countries with similar conditions to Türkiye.

The aims of this study are listed below:

- Determination of the effect of the waste characteristics such as elemental composition and organic content on the performance of the pyrolysis method by means of the quantity and quality of the final products
- Determination of the effect of the moisture content of the waste on the performance of the pyrolysis method and the quantity and quality of the products resulting from the process
- Determination of the effect of the particle size of the waste on the performance of the pyrolysis system and on the product quality
- Determining the efficiency of co-pyrolysis of biodegradable municipal waste with waste biomass by means of the quantity and quality of the final products
- Determining the effect of final temperature, sequential heating and residence time on pyrolysis system efficiency and product quality
- Defining optimum working conditions for the application of pyrolysis technology in municipal solid waste management within the framework of the National Waste Management and Action Plan
- Determining the performance of bio-drying, which is an economical and easily applicable method for reducing water content of the waste
- Producing a database that will contribute to the limited scientific literature focused on the application of thermal technologies in waste management in the world and in Türkiye.

CHAPTER THREE
MATERIAL & METHODS

3.1 Sampling

Municipal biodegradable solid waste, cattle manure, poultry manure, sewage sludge, yard waste and corn stalks were selected as samples for the study. Preliminary analyses and experiments were carried out with these samples. After determining the optimum conditions, they will be used in the final experiments. To determine the optimum conditions, dry cat/dog foods were used as they are very similar to biodegradable wastes in terms of content and analyzes were carried out to determine which food to use.

3.1.1 Sampling of Biodegradable Solid Wastes

At the beginning of the study, preliminary research was required to determine the experimental conditions. For this reason, biodegradable municipal solid waste samples were taken from various cities and various other biodegradable waste biomass samples were collected. Analyses were conducted on the biodegradable fractions of municipal solid wastes and various other types of biomasses. These samples will be used in the experiments once the systems have been optimized using dry cat/dog food as a reference.

The municipal solid waste samples were collected from different locations in Western part of Anatolia-Türkiye; including Aydın, Çanakkale, Manisa (Akhisar), and İzmir (Buca, Gaziemir, Karşıyaka, Konak, and Bornova). Waste samples of Aydın and Akhisar were obtained from the metropolitan municipality landfill, while the Çanakkale waste came from the municipal mechanical waste treatment plant. The waste samples from Buca, Gaziemir, Karşıyaka, Konak, and Bornova were collected from transfer stations. The Aydın and Çanakkale waste samples were taken in April 2022, while the samples from Karşıyaka, Konak, and Buca were collected in 2014 and properly dried and stored. The waste samples from Akhisar, Buca, and Gaziemir were sampled in 2018, dried, and stored appropriately. The waste samples were weighed and sorted into categories such as biodegradable waste, hygienic waste, and

recyclables, and the biodegradable fraction was sieved using a 70 mm sieve. The biodegradable fractions were promptly collected and prepared for analysis, while the remaining two fractions were discarded. The samples from Çanakkale and Aydın are composite samples that represent the entire city, whereas the samples from Akhisar, Karşıyaka, Bornova, Konak, Buca, and Gaziemir represent specific towns. The detailed information about cities was given in Table 3.1. You can find the compositions of the municipal solid wastes in Figure 3.1. The majority of the samples consist of biodegradable fractions, accounting for over 50%, with recyclables being the second most prominent category.

Table 3.1 The information of cities in the study

City	Population	Latitude & Longitude	Climate	Prevailing Economical Activities
Çanakkale	557,276	26.6225°E 40.073°N	Mediterranean-Black Sea	• Agriculture • Industry • Trade • Tourism
Akhisar	176,000	27.8366°E 38.9177°N	Mediterranean	• Agriculture • Industry
Karşıyaka	347,023	27.101667°E 38.476111°N	Mediterranean	• Service Sector • Industry
Bornova	452,867	27.221111°E 38.469722°N		• Trade • Service Sector • Agriculture
Konak	336,545	27.128333°E 38.418889°N		• Trade • Tourism • Service Sector
Buca	517,963	27.171667°E 38.388333°N		• Trade • Service Sector • Agriculture
Gaziemir	137,856	27.136944°E 38.325833°N		• Industry • Trade
Aydın	1,134,031	27.937222°E 37.728333°N	Mediterranean	• Agriculture • Industry

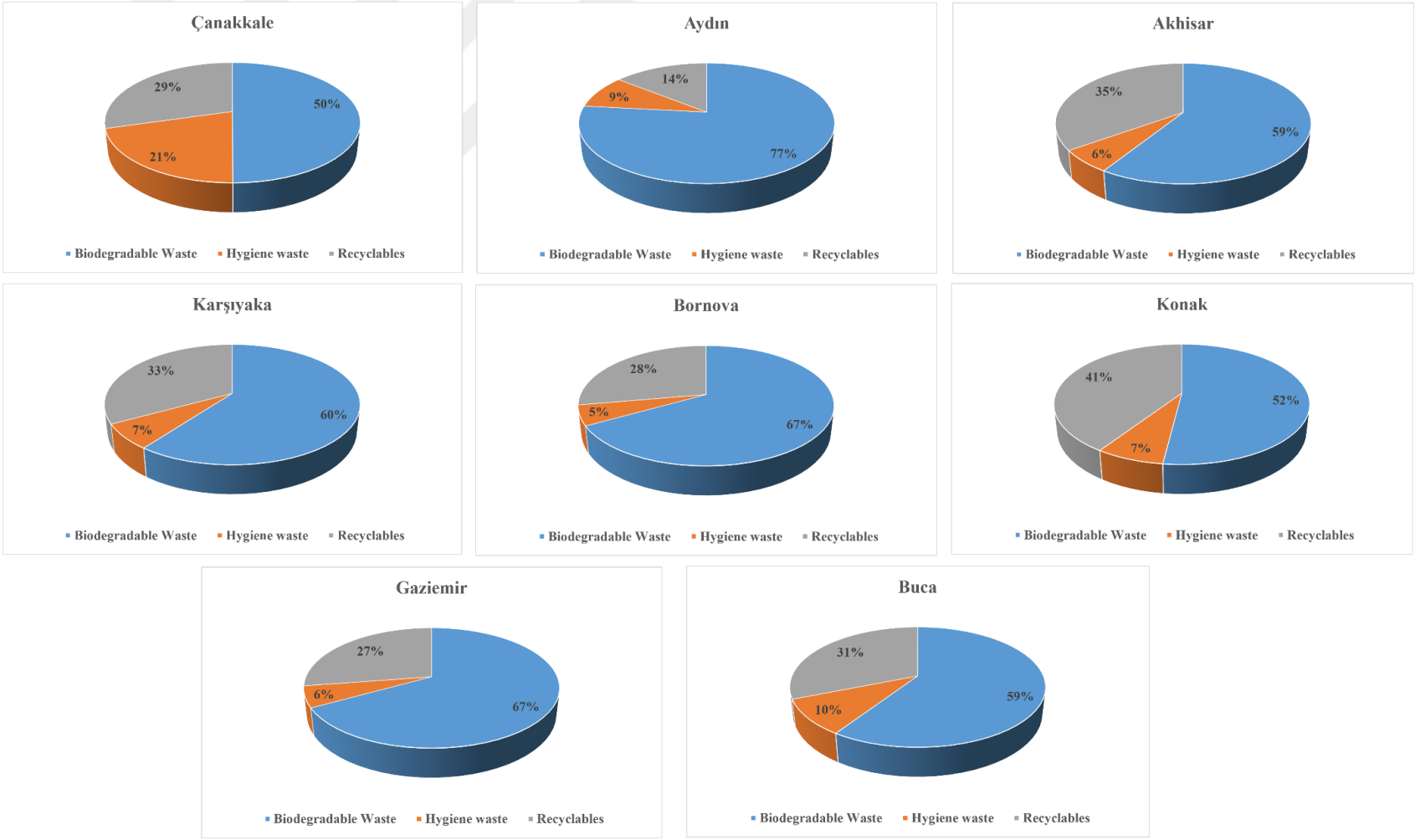

Figure 3.1 The composition of the waste samples

Cattle and poultry manure were sourced from farms in the Foça region of Izmir, Türkiye. Yard waste was obtained from the plant and tree trimmings at Tınaztepe Campus, while corn stalks were collected from a village in Aydın City. The WWTP (wastewater treatment plant) sludge was dried using solar energy and gathered from a municipal wastewater treatment plant in Izmir. As a result, 21 samples were collected and analyzed. You can see all samples and their descriptions in Table 3.2.

Table 3.2 The samples

Code	Definition
W1.1	Çanakkale (>70 mm)
W1.2	Çanakkale (<70 mm)
W2.1	Akhisar (>70 mm)
W2.2	Akhisar (<70 mm)
W3.1	Karşıyaka (>70 mm)
W3.2	Karşıyaka (<70 mm)
W4.1	Bornova (>70 mm)
W4.2	Bornova (<70 mm)
W5.1	Konak (>70 mm)
W5.2	Konak (<70 mm)
W6.1	Buca (>70 mm)
W6.2	Buca (<70 mm)
W7.1	Gaziemir (>70 mm)
W7.2	Gaziemir (<70 mm)
W8.1	Aydın (>70 mm)
W8.2	Aydın (<70 mm)
CM	Cattle Manure
PM	Poultry Manure
SS	Sewage Sludge
YW	Yard waste
CS	Corn stalk
BDW	Bio-dried waste

3.1.2 Selection of Dried Dog and Cat Foods for Experiments

Commercial cat and dog foods were purchased and their contents were examined, then analyzed and compared with biodegradable solid waste and four suitable dry cat/dog foods were identified and prepared for the experiments.

The dry cat and dog foods to be used in the study were selected by comparing their components with the contents of biodegradable solid waste. The contents of the commercial foods listed in Table 3.3, which also consists other detailed information, were compared with the biodegradable solid waste contents obtained in various studies can be found in Table 3.4 & 3.5. M18, M21, M27 and M28 foods were selected for use in the experiments based on their contents. This decision was also supported by proximate analysis.

Table 3.3 The properties of dry cat and dog foods

Number of dry cat/dog food	Type	Main food	Protein, % TS	Lipid, % TS	Ash, % TS	Cellulose, % TS
M1	Sterilized Cat	Beef	37	13	7.5	4
M2	Adult Cat	Chicken	34	14	7.5	2.5
M3	Kitten	Chicken	41	20	8	2.5
M4	Kitten	Chicken	37	13	7	1.5
M6	Adult Cat	Chicken	30	9	12	4.5
M7	Kitten	Chicken	33	10	13	4
M8	Puppy	Chicken	28	16	7	1.9
M9	Puppy	Lamb	26	13	8	4
M10	Adult Dog	Beef	22	10	9	2
M12	Adult Cat	Beef	32	12.5	8.7	1.5
M13	Adult Cat	Chicken	32	12.5	8.7	1.5
M14	Adult Cat	Fish	32	12.5	8.7	1.8
M15	Adult Cat	Lamb	27	10	8	2.5
M16	Adult Cat	Salmon	27	10	8	2.5
M17	Adult Dog	Lamb	20	9	8	4
M18	Adult Dog	Beef	18	7	8	4
M19	Adult Cat	Chicken	27	10	8	2.5
M20	Adult Cat	Chicken	27	10	8	2.5
M21	Adult Dog	Salmon	29	18	7.5	3
M22	Adult Dog	Lamb	24	12	8	3.5
M23	Adult Cat	Gourmet	27	10	8	2.5
M24	Adult Cat	Chicken	27	10	8	2.5
M25	Adult Dog	Lamb	22	10	9	6
M26	Adult Cat	Gourmet	28	14	7	4.5
M27	Adult Dog	Lamb	21	11	8	2.5
M28	Kitten	Chicken	41	20	6.5	1.5

Table 3.4 The components of some solid waste types

Components	Waste	Cow Manure	Domestic Waste	Waste Mix A	Waste Mix B	Waste Mix C	Meat-fish-cheese	Fruit	Vegetable	Bread-Pasta	Food Waste	Food Waste
	%	% TS	% TS	% TS	% TS	% TS	% TS	% TS	% TS	% TS	% TS	% TS
Cellulose	44	24	27.1	9	10	11	<1	3	3	<1		
Hemicellulose		11.9	13.65	5.1	5	5.1	2	2	3	2		
Crude protein	3	11.9	8.69	15	17	16	52	3	11	13	29.3	7.79
Starch		12.4	14.68	26	8	16	<1	<1	48	75	34.7	
Carbohydrates				67	45	57	12	94	72	82		9.52
Free Sugars							<1	89	18	5		
Glucose				6.2	4.1	5.1	<1	44	5	<1		
Fructose				3	3	3.1						
Sucrose				5	2.1	4	<1	<1	<1	5		
Lipid	2	0.1	0.8	11	31	19	33	<1	4	4	22.3	10.26
Lignin	13	12.1	14.5	5	4.9	5						
Ash	15											
Pentosan ve pektins	8			8.1	7.9	8						
Others	15										13.7	
Non-structural Carbohydrates							10	89	66	80		
Reference	(Erdin, 2005)	(Şenol & Açikel, 2019)		(Alibardi & Cossu, 2015)			(Alibardi & Cossu, 2016)				(F. Wang et al., 2016)	(Morales-Polo, Cledera-Castro, & Soria, 2018)

Table 3.5 The components of some solid waste types (Continued)

Components	Household FW	Household FW	Urban (Households, markets, restaurants)	University Dining Hall	Military Facilities	Institution Restaurant	Animal Kitchen Waste	Vegetable Kitchen Waste	Uneaten Animal Kitchen Waste	Uneaten Vegetable Kitchen Waste	Animal Food Waste	Vegetable Food Waste
	% TS	% TS	% TS	% TS	% TS	% TS	% TS	% TS	% TS	% TS	% TS	% TS
Cellulose							1.30	2.89	0.62	2.10	1.68	11.16
Hemicellulose								1.21			5.88	9.3
Crude protein	17.00	14.4	16.9	14.9	17.5	21.3	18.12	2.89	23.08	2.10	10.08	4.65
Starch												
Carbohydrates	55.00	60.7	78.2	64.5	56.79	63.9	3.30	7.91	5.02	7.50	43.68*	49.29*
Free Sugars												
Glucose												
Fructose												
Sucrose												
Lipid	13.00	14.4	4.9	17.5	22	12.4	11.89	2.60	10.50	1.20	21	13.02
Lignin											1.68	4.65
Ash												
Pentosan ve pektins												
Others												
Non-structural Carbohydrates												
Reference	(Iacovidou, Ohandja, & Voulvoulis, 2012)						(T. Kobayashi, Xu, Li, & Inamori, 2012)				(Naroznova, Møller, & Scheutz, 2016)	

3.2 Experimental Setup

3.2.1 Bio-Drying Experiments

Bio-drying experiments were attempted in the laboratory using various equipment, but the expected temperature increase could not be achieved due to insufficient isolation and ventilation. Therefore, bio-drying experiments were carried out using a composting machine (Figure 3.2). Bio-drying experiments were carried out using food preparation waste from the cafeteria. Samples were taken at regular intervals and the experimental process was monitored. The sample obtained as a result of bio-drying (BDW) was used in pyrolysis experiments.

Figure 3.2 Composting machine used for bio-drying

3.2.2 Preliminary Experiments for Pyrolysis

These experiments were done to decide on the conditions to be tested in the actual pyrolysis experiments.

3.2.2.1 System

The experimental setup as can be seen in Figure 3.3 consists of a muffle furnace, a condenser and a cooled circulator. Nitrogen was used as sweeping gas.

Figure 3.3 Preliminary experimental setup

3.2.2.2 Experimental Conditions

About 10 grams of the sample were placed into the pyrolysis chamber at room temperature, and a heating rate of 10°C per minute was applied under anaerobic conditions with a flow of nitrogen (1±0.3 L/min). The study involved investigating three different final pyrolysis temperatures: 350, 500, and 700 °C. Once the final temperature was reached, the pyrolysis system was maintained at that temperature for 30 minutes. The resulting char was collected from the system and utilized for further characterization studies. Biochar samples were named regarding their sample type and pyrolysis temperature such as W1.1-350.

Based on these experiments and biochar analysis together with TGA-DTA graphs, the temperatures to be tested in the actual pyrolysis experiments were decided.

3.2.3 Pyrolysis of Biomass

3.2.3.1 System

The system (Figure 3.4) consisting of a reactor (incineration chamber), a cooled circulator, a condenser, a nitrogen gas tube, a flowmeter and a gas collection bag. The reactor (Figure 3.5) is a cylindrical reactor tightly closed to prevent any leakage. The reactor is controlled with control unit adjusting temperature, time and waiting phases. During the experiments, the gas bag has been changed according to the need. The system drawing can be seen in appendices.

Figure 3.4 Experimental setup of pyrolysis system

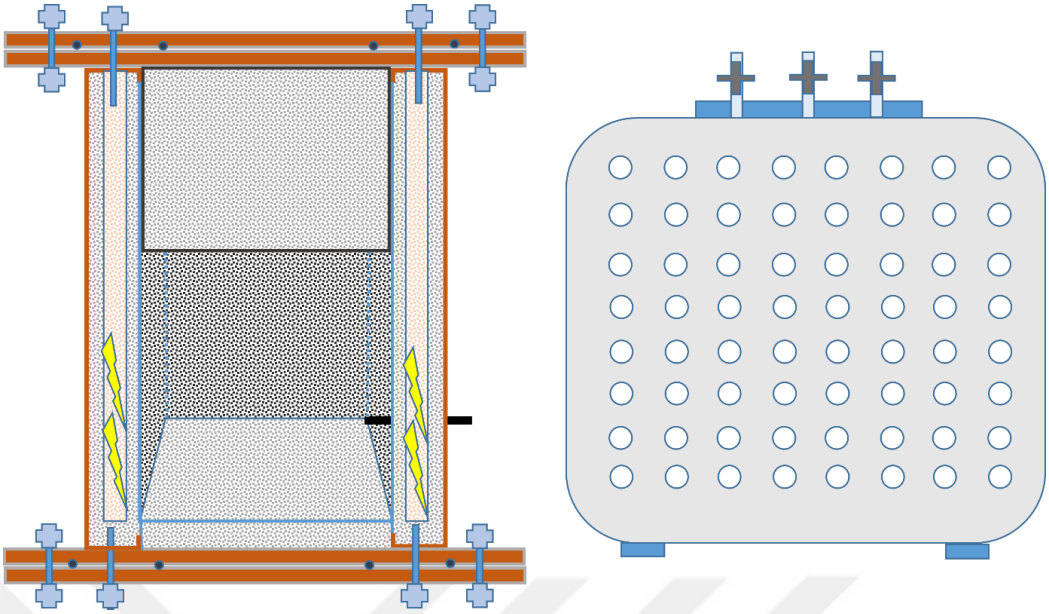

Figure 3.5 The cylindrical reactor cross sectional view and outer view

3.2.3.2 Experimental Conditions

As a result of preliminary experiments, conditions of pyrolysis experiments are given in Table 3.6 & 3.7 were obtained. When determining the conditions in the experiments, the experiments with waste samples carrying different levels of water content have been started. Three different water contents (25, 40 and 55%) were applied in duplicate. 40% water content was decided according to the amount of product obtained. Then the particle size was selected using the determined water content. Three different particle size ranges were tried in duplicate and 10-15 mm particle size range was selected according to the amount of product obtained. The next experiments continued with 40% water content and 10-15 mm particle diameter.

The study involved the testing of various parameters, including two different temperatures (500 & 700°C), two distinct heating rates (5 & 10 °C/min), and two varied residence times (20 & 40 min). Additionally, the experimentation encompassed two-stage heating ramp trials to comprehensively investigate the subject. All experiments were conducted under nitrogen flow (1.2±0.3 L/min). The capacity of the pyrolysis system used, i.e. the reactor, was also a factor in determining these experimental conditions. Since the reactor could not be efficient above 10 C^{o}/min as heating rate, this value could not be exceeded.

The pyrolysis of two distinct types of biodegradable waste was carried out at 500°C to ensure optimum conditions. The optimum conditions were determined as 700°C with a heating rate of 10 °C/min and residence time of 40 minutes. Afterwards, pyrolysis experiments were continued with wet or dry biodegradable waste samples and other biomasses using these conditions. The particle size of the wastes was between 10-15 mm, while the particle size of the other biomass was used as less than 5 mm. In addition, the bio-dried waste (BDW) sample was also used in pyrolysis experiments under optimum conditions. The detailed conditions can be seen in Table 3.8. First, pyrolysis was performed at two different temperatures with samples W1.1 and W8.1. Co-pyrolysis experiments were continued with W1.1 due to the product yield. CM and CS samples were used for co-pyrolysis because of their high carbon (C) content. SS was selected because of its low C content. Moreover, in order to observe the effects of sulphur (S) content, W7.1 was used in co-pyrolysis.

Table 3.6 Conditions of pyrolysis experiments

		# of experiment	Water content of sample, %	Particle size of sample, mm	Final Temperature, ºC	Heating rate, ºC/min	Retention Time	Code of Biochar Sample	Code of Bio-oil Sample
Properties of Samples	**Adjustment of water content**	1	25	-	700	10	20	BC1	BO1
		2	**40**	-	700	10	20	BC2	BO2
		3	55	-	700	10	20	BC3	BO3
	Adjustment of particle size	4	40	5-10	700	10	20	BC4	BO4
		5	40	**10-15**	700	10	20	BC5	BO5
		6	40	15-20	700	10	20	BC6	BO6
Working Conditions	**One Stage Heating**	7	40	10-15	500	5	-	BC7	BO7
		10	40	10-15	700	5	-	BC10	BO10
		8	40	10-15	500	10	-	BC8	BO8
		9	40	10-15	700	10	-	BC9	BO9
	One Stage Heating with retention phase	11	40	10-15	500	5	20	BC11	BO11
		12	40	10-15	500	5	40	BC12	BO12
		13	40	10-15	700	5	20	BC13	BO13
		14	40	10-15	700	5	40	BC14	BO14
		15	40	10-15	500	10	20	BC15	BO15
		16	40	10-15	500	10	40	BC16	BO16
		17	40	10-15	700	10	20	BC17	BO17
		18	40	10-15	700	10	40	BC18	BO18

Table 3.7 Conditions of pyrolysis experiments (continued)

		# of experiment	Water content of sample, %	Particle size of sample, mm	First Stage Final Temperature, ºC	First Stage Heating Rate, ºC/min	Second Stage Final Temperature, ºC	Second Stage Heating Rate, ºC/min	Code of Biochar Sample	Code of Bio-oil Sample
Working Conditions	**Two Stage Heating**	19	40	10-15	500	5	700	10	BC19	BO19
		20	40	10-15	500	10	700	5	BC20	BO20

Table 3.8 Conditions of pyrolysis experiments with biodegradable wastes and other biomasses

Sample	# of experiment	Water content of sample, %	Particle size of biodegradable waste sample, mm	Final Temperature, ºC	Heating rate, ºC/min	Retention Time	Code of Biochar Sample	Code of Bio-oil Sample
W1.1	21	40	10-15	700	10	40	BC21	BO21
W1.1	22	40	10-15	500	10	40	BC22	BO22
W8.1	23	40	10-15	700	10	40	BC23	BO23
W8.1	24	40	10-15	500	10	40	BC24	BO24
W1.1 + CM (50% + 50%)	25	40	10-15	700	10	40	BC25	BO25
W1.1 + SS (50% + 50%)	26	40	10-15	700	10	40	BC26	BO26
W1.1 + CS (50% + 50%)	27	40	10-15	700	10	40	BC27	BO27
W1.1 + W7.1 (50% + 50%)	28	40	10-15	700	10	40	BC28	BO28
CM	29	dry	<5	700	10	40	BC29	BO29
SS	30	dry	<5	700	10	40	BC30	BO30
CS	31	dry	<5	700	10	40	BC31	BO31
W1.1	32	dry	10-15	700	10	40	BC32	BO32
W7.1	33	dry	10-15	700	10	40	BC33	BO33
W1.1+W7.1 (50% + 50%)	34	dry	10-15	700	10	40	BC34	BO34
BDW	35	dry	<5	700	10	40	BC35	BO35

3.3 Analytical Method

Various analyses were applied to the raw materials at the beginning of the experiments and to the products at the end of the experiment. Detailed information showing which analysis was performed on which sample is shown in Table 3.9. Moreover, detailed procedures of the analyses are given in the sub-sections.

Table 3.9 Analyses of raw materials and products

Analysis	**Sample Type**				
	Raw materials		**Products**		
	Solid wastes/Biomasses	Dried dog and cat foods	Biochar/Ash	Bio-oil	Non-condensate gas/Flue gas
Water content	X	X			
Organic Matter Content	X	X			
Calorific Value	X	X			
Volatile matter	X	X			
Ash	X	X			
Fixed Carbon	X	X			
Ultimate analysis	X	X			
Lipid, cellulose, total protein and total sugar analyses		X			
TGA-DTA	X	X			
FT-IR	X	X	X		
BET			X		
SEM-EDS			X		
GC-MS				X	X
In-situ gas analysis					X

3.3.1 Proximate Analysis

3.3.1.1 Water Content Analysis

The water content of the samples was assessed in accordance with the TS EN ISO 11461 standard. The samples were placed in a drying oven with a capsule and kept at 105^{o}C for 24 hours. The water content was determined using the following equation (3.1).

$$\text{Water content} = (A-B)/A*100 \quad (3.1)$$

where:

A: weigh of sample with capsule at the beginning – weigh of capsule

B: weigh of sample with capsule at the end – weigh of capsule

3.3.1.2 Organic Matter Content

The organic matter content of the samples was analyzed in accordance with the ASTM D2974-13/TS 8336 standards. The samples were subjected to a muffle furnace at 550ºC for 1 hour. The following equation was used to calculate the organic matter content (3.2).

$$\text{Organic matter content} = (C- D)/C*100 = OM \quad (3.2)$$

where:

C: weigh of sample with crucible at the beginning- weigh of crucible

D: weigh of sample with crucible at the end- weigh of crucible

3.3.1.3 Calorific Value

The calorific values of the samples were measured using an IKA C 200 bomb calorimeter. The measurements were applied in duplicate and the calorimeter was calibrated before use.

3.3.1.4 Volatile Matter

The analysis was conducted following the ASTM E872-82 Standard Test Method for Volatile Matter in the Analysis of Particulate Wood Fuels (ASTM International, 2019). The sample was placed in a crucible, covered, and directly inserted into the furnace at a temperature of 950°C for a duration of 7 minutes. The calculation was performed based on the difference in weight before and after the heating process, using a gravimetric approach.

3.3.1.5 Ash

The analysis was conducted in accordance with the ASTM E1755-01 Standard Test Method for Ash in Biomass (ASTM International, 2020). The sample was placed into a crucible and placed in a muffle furnace at a temperature of 575°C for a duration of 3 hours. The calculation was performed based on the difference in weight before and after the heating process, using a gravimetric method.

3.3.1.6 Fixed Carbon

Fixed carbon is calculated by taking the difference, as stated in Equation 3.3 (Basu, 2013). Since our samples were already dried, the calculation was performed without considering the moisture content in the dry matter.

$$FC = 100- M - VM – ASH \quad (3.3)$$

where FC is fixed carbon, M is moisture and VM is volatile matter.

3.3.2 Ultimate Analysis

The elemental analysis for all samples, including four specific dried cat/dog foods, was carried out at the Ege University Biomass Energy Systems and Technologies Application and Research Center. The analysis was conducted using the Leco TruSpec CHNS instrument from the United States. Carbon, hydrogen, and nitrogen analysis followed the ASTM D5373 standard (ASTM International, 2021). The analysis for sulfur was performed according to the ASTM D4239 standard (ASTM International, 2018). The oxygen content was determined through the difference calculation.

3.3.3 Lipid, Cellulose, Total Protein and Total Sugar Analyses

The cellulose, total protein and total sugar analyses were applied to four selected dried cat/dog foods by Ege University Biomass Energy Systems and Technologies Application and Research Center. The cellulose, total protein and total sugar were determined according to modified Scharrer method, SM 4500-N_{org} standard and NREL, respectively. The analyses were conducted in triplicate.

Lipid contents of all dried cat/dog foods were analyzed with gravimetric method after ultrasonication-assisted organic solvent extraction in triplicate (Halim, Danquah, & Webley, 2012; Patel et al., 2019).

3.3.4 Thermogravimetric Analysis - Differential Thermal Analysis (TGA-DTA)

Thermogravimetric analysis was conducted by Perkin Elmer STA 6000 in The Center for Fabrication and Application of Electronic Materials. The samples were dried before the analysis. The temperature increased from room temperature to 950°C at a rate of 10 °C/min. The analysis was applied under nitrogen flow.

3.3.5 Fourier Transform Infrared Spectroscopy (FT-IR)

The Fourier transform infrared spectroscopy (FT-IR) analysis was applied by me at the Department of Metallurgical and Materials Science Engineering. The FT-IR analysis was conducted with Spectrum BX Perkin Elmer. The wavelength range was 4000 to 650 cm^{-1}, the resolution was 4 cm^{-1} and number of scans was 25.

3.3.6 Brunauer, Emmett and Teller (BET)

With the Brunauer, Emmett and Teller (BET) method, surface area measurements were made based on the nitrogen (N_2) gas adsorption technique in a liquid nitrogen environment at 77ºK. The degassing procedure took place at 250ºC for 4 h.

3.3.7 Scanning Electron Microscope - Energy-Dispersive X-Ray Spectroscopy (SEM-EDS)

Surface morphology of biochars was analyzed via scanning electron microscope (SEM) (Zeiss-Gemini560). Moreover, Energy-dispersive X-ray spectroscopy (EDS) was applied to raw materials and biochars to determine elemental composition.

3.3.8 In-Situ Gas Analysis

Pyrolysis gas samples were analyzed with MRU-Optima7 after collected in collection bags. CH_4, H_2S, CO_2, O_2, calorific value and N_2 were measured.

3.3.9 Gas Chromatography-Mass Spectrometry (GC-MS)

Gas chromatography-mass spectrometry analyses were applied to liquid and gas products. The liquid samples were centrifuged in a refrigerated centrifuge at 9000 rpm for 40 minutes. The supernatant was used for analysis. Approximately 150 mg of sample was taken and mixed with 3 ml of methanol. The mixture was then diluted to 10 ml with dichloromethane (Thangalazhy-Gopakumar et al., 2010). The mixture was then analyzed by GC-MS (Perkin Elmer Clarus 690 series-Clarus SQ 8T GC-MS) using an Elite-5MS column (30 m length, 0.25 mm inner diameter, 0.25 μm film thickness) and the results were searched in the NIST (National Institute of Standards and Technology) library to identify the bio-oil compounds. The initial temperature of the column, 40^{o}C, was maintained for 5 min, and the temperature was subsequently increased to 260^{o}C at 15^{o}C/min, and the final temperature was held for 20 min. Helium of ultra-high purity (99.99%) was used as a carrier gas and flowed at 1 mL/min. The injector and the GC/MS interface were kept at constant temperature of 250 and 200^{o}C, respectively.

The pyrolysis gases collected in collection bags were analyzed offline with GC-MS. Same column and temperature conditions have been used with analysis of bio-oil. Similarly, pyrolysis gas compounds were identified by using the NIST mass spectral library.

3.4 Statistical Analysis

Correlation analyses using Pearson's correlation coefficients were carried out to identify the interrelations among the analysis results of waste samples, other biomasses and dry cat & dog foods using SPSS version 25.0 for Windows software (IBM Inc., Chicago, Ill., USA). A Principal Component Analysis (PCA) was also applied to identify the possible interactions using SPSS version 25.0 software. Input variables are the results of proximate analysis, calorific value, the results of ultimate analysis and results of TGA-DTA analysis of corresponding samples. PCA was applied to the data set as the extraction method, and the raw calculated factor loading coefficients were rotated by Varimax with a Kaiser Normalization. Kaiser–Meyer–Olkin Measure of Sampling Adequacy and the significance of Bartlett's Test of Sphericity were

calculated as 0.733 and 0.000, respectively; therefore, the sample size was found suitable to be evaluated using PCA. The principal components (PCs) with clusters defined by factor loading coefficients ≥ 0.5 and with Eigenvalues greater than 1.0 were extracted.

Moreover, correlation analyses were conducted to investigate the relationships between various parameters. These parameters encompassed the initial conditions, such as waste amount, initial water amount, particle size, final temperature, heating rate, residence time, and the raw material properties including organic matter content, volatile matter, ash, fixed carbon, calorific value, carbon, hydrogen, nitrogen, sulfur. Additionally, the analysis considered biochar characteristics, comprising biochar amount, BET surface area, pore volume, and pore size, during both preliminary and final experiments. PCA was employed to process the dataset, and the initial factor loading coefficients were subjected to a Varimax rotation with Kaiser Normalization. To ensure the appropriateness of sample size for PCA, the Kaiser–Meyer–Olkin Measure of Sampling Adequacy was determined to be 0.735, and Bartlett's Test of Sphericity was found to be highly significant with a p-value of 0.000. In the PCA, principal components (PCs) were extracted based on specific criteria. These components were defined by factor loading coefficients ≥0.3 and had Eigenvalues exceeding 1.0.

CHAPTER FOUR
RESULTS AND DISCUSSION

4.1 Characteristics of Raw Materials

4.1.1 Proximate Analysis

The proximate analysis results, water contents, organic matter contents and calorific values of samples are given in the Table 4.1. The water content of samples changed from 54.51% to 77.05% except sewage sludge as expected, because it was solar dried. The organic matter content of samples was in the range of 50.22%$_{dw}$ to 88.02%$_{dw}$. Cattle manure had the highest volatility of 83.44%$_{dw}$. On the other hand, sewage sludge and W4.2 were higher in ash content with 39.24%$_{dw}$ and 39.51%$_{dw}$, respectively. Fixed carbon values changed between 1.36%$_{dw}$ and 16.22%$_{dw}$. The lowest calorific value was found in W4.2 as 2182 kcal/kg$_{dw}$ which was consistent with the ash content, while the highest calorific value was found in CM as 5476 kcal/kg$_{dw}$ which was consistent with the volatile matter. The results are consistent with the literature values (Volatile Matter: 39.16-84.42**%$_{dw}$**, Ash: 0.40-59.57**%$_{dw}$**, Fixed Carbon: 1.27-29.88**%$_{dw}$**) (Alves et al., 2022b; Charis et al., 2020; Y. Chen et al., 2021; Fang et al., 2017; J. Li et al., 2022; Y. Li, Zhao, Sui, Wang, & Ji, 2022a; W. Ma et al., 2019; Z. Ma, Chen, Gu, Bao, & Zhang, 2015; Nanda et al., 2013; Sukarni et al., 2018; Zhou, Meng, Long, Li, & Zhang, 2014).

Table 4.1 The proximate analysis results, water contents, organic matter contents and calorific values of samples

Sample #	Location and Size/Type	Water Content, %	Organic Matter Content, %$_{dw}$	Volatile Matter, %$_{dw}$	Ash, %$_{dw}$	Fixed Carbon, %$_{dw}$	Calorific Value, kcal/kg$_{dw}$
W1.1	Çanakkale (>70 mm)	75.81	82.27	78.7	7.17	14.13	4258
W1.2	Çanakkale (<70 mm)	72.85	79.91	78.94	7.95	13.11	4238
W2.1	Akhisar (>70 mm)	68.32	81.25	72.24	26.40	1.36	4179
W2.2	Akhisar (<70 mm)	67.23	71.36	62.64	29.36	8.00	3226

Table 4.1 The proximate analysis results, water contents, organic matter contents and calorific values of samples (continued)

Sample #	Location and Size/Type	Water Content, %	Organic Matter Content, $\%_{dw}$	Volatile Matter, $\%_{dw}$	Ash, $\%_{dw}$	Fixed Carbon, $\%_{dw}$	Calorific Value, $kcal/kg_{dw}$
W3.1	Karşıyaka (>70 mm)	59.01	85.77	74.51	16.89	8.60	3559
W3.2	Karşıyaka (<70 mm)	68.05	62.58	60.84	25.68	13.47	2851
W4.1	Bornova (>70 mm)	54.51	58.59	65.54	35.80	2.20	3291
W4.2	Bornova (<70 mm)	62.89	50.72	58.28	39.51	2.22	2182
W5.1	Konak (>70 mm)	58.94	71.24	75.24	17.88	6.88	2681
W5.2	Konak (<70 mm)	72.62	70.50	70.73	26.38	2.89	3243
W6.1	Buca (>70 mm)	65.42	88.02	76.37	11.63	12.01	4205
W6.2	Buca (<70 mm)	67.51	85.50	72.06	18.97	8.97	4198
W7.1	Gaziemir (>70 mm)	66.39	86.58	73.39	10.38	16.22	3832
W7.2	Gaziemir (<70 mm)	65.42	76.89	68.33	25.28	6.38	3583
W8.1	Aydın (>70 mm)	77.05	78.03	75.23	12.81	11.96	3904
W8.2	Aydın (<70 mm)	72.79	79.11	76.77	8.97	14.26	3935
CM	Cattle Manure	72.02	83.91	83.44	14.16	2.40	5476
PM	Poultry Manure	64.99	66.84	70.92	26.15	2.92	3355
SS	Sewage Sludge	8.63	50.22	58.48	39.24	2.28	3388
CS	Corn Stalk	11.25	96.86	84.08	2.92	13.01	3402
YW	Yarn Waste	55.04	50.52	62.42	33.02	4.55	3449
M18	Adult Dog/Beef	7.62	79.65	78.71	6.60	14.69	4513
M21	Adult Dog/Salmon	7.24	84.17	80.15	5.85	14.00	5025
M27	Adult Dog/Lamb	4.30	78.88	77.61	6.80	15.60	4895
M28	Kitten/Chicken	4.16	80.98	81.23	5.58	13.20	5293

4.1.2 Ultimate Analysis

The results of ultimate analysis are given in the Table 4.2. The least carbon content was found in W4.1 as 25.70%$_{dw}$, while cattle manure had the highest carbon content of 44.85%$_{dw}$ which is compatible with its volatility and calorific value. The hydrogen content of the samples was in the range of 4.61 to 8.40%$_{dw}$. The nitrogen and oxygen content of samples changed from 1.59 to 6.13%$_{dw}$ and 40.12 to 68.08%$_{dw}$, respectively. Compared with the other elemental contents, the sulfur content was found to be less (0- 0.73 %$_{dw}$). The results are in parallel with the values given in the literature (C: 16.46-51,56%$_{dw}$, H: 1.63-7.02%$_{dw}$, N: 0.039-3.48%$_{dw}$, S: 0-1.60%$_{dw}$ and O: 20.22-54.01%$_{dw}$). (Alves et al., 2022b; Anh et al., 2022; Charis et al., 2020; Y. Chen et al., 2021; Fang et al., 2017; J. Li et al., 2022; Y. Li et al., 2022a; W. Ma et al., 2019; Z. Ma et al., 2015; Nanda et al., 2013; Sukarni et al., 2018; Zhou et al., 2014)

Table 4.2 The results of ultimate analysis

Sample Code	C, %$_{dw}$	H, %$_{dw}$	N, %$_{dw}$	S, %$_{dw}$	O, %$_{dw}$
W1.1	39.28	6.86	2.12	0.06	51.67
W1.2	38.40	6.58	2.17	0.15	52.70
W2.1	38.35	6.28	2.17	0.06	53.14
W2.2	29.44	5.09	1.99	0.04	63.44
W3.1	33.11	6.09	2.01	0.08	58.72
W3.2	26.29	4.68	1.74	0.14	67.15
W4.1	25.70	4.61	1.60	0.02	68.08
W4.2	26.60	4.67	2.43	0.01	66.29
W5.1	32.56	5.39	1.59	0.08	60.39
W5.2	32.50	5.82	2.49	0.17	59.02
W6.1	39.83	6.99	2.05	0.00	51.12
W6.2	37.95	6.62	2.23	0.05	53.15
W7.1	37.57	6.16	2.30	0.12	53.84
W7.2	34.17	5.52	1.79	0.02	58.50
W8.1	36.66	6.36	2.82	0.40	53.77
W8.2	36.84	6.64	2.12	0.19	54.20
CM	44.85	8.40	6.13	0.50	40.12
PM	32.11	5.58	5.85	0.17	56.29
SS	28.24	4.85	4.85	0.73	61.33
CS	43.90	7.74	1.32	0.00	47.03
YW	31.34	5.02	1.25	0.00	62.38

Table 4.2 The results of ultimate analysis (continued)

Sample Code	C, $\%_{dw}$	H, $\%_{dw}$	N, $\%_{dw}$	S, $\%_{dw}$	O, $\%_{dw}$
M18	39.98	6.92	3.04	0.12	49.94
M21	43.40	7.62	4.47	0.30	44.21
M27	38.86	6.82	3.33	0.29	50.69
M28	46.18	7.50	6.84	0.46	39.02

4.1.3 Lipid, Cellulose, Total Protein and Total Sugar Analyses

The cellulose, total protein and total sugar analyses were applied to four selected dried cat and dog foods by Ege University Biomass Energy Systems and Technologies Application and Research Center. The results are given in the Table 4.3. The results are similar to given values by the manufacturer.

Table 4.3 The cellulose, total protein and total sugar results of four selected dried cat and dog foods

Sample	Cellulose	Total Protein	Total Sugar
M18	4.81	16.77	n.d
M21	6.15	28.24	n.d
M27	5.00	20.78	n.d
M28	2.34	42.59	n.d

Lipid contents of dried cat and dog foods were analyzed with gravimetric method after ultrasonication-assisted organic solvent extraction. The results are given in the Table 4.4. The results were compared with the lipid values given by producers. Some results are very similar, but some are different.

Table 4.4 The results of lipid analysis

Sample	**M1**	**M2**	**M3**	**M4**	**M6**	**M7**	**M8**	**M9**	**M10**
Lipid, $\%_{dw}$	8.30	9.37	14.12	10.63	9.58	10.56	13.27	20.58	6.55
Sample	**M12**	**M13**	**M14**	**M15**	**M16**	**M17**	**M18**	**M19**	**M20**
Lipid, $\%_{dw}$	7.54	8.78	7.34	9.88	7.99	9.22	4.15	9.79	10.81
Sample	**M21**	**M22**	**M23**	**M24**	**M25**	**M26**	**M27**	**M28**	
Lipid, $\%_{dw}$	13.71	9.80	9.08	10.84	9.28	11.06	6.05	12.67	

These analyses were performed to determine the accuracy of the ingredients used for selecting dry dog/cat food. A representative dry dog/cat food mix was determined based on the ratio of these values in biodegradable municipal waste.

4.1.4 Thermogravimetric Analysis - Differential Thermal Analysis (TGA-DTA)

TGA analysis provides important parameters for determining pyrolysis temperatures. Knowing the temperature range at which the main pyrolysis reaction will take place and the temperatures at which biochar formation will occur helps to determine the pyrolysis conditions. For this reason, TGA analysis was performed on the samples.

The table of TGA and DTA results, including main weight loss temperature interval, exothermic reaction temperature and char formation temperature, can be seen in the Table 4.5. The graphs of TGA-DTA results for waste, other biomass and dry dog/cat food samples are given in the Figures 4.1-4.10. There are three main phases that we would usually expect to observe on TGA graphs: evaporation of water (<130 ^{o}C), main devolatilization (<~500^{o}C) and minor devolatilization (>500^{o}C) (G. Chen & Leung, 2003; R. K. Singh, Patil, Pandey, Tekade, & Sawarkar, 2022; Yang, Heaven, et al., 2018). These phases are formed by the degradation of hemicellulose, cellulose and lignin (Xu & Chen, 2013; Yusuf, Inambao, Hassan, Nura, & Karthickeyan, 2020). In this study, main devolatilization, in other words main weight loss, was generally seen between 200-500^{o}C. Only in samples of W4.1, W4.2 and W5.2, the main weight losses continued up to 750 ^{o}C. This can be because of lignin whose interconnected structure allows for thermal breakdown to take place across a wide temperature range (Luo, Li, Meng, Long, & Zhang, 2018; R. K. Singh et al., 2022). In the second phase, weight loss generally ranging between 20% and 70% was observed. While there was very little weight loss in W3.2, there was a loss of 70% in the experiments with dry cat and dog foods. Samples W1.1, W1.2, and CS experienced a 65% mass loss. Samples W8.1, W8.2, and CM exhibited a 60% mass loss. Samples W7.1, W7.2, and PM had a 50% mass loss. Samples YW and SS showed a 35% mass loss. Probably due to the structure of the CS, a rapid weight loss is observed at a lower temperature. In this phase, at the beginning of the thermal degradation samples, weight loss occurred due to the depolymerization and decomposition of hemicellulose, as well as the less

stable portions of cellulose and lignin, leading to the generation of primary volatiles (Luo et al., 2018; R. K. Singh et al., 2022). In the third phase, as lignin degrades, there is a possibility of simultaneous polycondensation and aggregation reactions leading to the formation of new char at elevated temperatures. This phase exhibited a notably slower rate of thermal degradation and less weight loss compared to the previous phase (R. K. Singh et al., 2022).

The first curves in the DTA graph express that water was released. DTA curves show that there was an exothermic reaction (combustion) at around 280 ^{o}C. In other words, it can be said that the endothermic reaction lasted up to these temperatures (R. K. Singh et al., 2022). In addition, the char formation was observed between 420 and 850 ^{o}C.

Table 4.5 The summarized results of TGA and DTA

Sample	**Main weight loss temperature interval, °C**		**Exothermic reaction temperature, °C**	**Char formation temperature, °C**
Literature	127-600 (Abdullah, Tila, Hakim, Koestoer, & Putra, 2020; Alves et al., 2022b; G. Chen & Leung, 2003; El-Sayed, Khass, & Mostafa, 2023; F. Guo, He, Hassanpour, Gardy, & Zhong, 2020; Jerzak, Bieniek, & Magdziarz, 2021; Junga, Yilmaz, & Bozhenko, 2021; Kanca, 2020; Khan & Zeeshan, 2022; Kong et al., 2022; Y. Li, Zhao, Sui, Wang, & Ji, 2022b; Luo et al., 2018; Mu & Lai, 2017; Niu et al., 2022; Nzioka, Kim, Hwang, & Kim, 2019; Oyedun et al., 2012; R. K. Singh et al., 2022; Tabakaev et al., 2019; Xu & Chen, 2013; Yang, Heaven, et al., 2018; Yusuf et al., 2020)		200-240 (Abdullah et al., 2020; El-Sayed et al., 2023; Tabakaev et al., 2019)	332-650 (Abdullah et al., 2020; El-Sayed et al., 2023; Tabakaev et al., 2019)
W1.1	200	500	280	600
W1.2	200	500	280	600
W2.1	200	500	290	850
W2.2	200	500	290	725
W3.1	200	450	280	420, 560
W3.2	200	450	280	420, 575
W4.1	200	750	330	660
W4.2	200	750	330	660
W5.1	200	500	280	450

Table 4.5 The summarized results of TGA and DTA (continued)

Sample	Main weight loss temperature interval, °C		Exothermic reaction temperature, °C	Char formation temperature, °C
W5.2	200	750	340	490
W6.1	200	500	260	590
W6.2	200	500	260	650
W7.1	200	450	270	630
W7.2	200	450	270	650
W8.1	210	550	370	560
W8.2	210	550	260	420
CM	200	500	280	660, 750
PM	200	500	280	600
SS	200	500	280	450, 600
CS	200	350	280	450, 550
YW	200	500	280	450, 550
M18	210	390	290	400
M21	210	410	290	450
M27	210	390	290	650
M28	210	410	290	400

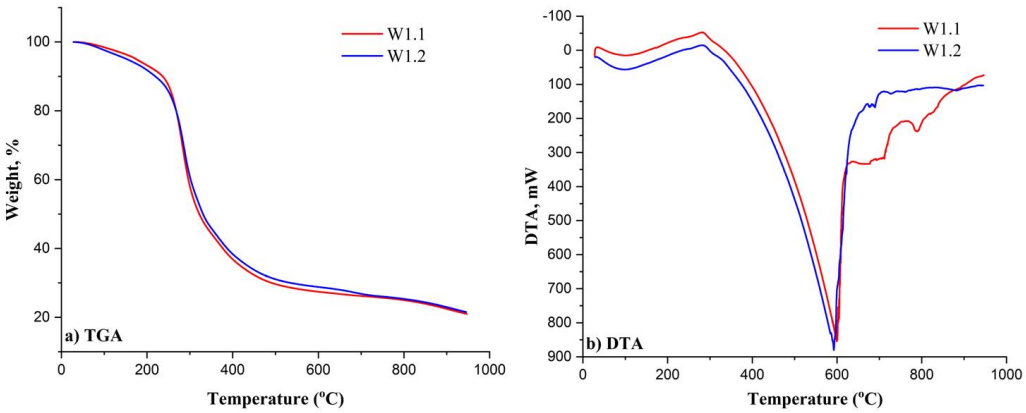

Figure 4.1 TGA-DTA graphs of W1.1-W1.2

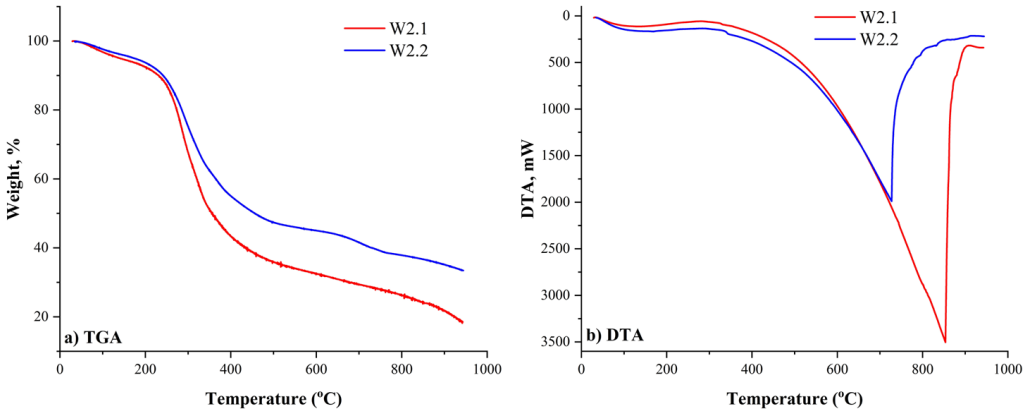

Figure 4.2 TGA-DTA graphs of W2.1-W2.2

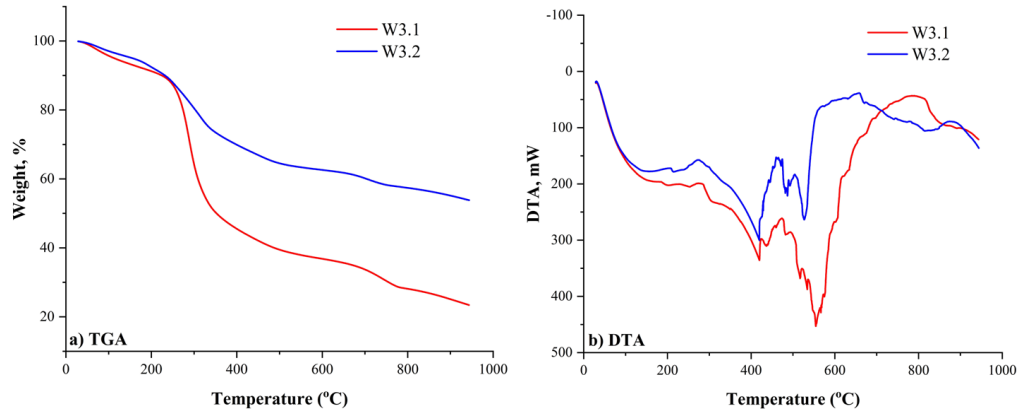

Figure 4.3 TGA-DTA graphs of W3.1-W3.2

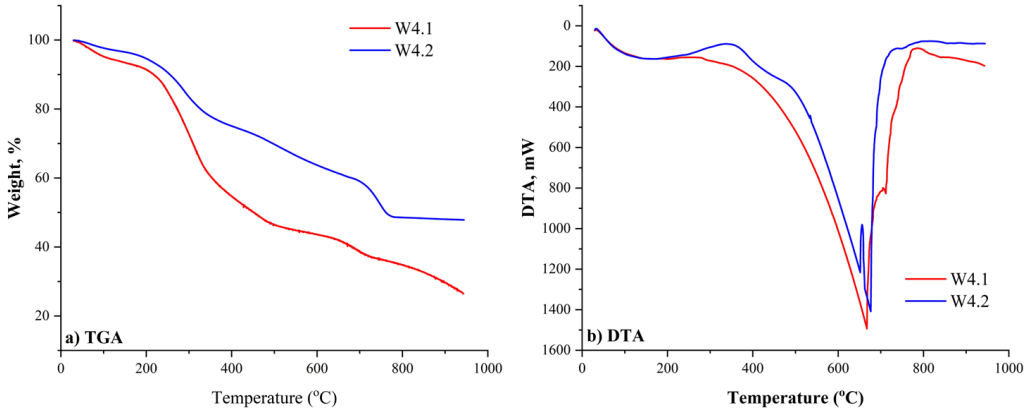

Figure 4.4 TGA-DTA graphs of W4.1-W4.2

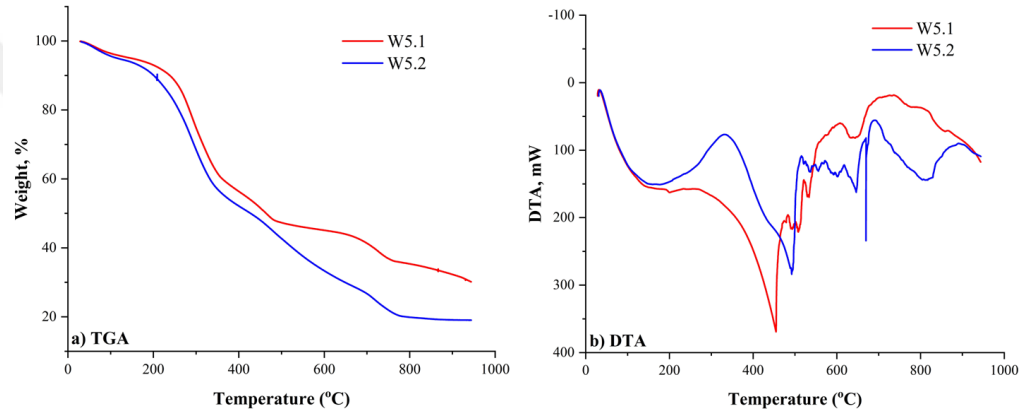

Figure 4.5 TGA-DTA graphs of W5.1-W5.2

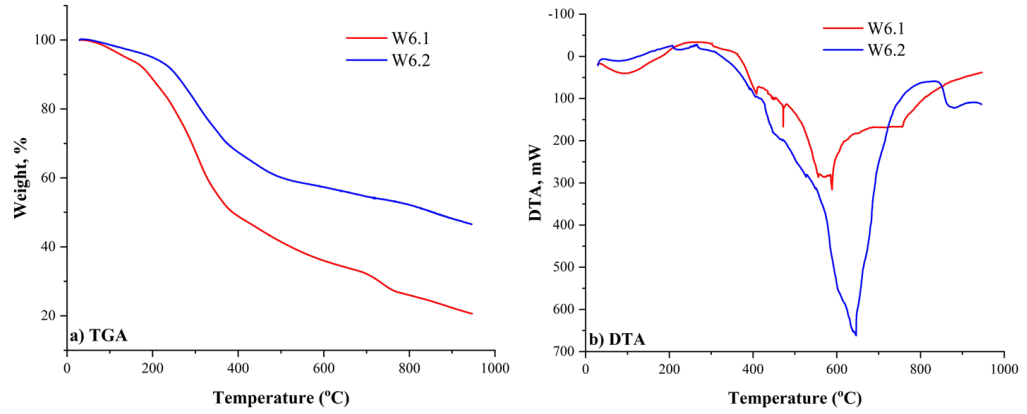

Figure 4.6 TGA-DTA graphs of W6.1-W6.2

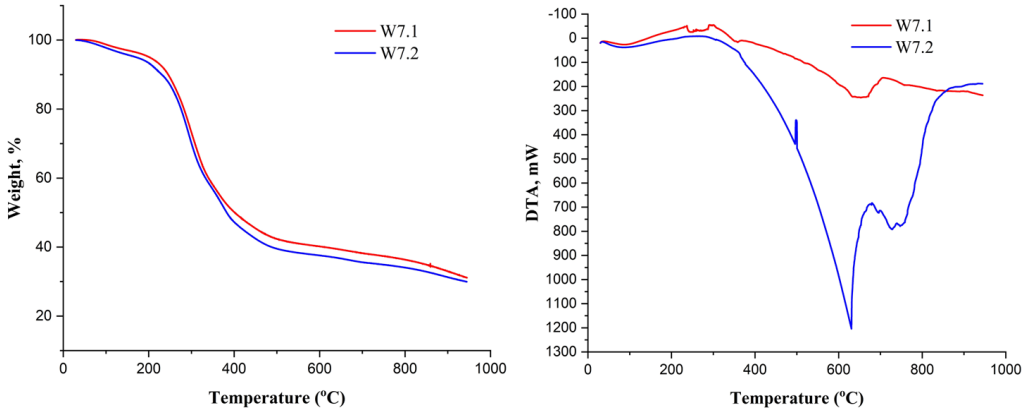

Figure 4.7 TGA-DTA graphs of W7.1-W7.2

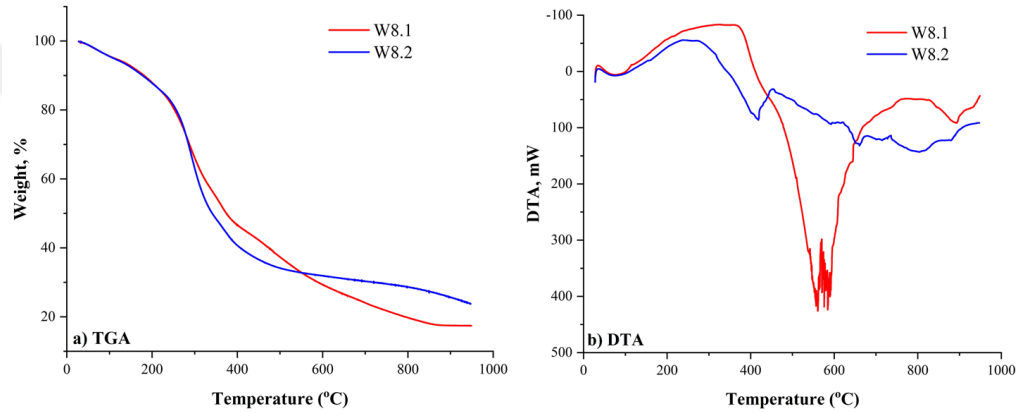

Figure 4.8 TGA-DTA graphs of W8.1-W8.2

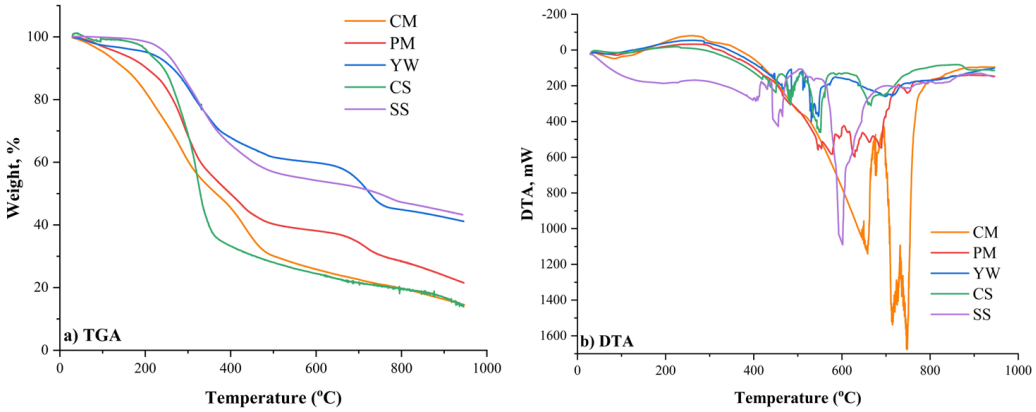

Figure 4.9 TGA-DTA graphs of CM, PM, YW, CS and SS

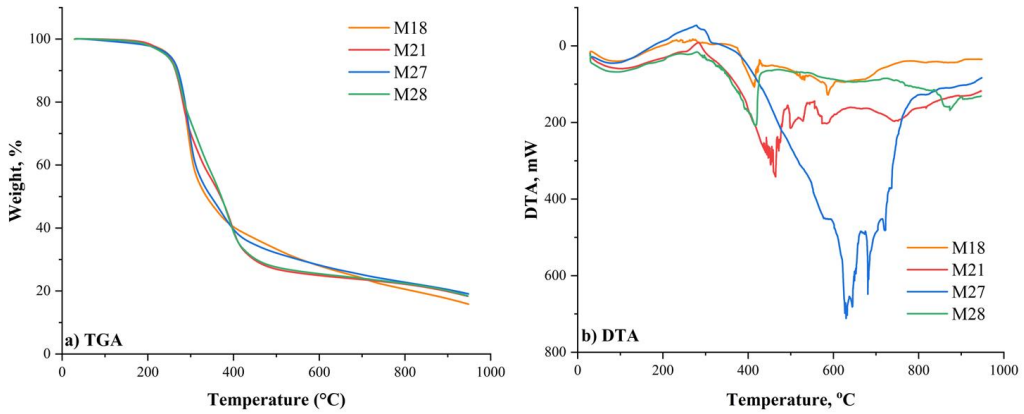

Figure 4.10 TGA-DTA graphs of M18, M21, M27 and M28

4.2 Results of Bio-drying Experiments

Bio-drying experiments were carried out with a composting machine. Samples were taken at the beginning, on the 7th day and on the last day (15th day). The results of these samples are given in Table 4.6.

While the water content decreased by approximately 31% in the first trial, it decreased by approximately 48% in the second trial. Besides the decrease in water content, there was no significant change in calorific value. This shows that the bio-drying experiment was successful. The final sample was then used in pyrolysis experiments (BDW).

Table 4.6 The results of bio-drying experiment

		Temperature °C	Water content %	Organic matter content $\%_{dw}$	Volatile Matter $\%_{dw}$	Ash, $\%_{dw}$	Fixed Carbon $\%_{dw}$	Calorific value $kcal/kg_{dw}$
1st trial	**Start-up**	42	91.06	89.13	76.00	10.62	13.38	4446.86
	7th day	32.4	75.25	85.00	73.80	15.07	11.13	4168.72
	15th day	31.7	59.85	80.35	70.06	15.26	14.68	4288.05
2nd trial	**Start-up**	38	84.53	82.04	73.78	16.30	9.92	4070.47
	7th day	32.1	59.85	82.94	71.20	17.22	11.59	4089.74
	15th day	31.5	36.77	79.46	67.43	18.23	14.34	4143.97

4.3 Results of Preliminary Experiments of Pyrolysis

4.3.1 Yields of Biochars

The yields of biochars produced from wastes and other biomasses are given in Table 4.7. As seen in the table, the amount of biochar decreases as the temperature increases.

Table 4.7 Yields of biochars

Code of samples	Biochar yield at 350°C	Biochar yield at 500 °C	Biochar yield at 700 °C
W1.1	36.68	26.54	25.74
W1.2	37.10	27.32	26.06
W2.1	52.88	46.55	32.05
W2.2	55.41	46.22	43.62
W3.1	49.49	41.51	27.24
W3.2	54.36	50.47	32.46
W4.1	63.56	61.27	33.08
W4.2	68.78	58.00	56.44
W5.1	61.6	47.31	41.33
W5.2	57.04	42.7	26.68
W6.1	43.83	30.71	20.85
W6.2	49.01	33.20	25.64
W7.1	43.03	30.58	24.77
W7.2	51.12	40.05	35.50
W8.1	38.89	28.86	27.09
W8.2	36.88	27.69	25.64
CM	52.07	30.09	22.56
PM	52.49	39.33	35.48
SS	63.64	52.74	37.79
CS	33.11	23.89	16.60
YW	57.56	46.28	44.38
M18	36.91	26.08	24.01
M21	37.86	26.26	23.33
M27	40.97	29.39	26.52
M28	40.90	26.62	23.41

4.3.2 FT-IR Results of Biochars

FT-IR spectroscopy was used to identify chemical compounds and functional groups in a sample observe the performance of pyrolysis experiments. FT-IR graphs of biochars produced from W1.1, W7.1, W8.1, CM, SS and CS samples are given in Figures 4.11-4.16. FT-IR graphs of other biochars including biochars of dried cat and dog foods can be seen in Appendices.

The spectra displayed several peaks specifying the complex nature of biomass and biochar samples. The major peaks are given in Table 4.8 showing different compounds and the type of bonds available in these fractions. We were expecting that O-H, CH and CH_2 bonds would remove, and C-O bonds would stay and form.

According to the results, there were water loss at 350 ^oC in all samples except CM and PM, because the O-H band, which can be seen at the wavelength of 3351-3280 cm^{-1}, disappears at this temperature (Elnour et al., 2019; Jouiad, Al-Nofeli, Khalifa, Benyettou, & Yousef, 2015; G. Li, Zhu, Zhu, & Chai, 2016; Nanda et al., 2013; Wu et al., 2012). The bands in the range of wavenumbers from 2924 to 2850 indicated that the presence of cellulose, hemi-cellulose and lignin. Moreover, C-H and C-H_2 bands (at 2924-2850 cm^{-1}) mostly disappeared at 350 ^oC. C-H band weakened at 350 ^oC for W2.1, W6.1, W6.2, W7.1, W8.1 and CM and disappeared at 500^oC (Elnour et al., 2019; Nanda et al., 2013; Reza et al., 2020; Wu et al., 2012). The loss of O-H stretching and C-H stretching shows that the samples were subjected to dehydration and depolymerization (Wu et al., 2012). Moreover, the disappear of these bands indicates the successful pyrolysis of the samples as we expected (Elnour et al., 2019; Jouiad et al., 2015; G. Li et al., 2016; Nanda et al., 2013; Reza et al., 2020; Wu et al., 2012).

The transmittance spectrum of the samples (W1.1, W1.2, W2.1, W2.2, W6.1, W6.2, W7.1, W7.2, W8.1, W8.2, CS and YW) presented distinct C=O band from carbonyl species (esters, carboxylic acid etc.) at about 1740 cm^{-1} which disappeared at 350 ^oC (Nanda et al., 2013; Siengchum, Isenberg, & Chuang, 2013; Wu et al., 2012)

The 1649-1517 cm^{-1} stretch in the spectra was caused by C=C stretching of aromatic components (Jouiad et al., 2015; Reza et al., 2020; Wu et al., 2012). C=C band was

mostly disappeared at 500 ^{o}C, while it was disappeared at 350 ^{o}C in W2.2, W4.1, W4.2, W5.2 and SS and it can be observed even at biochar produced from CS at 500 ^{o}C .

The transmittance spectrum of the samples and biochars except biochars of CM at 500 and 700 ^{o}C and biochars of CS produced at 350, 500 and 700 ^{o}C presented distinct C-H band from deformation in cellulose and hemicellulose between 1466-1313 cm^{-1} (G. Li et al., 2016; Reza et al., 2020; Wu et al., 2012).

C-O band caused by stretching vibration in cellulose and hemicelluloses can be seen at the wavelength of 1274-981 cm^{-1} (G. Li et al., 2016; Nanda et al., 2013; Reza et al., 2020; Wu et al., 2012). The peaks in this interval were mostly decreased with increasing temperature. In another words, as the temperature increased, the structure of the biochars became more regular in this wavelength range (Nanda et al., 2013). However, the effect of heterogeneity can be observed in some samples results.

Aromatic rings can be observed at the wavelength of 877-666 cm^{-1} (Nanda et al., 2013; Reza et al., 2020; Wu et al., 2012). The predominance of the transmittance spectrum at the wavelength between 1480-700 cm^{-1} for the samples and biochars indicates that the samples consist of lignin. Moreover, the existence of intense transmittance band between 1242-1030 cm^{-1} for C-O stretching suggests that the samples also comprise cellulose (Siengchum et al., 2013).

Furthermore, the board transmittance bands between 1745-1375 cm^{-1} for the samples and biochars indicates that they mainly comprise lignin and cellulose (Siengchum et al., 2013).

The FT-IR results show that the removal of O- and H- comprising functionalities in biochars regarding the contents of the samples due to pyrolysis at higher temperature. The absence of these bands in biochars indicates the formation of CO_2, CH_4 and H_2, due to the pyrolysis of cellulose, hemicelluloses and lignin (Nanda et al., 2013). Moreover, the FT-IR results point out that the soft-carbon components disappeared and hard-carbon components were preserved which are significant to produce the adsorbents for wastewater treatment (Reza et al., 2020). Intensity of bands mostly decreased as the process temperature increased. On the other hand, even at temperature

of 700 ^{o}C, C-H, C-O bands and aromatic rings were preserved. This can be defined by the presence of pyranose rings and guaiacyl monomers of cellulose and hemicellulose (Wu et al., 2012).

Table 4.8 The FT-IR results

		Functional Group						
		Wavelength, cm^{-1}						
Sample	**Temperature °C**	**O-H stretching of hydroxyl groups**	**C-H stretching of aliphatic CH_x**	**C=O stretching of carboxyl and ketones**	**C=C stretching of aromatic components**	**C-H deformation in cellulose and hemicellulose**	**C–O stretching vibration in cellulose and hemicelluloses**	**Aromatic rings**
Literature		3600-3200 (Elnour et al., 2019; Jouiad et al., 2015; G. Li et al., 2016; Nanda et al., 2013; Wu et al., 2012)	2960-2850 (Elnour et al., 2019; Nanda et al., 2013; Reza et al., 2020; Wu et al., 2012)	1745-1700 (Elnour et al., 2019; Nanda et al., 2013; Siengchum et al., 2013; Wu et al., 2012)	1630-1510 (Elnour et al., 2019; Jouiad et al., 2015; Reza et al., 2020; Wu et al., 2012)	1480-1375 (G. Li et al., 2016; Reza et al., 2020; Wu et al., 2012)	1242-1030 (G. Li et al., 2016; Nanda et al., 2013; Reza et al., 2020; Wu et al., 2012)	900–700 (Nanda et al., 2013; Reza et al., 2020; Wu et al., 2012)
W1.1	**Raw material**	3287	2921, 2852	1743	1646, 1540	1456	1240, 1151, 1077,1018	852, 761,706
	350				1578	1432	1116	877
	500					1428	1047	875
	700					1433	1030	874
W1.2	**Raw material**	3299	2923, 2853	1744	1636	1457	1240,1149, 1020	868, 815, 768, 719
	350				1575	1434	1102	875, 748
	500					1417	1049	875, 752
	700					1417	1036	875
W2.1	**Raw material**	3304	2923, 2854	1743	1626	1416	1240,1150, 1020	873, 779, 714
	350		2923, 2854		1558	1410	1034	873, 779
	500					1422	1033	875
	700					1417	1031	874

Table 4.8 The FT-IR results (continued)

		Functional Group						
		Wavelength, cm^{-1}						
Sample	**Temperature °C**	**O-H stretching of hydroxyl groups**	**C-H stretching of aliphatic CH_x**	**C=O stretching of carboxyl and ketones**	**C=C stretching of aromatic components**	**C-H deformation in cellulose and hemicellulose**	**C–O stretching vibration in cellulose and hemicelluloses**	**Aromatic rings**
W2.2	**Raw material**	3294	2924, 2854	1742	1616	1418	1239, 1026	873, 777, 712
	350					1416	1016	874, 779, 712
	500					1416	1030	873, 796, 712
	700					1438	1060	779, 694
W3.1	**Raw material**	3286	2919, 2852		1634	1418	1244, 1023	875, 765, 712
	350				1574	1418	1112	875, 770
	500					1417	1031	875, 712
	700					1416	1030	875, 712
W3.2	**Raw material**	3300	2921, 2852		1616	1415	1029	872, 779, 712
	350				1594	1435	1057	796, 778, 695
	500					1417	1044	874, 795, 712
	700					1415	1031	874, 712
W4.1	**Raw material**	3288	2918, 2852		1622	1409	1032	872, 712
	350					1410	1033	873, 712
	500					1416	1098, 1033	872, 712, 672
	700					1404	1037	872, 712

Table 4.8 The FT-IR results (continued)

		Functional Group						
		Wavelength, cm^{-1}						
Sample	**Temperature °C**	**O-H stretching of hydroxyl groups**	**C-H stretching of aliphatic CH_x**	**C=O stretching of carboxyl and ketones**	**C=C stretching of aromatic components**	**C-H deformation in cellulose and hemicellulose**	**C–O stretching vibration in cellulose and hemicelluloses**	**Aromatic rings**
W4.2	**Raw material**	3282	2922, 2853		1576, 1540	1417	1025	873, 712
	350					1394	1028	873, 712
	500					1417	1022	873, 712
	700					1410	1026	873, 712
W5.1	**Raw material**	3282	2919, 2851		1621	1418	1263, 1028	872, 780, 713
	350				1568	1400	1092, 1034	872, 780, 712
	500					1416	1107, 1034	873,712
	700					1414	1031	874, 712
W5.2	**Raw material**	3282	2919, 2851		1634, 1540	1418, 1318	1245, 1031	873, 720
	350					1420	1110, 1025	876, 712
	500					1420	1026	877, 712
	700					1417	1033	873, 712
W6.1	**Raw material**	3314	2923, 2854	1741	1607	1417	1242, 1029	816, 777, 722
	350		2923, 2854		1568	1417	1114, 1033	874
	500					1417	1027	874
	700					1435	1023	872

Table 4.8 The FT-IR results (continued)

		Functional Group						
		Wavelength, cm^{-1}						
Sample	**Temperature °C**	**O-H stretching of hydroxyl groups**	**C-H stretching of aliphatic CH_x**	**C=O stretching of carboxyl and ketones**	**C=C stretching of aromatic components**	**C-H deformation in cellulose and hemicellulose**	**C–O stretching vibration in cellulose and hemicelluloses**	**Aromatic rings**
W6.2	**Raw material**	3291	2923, 2853	1741	1616	1418	1150, 1017	764
	350		2923, 2853		1547	1418	1034	874, 780
	500					1418	1032	874, 750
	700					1418	1047	778, 695
W7.1	**Raw material**	3294	2922, 2853	1742	1616	1418, 1317	1239, 1151, 1023	877, 770, 711
	350		2922, 2853		1574	1416, 1313	1115, 1033	877, 756
	500					1416	1025	874, 692
	700					1413	1029	873, 700
W7.2	**Raw material**	3314	2922, 2853	1742	1636	1418	1154, 1024	874, 777, 712
	350				1558	1416	1028	874, 780
	500					1417	1018	872, 712
	700					1424	1027	874
W8.1	**Raw material**	3300	2922, 2852	1740	1615	1403, 1318	1241, 1025	830, 779, 720
	350		2922, 2852		1558	1418	1035	872, 782
	500					1415	1038	874, 692
	700					1416	1029	873

Table 4.8 The FT-IR results (continued)

		Functional Group						
		Wavelength, cm^{-1}						
Sample	**Temperature °C**	**O-H stretching of hydroxyl groups**	**C-H stretching of aliphatic CH_x**	**C=O stretching of carboxyl and ketones**	**C=C stretching of aromatic components**	**C-H deformation in cellulose and hemicellulose**	**C–O stretching vibration in cellulose and hemicelluloses**	**Aromatic rings**
W8.2	**Raw material**	3280	2922, 2853	1743	1622	1456	1238, 1152, 1024	874, 776, 720
	350				1574	1435	1072	874, 800
	500					1418	1032	874
	700					1417	1014	874
CM	**Raw material**		2918, 2850		1575, 1540	1466, 1412	1030	847, 772, 721, 666
	350		2918, 2850		1575	1455	1030	752
	500						1032	733
	700						1030	729
PM	**Raw material**		2920, 2852		1634, 1592	1408, 1344	1274, 1006	874, 794, 768, 723
	350				1652	1392	1034	873, 795, 770, 712
	500					1404	1032	872, 712
	700					1404	1030	872, 712
SS	**Raw material**	3299	2922, 2851		1649, 1517	1424	1234, 1029	875
	350					1428	1028	874
	500					1427	1029	874
	700					1418	1028	875

Table 4.8 The FT-IR results (continued)

		Functional Group						
		Wavelength, cm^{-1}						
Sample	**Temperature ºC**	**O-H stretching of hydroxyl groups**	**C-H stretching of aliphatic CH_x**	**C=O stretching of carboxyl and ketones**	**C=C stretching of aromatic components**	**C-H deformation in cellulose and hemicellulose**	**C–O stretching vibration in cellulose and hemicelluloses**	**Aromatic rings**
CS	**Raw material**	3330	2920, 2851	1732	1634	1374	1035	897,795
	350				1594		1110	750
	500				1583		1084	880, 802
	700						1032	
YW	**Raw material**	3351	2920, 2851	1732	1616	1418	1029	873, 779
	350					1404	1030	873
	500					1412	1025	874
	700					1410	981	873

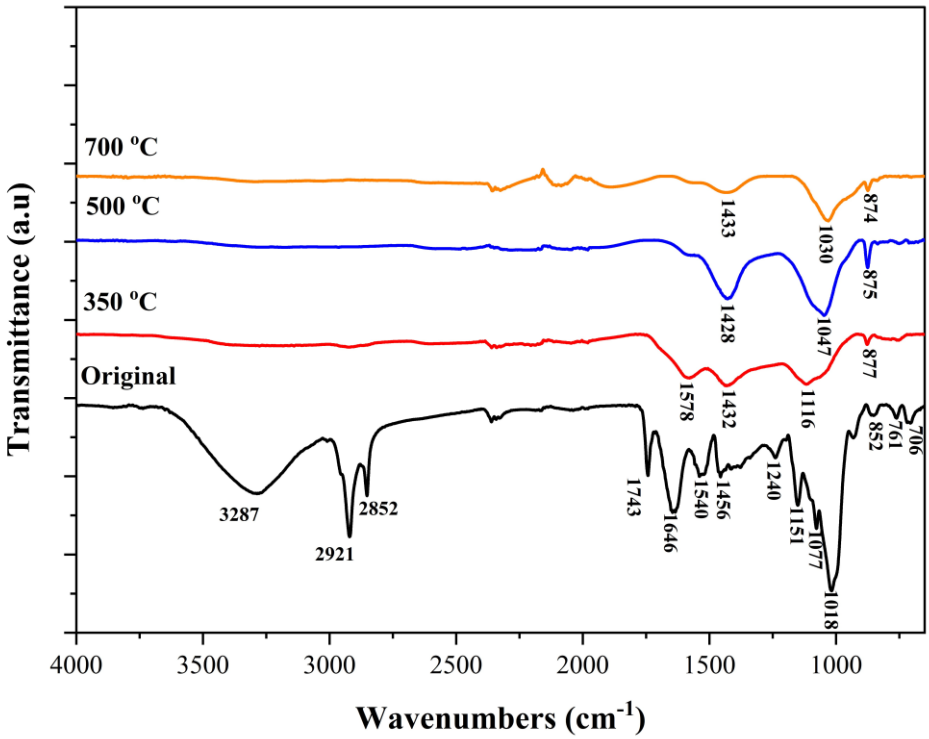

Figure 4.11 FT-IR graph of W1.1

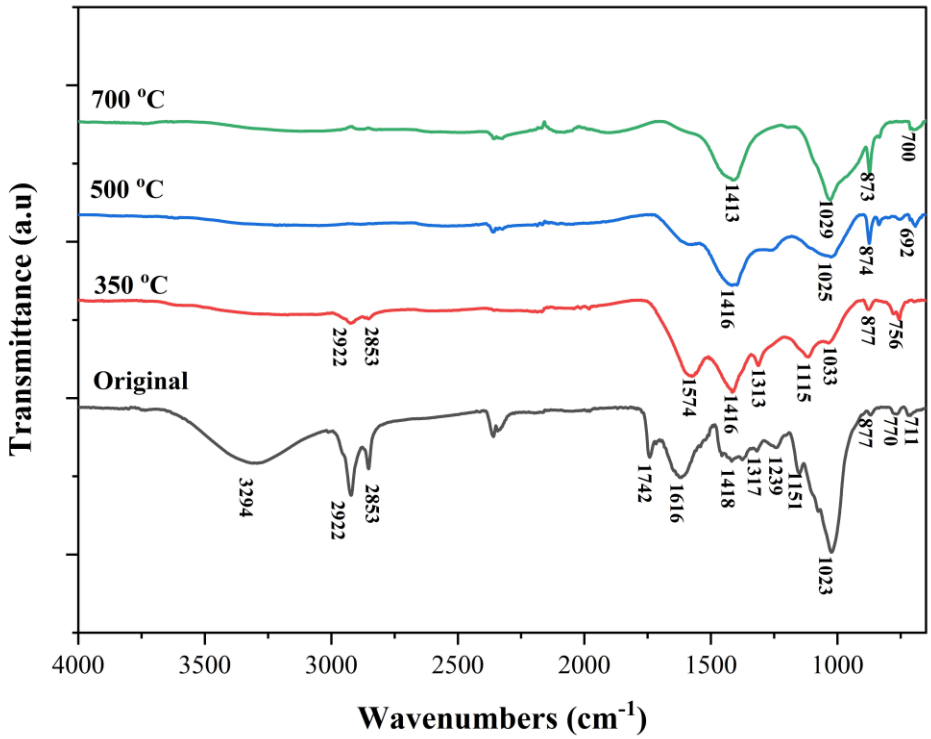

Figure 4.12 FT-IR graph of W7.1

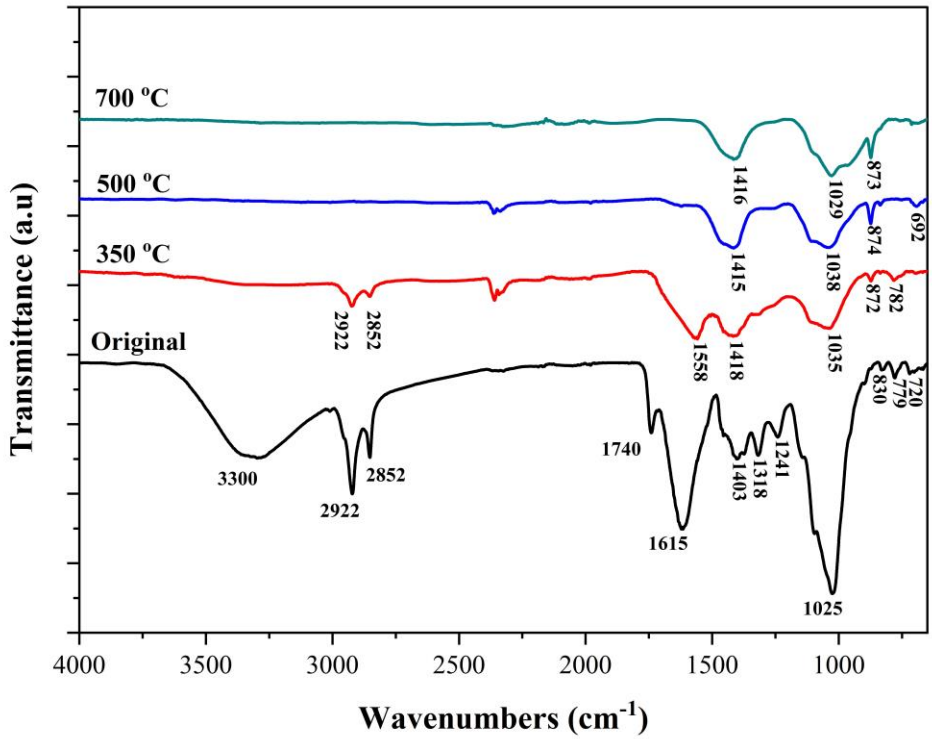

Figure 4.13 FT-IR graph of W8.1

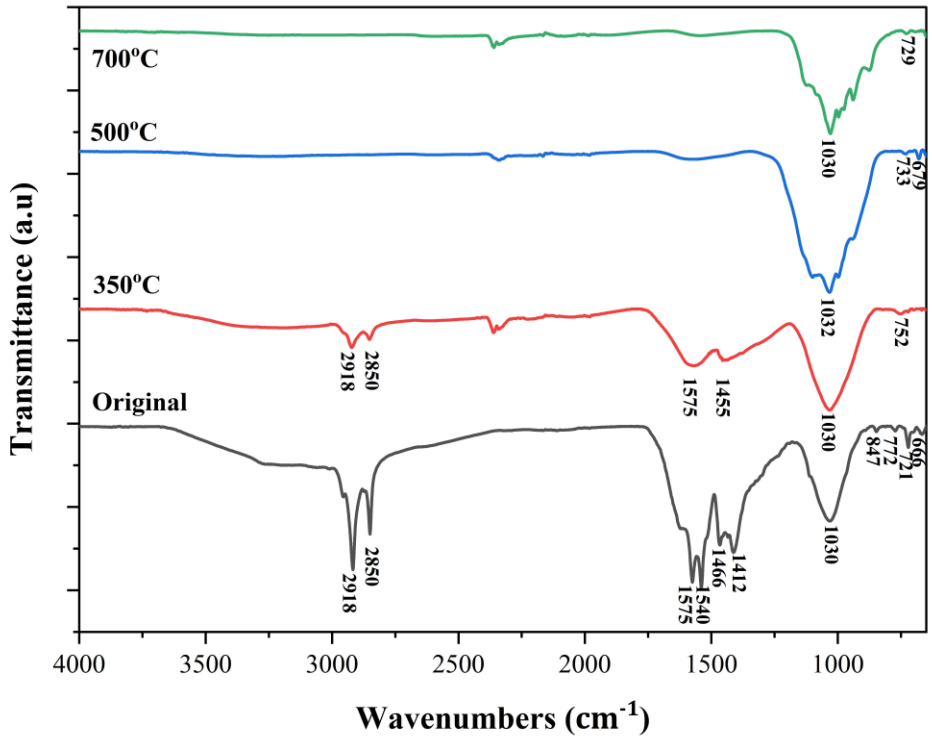

Figure 4.14 FT-IR graph of CM

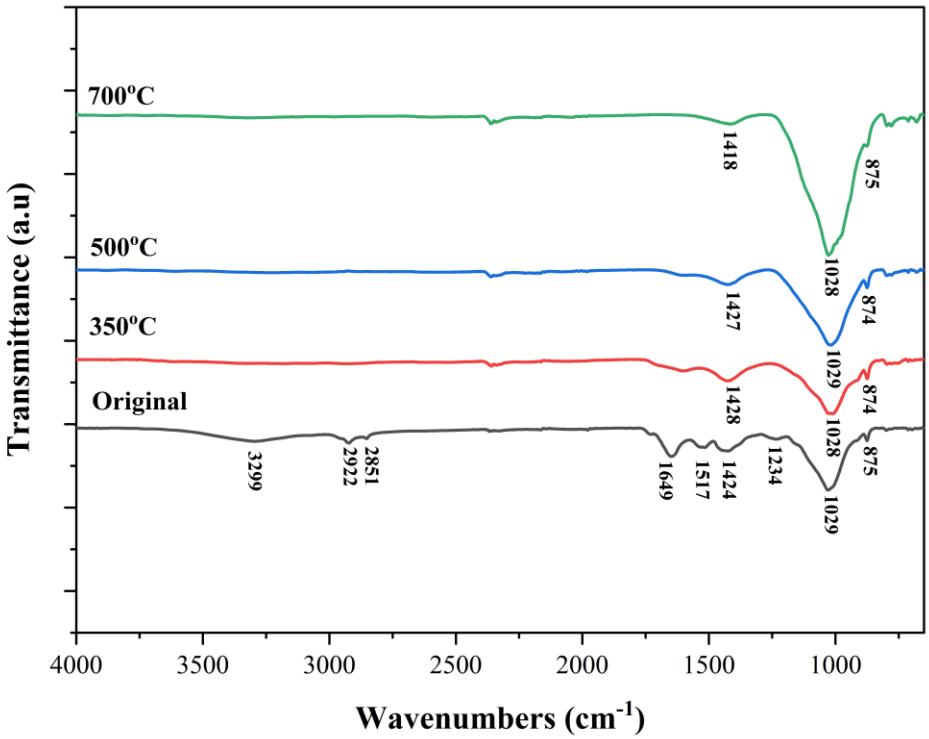

Figure 4.15 FT-IR graph of SS

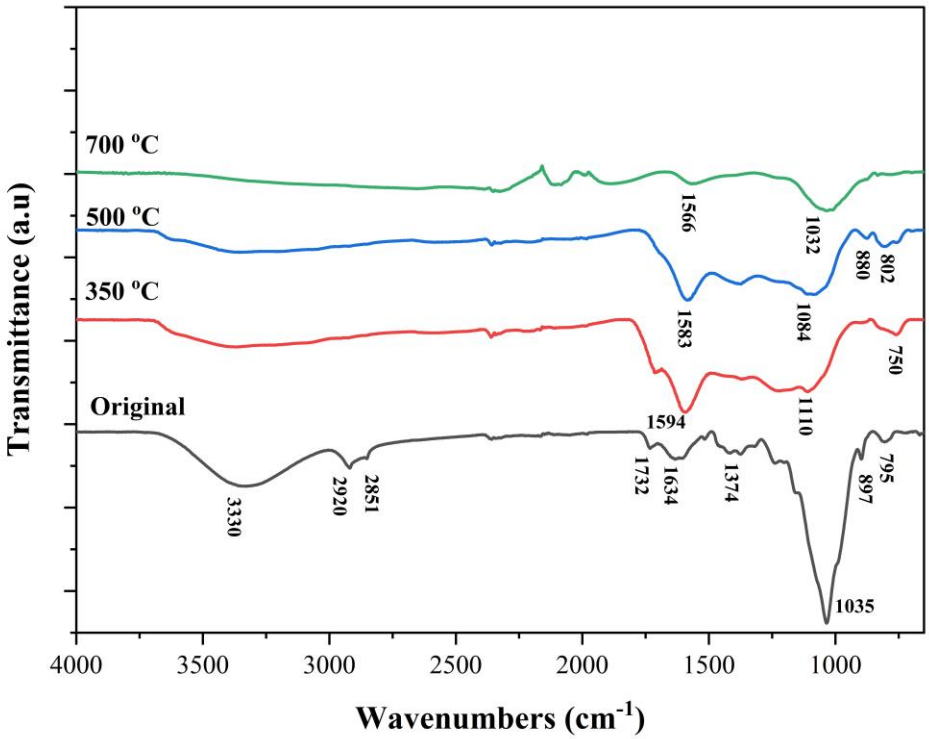

Figure 4.16 FT-IR graph of CS

4.3.3 BET Results of Biochars

BET analysis was used for biochars to assess their specific surface area and porosity. This analysis helps determine the biochar's capacity for adsorption, which is crucial for various applications, including environmental remediation, water purification, and soil improvement. Biochars produced from municipal solid waste samples, yard waste, corn stalk, cattle and poultry manure and sewage sludge were sent for BET analysis after the necessary pre-treatments. Table 4.9 presents the BET surface area and pore volume measurements for the biochar samples produced from sewage sludge (SS), cattle manure (CM), poultry manure (PM), corn stalk (CS), yard waste (YW), biodegradable municipal solid wastes and dried dog and cat foods at 350, 500 and 700 °C.

The results indicate a significant increase in both the BET surface areas and pore volumes of the biochars as the temperature rises, except for SS, W4.2 and W8.1, which exhibited a decrease in BET surface area at 700°C. This increase in surface area can be attributed to the release of volatile matter from the biomass during the pyrolysis process, leading to the formation of pores within the biochar (Elnour et al., 2019). Among the samples, CS biochar produced at 700°C exhibited the highest BET surface area (213.11 m^2/g), aligning well with the proximate and ultimate analysis data. CS is followed by W1.1 with a BET surface area of 152.07 m^2/g, which was selected for pyrolysis experiments. Although the reported BET values in the literature may vary, our findings are consistent with previous studies demonstrating the influence of temperature on the increase in BET surface area and pore volume of biochar. For instance, Singh et al. reported BET values ranging from 24.3-260 m^2/g for biochar derived from SS, with higher temperatures resulting in higher BET surface areas and pore volumes (S. Singh et al., 2020). In another study by Stylianou et al., biochar obtained from SS and CM at 550°C exhibited BET surface areas of 14.033 m^2/g and 3.98 m^2/g, respectively, which were considerably lower than the values obtained in our study (Stylianou et al., 2020).

While the highest BET surface area values observed in our study for biodegradable wastes and other biomasses are lower than those reported for illite in the literature,

they surpass the BET values of bentonite and kaolinite, which are recognized as effective absorbents (Murray & Quirk, 1990).

Table 4.9 BET results of biochars produced at 350, 500 and 700 °C

Sample Code	BET Surface Area, m^2/g	Pore Volume, cm^3/g	Pore Size, Å
W1.1-350	1.39	0.004	124.01
W1.1-500	1.37	0.006	175.23
W1.1-700	152.07	-	-
W1.2-350	1.29	0.005	168.20
W1.2-500	1.73	0.008	177.37
W1.2-700	58.67	-	-
W2.1-350	1.35	0.002	61.92
W2.1-500	9.04	0.017	77.26
W2.1-700	38.458	0.022547	23.4506
W2.2-350	1.55	0.003	86.00
W2.2-500	4.08	0.009	84.21
W2.2-700	49.1563	0.03161	25.7219
W3.1-350	13.66	0.046	135.98
W3.1-500	8.91	0.027	121.22
W3.1-700	14.9024	0.010963	29.4269
W3.2-350	17.71	0.046	103.23
W3.2-500	10.91	0.034	123.24
W3.2-700	56.2737	0.060022	42.6646
W4.1-350	1.76	0.003	75.91
W4.1-500	2.84	0.007	103.56
W4.1-700	26.0853	0.014533	22.2847
W4.2-350	1.58	0.002	60.79
W4.2-500	36.84	0.076	82.52
W4.2-700	6.3411	0.007431	46.8754
W5.1-350	2.13	0.005	91.16
W5.1-500	7.02	0.020	113.49
W5.1-700	8.4356	0.008003	37.9476
W5.2-350	7.82	0.021	105.17
W5.2-500	6.52	0.019	116.58
W5.2-700	25.917	0.023558	36.3586
W6.1-350	-	0.006	-
W6.1-500	1.88	0.004	84.61
W6.1-700	47.47	0.029	24.26
W6.2-350	2.36	0.014	233.13
W6.2-500	4.58	0.013	109.41
W6.2-700	48.09	0.020	-

Table 4.9 BET results of biochars produced at 350, 500 and 700 °C (continued)

Sample Code	BET Surface Area, m^2/g	Pore Volume, cm^3/g	Pore Size, Å
W7.1-350	4.02	1.417	14115.21
W7.1-500	1.92	0.004	89.75
W7.1-700	16.84	0.012	29.20
W7.2-350	1.14	1.343	47029.21
W7.2-500	2.26	0.005	81.82
W7.2-700	44.72	0.028	24.91
W8.1-350	2.24	0.768	13702.46
W8.1-500	3.48	1.847	21248.92
W8.1-700	2.99	1.812	24215.78
W8.2-350	1.24	0.766	24683.81
W8.2-500	1.25	1.573	50458.55
W8.2-700	6.48	0.029	175.88
CM-350	1.63	0.008	201.09
CM-500	22.95	0.138	240.73
CM-700	47.59	0.357	299.79
PM-350	7.84	0.055	279.93
PM-500	9.74	0.061	248.50
PM-700	11.31	0.606	2142.76
SS-350	1.92	0.287	5976.57
SS-500	41.76	0.024	22.68
SS-700	21.20	1.002	1390.72
CS-350	2.44	0.012	199.47
CS-500	26.41	0.014	20.88
CS-700	213.11	0.091	-
YW-350	1.89	0.026	556.85
YW-500	10.33	0.016	62.14
YW-700	95.18	0.066	27.72
M18-350	3.2828	0.006672	81.2914
M18-500	5.6415	0.011937	84.6404
M18-700	28.515	0.030361	42.5899
M21-350	2.1855	0.005017	91.8153
M21-500	4.4211	0.00991	89.7012
M21-700	8.2095	0.014876	72.4842
M27-350	2.4233	0.005173	85.3949
M27-500	16.1043	0.030583	75.9627
M27-700	3.9448	0.00554	56.2484
M28-350	1.2795	0.002992	93.525
M28-500	5.6906	0.011179	78.5784
M28-700	9.8643	0.01928	78.1949

While the BET values obtained in this study are generally satisfactory, there is room for improvement. Chemical activators and acid washing can be employed to enhance the BET value. Pehlivan (2017) suggested that the BET value can be increased through these methods (Pehlivan, 2017). For instance, Zaker et al. (2021) successfully increased the BET value of biochar produced from SS from 69.63 m^2/g to 899.33 m^2/g by subjecting it to chemical treatment using NaOH and HCl (Zaker et al., 2021).

In another study focusing on biochar derived from PM, the BET surface area increased from 2.68 m^2/g to 5.79 m^2/g as the pyrolysis temperature was raised from 300°C to 600°C. Although these values are comparable to the findings in this study, they do not exhibit the same characteristics as commercially available activated carbons, which typically have BET surface areas ranging from 500 m^2/g to 1000 m^2/g. Therefore, additional chemical activation is necessary to achieve similar properties (W. Song & Guo, 2012).

Furthermore, a study involving CM subjected to pyrolysis at higher temperatures resulted in a BET surface area of 170 m^2/g (M. Ma et al., 2020).

BET results of other waste samples will be re-evaluated when received from the corresponding laboratory.

4.3.4 SEM-EDS Results of Biochars

SEM analysis was employed for biochars to visualize and study its physical structure at the microscopic level. Besides, EDS was used because it is particularly useful for determining the presence of elements like carbon, hydrogen, oxygen, nitrogen, sulfur, and others in the biochar. The elemental composition can influence the biochar's effectiveness in applications such as soil improvement and pollutant adsorption.

4.3.4.1 SEM Results of Biochars

SEM figures of biochars produced from W1.1, W7.1, W8.1, CM, SS and CS samples are given in Figures 4.17-4.22. SEM figures of other biochars can be seen in Appendices.

The biochars derived from different sources such as municipal solid waste, yard waste, corn stalk, cattle and poultry manure, and sewage sludge underwent pre-treatments before being subjected to SEM analysis to determine their surface characteristics. Surface morphology of biochars was analyzed via scanning electron microscope (SEM) (Zeiss-Gemini560). Cracked structures are evident in all samples, which is consistent with the findings of Ma et al. (2020) for CM biochar. Additionally, the SEM images of SS and CM biochars obtained by Stylianou et al. (2020) at 550°C exhibit similarities to the biochars in this study. Increasing the temperature promotes the development of cracks and fragmentation in the biochar structures, as also observed by Zhang et al. (2015). Cuixia et al. (2020) supported these findings through their study on biochar synthesized from PM, where characteristic structures were observed, particularly in the PM-derived biochars.

Furthermore, when examining the SEM image of SS biochar produced at 500°C, it is apparent that it possesses a more porous structure compared to the biochar synthesized at 700°C. This observation aligns with the BET values, and it is possible that the reaction of inorganic additives in the SS, which melt at high temperatures, contributed to this outcome. SEM analysis confirms that the SS biochar synthesized at 700°C exhibits a less porous appearance than the one produced at 500°C, thereby supporting the hypothesis.

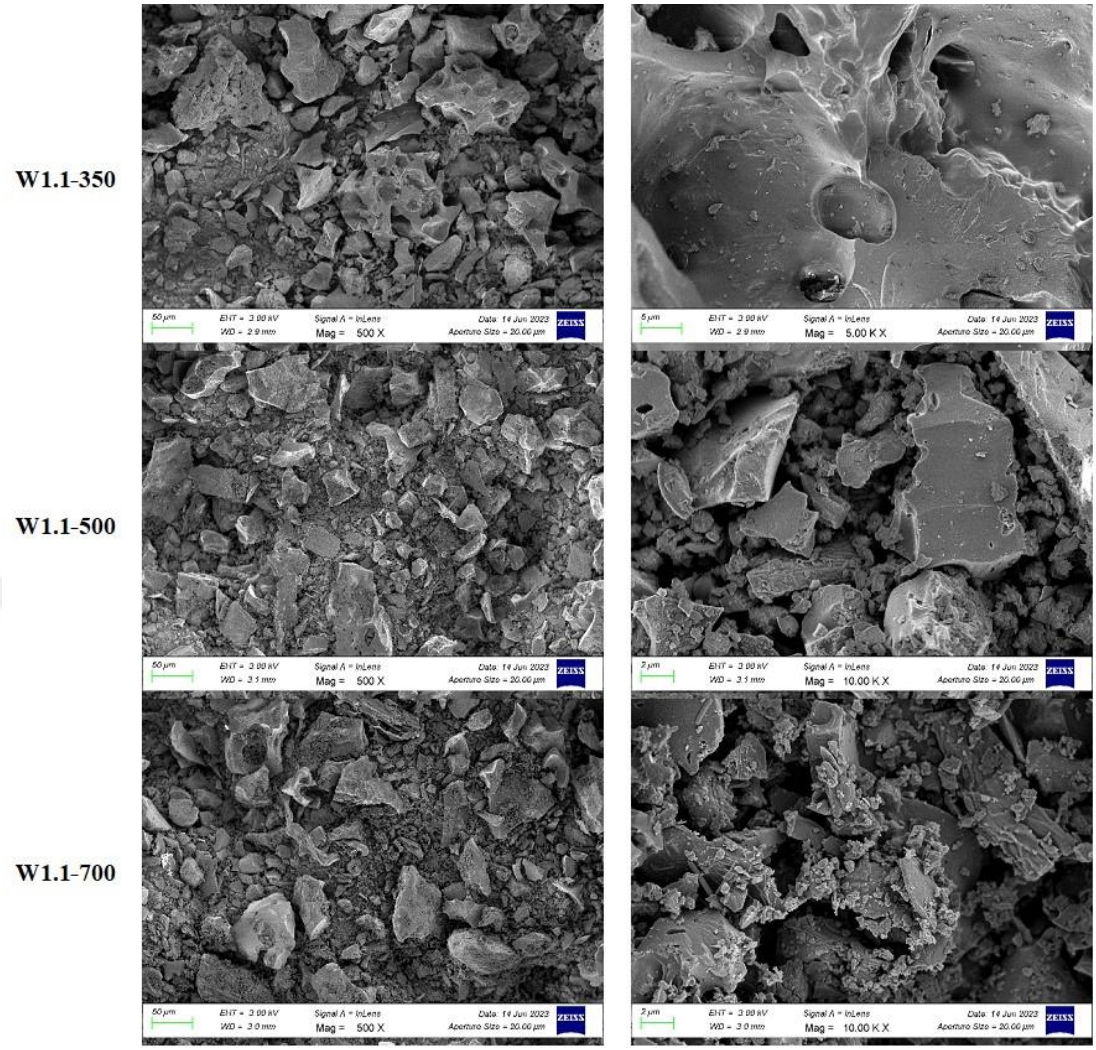

Figure 4.17 SEM figure of W1.1

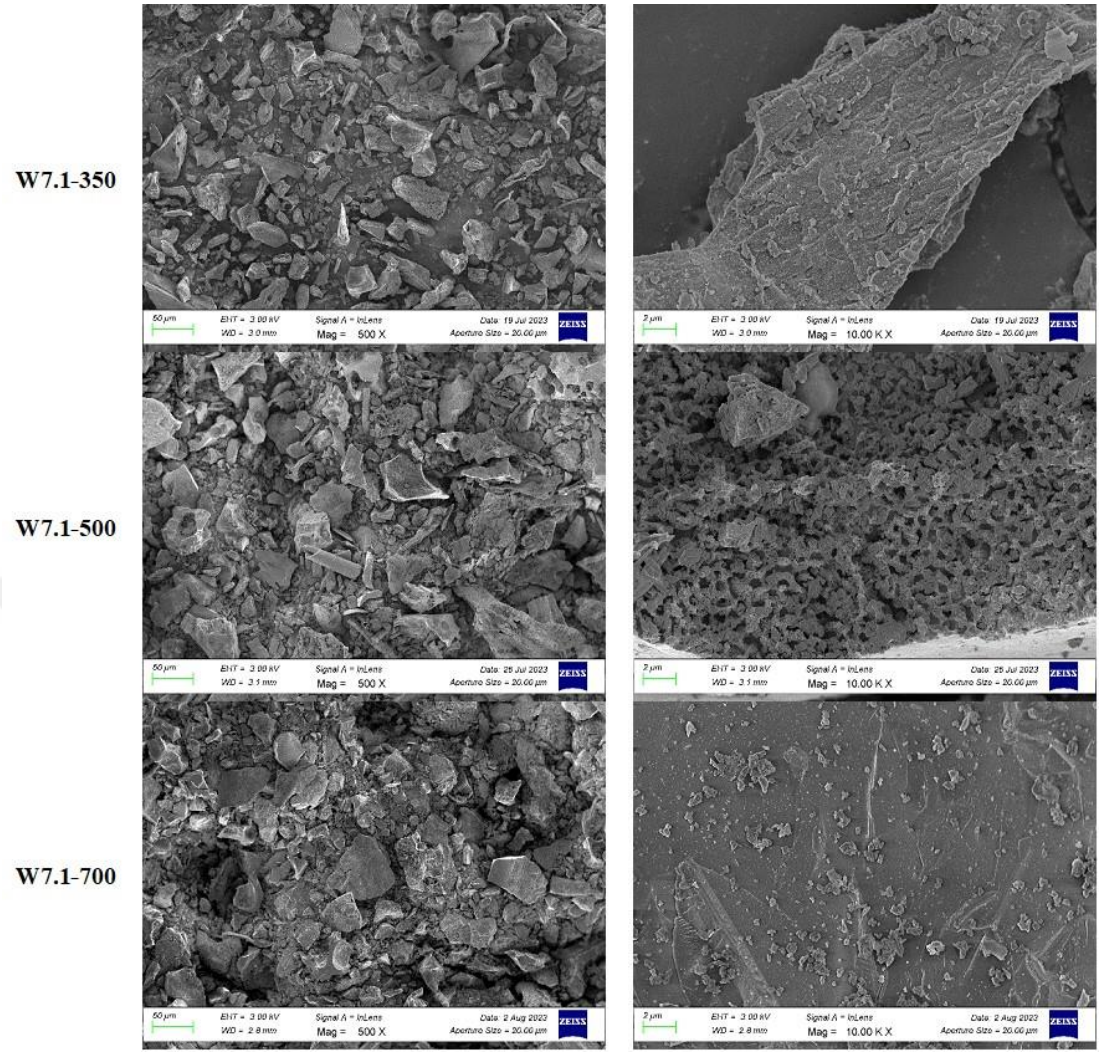

Figure 4.18 SEM figure of W7.1

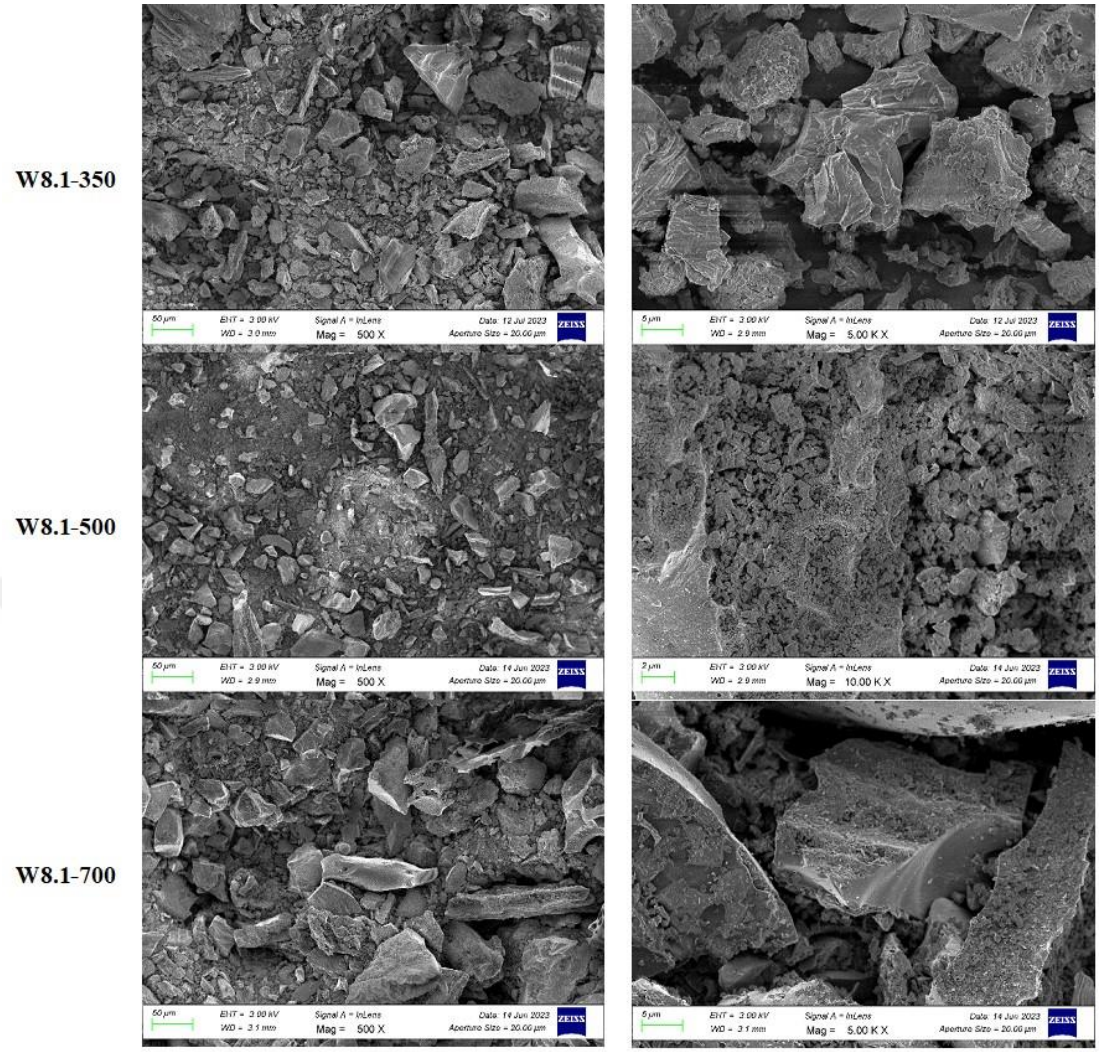

Figure 4.19 SEM figure of W8.1

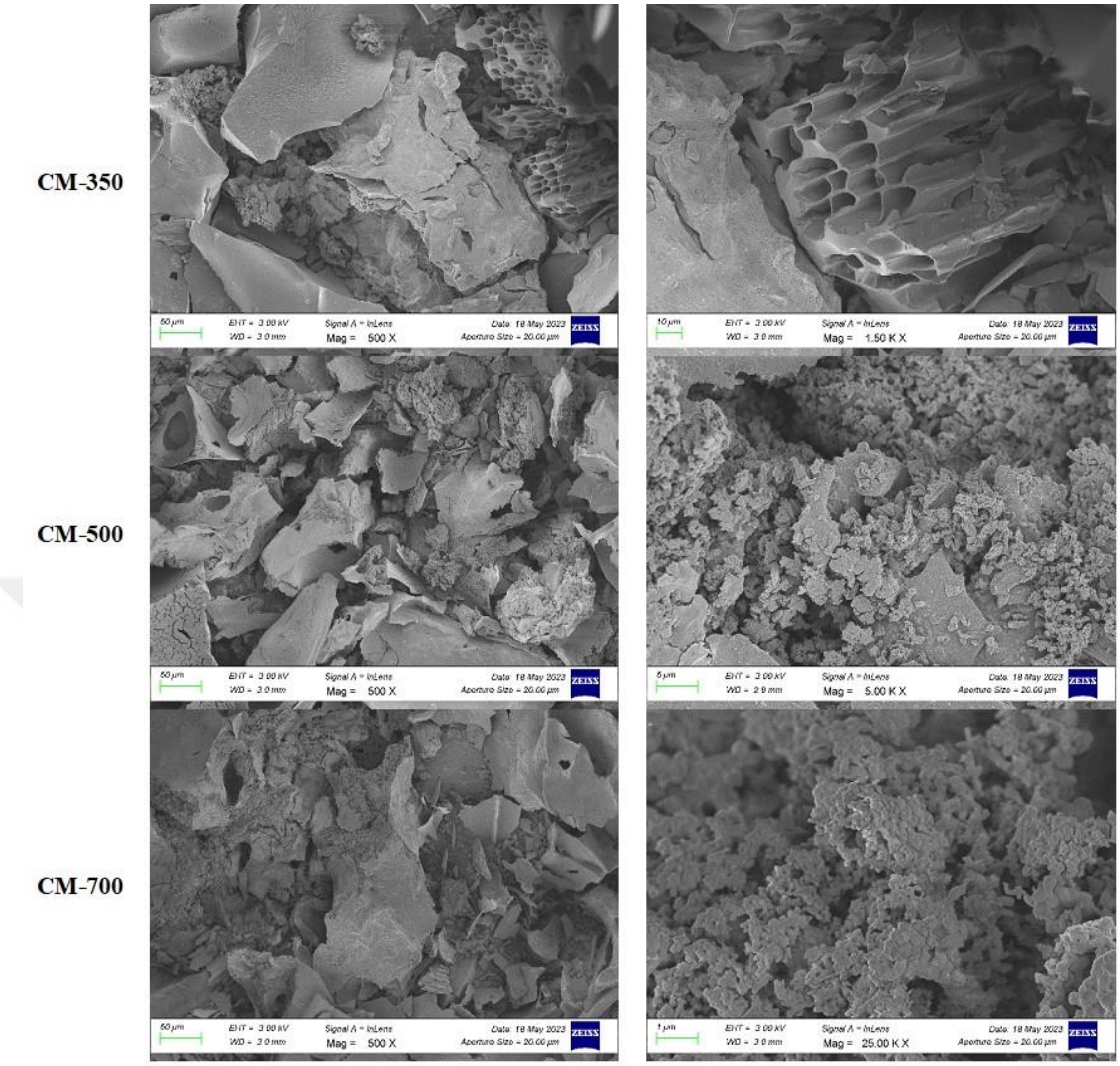

Figure 4.20 SEM figure of CM

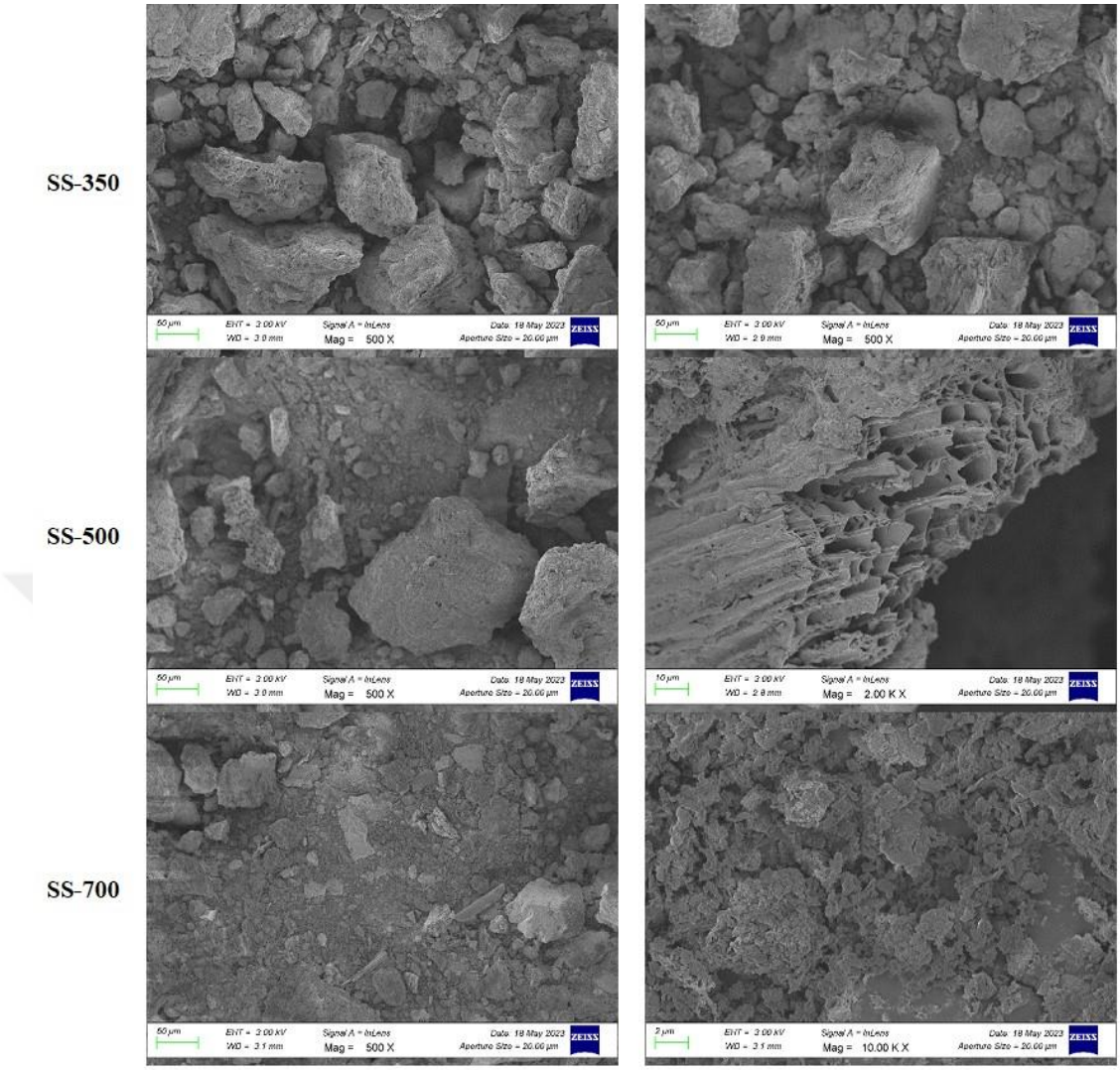

Figure 4.21 SEM figure of SS

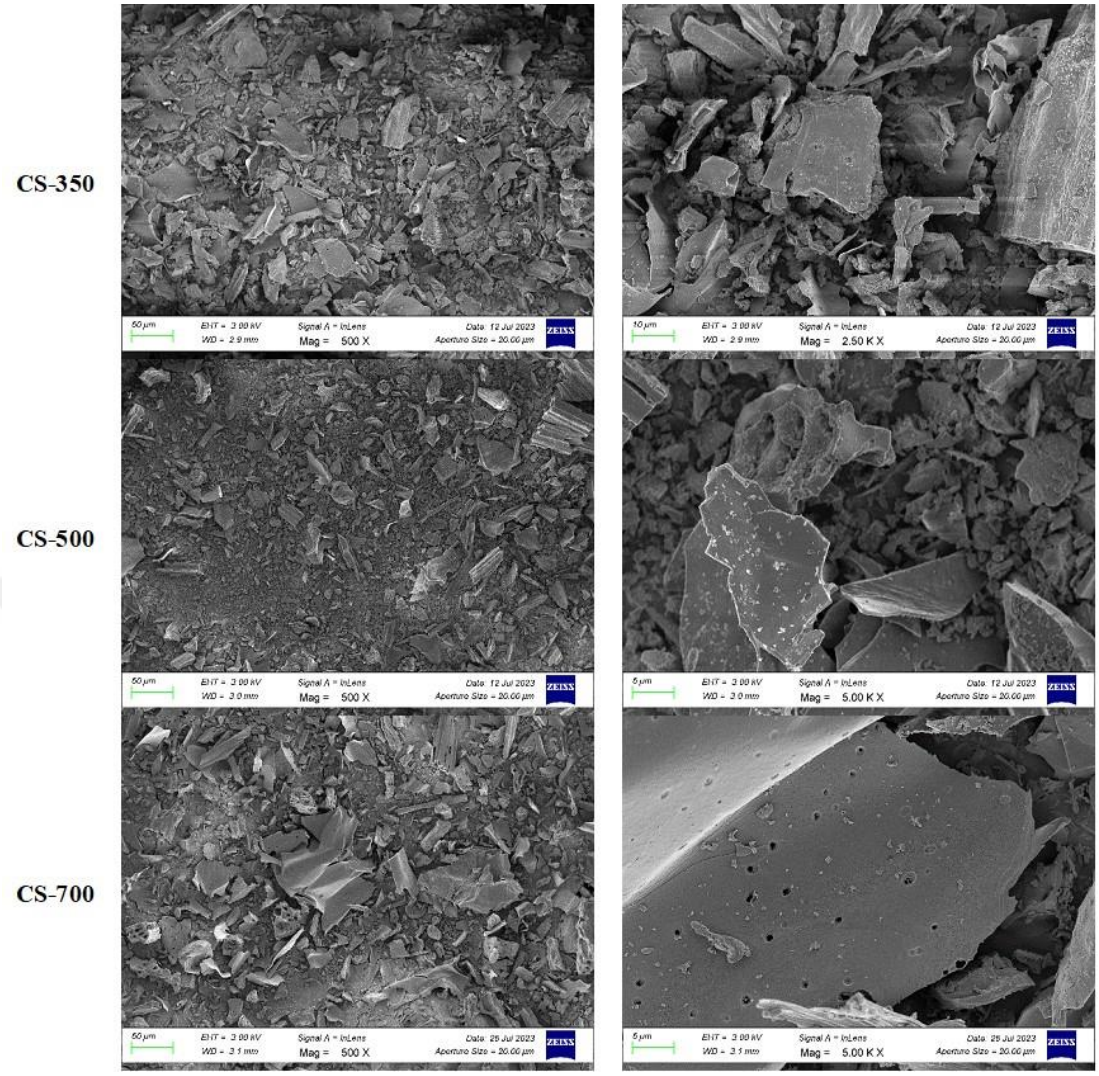

Figure 4.22 SEM figure of CS

4.3.4.2 EDS Results of Biochars

SEM-EDS figures of biochars produced from W1.1, W7.1, W8.1, CM, SS and CS samples at 700^{o}C are given in Figures 4.23-4.28. SEM-EDS figures of other biochars can be seen in Appendices. Although there is no significant difference in the carbon content of biochars produced at three different temperatures, as expected, carbon (C) and oxygen (O) are the most abundant, followed by calcium (Ca), potassium (K), chlorine (Cl) and sodium (Na). In addition, silicium (Si) is present in the biochars except biochars produced from W1.1, W1.2, W6.1, CM and PM samples. There is also iron (Fe) in the biochar produced from CM. In particular, the biochar resulting from

pyrolysis at 700^{o}C contains 31.5% Fe (Figure 4.26). These contents are probably related to the initial contents of the wastes.

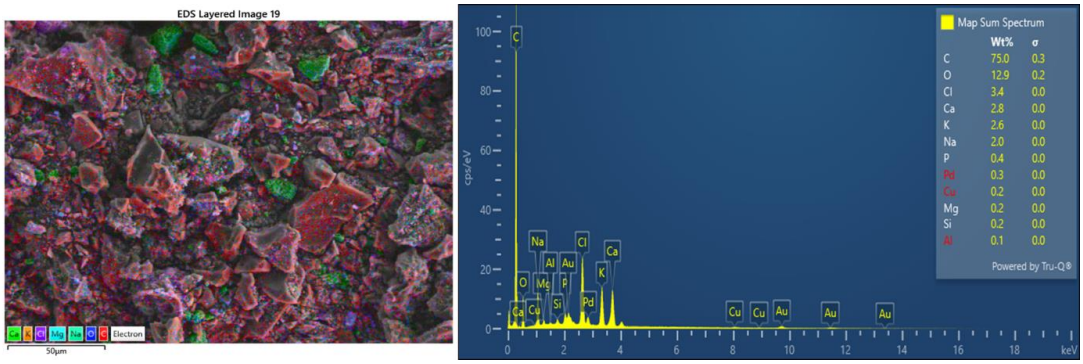

Figure 4.23 SEM-EDS results of W1.1-700

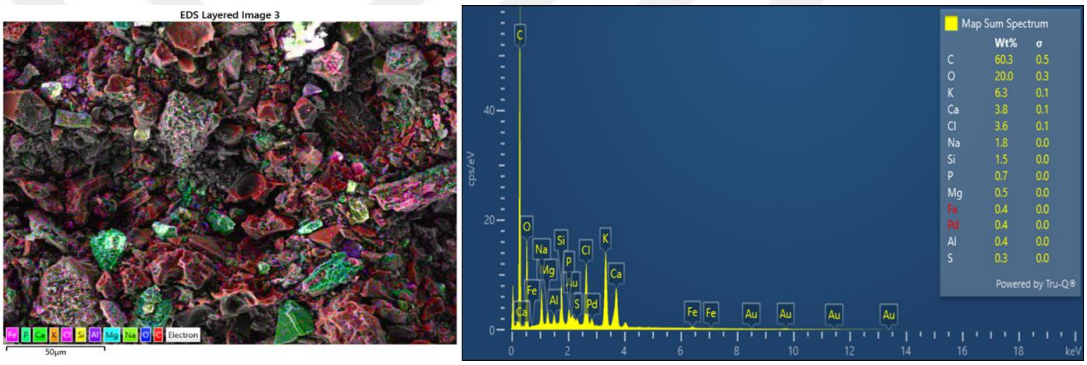

Figure 4.24 SEM-EDS results of W7.1-700

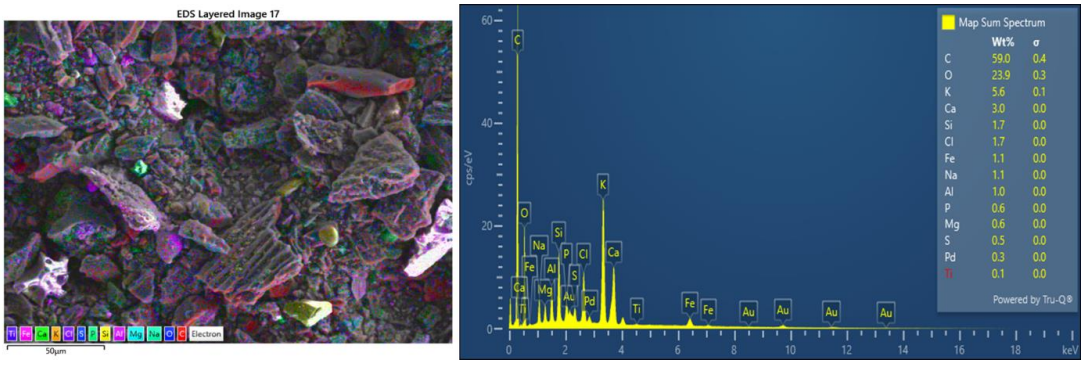

Figure 4.25 SEM-EDS results of W8.1-700

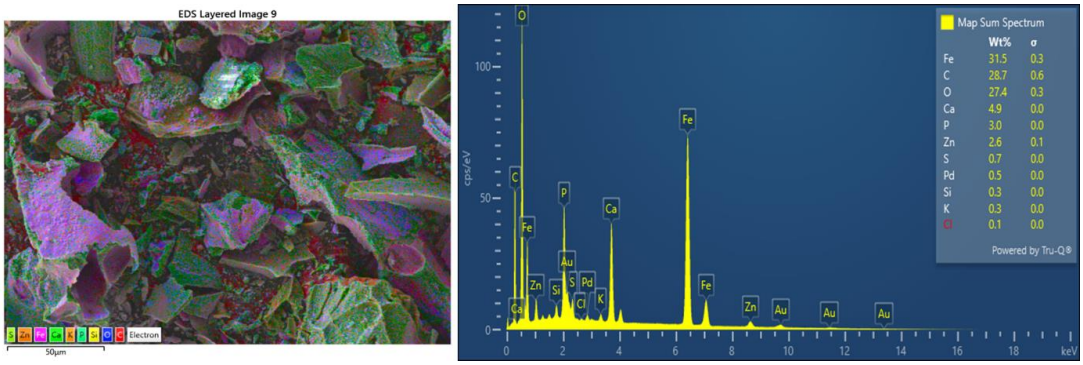

Figure 4.26 SEM-EDS results of CM-700

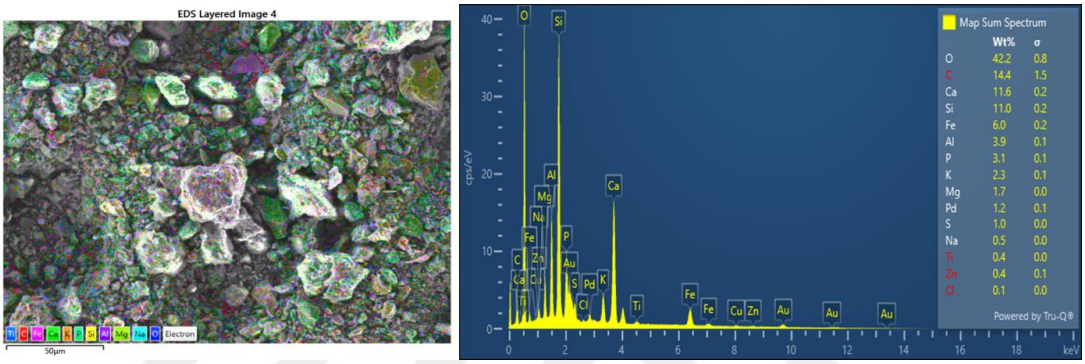

Figure 4.27 SEM-EDS results of SS-700

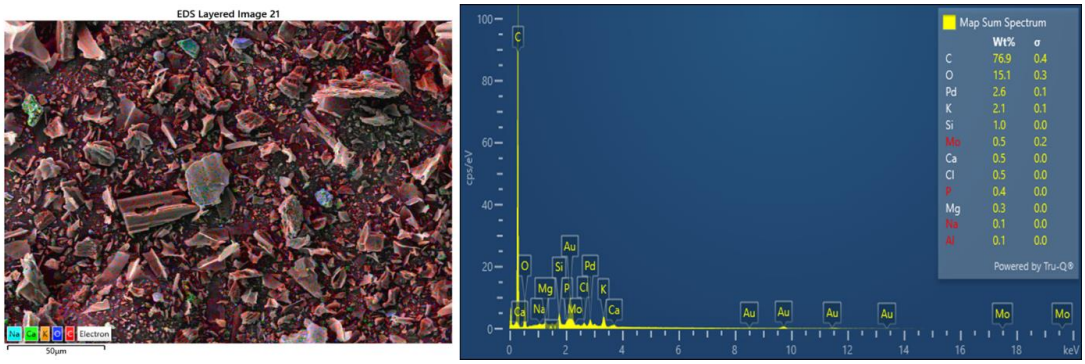

Figure 4.28 SEM-EDS results of CS-700

4.4 Results of Pyrolysis Experiments

4.4.1 Yields of Products

Yield calculations are based on mass balance. Assuming that the nitrogen gas released at the end of the process comes entirely from the supplied nitrogen gas as studies in literature (Yang, Heaven, et al., 2018), the amount of gas was determined based on the gas composition determined by in-situ measurement. Since the amount of liquid product could not be calculated exactly due to the system during the process, the loss of liquid product was added to the mass balance in this way. As a result of this arrangement, the production ratios of the products formed as a result of pyrolysis according to the initial amounts are given in Table 4.10. The liquid product was most produced from pyrolysis using only dry municipal waste (32). While the most gaseous product was produced in the experiment where corn stalks (31) were used, the most biochar was produced as a result of the pyrolysis process where sewage sludge was used (30) in accordance with the ultimate analysis. The results of the experiments with dry dog/ cat food (18) and waste (21) under optimum conditions are very similar. Experiments 1 to 20 were conducted with dry dog/cat food to find the optimum conditions. Three different water contents (25, 40 and 55%) were tried in duplicate (Figure 4.29). 40% water content was decided according to the amount of product obtained. Because it was desired to obtain a sufficient amount of both liquid product and biochar. Then the particle size was decided using the determined water content (Figure 4.30). Three different particle size ranges were tried in duplicate and 10-15 mm particle size range was selected according to the amount of biochar and liquid product obtained. The next experiments continued with 40% water content and 10-15 mm particle diameter. In addition, experiments with biomasses other than dry dog/cat food were also performed without adding water. As seen in Figure 4.31, although there is no clear independent effect of final temperature, heating rate and residence time, 700^{o}C, 10 ^{o}C/min of heating rate and 40 minutes residence time gave more preferable results in terms of yield. If we look at the effect of co-pyrolysis, most liquid yield were formed as a result of pyrolysis of CS and W1.1 together (Figure 4.32). In addition, most biochar production was observed as a result of co-pyrolysis with sewage sludge. This was due to the C, H and inorganic matter contents of the raw materials. It was

observed that adding water to the feedstock increased the liquid product. It was also observed that water affects the pyrolysis performance of the feedstocks and can negatively affect the product yields.

Table 4.10 Yields of products

# of experiment	Condition	Biochar, %	Liquid, %	Gas, %
1	25% WC	14.17	20.60	65.23
2	40% WC	12.24	24.37	63.39
3	55% WC	7.80	35.55	56.65
4	5-10 mm particle size	11.45	22.04	66.51
5	10-15 mm particle size	11.58	25.33	63.09
6	15-20 mm particle size	8.10	19.57	72.33
7	500ºC, 5 ºC/min	16.22	17.77	66.01
8	500ºC, 10 ºC/min	19.85	14.61	65.54
9	700ºC, 10 ºC/min	11.49	19.47	69.04
10	700ºC, 5 ºC/min	15.55	17.65	66.80
11	500ºC, 5 ºC/min, Residence time: 20 min	19.13	17.40	63.46
12	500ºC, 5 ºC/min, Residence time: 40 min	19.32	18.13	62.55
13	700ºC, 5 ºC/min, Residence time: 20 min	13.15	25.47	61.38
14	700ºC, 5 ºC/min, Residence time: 40 min	11.63	27.39	60.98
15	500ºC, 10 ºC/min, Residence time: 20 min	18.47	18.63	62.90
16	500ºC, 10 ºC/min, Residence time: 40 min	18.11	22.88	59.01
17	700ºC, 10 ºC/min, Residence time: 20 min	11.58	25.33	63.09
18	700ºC, 10 ºC/min, Residence time: 40 min	14.14	35.51	50.35
19	500&700 ºC 5&10ºC/min	17.36	15.06	67.57
20	500&700 ºC 10&5ºC/min	16.84	17.54	65.62
21	W1.1 700ºC, 10 ºC/min, Residence time: 40 min	13.35	35.66	50.99
22	W1.1 500ºC, 10 ºC/min, Residence time: 40 min	17.40	42.08	40.52
23	W8.1 700ºC, 10 ºC/min, Residence time: 40 min	16.61	45.06	38.20
24	W8.1 500ºC, 10 ºC/min, Residence time: 40 min	13.38	44.07	42.67

Table 4.10 Yields of products (continued)

# of experiment	Condition	Biochar, %	Liquid, %	Gas, %
25	W1.1+CM (50%+50%) 700°C, 10 °C/min, Residence time: 40 min	14.69	46.67	38.64
26	W1.1+SS (50%+50%) 700°C, 10 °C/min, Residence time: 40 min	20.16	37.37	42.47
27	W1.1+CS (50%+50%) 700°C, 10 °C/min, Residence time: 40 min	12.17	48.00	39.83
28	W1.1+W7.1 (50%+50%) 700°C, 10 °C/min, Residence time: 40 min	13.61	36.68	49.71
29	CM 700°C, 10 °C/min, Residence time: 40 min, dry	15.50	48.33	36.16
30	SS 700°C, 10 °C/min, Residence time: 40 min, dry	50.58	37.71	11.70
31	CS 700°C, 10 °C/min, Residence time: 40 min, dry	25.21	21.50	53.29
32	W1.1 700°C, 10 °C/min, Residence time: 40 min, dry	28.40	66.29	16.44
33	W7.1 700°C, 10 °C/min, Residence time: 40 min, dry	24.45	51.14	24.41
34	W1.1+W7.1 (50%+50%) 700°C, 10 °C/min, Residence time: 40 min, dry	25.14	24.72	50.14
35	BDW 700°C, 10 °C/min, Residence time: 40 min, dry	35.35	27.02	37.63

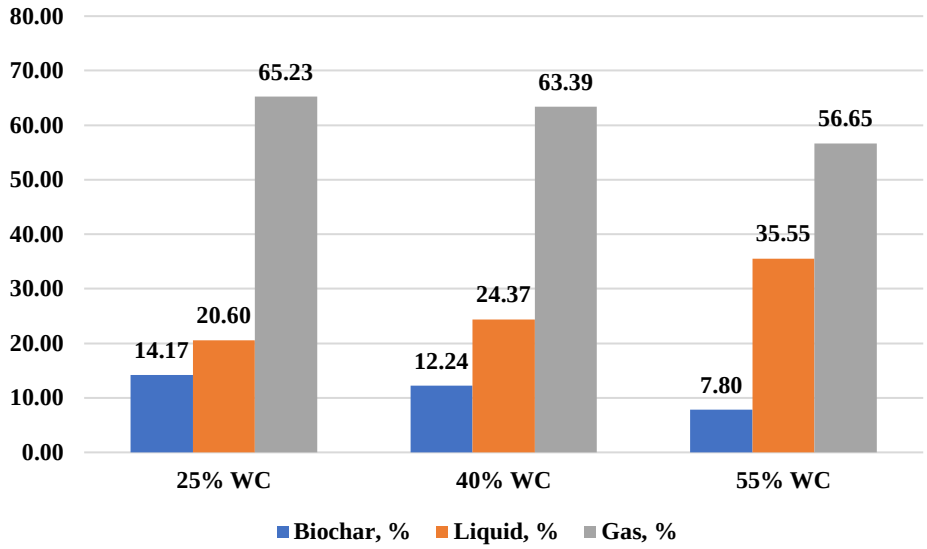

Figure 4.29 Yields of products regarding water content

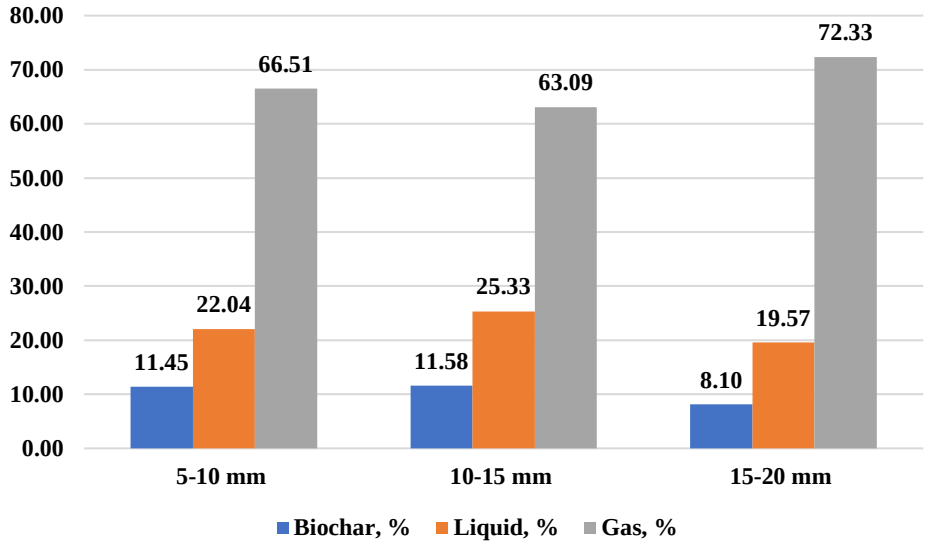

Figure 4.30 Yields of products regarding particle size

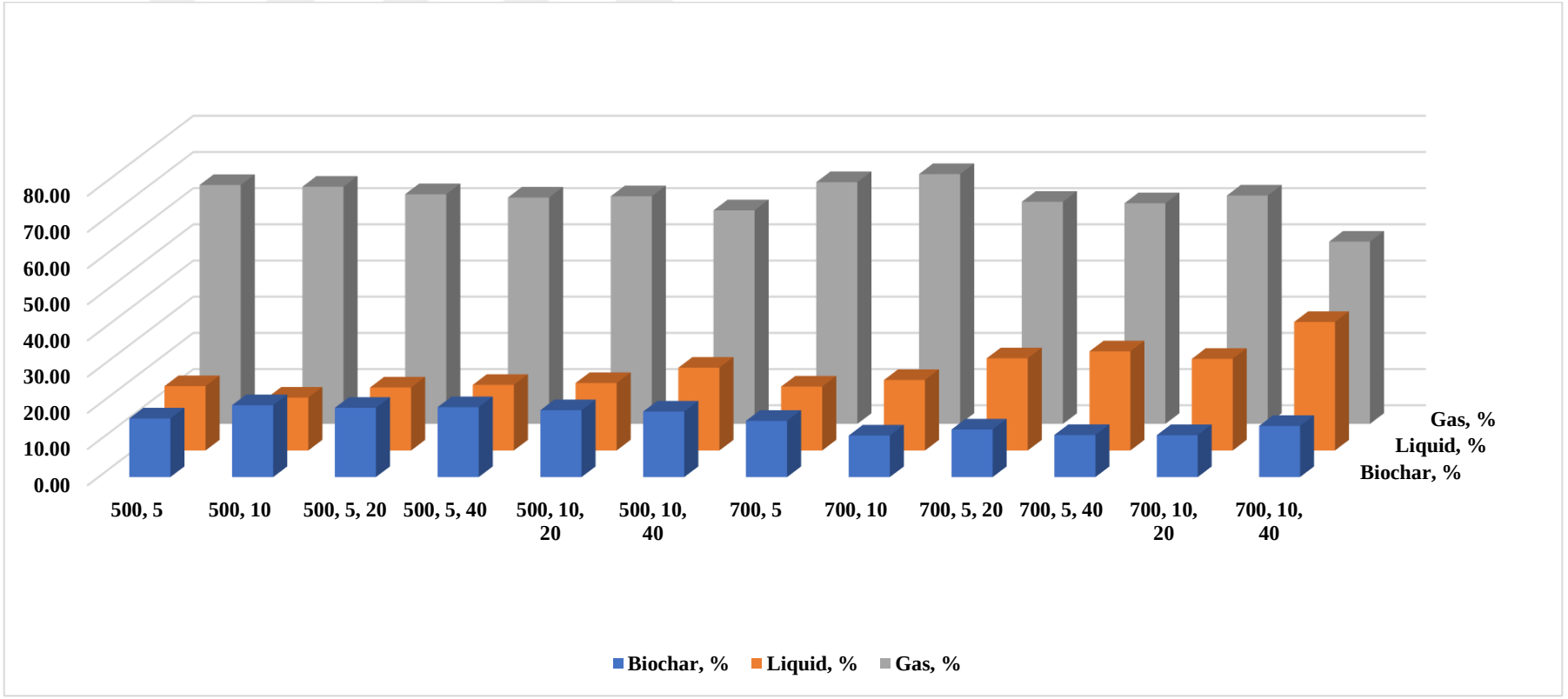

Figure 4.31 Yields of products regarding final temperature, heating rate and residence time

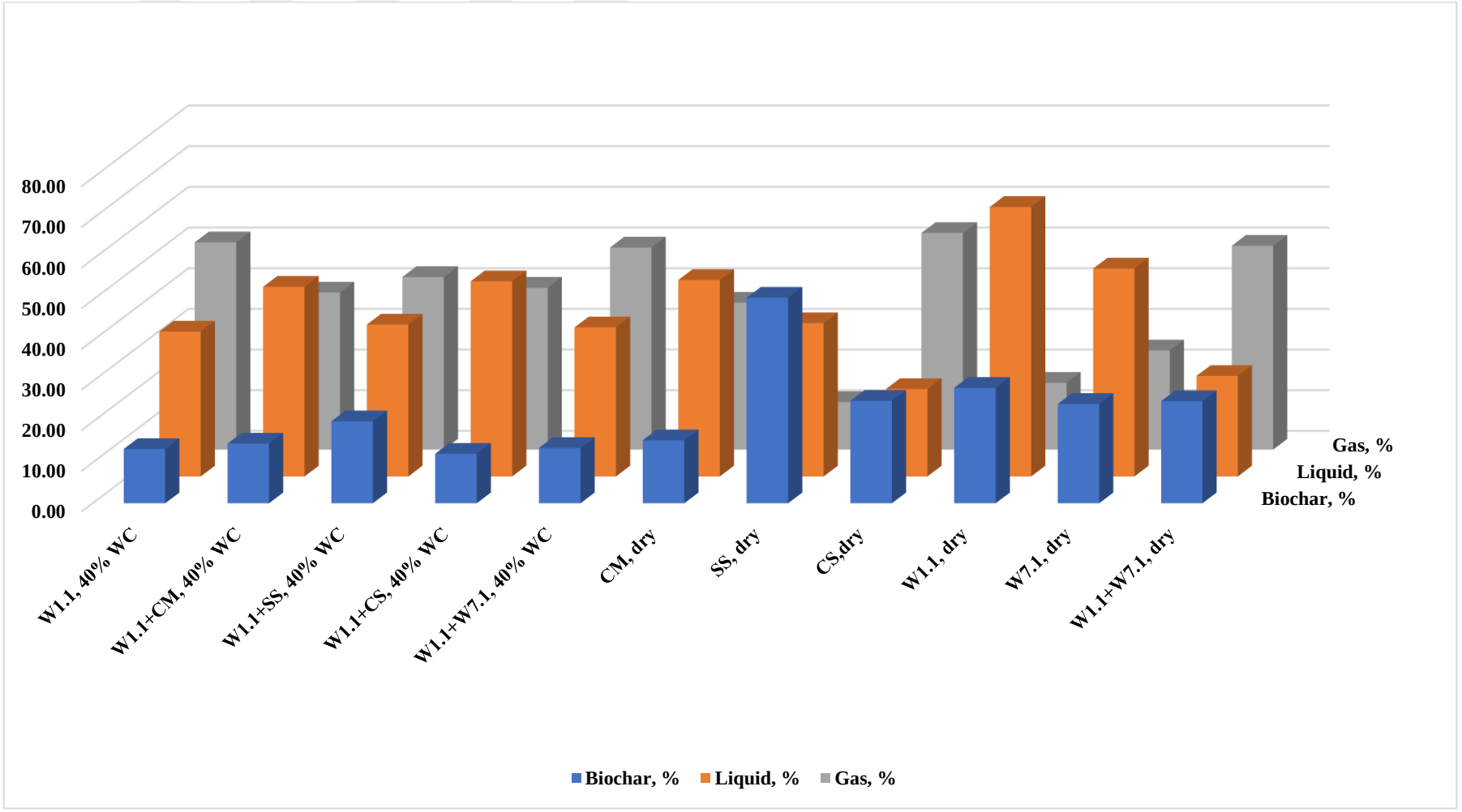

Figure 4.32 Yields of products regarding waste type

4.4.2 FT-IR Results of Biochars

FT-IR spectroscopy was employed for the identification of chemical compounds and functional groups within the sample, enabling the observation of pyrolysis experiment outcomes. FT-IR graphs of biochars produced as a result of pyrolysis with dry cat and dog food to determine the optimum conditions can be seen in Figures 4.33-4.40.

According to FT-IR results (Figure 4.33), it was observed that water content had no effect on biochar formation. Considering the raw material results, biochar production was realized efficiently in experiments where three different water contents were applied.

In the experiments where particle size was tested (Figure 4.34), it was observed that particle size had no significant effect on the biochar produced.

According to the FT-IR results (Figure 4.35-4.38) of the biochars produced as a result of the experiments, in which the effect of the final temperature, heating rate and retention time were investigated, the final temperature had a significant positive effect on the biochar quality, but the heating rate and residence time did not have such an effect.

Moreover, one stage heating or two stage heating (Figure 4.38) doesn't have different effects on the quality of biochar.

Co-pyrolysis with CM, SS and CS had a positive effect on the quality of biochar, based on experiments with wastes and other biomasses (Figure 4.39). FT-IR lines of co-pyrolysis with CM, SS and CS are smoother than ones of only wastes.

In addition, if we compare the FT-IR results of the biochars produced as a result of wet and dry pyrolysis experiments, it is seen that water content does not have a negative effect on biochar quality (Figure 4.39-4.40).

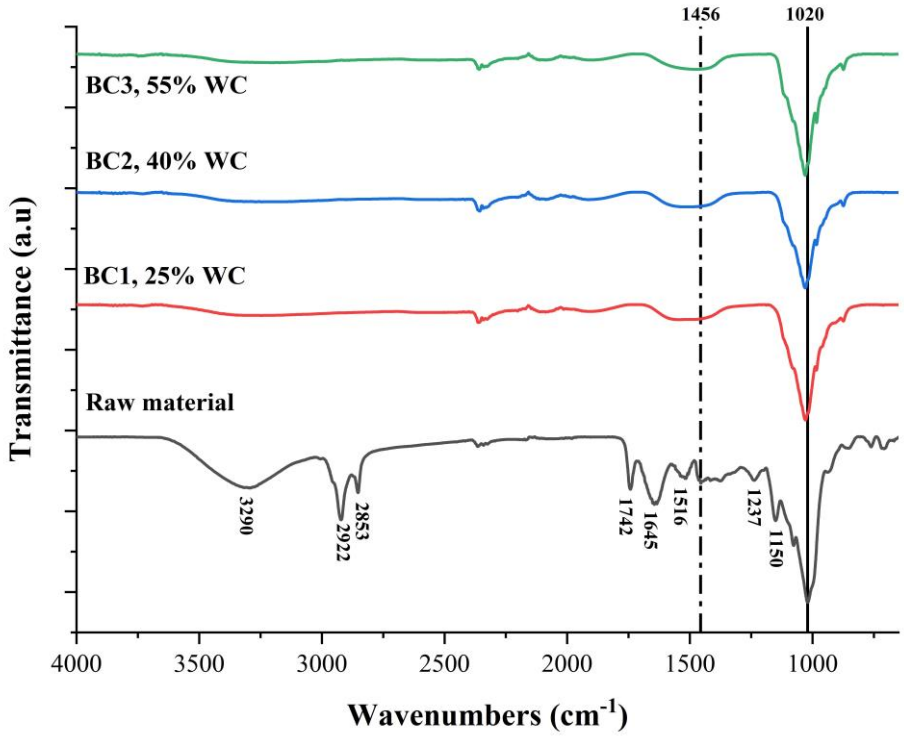

Figure 4.33 FT-IR results of biochars for water content comparison

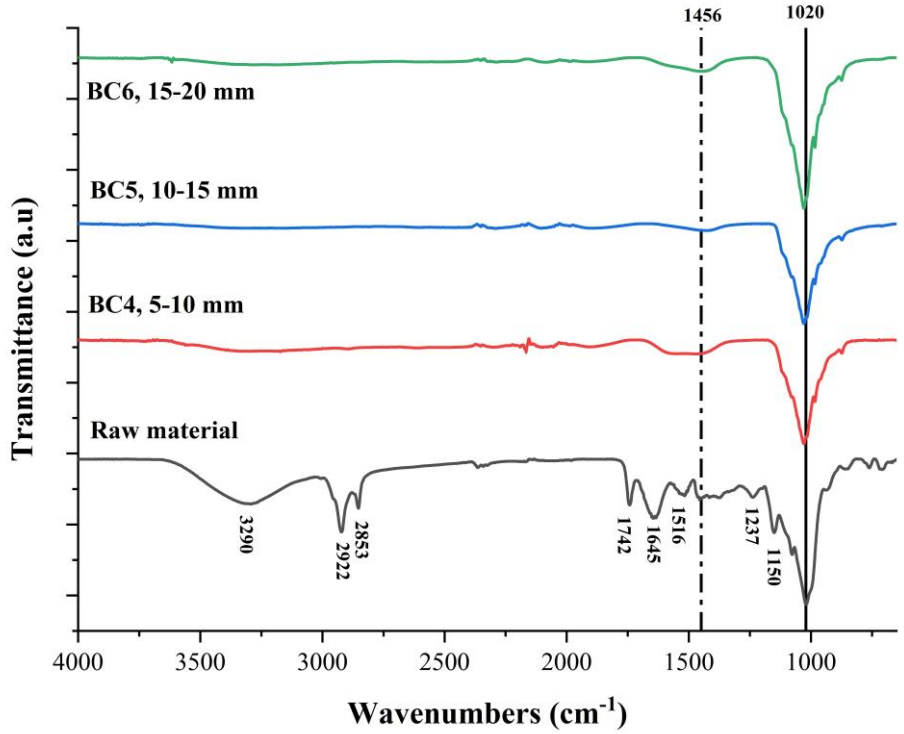

Figure 4.34 FT-IR results of biochars for particle size comparison

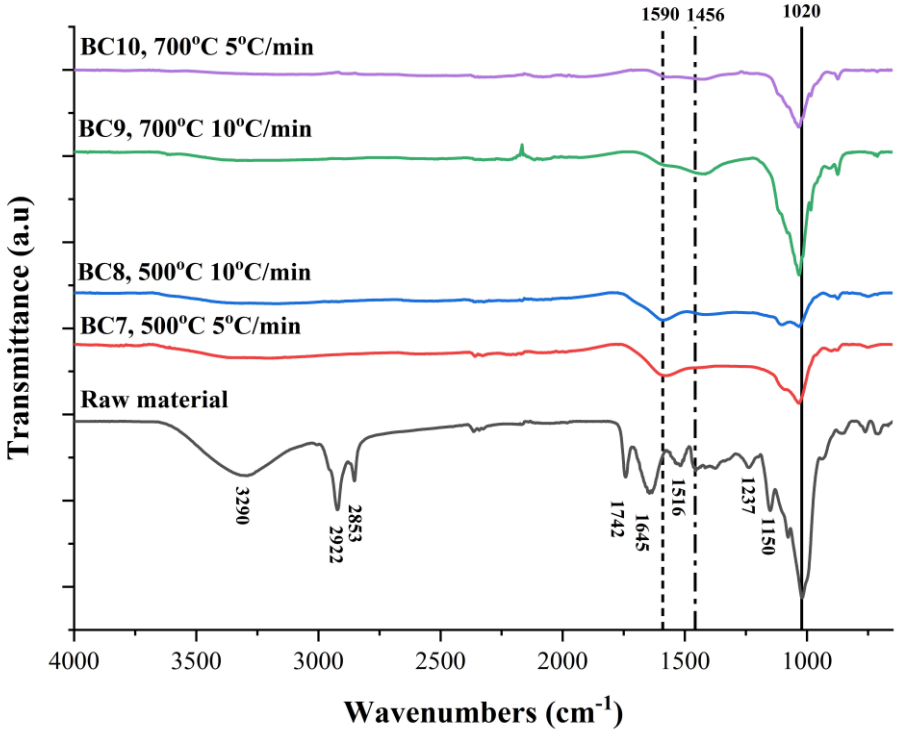

Figure 4.35 FT-IR results of biochars for comparing final temperature and heating rate

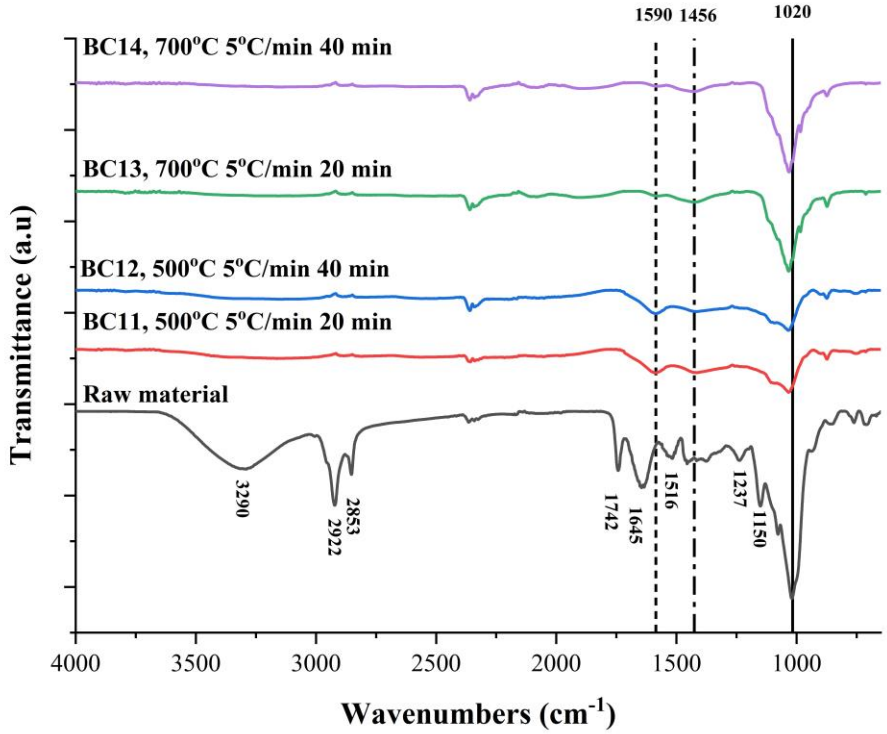

Figure 4.36 FT-IR results of biochars for comparing final temperature and retention time with 5°C/min heating rate

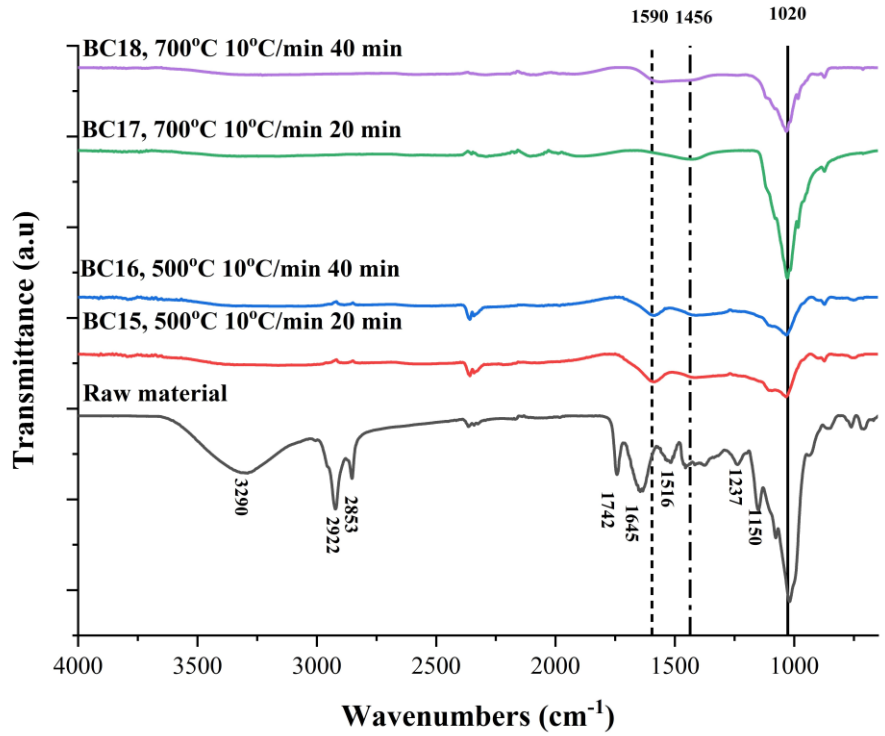

Figure 4.37 FT-IR results of biochars for comparing final temperature and retention time with 10°C/min heating rate

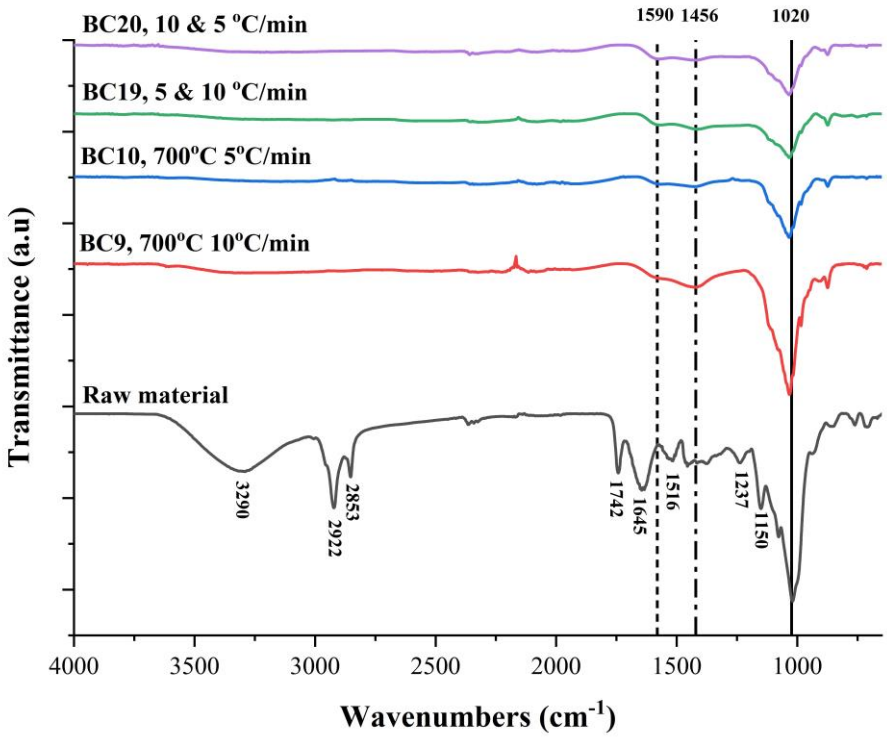

Figure 4.38 FT-IR results of biochars for comparing one stage and two stage heating

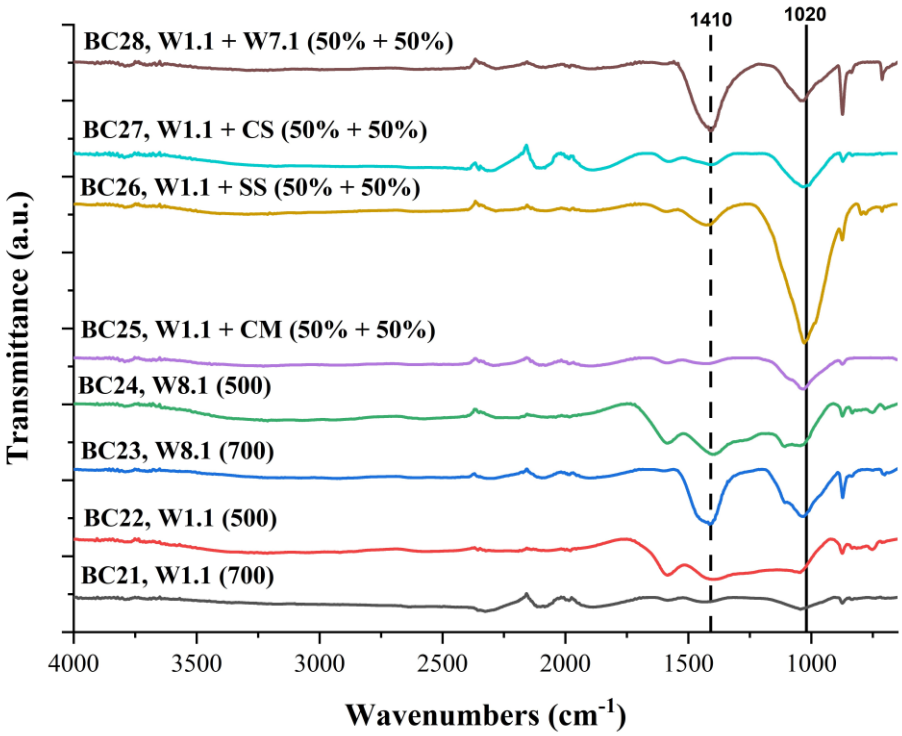

Figure 4.39 FT-IR results of biochars of waste and other biomass samples (Wet trial)

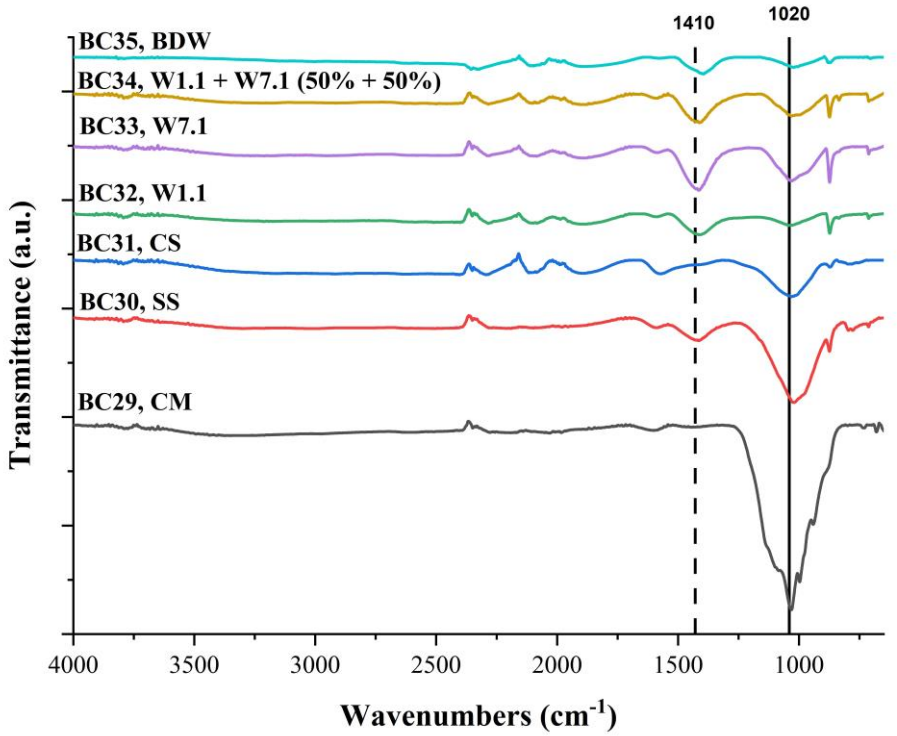

Figure 4.40 FT-IR results of biochars of waste and other biomass samples (Dry trial)

4.4.3 BET Results of Biochars

BET analysis was employed for biochars to evaluate their specific surface area and pore characteristics. This assessment is essential for investigating biochar's adsorption capacity. A higher specific surface area, as determined by BET analysis, often signifies improved adsorption potential, enhancing biochar's effectiveness in these applications. Some BET results of biochars produced from mixed dried dog/cat food and wastes can be seen in Table 4.11. The highest BET value was obtained in the BC18 sample (169.2053 m^2/g) in experiments conducted with dry dog/cat food. When the parameters are evaluated as a whole, the most effective conditions are the final temperature of 700ºC, heating rate of 10 ºC/min and 40 minutes residence time. According to this BET result and other analysis results, 700 ºC final temperature with a heating rate of 10 ºC/min and 40 minutes of residence time was determined as the optimum condition. It was also observed that the BET values of biochar produced from wastes were very low but co-pyrolysis had a positive effect. The BET value of the biochar produced as a result of co-pyrolysis of W1.1 with CS is high (170.18 m^2/g) due to the effect of corn stalk. Besides, the BET value of biochar produced from CS is the highest (206.06 m^2/g). Although the highest BET surface area values observed in this study after pyrolysis at 700°C are less than what has been reported for illite in prior research, they do exceed the BET values of bentonite and kaolinite, which are acknowledged for their effectiveness as absorbents (I. Kobayashi, Owada, Ishii, & Iizuka, 2017; Murray & Quirk, 1990). Illite, bentonite and kaolinite are adsorbents used for the removal of heavy metals such as cadmium and chromium from water and/or wastewater. Comparison with low-cost adsorbents such as illite, bentonite and kaolinite is important to evaluate the possibility of using biochars as adsorbents (Ghorbel-Abid, Galai, & Trabelsi-Ayadi, 2010; Inyang et al., 2016; J. Ma et al., 2012; Mustapha et al., 2019; Naseem & Tahir, 2001; G. Wang, Wang, Sun, Sun, & Zheng, 2017).

Table 4.11 BET results of biochars

Sample Code	Condition	BET Surface Area, m^2/g	Pore Volume, cm^3/g	Pore Size, Å
BC1	25% WC	91.15	0.08	34.30
BC2	40% WC	107.06	0.09	32.23
BC3	55% WC	78.95	0.07	34.25
BC4	5-10 mm particle size	102.76	0.08	32.61
BC5	10-15 mm particle size	8.52	0.02	85.15
BC6	15-20 mm particle size	27.78	0.04	51.36
BC7	500ºC, 5 ºC/min	41.97	0.04	41.43
BC8	500ºC, 10 ºC/min	9.29	0.02	79.13
BC9	700ºC, 10 ºC/min	29.01	0.04	49.15
BC10	700ºC, 5 ºC/min	12.08	0.02	71.33
BC11	500ºC, 5 ºC/min, Residence time: 20 min	8.87	0.02	74.99
BC12	500ºC, 5 ºC/min, Residence time: 40 min	20.26	0.02	46.49
BC13	700ºC, 5 ºC/min, Residence time: 20 min	45.65	0.02	20.36
BC14	700ºC, 5 ºC/min, Residence time: 40 min	35.70	0.03	39.03
BC15	500ºC, 10 ºC/min, Residence time: 20 min	13.71	0.02	64.70
BC16	500ºC, 10 ºC/min, Residence time: 40 min	62.61	0.05	34.80
BC17	700ºC, 10 ºC/min, Residence time: 20 min	8.52	0.02	85.15
BC18	700ºC, 10 ºC/min, Residence time: 40 min	169.21	0.12	28.13
BC19	500&700 ºC 5&10ºC/min	15.93	0.02	57.35
BC20	500&700 ºC 10&5ºC/min	106.30	0.08	29.21
BC21	W1.1 700ºC, 10 ºC/min, Residence time: 40 min	2.57	0.01	124.66
BC22	W1.1 500ºC, 10 ºC/min, Residence time: 40 min	2.34	0.002	37.53
BC23	W8.1 700ºC, 10 ºC/min, Residence time: 40 min	12.69	0.01	37.93
BC24	W8.1 500ºC, 10 ºC/min, Residence time: 40 min	1.95	0.002	46.69
BC25	W1.1+CM (50%+50%) 700ºC, 10 ºC/min, Residence time: 40 min	4.45	0.01	63.92

Table 4.11 BET results of biochars (continued)

Sample Code	Condition	BET Surface Area, m^2/g	Pore Volume, cm^3/g	Pore Size, Å
BC26	W1.1+SS (50%+50%) 700°C, 10 °C/min, Residence time: 40 min	62.80	0.05	32.53
BC27	W1.1+CS (50%+50%) 700°C, 10 °C/min, Residence time: 40 min	170.18	0.10	22.36
BC28	W1.1+W7.1 (50%+50%) 700°C, 10 °C/min, Residence time: 40 min	14.47	0.01	28.38
BC29	CM 700°C, 10 °C/min, Residence time: 40 min, dry	31.78	0.06	75.00
BC30	SS 700°C, 10 °C/min, Residence time: 40 min, dry	66.61	0.04	26.95
BC31	CS 700°C, 10 °C/min, Residence time: 40 min, dry	206.06	0.11	20.82
BC32	W1.1 700°C, 10 °C/min, Residence time: 40 min, dry	43.44	0.03	24.29
BC33	W7.1 700°C, 10 °C/min, Residence time: 40 min, dry	81.65	0.05	24.96
BC34	W1.1+W7.1 (50%+50%) 700°C, 10 °C/min, Residence time: 40 min, dry	80.43	0.03	20
BC35	BDW 700°C, 10 °C/min, Residence time: 40 min, dry	3.73	0.004	43.67

4.4.4 SEM-EDS Results of Biochars

SEM analysis was used to provide high-resolution images of the biochar's microstructure, while EDS was used to detect the elements present within the sample. This combination allowed us to assess the biochar's texture, pore structure, and particle distribution while simultaneously identifying the elemental composition. This is

essential because the physical structure and chemical composition of biochar are critical for its intended applications, such as in agriculture, environmental remediation, or water treatment.

4.4.4.1 SEM Results of Biochars

SEM figures of feedstock sample and biochars can be seen in Figures 4.41-4.51. SEM analysis was also performed for the feedstock to better understand the difference (Figure 4.41). SEM figures of biochars produced as a result of pyrolysis experiment comparing water content can be seen in Figure 4.42. There is no significant difference in biochars produced with these three different water contents.

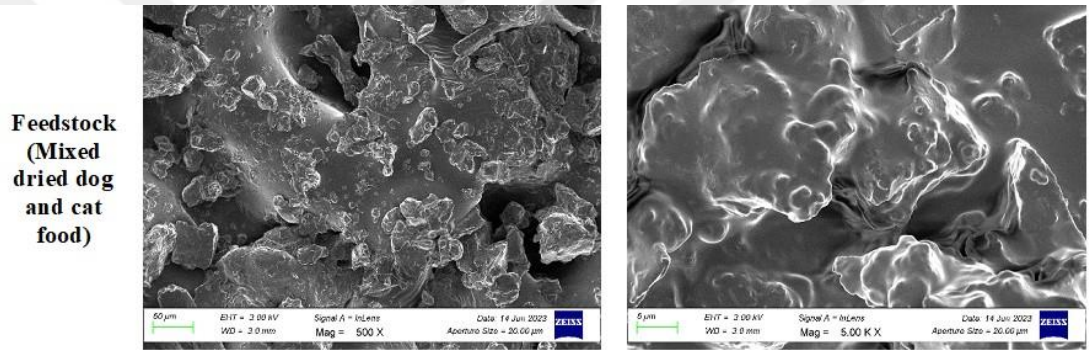

Figure 4.41 SEM figure of feedstock

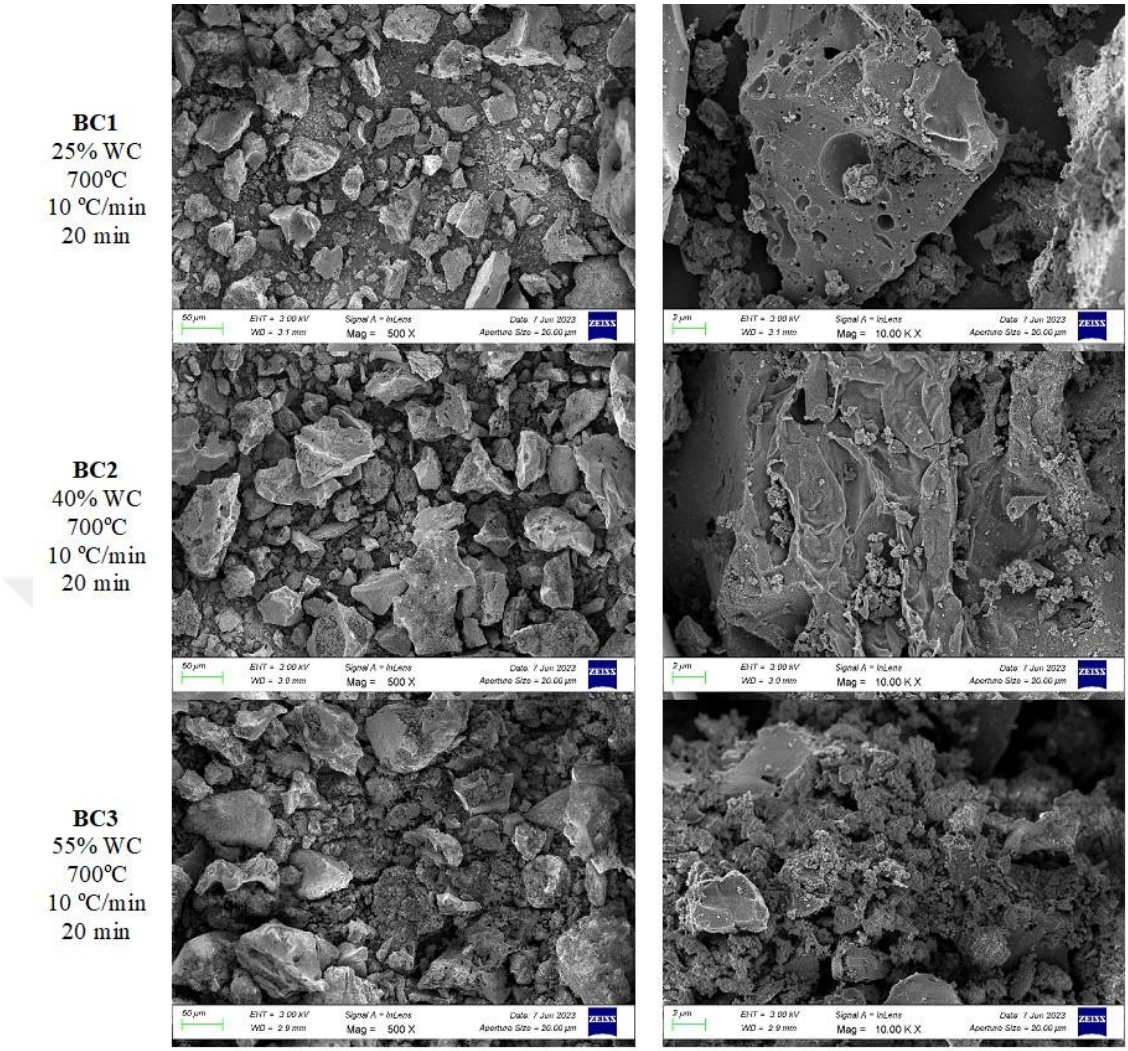

Figure 4.42 SEM figures of biochars with different water contents

SEM figures of biochars produced as a result of pyrolysis experiment comparing particle size can be seen in Figure 4.43. There is no significant difference in biochars produced with these three different particle sizes.

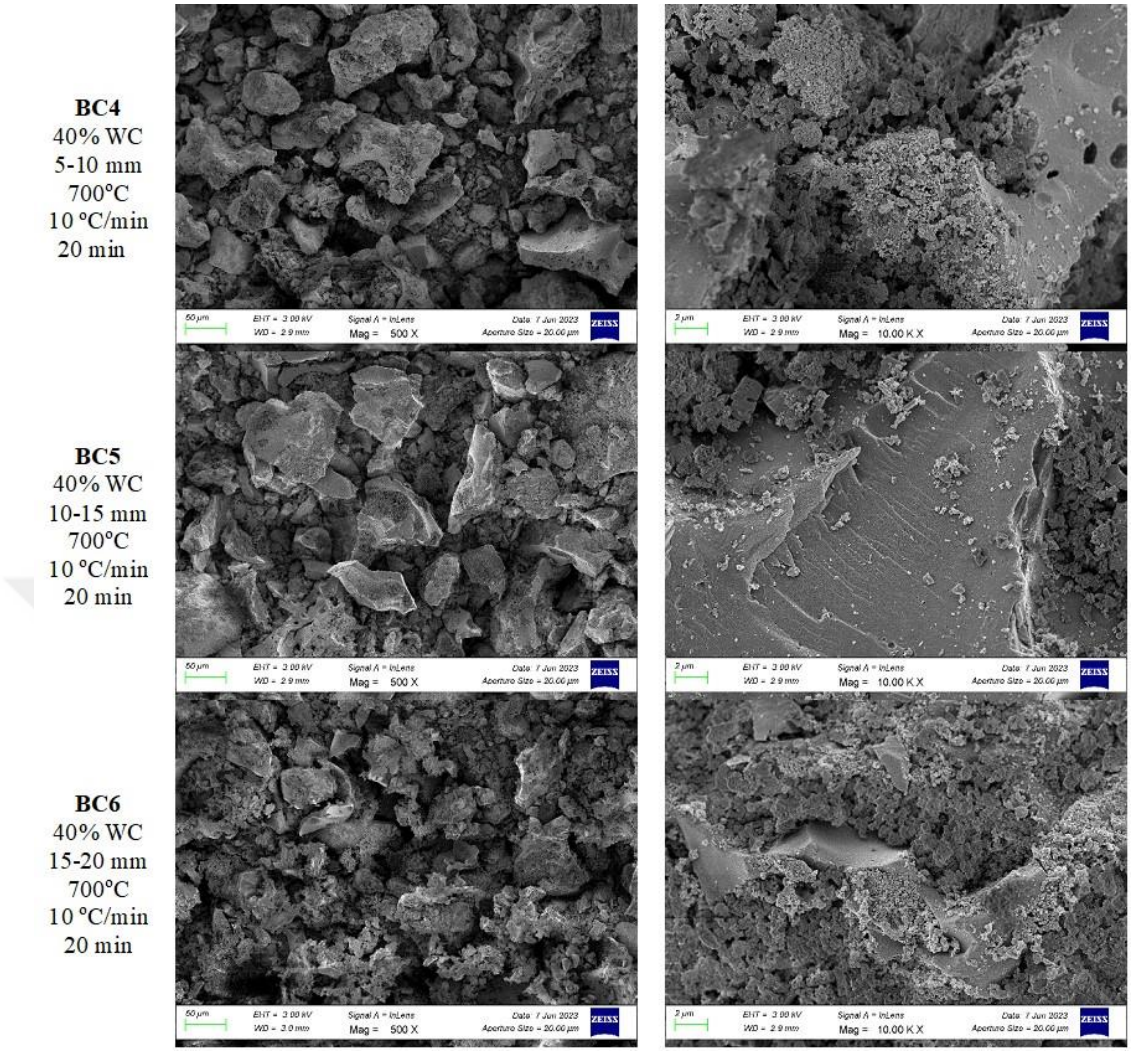

Figure 4.43 SEM figures of biochars with different particle sizes

SEM figures of biochars produced with different final temperatures and heating rates can be seen in Figure 4.44. The presence of cracked structures is noticeable in all samples, aligning with the observations made by Ma et al. (2020). It's worth noting that elevating the temperature encourages the further formation of cracks and the fragmentation of biochar structures, which corresponds with findings from Zhang et al. (2015).

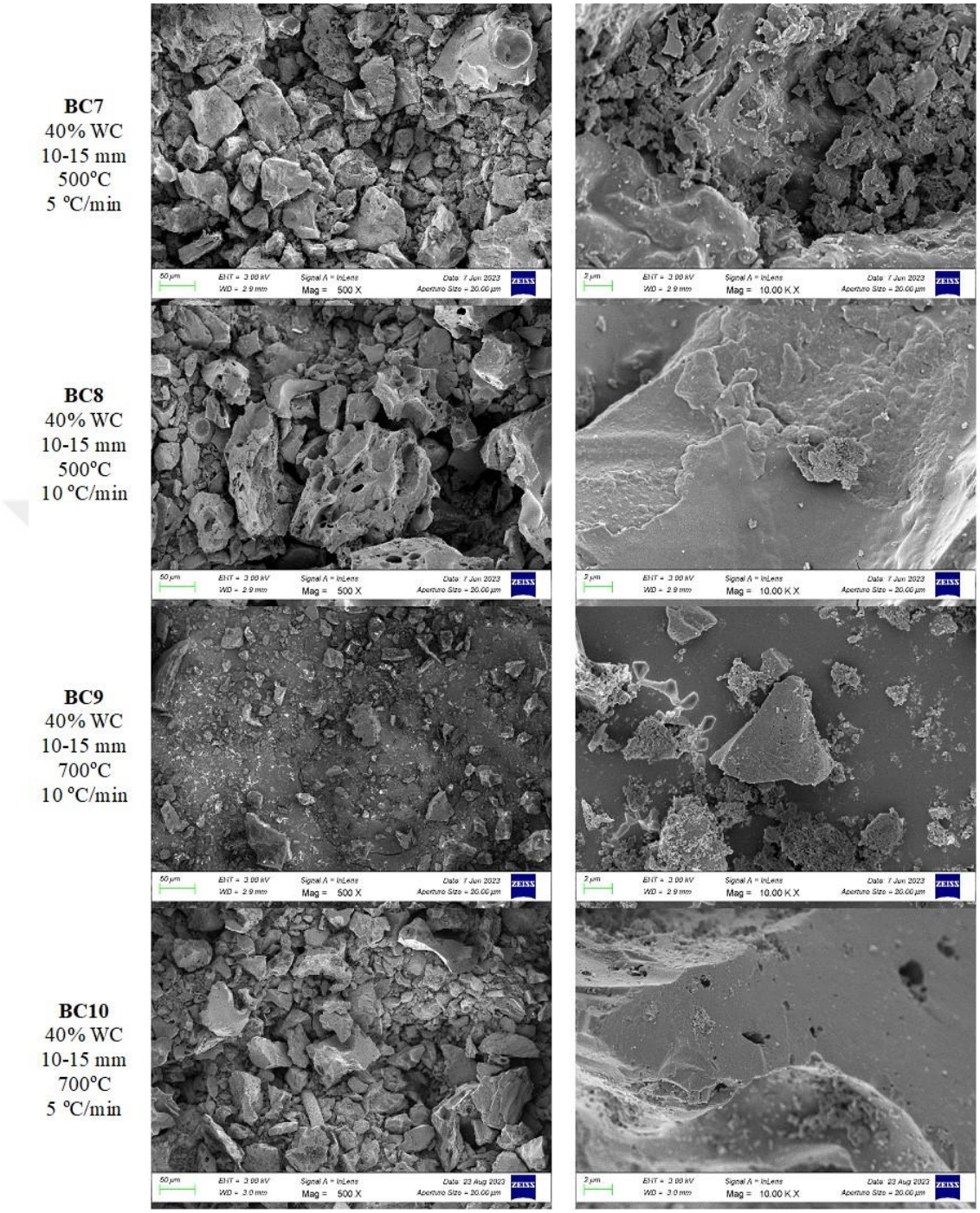

Figure 4.44 SEM figures of biochars with one stage heating condition

SEM figures of biochars produced with different final temperatures, heating rates and retention times can be seen in Figure 4.45-4.46. There is no significant difference in biochars. However, when looking at the details, it can be said that there are more pores and cracked structures in biochars produced at 700°C, although it is not very obvious.

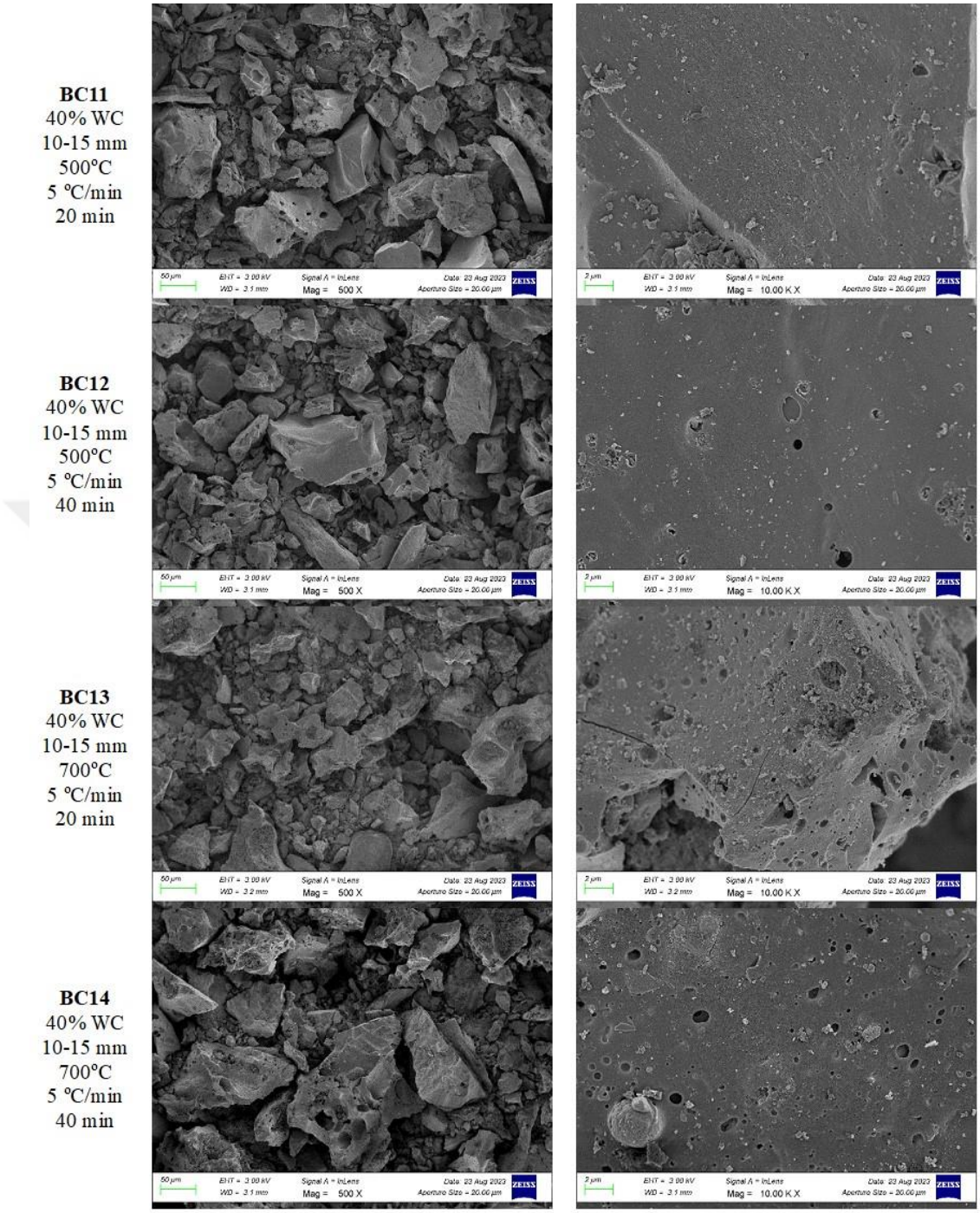

Figure 4.45 SEM figures of biochars with one stage heating (5 °C/min) and retention time conditions

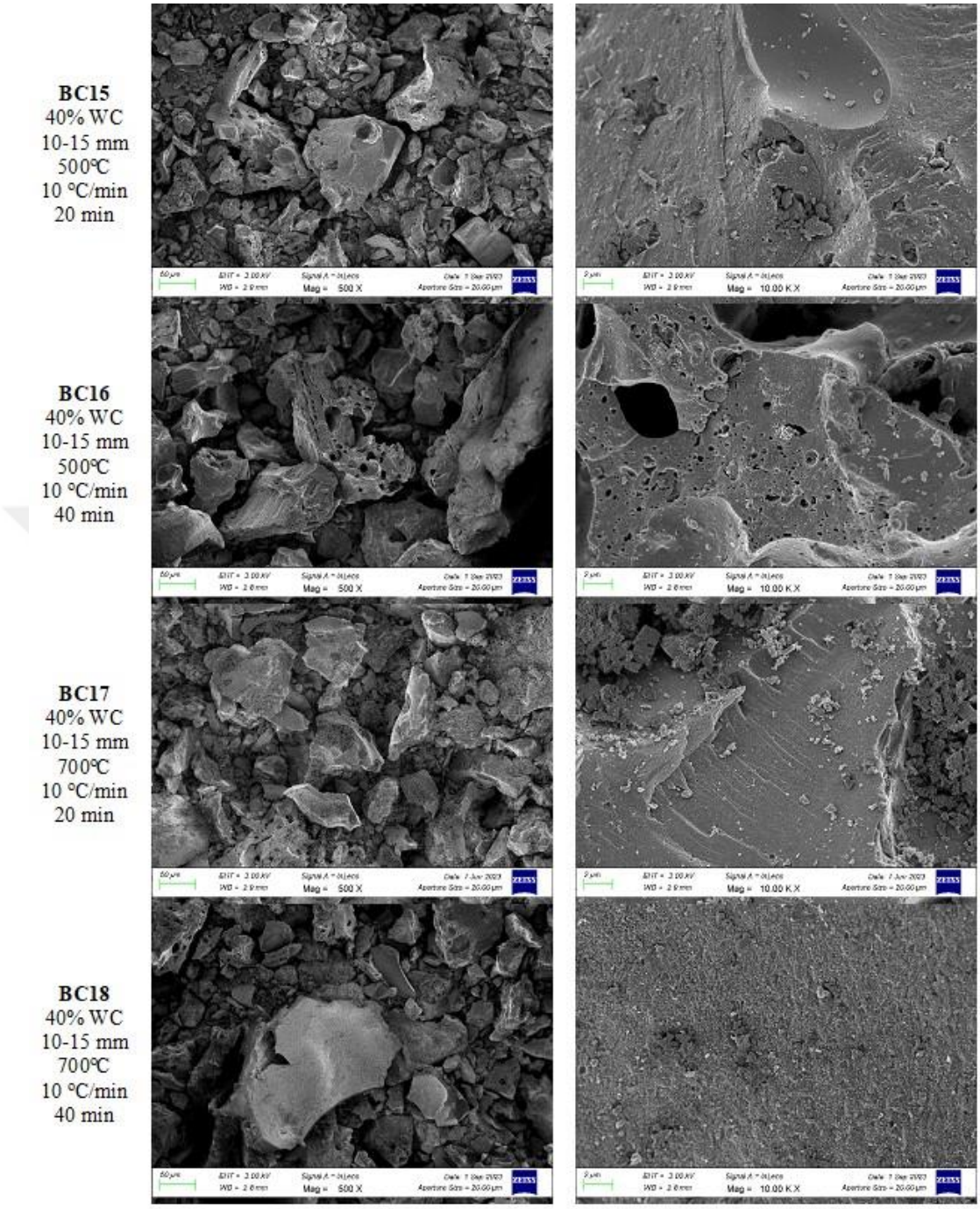

Figure 4.46 SEM figures of biochars with one stage heating (10 ^{o}C/min) and retention time conditions

No significant difference was observed in the SEM figures of the biochars produced as a result of the experiments using two-stage heating rate (Figure 4.47).

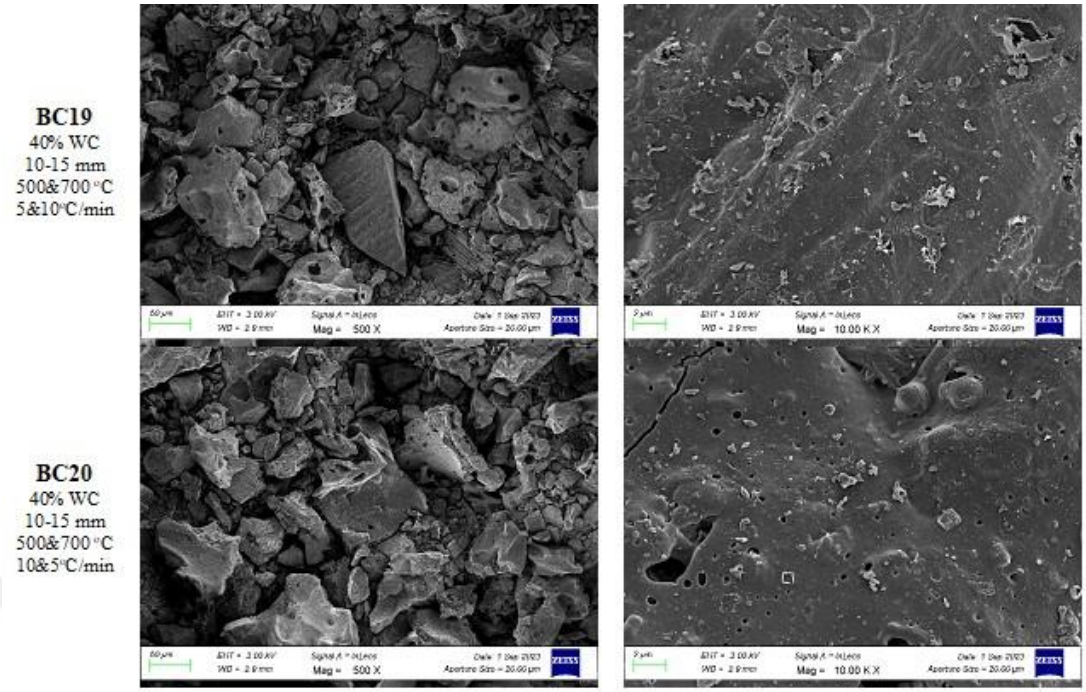

Figure 4.47 SEM figures of biochars with two stage heating and retention time conditions

Cracked structures are seen clearly in biochars produced from waste and other biomass (Figure 4.48-4.51), but the porous structure is not clear. It would be more accurate to evaluate together with BET results. When BET results were analyzed, co-pyrolysis gave better results. Therefore, co-pyrolysis of biodegradable wastes with other biomasses and addition of catalysis will improve the quality of biochar.

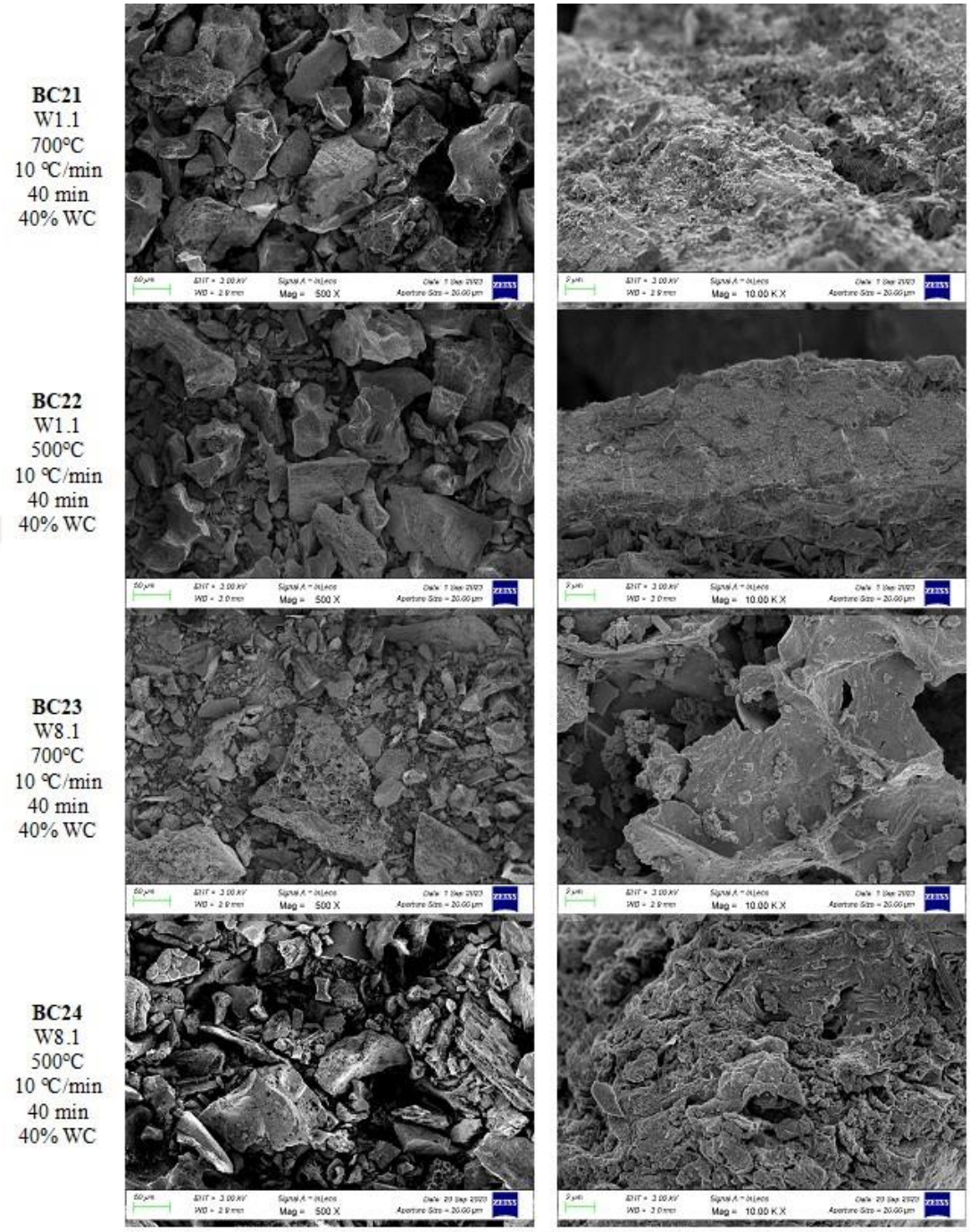

Figure 4.48 SEM figures of biochars produced from two different biodegradable wastes by pyrolysis at optimum conditions

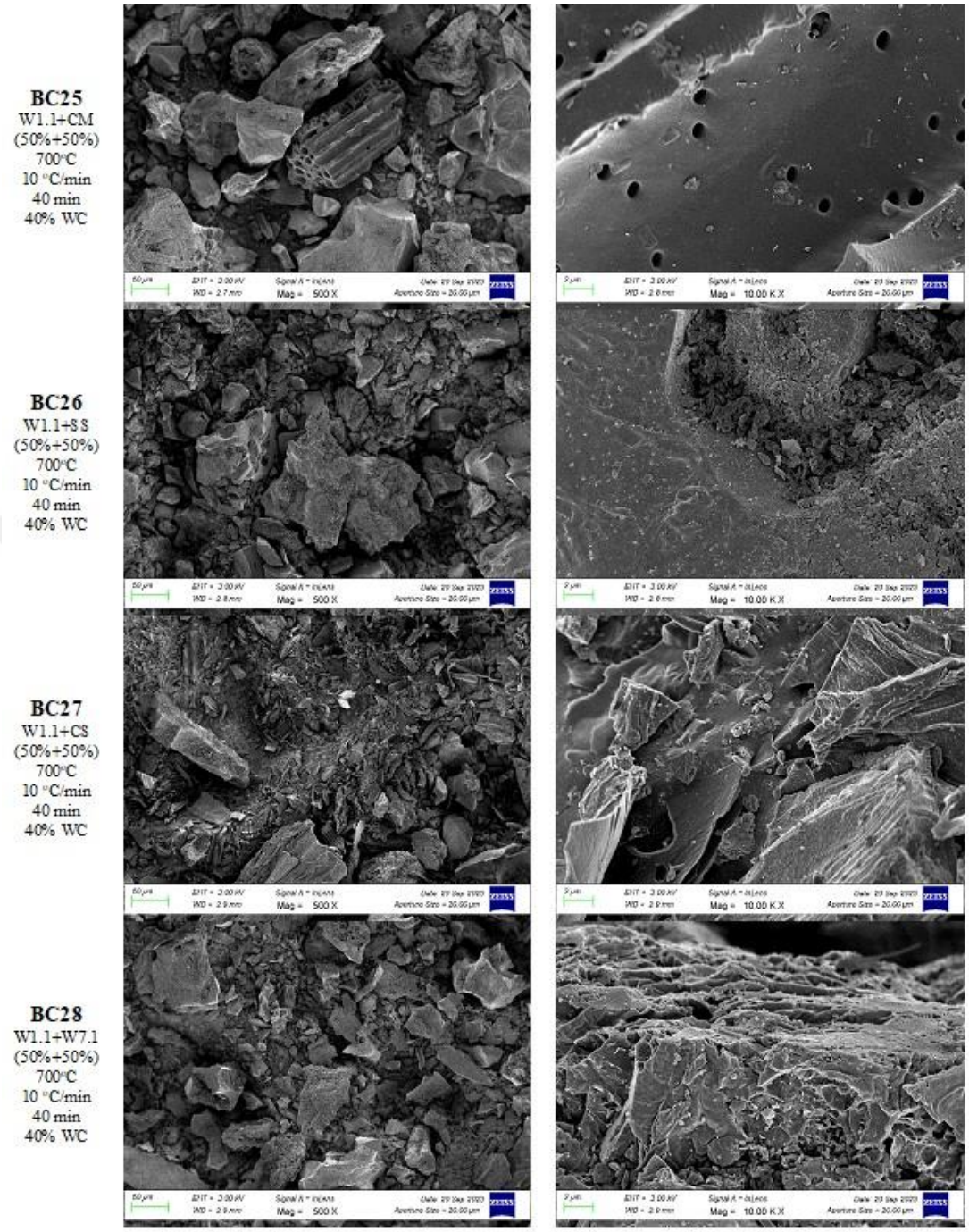

Figure 4.49 SEM figures of biochars produced by co-pyrolysis of biodegradable wastes and other biomasses at optimum conditions

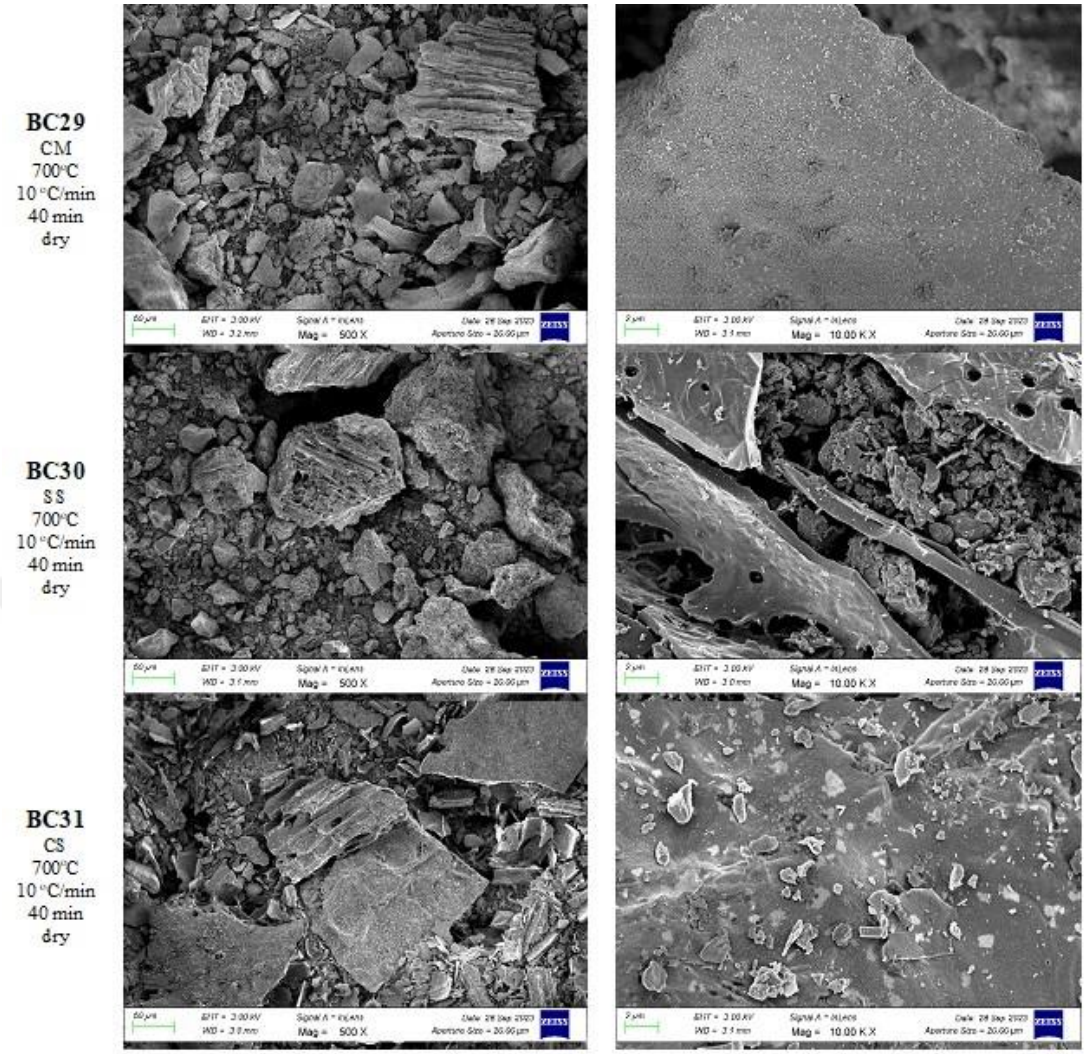

Figure 4.50 SEM figures of biochars produced by pyrolysis of dry biomasses

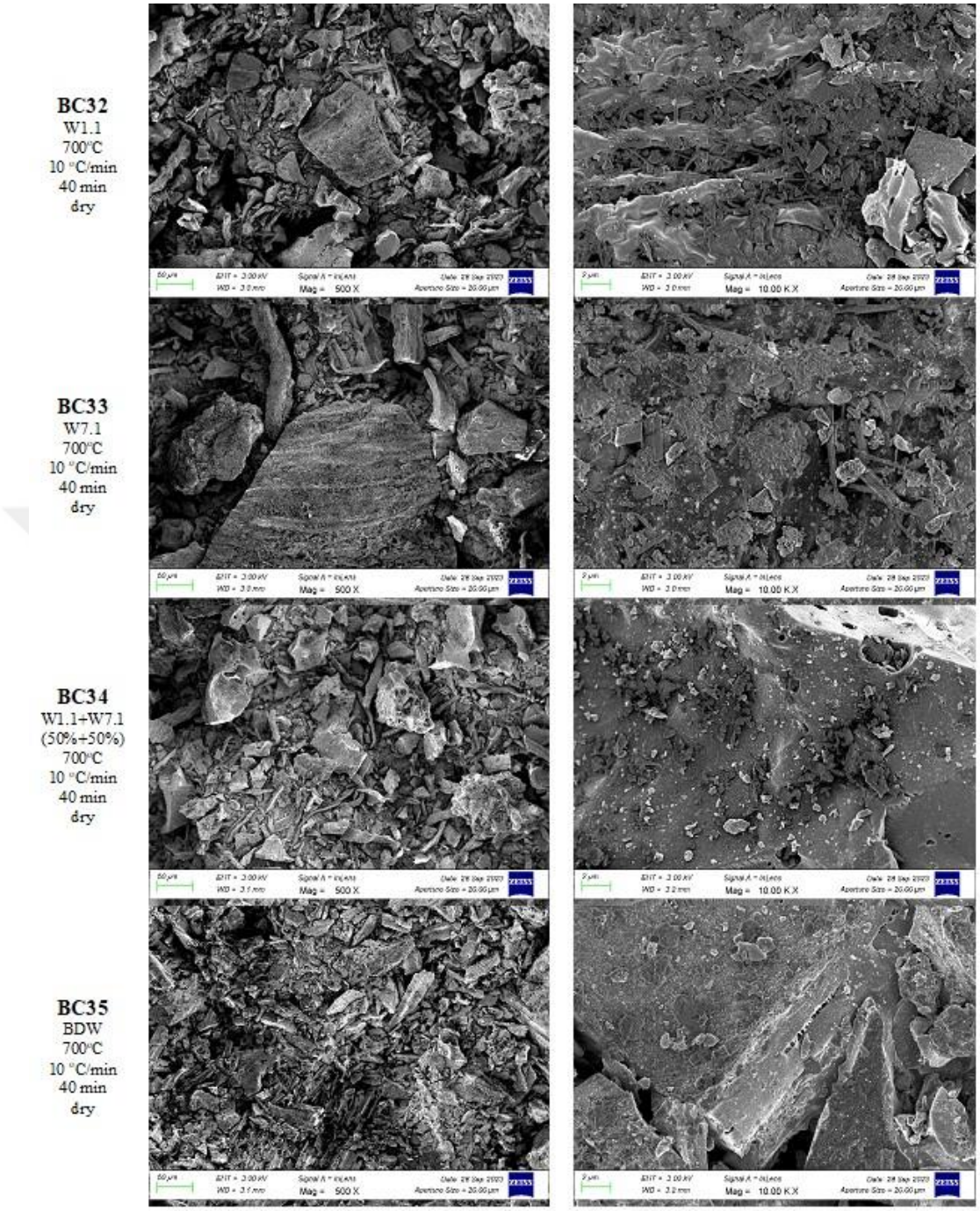

Figure 4.51 SEM figures of biochars produced by pyrolysis of dry biodegradable wastes and bio-dried biodegradable waste at optimum conditions

4.4.4.2 EDS Results of Biochars

SEM-EDS figures of feedstock and biochars produced as result of pyrolysis experiments can be seen in appendices. When we look at the results of biochar

produced as a result of pyrolysis, the carbon content varies between 10.5% (Figure-S 127 BC29) and 79.9% (Figure-S 119 BC21). While the initial carbon content of BC 21 sample was 82.27%, this rate was 79.9% in biochar. In addition, there was a slight decrease in the carbon content of the biochar formed as a result of pyrolysis with dry dog/cat food under optimum conditions (Figure-S 116 BC18) compared to the initial concentration (Figure-S 98 Feedstock). This is one of the results showing that pyrolysis is successful.

In addition to carbon and oxygen, although other contents vary according to the structure of the waste, the presence of potassium, calcium and chlorine is observed in biochars. The presence of iron (36.1%) is also observed in the biochar produced from CM (Figure-S 127 BC29). Also the co-pyrolysis of this biomass with W1.1 (Figure-S 123 BC25) has a high iron content (7.2%) compared to other samples.

Silicium is present in the biochar sample resulting from the pyrolysis of the SS sample (Figure-S 128 BC30). Its concentration decreased from 4.8% to 2.4% in the co-pyrolysis of SS sample with W1.1 (Figure-S 124 BC26).

4.4.5 In-situ gas analysis

Pyrolysis gas samples were analyzed with MRU-Optima7 after collected in collection bags. The results are given in Table 4.12. The highest amount of methane was found in the pyrolysis with CM. This was followed by the co-pyrolysis of W1.1 and CM.

Table 4.12 Methane (CH_4) results of pyrolysis gases

Experiment #	**CH_4 (L per 100 g dry waste)**	**Experiment #**	**CH_4 (L per 100 g dry waste)**
1	2.76	**19**	3.81
2	1.86	**20**	5.44
3	1.13	**21**	4.66
4	5.77	**22**	4.99
5	6.11	**23**	7.32
6	7.26	**24**	8.36
7	2.39	**25**	8.60
8	1.79	**26**	4.94

Table 4.12 Methane (CH_4) results of pyrolysis gases (continued)

Experiment #	CH_4 (L per 100 g dry waste)	Experiment #	CH_4 (L per 100 g dry waste)
9	4.51	**27**	4.72
10	4.18	**28**	5.99
11	3.39	**29**	10.63
12	3.15	**30**	3.60
13	3.63	**31**	2.99
14	2.57	**32**	4.79
15	4.36	**33**	3.81
16	4.15	**34**	3.69
17	6.11	**35**	6.44
18	7.39		

4.4.6 GC-MS Results of Bio-oils

As a result of the GC-MS analysis of the liquid product produced by pyrolysis from waste samples, a library search was performed and the results obtained together with the area distribution are given comparatively between Tables 4.13-4.21. When we look at the results in general, it is seen that mostly alkane group was formed, besides alcohols, aldehydes, ketones, alkenes and some special groups were formed. In previous studies, the most common compounds were found as alkane and alkene in bio-oil (Suriapparao & Vinu, 2015). These are followed by alcohols, aldehydes, ketones as compounds of bio-oil (Balat et al., 2009; Suriapparao & Vinu, 2015).

Alkanes belong to a category of organic substances predominantly located in fossil fuels and natural gas reservoirs. They represent the primary constituents of crude oil, comprising a substantial portion of widely used fuels like gasoline, diesel, and kerosene, crucial for powering vehicles and providing heat. Additionally, alkanes find application as foundational materials in the chemical sector, enabling the creation of a diverse range of products, including plastics, synthetic rubber, and various solvents. They frequently serve as initial building blocks for the construction of more intricate organic compounds. Alkanes assume a vital role in energy generation, transportation, and diverse industrial procedures owing to their capacity to combust and their

adaptability in chemical synthesis (Kostecki, Morrison, & Dragun, 2005; Stout & Wang, 2016).

When we look at the results of BO21(W1.1 wet) & BO32 (W1.1 dry) and BO28 (W1.1 + W7.1 wet) & BO34 (W1.1 + W7.1 dry) samples (Table 4.13 & 4.17), we can see the effect of water content. In the experiments with wet samples, we see that extra diol and ketone groups were formed. Moreover, the formation of fatty acids was observed as a result of co-pyrolysis of biodegradable municipal solid waste (W1.1) with SS (Table 4.18).

Table 4.13 GC-MS results of liquid samples of BO21 & BO32

BO21					BO32				
#	Retention Time, min	Compound Name	Area, %	Types of compounds	#	Retention Time, min	Compound Name	Area, %	Types of compounds
5	6.847	1,3,5-Pentanetriol, 3-methyl-	1.607	Alcohol	**3**	5.433	1-Hexanol	1.53	Alcohol
6	**7**	**2-Furanmethanol**	**7.63**	**Alcohol**	**6**	**6.98**	**2-Furanmethanol**	**13.811**	**Alcohol**
10	8.948	2-Furancarboxaldehyde, 5-methyl-	4.447	Aldehyde	**8**	8.935	2-Furancarboxaldehyde, 5-methyl-	1.411	Aldehyde
19	16.731	10-Octadecenal	1.579	Aldehyde	**2**	4.606	Heptane, 4-methyl-	1.704	Alkane
14	10.782	Undecane	2.043	Alkane	**10**	10.235	Dodecane	1.344	Alkane
15	13.05	Heptadecane	2.499	Alkane	**11**	10.775	Undecane	3.206	Alkane
16	13.757	Octadecane, 3-ethyl-5-(2-ethylbutyl)-	1.367	Alkane	**12**	10.842	Dodecane, 2,6,11-trimethyl-	1.961	Alkane
17	14.897	Hexadecane, 2,6,11,15-tetramethyl-	1.869	Alkane	**13**	10.929	Undecane, 4-methyl-	1.334	Alkane
18	16.518	Heptacosane	1.158	Alkane	**14**	12.604	Tetradecane, 2,6,10-trimethyl-	1.394	Alkane
4	**6.687**	**2,4-Dimethyl-1-heptene**	**1.429**	**Alkene**	**15**	13.044	Hexadecane	2.96	Alkane
12	9.028	1,4-Butanediol, 2,3-bis(methylene)-	1.509	Diols/glycols	**16**	13.131	Dodecane, 2,6,11-trimethyl-	1.824	Alkane
1	4.439	2,2-Dimethoxybutane	2.382	Ether	**17**	13.211	Dodecane, 2,6,11-trimethyl-	1.804	Alkane
2	**6.48**	**Furfural**	**5.398**	**Furan derivatives**	**18**	14.885	Tetradecane, 2-methyl-	2.834	Alkane
3	6.554	2-Cyclopenten-1-one	1.507	Ketone	**19**	16.506	Heptacosane	1.346	Alkane
7	7.354	2-Propanone, 1-(acetyloxy)-	1.735	Ketone	**5**	**6.68**	**2,4-Dimethyl-1-heptene**	**2.807**	Alkene
8	8.081	Ethanone, 1-(2-furanyl)-	5.76	Ketone	**20**	24.449	Octadecanoic acid, 2,3-dihydroxypropyl ester	2.769	Ester
11	8.995	2-Butanone, 1-(acetyloxy)-	1.121	Ketone	**1**	4.413	2,2-Dimethoxybutane	3.257	Ether
13	9.188	Phenol	2.032	Phenol	**4**	**6.474**	**Furfural**	**4.322**	**Furan derivatives**

Table 4.13 GC-MS results of liquid samples of BO21 & BO32 (continued)

BO21					BO32				
#	**Retention Time, min**	**Compound Name**	**Area, %**	**Types of compounds**	**#**	**Retention Time, min**	**Compound Name**	**Area, %**	**Types of compounds**
20	23.948	Thieno[2,3-c]furan-3-carbonitrile, 2-amino-4,6dihydro-4,4,6,6-tetramethyl	1.722	Thiophene	**7**	8.061	N-Cyano-2-methylpyrrolidine	6.531	Nitrile
9					**9**	9.181	Phenol	2.716	Phenol

Table 4.14 GC-MS results of liquid samples of BO22 & BO21

BO22					BO21				
#	**Retention Time, min**	**Compound Name**	**Area, %**	**Types of compounds**	**#**	**Retention Time, min**	**Compound Name**	**Area, %**	**Types of compounds**
6	7.054	2-Furanmethanol	10.921	Alcohol	**5**	6.847	1,3,5-Pentanetriol, 3-methyl-	1.607	Alcohol
9	8.988	2-Furancarboxaldehyde, 5-methyl-	5.533	Aldehyde	**6**	7	2-Furanmethanol	7.63	Alcohol
11	10.816	Octane, 3,5-dimethyl-	3.284	Alkane	**10**	8.948	2-Furancarboxaldehyde, 5-methyl-	4.447	Aldehyde
12	10.882	Octane, 3,5-dimethyl-	1.558	Alkane	**19**	16.731	10-Octadecenal	1.579	Aldehyde
13	13.077	Undecane, 3,7-dimethyl-	2.701	Alkane	**14**	10.782	Undecane	2.043	Alkane
14	13.163	Undecane	1.403	Alkane	**15**	13.05	Heptadecane	2.499	Alkane
15	13.25	Octane, 2,3,6,7-tetramethyl-	1.539	Alkane	**16**	13.757	Octadecane, 3-ethyl-5-(2-ethylbutyl)-	1.367	Alkane
16	14.911	2-Bromo dodecane	2.497	Alkane	**17**	14.897	Hexadecane, 2,6,11,15-tetramethyl-	1.869	Alkane
19	16.199	Dodecane, 1-iodo-	3.563	Alkane	**18**	16.518	Heptacosane	1.158	Alkane
20	16.513	Heptadecane, 2,6,10,15-tetramethyl-	1.843	Alkane	**4**	6.687	2,4-Dimethyl-1-heptene	1.429	Alkene
4	6.74	2,4-Dimethyl-1-heptene	2.822	Alkene	**12**	9.028	1,4-Butanediol, 2,3-bis(methylene)-	1.509	Diols/glycols
18	15.966	1-Methyldodecylamine	3.045	Amine	**1**	4.439	2,2-Dimethoxybutane	2.382	Ether
1	4.513	2,2-Dimethoxybutane	3.751	Ether	**2**	6.48	Furfural	5.398	Furan derivatives
2	6.54	Furfural	6.616	Furan derivatives	**3**	6.554	2-Cyclopenten-1-one	1.507	Ketone
3	6.6	2-Cyclopenten-1-one	2.671	Ketone	**7**	7.354	2-Propanone, 1-(acetyloxy)-	1.735	Ketone
7	7.408	2-Propanone, 1-(acetyloxy)-	2.136	Ketone	**8**	8.081	Ethanone, 1-(2-furanyl)-	5.76	Ketone
8	8.121	1-(3H-Imidazol-4-yl)-ethanone	6.23	Ketone	**11**	8.995	2-Butanone, 1-(acetyloxy)-	1.121	Ketone
5	6.901	2-Butanamine, N-nitro-	1.513	Nitroamine	**13**	9.188	Phenol	2.032	Phenol

Table 4.14 GC-MS results of liquid samples of BO22 & BO21 (continued)

BO22					BO21				
#	**Retention Time, min**	**Compound Name**	**Area, %**	**Types of compounds**	**#**	**Retention Time, min**	**Compound Name**	**Area, %**	**Types of compounds**
10	9.228	Phenol	2.124	Phenol	**20**	23.948	Thieno[2,3-c]furan-3-carbonitrile, 2-amino-4,6dihydro-4,4,6,6-tetramethyl	1.722	Thiophene
17	15.725	Nitrous oxide	3.036	Other					

Table 4.15 GC-MS results of liquid samples of BO23 & BO24

BO23					BO24				
#	**Retention Time, min**	**Compound Name**	**Area, %**	**Types of compounds**	**#**	**Retention Time, min**	**Compound Name**	**Area, %**	**Types of compounds**
6	7.061	2-Furanmethanol	11.159	Alcohol	**4**	6.513	13-Heptadecyn-1-ol	1.439	Alcohol
2	4.686	Pentane, 3-ethyl-	1.815	Alkane	**7**	6.994	2-Furanmethanol	5.037	Alcohol
10	10.282	Nonane, 1-iodo-	1.5	Alkane	**8**	8.067	Cyclohexanol, 2,3-dimethyl-	3.882	Alcohol
11	10.816	Undecane, 4,7-dimethyl-	4.087	Alkane	**10**	10.782	Octadecane, 3-ethyl-5-(2-ethylbutyl)-	1.036	Alkane
13	13.077	Hexane, 3,3-dimethyl-	2.719	Alkane	**5**	6.687	2,4-Dimethyl-1-heptene	1.085	Alkene
14	13.17	Nonane, 1-iodo-	1.306	Alkane	**19**	21.006	Ethyl iso-allocholate	1.518	Allocholic acid
15	13.243	Pentane, 3,3-dimethyl-	1.269	Alkane	**14**	19.872	1,4-Benzenediol, 2,6-bis(1,1-dimethylethyl)-	1.857	Diol
5	6.747	2,4-Dimethyl-1-heptene	3.726	Alkene	**9**	9.181	Carbamic acid, phenyl ester	2.003	Ester
1	4.506	2,2-Dimethoxybutane	4.912	Ether	**1**	4.413	2,2-Dimethoxybutane	2.474	Ether
4	6.574	Furfural	1.443	Furan derivatives	**6**	6.834	Octaethylene glycol monododecyl ether	0.876	Ether
3	5.533	Cyclopentanone	1.176	Ketone	**11**	15.41	2-Myristynoyl pantetheine	1.406	Fatty acid
7	8.068	2-Cyclopenten-1-one, 2-methyl-	2.394	Ketone	**12**	17.991	2-Myristynoyl pantetheine	0.899	Fatty acid
8	8.128	Ethanone, 1-(2-furanyl)-	7.393	Ketone	**3**	6.48	Furfural	1.418	Furan derivatives
16	14.911	3-Hexanone, 2,5-dimethyl-	2.168	Ketone	**15**	20.052	Tetraacetyl-d-xylonic nitrile	1.569	Nitrile
9	9.228	Phenol	4.118	Phenol	**13**	19.612	1-(2-Acetoxyethyl)-3,6-diazahomoadamantan-9one oxime	2.382	Other

Table 4.15 GC-MS results of liquid samples of BO23 & BO24 (continued)

BO23					BO24				
#	**Retention Time, min**	**Compound Name**	**Area, %**	**Types of compounds**	**#**	**Retention Time, min**	**Compound Name**	**Area, %**	**Types of compounds**
12	10.882	1H-Tetrazol-5-amine	2.238	Tetrazole	**18**	20.672	1-(2-Acetoxyethyl)-3,6-diazahomoadamantan-9one oxime	1.051	Other
17	19.486	Nitrous oxide	1.205	Other	**20**	23.647	1-(2-Acetoxyethyl)-3,6-diazahomoadamantan-9one oxime	0.967	Other
18	19.966	Nitrous oxide	8.733	Other	**2**	5.42	2-Amino-oxazole	1.797	Oxazole
19	20.326	Nitrous oxide	8.862	Other	**17**	20.492	Pterin-6-carboxylic acid	1.776	Pterin
20	20.574	Nitrous oxide	7.864	Other	**16**	20.266	Pyrazole[4,5-b]imidazole, 1-formyl-3-ethyl-6-á-dribofuranosyl	1.532	Pyrazole

Table 4.16 GC-MS results of liquid samples of BO25 & BO29

BO25					BO29				
#	**Retention Time, min**	**Compound Name**	**Area, %**	**Types of compounds**	**#**	**Retention Time, min**	**Compound Name**	**Area, %**	**Types of compounds**
7	13.696	1-Hexadecanol	1.635	Alcohol	**10**	13.71	1-Hexadecanol	1.595	Alcohol
5	10.802	Undecane	1.517	Alkane	**4**	8.008	Cyclopropane-1,1,2,2-tetracarbonitrile, 3-ethyl-3methyl	1.724	Alkane
6	12.863	Tetradecane	2.039	Alkane	**6**	10.715	4-Trifluoroacetoxytetradecane	1.87	Alkane
8	13.77	Tetradecane	1.542	Alkane	**7**	10.815	Undecane	2.738	Alkane
9	14.55	1-Nonadecene	2.16	Alkane	**8**	11.896	Dodecane	1.349	Alkane
10	14.617	Nonadecane	3.205	Alkane	**9**	12.87	Tridecane	2.94	Alkane
11	15.41	Hexadecane	1.261	Alkane	**11**	13.777	Tetradecane	2.005	Alkane
13	16.17	Heptadecane	2.608	Alkane	**12**	14.564	2-Trifluoroacetoxypentadecane	1.951	Alkane
2	6.734	2,4-Dimethyl-1-heptene	1.489	Alkene	**13**	14.624	Pentadecane	3.671	Alkane
4	10.468	p-Cresol	1.609	Cresol	**14**	15.424	Hexadecane	1.364	Alkane
12	16.117	Acetic acid, chloro-, octadecyl ester	1.219	Ester	**16**	16.179	Heptadecane	2.315	Alkane
1	4.479	2,2-Dimethoxybutane	1.62	Ether	**3**	6.74	2,4-Dimethyl-1-heptene	2.459	Alkene
15	17.945	n-Hexadecanoic acid	8.793	Fatty acid	**2**	4.686	Benzene, (3-octylundecyl)-	1.334	Benzene
18	19.072	Oleic Acid	1.786	Fatty acid	**5**	9.228	Carbamic acid, phenyl ester	1.715	Ester
19	19.212	Octadecanoic acid	1.562	Fatty acid	**1**	4.499	2,2-Dimethoxybutane	2.06	Ether
20	19.338	9-Octadecenamide, (Z)-	2.55	Fatty acid	**18**	17.953	n-Hexadecanoic acid	2.368	Fatty acid
14	17.578	Hexadecanenitrile	13.632	Nitrile	**15**	16.139	Hexadecanenitrile	1.341	Nitrile
16	18.758	9-Octadecenenitrile, (Z)-	7.295	Nitrile	**17**	17.593	Hexadecanenitrile	21.076	Nitrile
17	18.898	Octadecanenitrile	9.355	Nitrile	**19**	18.766	9-Octadecenenitrile, (Z)-	9.475	Nitrile
3	9.214	Phenol	2.329	Phenol	**20**	18.906	Octadecanenitrile	12.856	Nitrile

Table 4.17 GC-MS results of liquid samples of BO28 & BO34

BO28					BO34				
#	Retention Time, min	Compound Name	Area, %	Types of compounds	#	Retention Time, min	Compound Name	Area, %	Types of compounds
7	7.054	2-Furanmethanol	7.511	Alcohol	**4**	7.047	2-Furanmethanol	10.914	Alcohol
9	8.128	Cyclohexanol, 3,3-dimethyl-	5.729	Alcohol	**13**	13.043	1-Hexadecanol, 2-methyl-	1.39	Alcohol
19	35.333	d-Mannitol, 1-decylsulfonyl-	1.532	Alcohol	**2**	4.693	Heptane, 4-methyl-	2.348	Alkane
10	8.988	2-Furancarboxaldehyde, 5-methyl-	1.733	Aldehyde	**7**	9.655	3-Ethyl-3-methylnonadecane	1.461	Alkane
2	4.693	Heptane, 4-methyl-	1.573	Alkane	**8**	10.275	Dodecane, 2,6,10-trimethyl-	1.856	Alkane
12	10.815	Dodecane, 2,6,10-trimethyl-	3.056	Alkane	**9**	10.815	Nonane, 4,5-dimethyl-	4.25	Alkane
13	10.882	Tetradecane, 2,6,10-trimethyl-	1.862	Alkane	**10**	10.882	Dodecane	2.096	Alkane
14	13.076	Dodecane, 2,6,11-trimethyl-	2.336	Alkane	**11**	10.962	Undecane, 4-methyl-	1.507	Alkane
15	13.163	Heptadecane, 9-hexyl-	1.437	Alkane	**12**	12.643	Nonadecane	1.693	Alkane
16	13.243	Heptadecane, 9-hexyl-	1.481	Alkane	**14**	13.076	Dodecane, 2,6,11-trimethyl-	3.589	Alkane
17	14.91	Hexadecane, 2,6,11,15-tetramethyl-	2.138	Alkane	**15**	13.163	Dodecane, 2,6,11-trimethyl-	2.303	Alkane
18	16.511	Heptadecane, 9-hexyl-	1.476	Alkane	**16**	13.243	Hexadecane, 2,6,11,15-tetramethyl-	2.156	Alkane
5	6.74	2,4-Dimethyl-1-heptene	2.635	Alkene	**17**	14.911	Hexadecane, 2,6,11,15-tetramethyl-	3.744	Alkane
6	6.9	Octaethylene glycol monododecyl ether	1.468	Diol	**18**	14.991	Hexadecane, 2,6,11,15-tetramethyl-	1.383	Alkane
1	4.513	2,2-Dimethoxybutane	3.659	Ether	**19**	16.511	Nonadecane, 2-methyl-	1.574	Alkane
20	35.6	1-(2-Acetoxyethyl)-3,6-diazahomoadamantan-9one oxime	1.525	Ethyl	**3**	6.747	2,4-Dimethyl-1-heptene	4.089	Alkene
3	6.547	Furfural	2.874	Furan derivatives	**5**	8.128	Butyrolactone	5.461	Ester
4	6.587	2-Cyclopenten-1-one	2.864	Ketone	**20**	24.014	Octadecanoic acid, 2,3-dihydroxypropyl ester	3.898	Ester
8	8.061	2-Cyclopenten-1-one, 2-methyl-	1.713	Ketone	**1**	4.506	2,2-Dimethoxybutane	3.225	Ether
11	9.228	Phenol	3.735	Phenol	**6**	9.228	Phenol	1.43	Phenol

Table 4.18 GC-MS results of liquid samples of BO26 & BO30

BO26					BO30				
#	Retention Time, min	Compound Name	Area, %	Types of compounds	#	Retention Time, min	Compound Name	Area, %	Types of compounds
1	4.693	Heptane, 4-methyl-	2.692	Alkane	**1**	7.847	Dodecanal	2.933	Aldehyde
3	9.662	Nonane, 2,6-dimethyl-	1.582	Alkane	**5**	11.289	10-Octadecenal	1.476	Aldehyde
4	9.722	Octane, 3,3-dimethyl-	1.793	Alkane	**8**	12.523	10-Octadecenal	1.973	Aldehyde
5	10.282	Undecane, 4,7-dimethyl-	2.595	Alkane	**9**	13.183	10-Octadecenal	3.17	Aldehyde
7	10.595	2,6-Dimethyl-6-trifluoroacetoxyoctane	1.647	Alkane	**12**	13.59	Octadecanal	2.399	Aldehyde
8	10.815	Undecane, 5,7-dimethyl-	6.031	Alkane	**16**	19.372	10-Octadecenal	1.639	Aldehyde
9	10.882	Undecane, 4,7-dimethyl-	3.057	Alkane	**2**	7.981	Cyclobutane, 1,1-dimethyl-2-octyl-	2.792	Alkane
10	10.969	Octane, 6-ethyl-2-methyl-	2.042	Alkane	**7**	12.429	Tetradecane, 2,6,10-trimethyl-	2.276	Alkane
11	12.643	Dodecane, 2,6,11-trimethyl-	2.126	Alkane	**11**	13.436	Pentadecane	4.46	Alkane
14	13.083	Dodecane, 2,7,10-trimethyl-	5.063	Alkane	**14**	14.884	Tetradecane, 2,6,10-trimethyl-	1.485	Alkane
15	13.17	Dodecane, 2,6,10-trimethyl-	2.84	Alkane	**15**	14.977	Tetradecane, 2,6,10-trimethyl-	1.733	Alkane
16	13.25	Dodecane, 2,6,11-trimethyl-	2.778	Alkane	**6**	11.649	5,9-Undecadien-2-one, 6,10-dimethyl-	6.782	Ketone
17	14.911	Dodecane, 2,6,11-trimethyl-	4.906	Alkane	**10**	13.31	2,6-Dihydroxyacetophenone, 2TMS derivative	9.867	Ketone
19	16.518	Hexadecane, 2,6,11,15-tetramethyl-	2.621	Alkane	**18**	20.259	Tetraacetyl-d-xylonic nitrile	1.688	Nitrile
2	6.747	2,4-Dimethyl-1-heptene	6.292	Alkene	**4**	11.175	Pterin-6-carboxylic acid	1.656	Pterin
6	10.542	1-Octene, 3,7-dimethyl-	1.745	Alkene	**17**	19.639	Pterin-6-carboxylic acid	3.079	Pterin
12	12.976	1-Nonene, 4,6,8-trimethyl-	1.883	Alkene	**19**	20.799	Pterin-6-carboxylic acid	1.383	Pterin
13	13.05	1-Nonene, 4,6,8-trimethyl-	1.963	Alkene	**20**	20.986	Pterin-6-carboxylic acid	1.447	Pterin
18	14.997	Sulfurous acid, hexyl pentadecyl ester	1.842	Ester	**13**	14.257	tert-Hexadecanethiol	2.038	Thiol
20	24.028	Octadecanoic acid, 2,3-dihydroxypropyl ester	5.685	Ester					

Table 4.19 GC-MS results of liquid samples of BO27 & BO31

BO27					BO31				
#	Retention Time, min	Compound Name	Area, %	Types of compounds	#	Retention Time, min	Compound Name	Area, %	Types of compounds
6	7.054	2-Furanmethanol	9.971	Alcohol	**5**	6.907	1,3,5-Pentanetriol, 3-methyl-	1.236	Alcohol
11	9.662	2-Furanmethanol, tetrahydro-	3.08	Alcohol	**6**	7.061	2-Furanmethanol	5.099	Alcohol
2	4.693	Pentane, 3-ethyl-	2.161	Alkane	**2**	4.686	Butane, 1-(ethenyloxy)-3-methyl-	1.5	Alkane
14	10.816	Hexane, 3,3-dimethyl-	4.855	Alkane	**11**	9.655	Octane, 2,6-dimethyl-	1.759	Alkane
15	10.882	Octane, 2,6,6-trimethyl-	2.156	Alkane	**12**	10.275	Tetradecane, 2,6,10-trimethyl-	1.181	Alkane
17	13.083	Hexane, 3,3-dimethyl-	4.44	Alkane	**13**	10.815	Undecane	2.726	Alkane
20	14.911	Decane, 1-iodo-	2.866	Alkane	**14**	10.882	Decane	1.304	Alkane
5	6.747	2,4-Dimethyl-1-heptene	4.216	Alkene	**15**	12.643	Heptadecane, 2,6,10,15-tetramethyl-	1.185	Alkane
8	8.134	Azetidine, 1-nitroso-	9.424	Azetidine	**16**	13.076	Dodecane, 2,6,11-trimethyl-	2.294	Alkane
9	8.995	Benzeneethanol, 3-fluoro-	2.656	Benzene	**17**	13.163	Tetradecane, 2,6,10-trimethyl-	1.492	Alkane
13	10.495	Carbamic acid, methyl-, 3-methylphenyl ester	1.354	Ester	**18**	13.243	Tetradecane, 2,6,10-trimethyl-	1.373	Alkane
1	4.513	2,2-Dimethoxybutane	4.613	Ether	**19**	14.91	Nonadecane	2.465	Alkane
10	9.228	2-Vinylfuran	7.024	Furan	**20**	16.511	Tetradecane, 2,6,10-trimethyl-	1.769	Alkane
3	6.54	Furfural	9.436	Furan derivatives	**4**	6.74	2,4-Dimethyl-1-heptene	2.59	Alkene
7	7.387	2-Propanone, 1-(acetyloxy)-	5.684	Ketone	**1**	4.506	2,2-Dimethoxybutane	2.781	Ether
12	10.282	3-Hexanone, 2,5-dimethyl-	1.713	Ketone	**3**	6.534	Furfural	6.144	Furan derivatives
16	12.643	3-Hexanone, 2,5-dimethyl-	1.371	Ketone	**9**	9.001	Imidazole, 2-amino-5-[(2-carboxy)vinyl]-	1.024	Imidazole
18	13.17	4-Heptanone, 3-methyl-	1.609	Ketone	**7**	7.387	2-Propanone, 1-(acetyloxy)-	3.883	Ketone
19	13.243	3-Hexanone, 2,5-dimethyl-	1.64	Ketone	**10**	9.228	Phenol	1.83	Phenol
4	6.607	1,2,4,5-Tetrazine	1.748	Tetrazine	**8**	8.134	endo-Borneol	3.321	Terpene

Table 4.20 GC-MS results of liquid samples of BO33 & BO35

BO33					BO35				
#	Retention Time, min	Compound Name	Area, %	Types of compounds	#	Retention Time, min	Compound Name	Area, %	Types of compounds
5	7	2-Furanmethanol	8.575	Alcohol	**6**	6.994	2-Furanmethanol	5.514	Alcohol
2	4.606	Heptane, 4-methyl-	2.139	Alkane	**10**	9.582	2-Furanmethanol, tetrahydro-	1.441	Alcohol
7	9.622	Nonane, 2,6-dimethyl-	1.308	Alkane	**3**	4.606	Heptane, 4-methyl-	1.84	Alkane
8	10.242	Dodecane, 2,6,10-trimethyl-	1.796	Alkane	**11**	10.502	3-Trifluoroacetoxydodecane	1.368	Alkane
9	10.782	2,6-Dimethyldecane	4.237	Alkane	**13**	10.776	Dodecane, 2,6,10-trimethyl-	3.019	Alkane
10	10.842	2,6-Dimethyldecane	2.144	Alkane	**14**	10.842	Tridecane	2.335	Alkane
11	10.929	Undecane, 4-methyl-	1.452	Alkane	**16**	13.05	Dodecane, 2,6,11-trimethyl-	2.456	Alkane
12	12.616	Dodecane, 2,6,11-trimethyl-	1.539	Alkane	**17**	13.137	Heptacosane	1.552	Alkane
13	13.05	Dodecane, 2,6,11-trimethyl-	3.46	Alkane	**18**	13.217	Heptacosane	1.572	Alkane
14	13.136	Pentadecane	2.105	Alkane	**19**	14.891	Hexadecane, 2,6,11,15-tetramethyl-	2.564	Alkane
15	13.216	Dodecane, 2,6,11-trimethyl-	2.145	Alkane	**5**	6.687	2,4-Dimethyl-1-heptene	3.449	Alkene
16	14.89	Dodecane, 2,6,11-trimethyl-	3.575	Alkane	**20**	24.501	Ethyl iso-allocholate	2.188	Allocholic acid
17	14.971	Hexadecane, 2,6,11,15-tetramethyl-	1.379	Alkane	**15**	11.016	3-Hydroxymandelic acid, ethyl ester, di-TMS	2.119	Benzene
18	16.505	Heptacosane	2.148	Alkane	**7**	8.068	Butyrolactone	5.881	Ester
19	16.711	Heptacosane	1.284	Alkane	**2**	4.419	2,2-Dimethoxybutane	2.983	Ether
3	6.687	2,4-Dimethyl-1-heptene	3.845	Alkene	**9**	9.188	Phenol	2.144	Phenol
6	8.088	Butyrolactone	4.354	Ester	**12**	10.622	Phenol, 2-methoxy-	4.051	Phenol
20	24.248	Octadecanoic acid, 2,3-dihydroxypropyl ester	4.105	Ester	**4**	6.333	Pyrimidine, 2-methyl-	2.338	Pyrimidine
1	4.426	2,2-Dimethoxybutane	3.283	Ether	**1**	4.159	Pyrrole	1.406	Pyrrole
4	6.84	1,3,3-Trimethoxybutane	1.331	Ether					

Table 4.21 GC-MS results of liquid samples of BO18 & BO21

BO18					BO21				
	Retention Time, min	Compound Name	Area, %	Types of compounds	#	Retention Time, min	Compound Name	Area, %	Types of compounds
1	4.686	Heptane, 4-methyl-	1.767	Alkane	**5**	6.847	1,3,5-Pentanetriol, 3-methyl-	1.607	Alcohol
2	10.269	Undecane	1.895	Alkane	**6**	7	2-Furanmethanol	7.63	Alcohol
3	10.582	Cyclooctane, 1,4-dimethyl-, cis-	1.437	Alkane	**10**	8.948	2-Furancarboxaldehyde, 5-methyl-	4.447	Aldehyde
4	10.809	Undecane	4.695	Alkane	**19**	16.731	10-Octadecenal	1.579	Aldehyde
5	10.869	Dodecane	2.485	Alkane	**14**	10.782	Undecane	2.043	Alkane
6	10.956	Undecane, 4-methyl-	1.696	Alkane	**15**	13.05	Heptadecane	2.499	Alkane
7	12.636	Dodecane, 2,6,11-trimethyl-	1.803	Alkane	**16**	13.757	Octadecane, 3-ethyl-5-(2-ethylbutyl)-	1.367	Alkane
8	12.963	1-Nonene, 4,6,8-trimethyl-	1.874	Alkane	**17**	14.897	Hexadecane, 2,6,11,15-tetramethyl-	1.869	Alkane
9	13.07	Dodecane, 2,6,11-trimethyl-	4.241	Alkane	**18**	16.518	Heptacosane	1.158	Alkane
10	13.156	Dodecane, 2,6,11-trimethyl-	2.553	Alkane	**4**	6.687	2,4-Dimethyl-1-heptene	1.429	Alkene
11	13.236	Dodecane, 2,6,11-trimethyl-	2.522	Alkane	**12**	9.028	1,4-Butanediol, 2,3-bis(methylene)-	1.509	Diols/glycols
12	14.904	Dodecane, 2,6,11-trimethyl-	4.26	Alkane	**1**	4.439	2,2-Dimethoxybutane	2.382	Ether
13	14.984	Dodecane, 2,6,11-trimethyl-	1.77	Alkane	**2**	6.48	Furfural	5.398	Furan derivatives
14	16.505	Eicosane, 2-methyl-	1.851	Alkane	**3**	6.554	2-Cyclopenten-1-one	1.507	Ketone
15	17.945	2-Methylhexacosane	2.241	Alkane	**7**	7.354	2-Propanone, 1-(acetyloxy)-	1.735	Ketone
16	6.734	2,4-Dimethyl-1-heptene	4.222	Alkene	**8**	8.081	Ethanone, 1-(2-furanyl)-	5.76	Ketone

Table 4.21 GC-MS results of liquid samples of BO18 & BO21 (continued)

17	13.043	Trichloroacetic acid, pentadecyl ester	1.818	Ester
19	24.034	Octadecanoic acid, 2,3-dihydroxypropyl ester	10.133	Ester
11	8.995	2-Butanone, 1-(acetyloxy)-	1.121	Ketone
13	9.188	Phenol	2.032	Phenol
20	23.948	Thieno[2,3-c]furan-3-carbonitrile, 2-amino-4,6dihydro-4,4,6,6-tetramethyl	1.722	Thiophene

4.4.7 GC-MS Results of Non-Condensable Gases

The GC-MS results of two gas samples are be given in Figure 4.52 & 4.53.

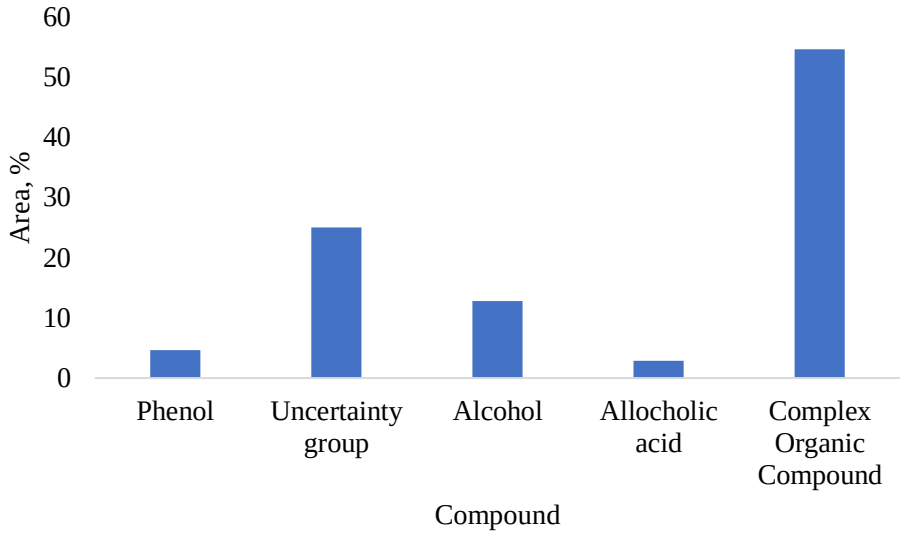

Figure 4.52 GC-MS result of gas sample from experiment 28

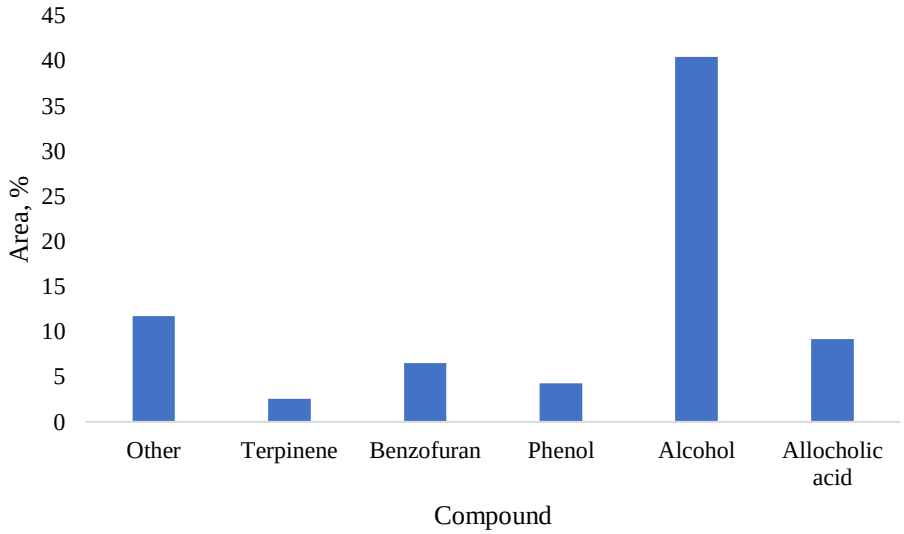

Figure 4.53 GC-MS result of gas sample from experiment 31

4.5 Results of Statistical Analysis

4.5.1 Results of statistical analysis for characteristics of raw materials

Correlation analyses using Pearson's correlation coefficients were carried out to identify the interrelations among the analysis results, which are size, organic matter content (OMC), volatile matter (VM), ash, fixed carbon (FC), calorific value (CV), C, H, S, O, lowest weight loss temperature (LWL), highest weight loss temperature (HLW), exothermic reaction temperature (ER), first char formation temperature (FCF) and second char formation temperature (SCF) using SPSS version 24.0.

The effect from the organic structure of the substance (OMC, VM, FC, CV, C, H, N, S and O) is seen in the correlation results (Table 4.22). Principal component analysis explained 89.094% of variance (Table 4.23). KMO and Bartlett's Test results are given in Table 4.24.

If we look at the component analysis (Table 4.25), four components were identified. The first component can be explained by the organic and inorganic content of the raw materials. The second component shows the presence of protein in the wastes. The sulfur and nitrogen contents are due to the protein present in the waste. The third component shows the effect of inorganic content on weight loss and exothermic reaction. The temperature increases as the inorganic content volatilizes later, which is supported by the correlation between ash and highest weight loss temperature (r:0.565, $p \leq 0,01$). Likewise, the fourth component is linked to the inorganic content. Since inorganics volatilize later, char formation takes place later. This situation is also observed in correlation between ash and second char formation temperature (r:0.417, $p \leq 0,05$). These results can be better evaluated after the XRD results are available. In addition, the increase in organic content allows the raw material to be exposed to the degradation at lower temperatures. Correlations between highest weight loss temperature and OMC, VM, FC, CV, C and H are the proof of this situation (r:-0.464, $p \leq 0,05$; r:-0.410, $p \leq 0,05$; r:-0.574, $p \leq 0,01$; r:-0.541, $p \leq 0,01$; r:-0.521, $p \leq 0,01$; r:-0.441, $p \leq 0,05$, respectively.)

Table 4.22 Correlations among the analysis results of raw materials

		Size, cm	OMC $\%_{dw}$	VM $\%_{dw}$	Ash $\%_{dw}$	FC $\%_{dw}$	CV $kcal/kg_{dw}$	C $\%_{dw}$	H $\%_{dw}$	N $\%_{dw}$	S $\%_{dw}$	O $\%_{dw}$	LWL °C	HLW °C	ER °C	FCF °C	SCF °C
Size cm	r	1	0.211	0.113	-0.067	0.021	-0.094	-0.045	-0.066	-0.336	-0.241	0.117	-0.185	0.105	0.154	0.229	0.177
	p		*0.312*	*0.591*	*0.752*	*0.919*	*0.655*	*0.829*	*0.753*	*0.101*	*0.246*	*0.576*	*0.377*	*0.618*	*0.461*	*0.270*	*0.398*
OMC $\%_{dw}$	r		1	**,850****	**-,845****	**,576****	**,582****	**,812****	**,822****	0.013	-0.106	**-,732****	0.227	**-,464***	-0.319	0.043	-0.066
	p			*0.000*	*0.000*	*0.003*	*0.002*	*0.000*	*0.000*	*0.950*	*0.613*	*0.000*	*0.276*	*0.020*	*0.121*	*0.836*	*0.753*
VM $\%_{dw}$	r			1	**-,915****	**,521****	**,718****	**,906****	**,923****	0.258	0.111	**-,872****	**,423***	**-,410***	-0.188	-0.150	-0.296
	p				*0.000*	*0.008*	*0.000*	*0.000*	*0.000*	*0.213*	*0.596*	*0.000*	*0.035*	*0.042*	*0.367*	*0.474*	*0.150*
Ash $\%_{dw}$	r				1	**-,818****	**-,664****	**-,850****	**-,846****	-0.136	-0.072	**,793****	**-,537****	**,565****	0.266	0.272	**,417***
	p					*0.000*	*0.000*	*0.000*	*0.000*	*0.517*	*0.734*	*0.000*	*0.006*	*0.003*	*0.199*	*0.189*	*0.038*
FC $\%_{dw}$	r					1	0.391	**,494***	**,467***	-0.102	-0.029	**-,420***	**,548****	**-,574****	-0.265	-0.354	**-,465***
	p						*0.054*	*0.012*	*0.019*	*0.628*	*0.892*	*0.037*	*0.005*	*0.003*	*0.200*	*0.083*	*0.019*
CV $kcal/kg_{dw}$	r						1	**,838****	**,831****	**,549****	**,431***	**-,874****	**,533****	**-,541****	-0.226	0.031	-0.061
	p							*0.000*	*0.000*	*0.005*	*0.032*	*0.000*	*0.006*	*0.005*	*0.277*	*0.883*	*0.773*
C $\%_{dw}$	r							1	**,969****	0.381	0.215	**-,978****	**,444***	**-,521****	-0.272	-0.074	-0.196
	p								*0.000*	*0.060*	*0.302*	*0.000*	*0.026*	*0.008*	*0.189*	*0.726*	*0.347*
H $\%_{dw}$	r								1	0.390	0.243	**-,961****	**,426***	**-,441***	-0.238	-0.088	-0.175
	p									*0.054*	*0.242*	*0.000*	*0.034*	*0.027*	*0.253*	*0.674*	*0.404*
N $\%_{dw}$	r									1	**,763****	**-,564****	0.347	-0.252	0.004	-0.104	-0.113
	p										*0.000*	*0.003*	*0.089*	*0.225*	*0.985*	*0.619*	*0.591*

Table 4.22 Correlations among the analysis results of raw materials (continued)

		Size, cm	OMC $\%_{dw}$	VM $\%_{dw}$	Ash $\%_{dw}$	FC $\%_{dw}$	CV kcal/kg_{dw}	C $\%_{dw}$	H $\%_{dw}$	N $\%_{dw}$	S $\%_{dw}$	O $\%_{dw}$	LWL °C	HLW °C	ER °C	FCF °C	SCF °C
S $\%_{dw}$	r										1	-0.375	0.392	-0.210	0.136	-0.245	-0.137
	p											*0.065*	*0.052*	*0.314*	*0.517*	*0.237*	*0.513*
O $\%_{dw}$	r											1	**-,477***	**,514****	0.236	0.095	0.200
	p												*0.016*	*0.009*	*0.255*	*0.650*	*0.339*
LWL °C	r												1	-0.344	0.199	-0.358	**-,548****
	p													*0.092*	*0.340*	*0.079*	*0.005*
HLW °C	r													1	**,605****	0.223	0.161
	p														*0.001*	*0.285*	*0.441*
ER °C	r														1	0.089	0.001
	p															*0.671*	*0.997*
FCF °C	r															1	**,891****
	p																0.000
SCF °C	r																1
	p																

**. Correlation is significant at the 0.01 level (2-tailed).
*. Correlation is significant at the 0.05 level (2-tailed).

Table 4.23 Total variance explained with PCA

Component	Initial Eigenvalues			Extraction Sums of Squared Loadings			Rotation Sums of Squared Loadings		
	Total	**% of Variance**	**Cumulative %**	**Total**	**% of Variance**	**Cumulative %**	**Total**	**% of Variance**	**Cumulative %**
1	5.511	50.102	50.102	5.511	50.102	50.102	4.342	39.472	39.472
2	1.835	16.683	66.785	1.835	16.683	66.785	2.145	19.505	58.976
3	1.377	12.522	79.307	1.377	12.522	79.307	1.662	15.111	74.087
4	1.077	9.787	89.094	1.077	9.787	89.094	1.651	15.007	**89.094**
5	0.515	4.678	93.772						
6	0.251	2.282	96.054						
7	0.191	1.740	97.794						
8	0.104	0.948	98.742						
9	0.081	0.739	99.481						
10	0.036	0.325	99.806						
11	0.021	0.194	100						

Extraction Method: Principal Component Analysis.

Table 4.24 KMO and Bartlett's Test

Kaiser-Meyer-Olkin Measure of Sampling Adequacy.		0.733
Bartlett's Test of Sphericity	Approx. Chi-Square	252.342
	df	55
	Sig.	0.000

Table 4.25 Rotated Component Matrix[a]

	Component			
	1	2	3	4
H, $\%_{dw}$	**0.952**			
Volatile Matter, $\%_{dw}$	**0.944**			
C, $\%_{dw}$	**0.936**			
Ash, $\%_{dw}$	**-0.858**			
Calorific Value, $kcal/kg_{dw}$	**0.778**			
S, $\%_{dw}$		**0.923**		
N, $\%_{dw}$		**0.898**		
Exothermic reaction temperature, °C			**0.925**	
Highest weight loss temperature, °C			**0.796**	
Second char formation temperature, °C				**0.926**
Lowest weight loss temperature, °C				**-0.720**

Extraction Method: Principal Component Analysis.
Rotation Method: Varimax with Kaiser Normalization.
a. Rotation converged in 5 iterations.

4.5.2 Results of statistical analysis for biochar properties

Correlation analyses using Pearson's correlation coefficients were carried out to identify the interrelations among the initial conditions which are waste amount (WA), initial water amount (IWA), particle size (PS), final temperature (FT), heating rate (HR), retention time (RT), raw material properties which are organic matter content (OMC), volatile matter (VM), ash (A), fixed carbon (FC), calorific value (CV), carbon (C), hydrogen (H), nitrogen (N), sulfur (S) and the biochar characteristics, which are biochar (BC), BET surface area (BET), pore volume (PV) and pore size (POS) for both preliminary and final experiments.

The correlation results are given in Table 4.26. Since the first six parameters are the initial conditions determined for experiments, they were not expected to have an effect on the properties of the raw material, so this part was not evaluated. However, their effects on the amount and surface area of biochar are significant. As the amount of waste increases, the amount of biochar will increase (r:0.873, p≤0,01). Also, the amount of biochars increases as the initial amount of water increases, because waste is added as water is added to maintain a certain percentage of water (r:0.313, p≤0,01). If we look at the effect of particle size on the amount of biochars, increasing the particle size of the feedstock can lead to a higher biochar yield (r:0.294, p≤0,01). This is because larger particles may undergo slower pyrolysis, allowing more of the biomass to be converted into char rather than volatiles or gases. However, there is an optimal particle size range for maximizing biochar yield (Asadullah, Zhang, & Li, 2010). Also, if the effect of particle size on the BET surface area value is analyzed, larger feedstock particles can lead to biochar with a higher BET surface area in some cases (r:0.221, p≤0,05). This is because the internal pore structure of the biochar can be more developed when produced from larger particles. Larger particles allow for greater development of macropores and mesopores, which contribute to higher surface area. Similar to biochar yield, there is an optimal particle size range for maximizing BET surface area (Sun, Hockaday, Masiello, & Zygourakis, 2012). Furthermore, the increase in surface area as the final temperature increases is an expected result in pyrolysis (r:0.490, p≤0,01) (Sun et al., 2012).

Organic matter content, volatile matter, fixed carbon, calorific value, carbon, hydrogen, nitrogen increase in parallel with each other while ash content decreases. As organic matter content and volatile matter increase, the amount of biochar decreases (r:-0.335, p≤0,01 and r:-0.217, p≤0,05) (Encinar, Beltrán, Bernalte, Ramiro, & González, 1996). Increasing ash content has the opposite effect (r:0.199, p≤0,05). In addition, the increase in sulfur and nitrogen amounts together is due to the protein content of the raw material (r:0.778, p≤0,01). Similarly, sulfur and nitrogen may increase the amount of biochars due to their protein content (r:0.669, p≤0,01 and r:0.385, p≤0,01) (Greenough et al., 2022).

Moreover, an increase in ash content in biochar typically has a negative effect on its BET surface area (r:-0.191, p≤0,05). Ash consists of inorganic minerals and impurities present in the feedstock biomass. When the ash content in biochar increases, it essentially dilutes the carbon content, which is the component responsible for creating the porous structure of biochar. As the proportion of carbon decreases relative to the total mass, the potential for porous structure development is reduced. This also explains why the amount of carbon and hydrogen increases the BET value (r:0.204, p≤0,05 and r:0.200, p≤0,05) (Calvelo Pereira et al., 2011). Furthermore, ash particles do not contribute to the development of the porous structure in the same way that carbon does. Instead, they can occupy the pore spaces within the biochar, obstructing the formation of a well-developed network of pores. This reduces the biochar's ability to adsorb gases, liquids, or solutes (Ronsse, van Hecke, Dickinson, & Prins, 2013).

There is a positive relation between pore volume and pore size (r:0.840, p≤0,01). Because larger pores contribute more to the pore volume compared to smaller pores because they occupy more space. The distribution of pore sizes throughout the material can greatly impact the overall pore volume (Lu & Zong, 2018).

There is a correlation between the amount of pore volume and the sulfur content (r:0.197, p≤0,05). The relationship between pore volume and sulfur content in materials, especially in the context of biochar, can be complex and depends on several factors, including the type of sulfur, the source material, and the pyrolysis conditions. Generally, as the sulfur content in the feedstock used to produce biochar increases, it can lead to the formation of more volatile sulfur compounds during pyrolysis. These volatile sulfur compounds contribute to gas and liquid products, and they may also impact the porous structure of the resulting biochar (S. Guo, Xiong, Che, Liu, & Sun, 2021).

Principal component analysis explained 80.656% of variance (Table 4.27). KMO and Bartlett's Test results are given in Table 4.28. According to this table, the KMO value was 0.735. In other words, the sample size is sufficient for correlation.

Furthermore, in the rotated component matrix created as a result of principal component analysis, 5 component extracts were obtained (Table 4.29). It is seen that

the first component is due to the chemical properties of the raw material. It is understood from this that the carbon-dependent properties of the waste reduce the amount of biochar. On the contrary, as the amount of ash increases, the amount of biochar also increases (Encinar et al., 1996). When we look at the second component, we can see that the heating rate and retention time negatively affect the amount of biochar. In the third component, we observe the effect of the protein content of the waste on the amount of biochar and calorific value. The fourth component explains the relationship between pore size and pore volume, which also appears in the correlation. The last component shows the positive effect of final temperature and retention time on the BET surface area (Sun et al., 2012).

Table 4.26 Correlations among the initial conditions, raw material properties and biochar characteristics

		WA, g dry	IWA, g	PS, mm	FT,°C	HR, °C/min	RT, min	OMC, $\%_{dw}$	VM, $\%_{dw}$	A, $\%_{dw}$	FC, $\%_{dw}$	CV, $kcal/kg_{dw}$	C, $\%_{dw}$	H, $\%_{dw}$	N, $\%_{dw}$	S, $\%_{dw}$	BC, g	BET , m^2/g	PV, cm^3/g	POS, Å
WA, g dry	**r**	1	,658**	,644**	,263**	-,314**	-0.079	-0.117	0.056	-0.086	0.094	,334**	0.171	0.165	,485**	,665**	**,873****	0.122	-0.043	-0.124
	p		*0.000*	*0.000*	*0.006*	*0.001*	*0.417*	*0.231*	*0.565*	*0.379*	*0.335*	*0.000*	*0.079*	*0.089*	*0.000*	*0.000*	*0.000*	*0.212*	*0.662*	*0.203*
IWA, g	**r**		1	,904**	,299**	-,457**	-,233*	0.184	,326**	-,390**	,380**	,426**	,364**	,336**	,289**	,233*	**,313****	0.130	-0.155	-0.138
	p			*0.000*	*0.002*	*0.000*	*0.016*	*0.058*	*0.001*	*0.000*	*0.000*	*0.000*	*0.000*	*0.000*	*0.003*	*0.016*	*0.001*	*0.181*	*0.112*	*0.155*
PS, mm	**r**			1	,365**	-,407**	-0.143	,230*	,340**	-,424**	,435**	,411**	,375**	,339**	,238*	0.179	**,294****	**,221***	-0.164	-0.151
	p				*0.000*	*0.000*	*0.142*	*0.017*	*0.000*	*0.000*	*0.000*	*0.000*	*0.000*	*0.000*	*0.013*	*0.065*	*0.002*	*0.022*	*0.091*	*0.122*
FT,°C	**r**				1	-0.074	0.019	0.097	0.138	-0.156	0.142	0.157	0.159	0.153	0.108	0.102	0.037	**,490****	-0.084	-0.189
	p					*0.450*	*0.845*	*0.318*	*0.158*	*0.108*	*0.145*	*0.107*	*0.103*	*0.116*	*0.266*	*0.297*	*0.704*	*0.000*	*0.391*	*0.052*
HR, °C/min	**r**					1	,304**	-0.088	-0.175	,208*	-,203*	-,267**	-,214*	-,190*	-,217*	-0.132	-0.190	0.008	0.074	0.061
	p						*0.001*	*0.368*	*0.071*	*0.031*	*0.036*	*0.005*	*0.027*	*0.050*	*0.025*	*0.174*	*0.050*	*0.934*	*0.447*	*0.533*
RT, min	**r**						1	-0.023	-0.107	0.133	-0.139	-,232*	-0.150	-0.120	-,219*	-0.086	-0.013	0.117	0.015	0.012
	p							*0.818*	*0.271*	*0.171*	*0.152*	*0.016*	*0.124*	*0.220*	*0.024*	*0.377*	*0.896*	*0.229*	*0.876*	*0.905*
OMC, $\%_{dw}$	**r**							1	**,857****	**-,847****	**,603****	**,556****	**,810****	**,815****	0.019	-0.144	**-,335****	0.185	-0.026	0.016
	p								*0.000*	*0.000*	*0.000*	*0.000*	*0.000*	*0.000*	*0.842*	*0.138*	*0.000*	*0.056*	*0.789*	*0.870*
VM, $\%_{dw}$	**r**								1	**-,923****	**,574****	**,737****	**,923****	**,935****	**,297****	0.094	**-,217***	0.175	-0.057	-0.029
	p									*0.000*	*0.000*	*0.000*	*0.000*	*0.000*	*0.002*	*0.334*	*0.025*	*0.071*	*0.558*	*0.764*
A, $\%_{dw}$	**r**									1	**-,842****	**-,696****	**-,874****	**-,857****	**-,196***	-0.057	**,199***	**-,191***	0.026	-0.008
	p										*0.000*	*0.000*	*0.000*	*0.000*	*0.043*	*0.559*	*0.040*	*0.048*	*0.789*	*0.936*

Table 4.26 Correlations among the initial conditions, raw material properties and biochar characteristics (continued)

FC, %$_{dw}$	**r**	1	**,456****	**,560****	**,509****	-0.015	-0.029	-0.136	0.162	0.017	0.055
	p		*0.000*	*0.000*	*0.000*	*0.880*	*0.765*	*0.164*	*0.095*	*0.859*	*0.577*
CV, kcal/kg$_{dw}$	**r**		1	**,849****	**,838****	**,632****	**,448****	0.079	0.040	-0.083	-0.077
	p			*0.000*	*0.000*	*0.000*	*0.000*	*0.419*	*0.686*	*0.398*	*0.430*
C, %$_{dw}$	**r**			1	**,973****	**,431****	**,212***	-0.095	**,204***	-0.074	-0.059
	p				*0.000*	*0.000*	*0.028*	*0.331*	*0.035*	*0.447*	*0.546*
H, %$_{dw}$	**r**				1	**,436****	**,235***	-0.096	**,200***	-0.072	-0.059
	p					*0.000*	*0.015*	*0.325*	*0.039*	*0.461*	*0.544*
N, %$_{dw}$	**r**					1	**,778****	**,385****	-0.051	-0.013	-0.117
	p						*0.000*	*0.000*	*0.605*	*0.893*	*0.229*
S, %$_{dw}$	**r**						1	**,669****	-0.055	**,197***	0.041
	p							*0.000*	*0.573*	*0.042*	*0.673*
BC, g	**r**							1	0.022	0.007	-0.063
	p								*0.820*	*0.942*	*0.521*
BET, m^2/g	**r**								1	-0.105	-0.155
	p									*0.281*	*0.111*
PV, cm^3/g	**r**									1	**,840****
	p										*0.000*
POS, Å	**r**										1
	p										

**. Correlation is significant at the 0.01 level (2-tailed).

*. Correlation is significant at the 0.05 level (2-tailed).

Table 4.27 Total variance explained with PCA for biochar

Component	Initial Eigenvalues			Extraction Sums of Squared Loadings			Rotation Sums of Squared Loadings		
	Total	% of Variance	Cumulative %	Total	% of Variance	Cumulative %	Total	% of Variance	Cumulative %
1	7.084	35.422	35.422	7.084	35.422	35.422	5.790	28.950	28.950
2	3.696	18.478	53.900	3.696	18.478	53.900	3.713	18.564	47.515
3	2.210	11.051	64.951	2.210	11.051	64.951	3.105	15.525	63.040
4	1.699	8.496	73.447	1.699	8.496	73.447	1.900	9.500	72.540
5	1.442	7.209	80.656	1.442	7.209	80.656	1.623	8.117	**80.656**
6	0.941	4.706	85.362						
7	0.664	3.318	88.680						
8	0.622	3.108	91.787						
9	0.505	2.527	94.315						
10	0.370	1.852	96.166						
11	0.197	0.986	97.152						
12	0.134	0.669	97.821						
13	0.125	0.624	98.445						
14	0.104	0.521	98.965						
15	0.087	0.436	99.401						
16	0.052	0.261	99.662						
17	0.032	0.158	99.821						
18	0.021	0.104	99.924						
19	0.014	0.070	99.995						
20	0.001	0.005	100.000						

Extraction Method: Principal Component Analysis.

Table 4.28 KMO and Bartlett's Test for biochar

Kaiser-Meyer-Olkin Measure of Sampling Adequacy.		0.735
Bartlett's Test of Sphericity	Approx. Chi-Square	2906.081
	df	190
	Sig.	0.000

Table 4.29 Rotated Component Matrix[a] for biochar

	Component				
	1	2	3	4	5
Volatile Matter, %dw	**0.953**				
C, %dw	**0.947**				
H, %dw	**0.947**				
Ash, %dw	**-0.927**				
Organic Matter Content, %dw	**0.892**				
Calorific Value, kcal/kgdw	**0.786**		**0.426**		
Fixed Carbon, %dw	**0.640**	**0.398**			
Initial Water amount, g		**0.906**			
Initial Water Content, %		**0.893**			
Particle size, mm		**0.871**			
Heating Rate, °C/min		**-0.597**			
S, %dw			**0.934**		
N, %dw	**0.307**		**0.823**		
Biochar, g	**-0.302**	**0.310**	**0.756**		
Waste Amount, g dry		**0.590**	**0.715**		
Pore Volume, cm3/g				**0.944**	
Pore Size, Å				**0.943**	
BET Surface Area, m2/g					**0.775**
Final Temperature,°C					**0.681**
Residence time, min		**-0.358**			**0.532**

Extraction Method: Principal Component Analysis.
Rotation Method: Varimax with Kaiser Normalization.

a. Rotation converged in 5 iterations.

CHAPTER FIVE
CONCLUSION

The primary objective of this research was to explore a strategy for effectively using municipal biodegradable waste alongside other locally abundant and valuable biomass residues, taking into account their specific waste attributes. This study also placed a particular emphasis on addressing issues related to waste quality, particularly water content. These aspects are pivotal in determining the feasibility of employing pyrolysis technology for municipal waste management in Türkiye. Furthermore, the findings from this study can offer valuable insights for nations facing similar circumstances to Türkiye.

Since waste diversity will affect pyrolysis performance, dry dog/cat food was used to determine the optimum conditions. For this reason, the protein, cellulose and lipid contents of the wastes and foods were compared and foods with similar contents to biodegradable wastes were selected. In addition, this selection was supported by proximate and ultimate analyses.

Moreover, the main experimental conditions were determined according to the results of the preliminary analyses and thermogravimetric analysis. It was seen that biochar production from the biodegradable fraction of municipal waste and other biomass sources is possible when appropriate conditions are provided. According to TGA, the primary devolatilization, or the main weight loss, typically occurred within the temperature range of 200 to 500°C due to the degradation of hemicellulose, cellulose and lignin. The initial curves of the DTA graph indicate the release of water. DTA curves reveal the occurrence of an exothermic reaction (combustion) at approximately 280°C. In simpler terms, this means that the endothermic reaction extended up to these temperatures. Additionally, the formation of char was observed within the temperature range of 420 to 850°C.

Bio-drying experiments were conducted as a low-cost and easily applicable method to reduce the high water content of the waste. Throughout the bio-drying experiment, the moisture content reduced by about 48% in 15 days. Apart from the decline in water

content, there were no substantial alterations in the calorific value. This outcome indicates the effectiveness of the bio-drying experiment.

Based on preliminary pyrolysis trials, it was observed that the quantity of biochar produced decreased with rising temperatures. Moreover, the FT-IR findings indicated the elimination of oxygen and hydrogen-based functional groups in the biochars as a result of pyrolysis at elevated temperatures. The absence of these characteristic bands in the biochars suggests the generation of CO_2, CH_4, and H_2 through the pyrolysis of cellulose, hemicelluloses, and lignin. Furthermore, the FT-IR results highlight the disappearance of soft-carbon components and the preservation of hard-carbon components, which are crucial for the production of adsorbents used in wastewater treatment. Moreover, the BET analysis results demonstrated a notable rise in the BET surface areas of the biochars up to 213.11 m^2/g as the temperature increases. This enhanced surface area can be because of the release of volatile components from the biomass throughout pyrolysis, resulting in the creation of pores within the biochar. As per SEM analysis, fractured structures are visible in all samples, aligning with prior research results. Furthermore, an increase in temperature was noted to enhance the formation of cracks and the fragmentation of biochar structures as supporting BET analysis. As previsedd, there was no substantial variation in the carbon content of biochars generated at three distinct temperatures. The most prevalent elements detected in EDS analysis were carbon (C) and oxygen (O), with calcium (Ca), potassium (K), chlorine (Cl), and sodium (Na) following in abundance.

Based on the final pyrolysis experiments, it was noted that the quantity of biochar produced decreased with rising temperatures. Furthermore, while there wasn't a distinct individual effect of the final temperature, heating rate, and retention time, the most favorable results in terms of yield were achieved at 700°C, with a heating rate of 10°C/min and a retention time of 40 minutes. On the other hand, the quality of the biochar was positively affected by the elevated temperature which was proved by FT-IR, BET and SEM-EDS analyses.

Based on the findings from FT-IR analysis, it was evident that neither initial water content of the waste nor its particle size had any impact on the properties of biochar. In the experiments exploring the influence of final temperature, heating rate, and

retention time on biochar production, it was clear that the higher final temperature had a notably positive influence on biochar quality. Conversely, heating rate and residence time did not exhibit a significant impact on biochar quality. Furthermore, the co-pyrolysis of biodegradable solid waste with CM (Cattle Manure), SS (Sewage Sludge), and CS (Corn Stalk) demonstrated a favorable impact on the biochar's quality regarding FT-IR lines.

While the BET surface area was 62.61 m^2/g at 500^oC, it increased to 169.21 m^2/g at 700 ^oC under the same initial conditions. The study noted that biochar generated from waste materials initially had quite low BET values (2.34-2.57 m^2/g). Biochars produced from CM, SS and CS were resulted with higher BET values were 4.45 m^2/g, 62.80 m^2/g, and 170.18 m^2/g, respectively. It was observed that, when biodegradable waste was co-pyrolyzed with these biomass, a significant improvement in BET values was observed. In fact, the highest BET value recorded, reaching 170.18 m^2/g, was associated with the biochar produced through the co-pyrolysis of biodegradable solid waste and CS. Even though the mix ratio of waste and CS was 1:1, the final BET surface area of the produced biochar was much higher than the mean value of the BET surface areas of both materials. This is also supported by SEM results showing favorable cracked structures, where further studies are necessary to explain this phenomenon. Although this value seems to be suitable for the use of biochar as adsorbent, it may be recommended to use a catalyst in the pyrolysis process to make the surface area equivalent to known adsorbents such as illite.

Furthermore, based on the EDS findings, a slight reduction in the carbon content of the biochar produced by the pyrolysis of biodegradable solid waste was observed in comparison to the initial carbon concentration. This outcome serves as an indicator of the successful pyrolysis process.

Analyzing the GC-MS findings of the bio-oil in general, it's evident that the predominant components formed are from the alkane group. Additionally, alcohols, aldehydes, ketones, and alkenes were also detected, as consistent with existing literature.

In the light of all these analysis results, correlation and principal component analysis were performed both for the preliminary analysis results and for all results. The statistical results helped to identify some important factors affecting pyrolysis. As the inorganic components undergo later stages of volatilization, there is an associated increase in temperature. This relationship is substantiated by the correlation between ash content and the temperature at which the highest weight loss occurs (r: 0.565, $p \leq 0.01$). Similarly, since inorganic substances volatilize at later stages, the formation of char also occurs subsequently. This pattern is further evident in the correlation between ash content and the temperature at which secondary char formation takes place (r: 0.417, $p \leq 0.05$).

When considering the impact of particle size on biochar production, increasing the size of the feedstock particles can result in a higher biochar yield (r: 0.294, $p \leq 0.01$). This is due to the fact that larger particles tend to undergo slower pyrolysis, which permits more of the biomass to be converted into char rather than volatile compounds or gases. Furthermore, when examining the influence of particle size on the BET surface area, it's observed that larger feedstock particles can, in some cases, lead to biochar with a higher BET surface area (r: 0.221, $p \leq 0.05$). Moreover, the expected outcome in pyrolysis is the increase in BET surface area as the final temperature rises (r: 0.490, $p \leq 0.01$).

When examining the rotated component matrix, it becomes apparent that heating rate and retention time have a negative influence on the biochar yield. Conversely, the final component shows the positive impact of final temperature and retention time on the BET surface area. The sum of these two components is 26.68%, which means that the effect of operating conditions on the quality of biochar obtained by pyrolysis is 26.68%.

The experiments and statistical analyses revealed that elevating the moisture level in the waste had no impact on the quality of the biochar. However, it did result in an augmentation of the liquid product formed during pyrolysis and contributed to a rise in the ketone content of the liquid product.

The study concluded that biodegradable municipal wastes with elevated water content can be effectively processed with a product-oriented approach using the pyrolysis technique following biodrying. Analyses conducted on the wastes and the final products of pyrolysis indicate the feasibility of co-pyrolysis involving biodegradable municipal wastes and other biomasses. Furthermore, co-pyrolysis was found to positively influence the quality of the final products obtained from the process.

REFERENCES

Abdullah, N. A., Tila, J., Hakim, I. I., & Koestoer, R. A. (n.d.). *Influence of Feedstock Particle Size from Merbau Wood (Intsia bijuga) on Bio-Oil Production Using a Heat Pipe Fin L-Shaped Condenser in a Pyrolysis Process*. *July 2020*, 14–16. https://doi.org/10.4186/ej.2020.24.4.261

Abdullah, N. A., Tila, J., Hakim, I. I., Koestoer, R. A., & Putra, N. (2020). Influence of feedstock particle size from merbau wood (Intsia bijuga) on bio-oil production using a heat pipe fin l-shaped condenser in a pyrolysis process. *Engineering Journal*, *24*(4), 261–271. https://doi.org/10.4186/ej.2020.24.4.261

Agrafioti, E., Bouras, G., Kalderis, D., & Diamadopoulos, E. (2013). Biochar production by sewage sludge pyrolysis. *Journal of Analytical and Applied Pyrolysis*, *101*, 72–78. https://doi.org/10.1016/j.jaap.2013.02.010

Aksoğan Korkmaz, A., & Bentli, İ. (2019). Kömür Zenginleştirmenin Piroliz Ürün Verimlerine Etkisinin Araştırılması. *Fırat Üniversitesi Mühendislik Bilimleri Dergisi*, *31*(2), 259–267. https://doi.org/10.35234/fumbd.499279

Al Arni, S., Bosio, B., & Arato, E. (2010). Syngas from sugarcane pyrolysis: An experimental study for fuel cell applications. *Renewable Energy*, *35*(1), 29–35. https://doi.org/10.1016/j.renene.2009.07.005

Ali, N., Saleem, M., Shahzad, K., Hussain, S., & Chughtai, A. (2016). *Effect of operating parameters on production of bio-oil from fast pyrolysis of maize stalk in bubbling fl uidized bed reactor*. 88–96.

Alibardi, L., & Cossu, R. (2015). Composition variability of the organic fraction of municipal solid waste and effects on hydrogen and methane production potentials. *Waste Management*, *36*, 147–155. https://doi.org/10.1016/j.wasman.2014.11.019

Alibardi, L., & Cossu, R. (2016). Effects of carbohydrate, protein and lipid content of organic waste on hydrogen production and fermentation products. *Waste Management*, *47*, 69–77. https://doi.org/10.1016/j.wasman.2015.07.049

Alves, J. L. F., da Silva, J. C. G., Mumbach, G. D., Domenico, M. Di, Bolzan, A., Machado, R. A. F., & Marangoni, C. (2022a). Evaluating the bioenergy potential of cupuassu shell through pyrolysis kinetics, thermodynamic parameters of activation, and evolved gas analysis with TG/FTIR technique. *Thermochimica Acta*, *711*(March). https://doi.org/10.1016/j.tca.2022.179187

Alves, J. L. F., da Silva, J. C. G., Mumbach, G. D., Domenico, M. Di, Bolzan, A., Machado, R. A. F., & Marangoni, C. (2022b). Evaluating the bioenergy potential of cupuassu shell through pyrolysis kinetics, thermodynamic parameters of activation, and evolved gas analysis with TG/FTIR technique. *Thermochimica Acta*, *711*(January). https://doi.org/10.1016/j.tca.2022.179187

Amalina, F., Krishnan, S., Zularisam, A. W., & Nasrullah, M. (2023). Effect of process parameters on bio-oil yield from lignocellulosic biomass through microwave-assisted pyrolysis technology for sustainable energy resources: Current status. *Journal of Analytical and Applied Pyrolysis*, *171*(March), 105958. https://doi.org/10.1016/j.jaap.2023.105958

Anh, T., Khanh, Q., Vu, H., Kwon, B., Tae, H., Kim, J., & Kim, S. (2022). Co-pyrolysis of lignocellulosic biomass and plastics : A comprehensive study on pyrolysis kinetics and characteristics. *Journal of Analytical and Applied Pyrolysis*, *163*(September 2021), 105464. https://doi.org/10.1016/j.jaap.2022.105464

Arni, S. Al. (2018). Comparison of slow and fast pyrolysis for converting biomass into fuel. *Renewable Energy*, *124*, 197–201. https://doi.org/10.1016/j.renene.2017.04.060

Asadullah, M., Zhang, S., & Li, C. Z. (2010). Evaluation of structural features of chars from pyrolysis of biomass of different particle sizes. *Fuel Processing Technology*, *91*(8), 877–881. https://doi.org/10.1016/j.fuproc.2009.08.008

Ashraf, M., Ramzan, N., Khan, R. U., & Durrani, A. K. (2021). Analysis of mixed cattle manure: Kinetics and thermodynamic comparison of pyrolysis and combustion processes. *Case Studies in Thermal Engineering*, *26*(May), 101078. https://doi.org/10.1016/j.csite.2021.101078

ASTM International. (2018). *ASTM D4239-18e1-Standard Test Method for Sulfur in the Analysis Sample of Coal and Coke Using High-Temperature Tube Furnace Combustion*. https://doi.org/10.1520/D4239-18E01

ASTM International. (2019). *ASTM E872-82- Standard Test Method for Volatile Matter in the Analysis of Particulate Wood Fuels*. https://doi.org/10.1520/E0872-82R19.2

ASTM International. (2020). *ASTM E1755-01- Standard Test Method for Ash in Biomass*. https://doi.org/10.1520/E1755-01R20.2

ASTM International. (2021). *ASTM D5373-21- Standard Test Methods for Determination of Carbon, Hydrogen and Nitrogen in Analysis Samples of Coal and Carbon in Analysis Samples of Coal and Coke*. https://doi.org/10.1520/D5373-21

Atienza-Martínez, M., Ábrego, J., Gea, G., & Marías, F. (2020). Pyrolysis of dairy cattle manure: evolution of char characteristics. *Journal of Analytical and Applied Pyrolysis*, *145*(July 2019), 104724. https://doi.org/10.1016/j.jaap.2019.104724

Ayiania, M., Terrell, E., Dunsmoor, A., Carbajal-Gamarra, F. M., & Garcia-Perez, M. (2019). Characterization of solid and vapor products from thermochemical conversion of municipal solid waste woody fractions. *Waste Management*, *84*, 277–285. https://doi.org/10.1016/j.wasman.2018.11.042

Ayilara, M. S., Olanrewaju, O. S., Babalola, O. O., & Odeyemi, O. (2020). Waste management through composting: Challenges and potentials. *Sustainability (Switzerland)*, *12*(11), 1–23. https://doi.org/10.3390/su12114456

Azim, K., Soudi, B., Boukhari, S., Perissol, C., Roussos, S., & Thami Alami, I. (2018). Composting parameters and compost quality: a literature review. *Organic Agriculture*, *8*(2), 141–158. https://doi.org/10.1007/s13165-017-0180-z

Balat, M., Balat, M., Kirtay, E., & Balat, H. (2009). Main routes for the thermo-conversion of biomass into fuels and chemicals. Part 1: Pyrolysis systems. *Energy Conversion and Management*, *50*(12), 3147–3157. https://doi.org/10.1016/j.enconman.2009.08.014

Banar, M., Akyildiz, V., Özkan, A., Çokaygil, Z., & Onay, Ö. (2012). Characterization of pyrolytic oil obtained from pyrolysis of TDF (Tire Derived Fuel). *Energy Conversion and Management*, *62*, 22–30. https://doi.org/10.1016/j.enconman.2012.03.019

Basu, P. (2013). Biomass Gasification, Pyrolysis and Torrefaction: Practical Design and Theory. In *Academic Press* (2nd ed.). https://doi.org/10.1016/C2011-0-07564-6

Bhoi, P. R., Ouedraogo, A. S., Soloiu, V., & Quirino, R. (2020a). Recent advances on catalysts for improving hydrocarbon compounds in bio-oil of biomass catalytic pyrolysis. *Renewable and Sustainable Energy Reviews*, *121*(March 2019), 109676. https://doi.org/10.1016/j.rser.2019.109676

Bhoi, P. R., Ouedraogo, A. S., Soloiu, V., & Quirino, R. (2020b). Recent advances on catalysts for improving hydrocarbon compounds in bio-oil of biomass catalytic pyrolysis. *Renewable and Sustainable Energy Reviews*, *121*(March 2019), 109676. https://doi.org/10.1016/j.rser.2019.109676

Bridgwater, A. V., & Bridge, S. A. (1991). A Review of Biomass Pyrolysis and Pyrolysis Technologies. In *Biomass Pyrolysis Liquids Upgrading and Utilization* (pp. 11–92). https://doi.org/10.1007/978-94-011-3844-4_2

Buah, W. K., Cunliffe, A. M., & Williams, P. T. (2007). Characterization of products from the pyrolysis of municipal solid waste. *Process Safety and Environmental Protection*, *85*(5 B), 450–457. https://doi.org/10.1205/psep07024

Calvelo Pereira, R., Kaal, J., Camps Arbestain, M., Pardo Lorenzo, R., Aitkenhead, W., Hedley, M., Macías, F., Hindmarsh, J., & Maciá-Agulló, J. A. (2011). Contribution to characterisation of biochar to estimate the labile fraction of carbon. *Organic Geochemistry*, *42*(11), 1331–1342. https://doi.org/10.1016/j.orggeochem.2011.09.002

Cantrell, K. B., Hunt, P. G., Uchimiya, M., Novak, J. M., & Ro, K. S. (2012). Impact of pyrolysis temperature and manure source on physicochemical characteristics of

biochar. *Bioresource Technology*, *107*, 419–428. https://doi.org/10.1016/j.biortech.2011.11.084

Charis, G., Danha, G., & Muzenda, E. (2020). Characterizations of biomasses for subsequent thermochemical conversion: A comparative study of pine sawdust and acacia tortilis. *Processes*, *8*(5). https://doi.org/10.3390/PR8050546

Chen, G., & Leung, D. Y. C. (2003). Experimental Investigation of Biomass Waste, (Rice Straw, Cotton Stalk, and Pine Sawdust), Pyrolysis Characteristics. *Energy Sources*, *25*(4), 331–337. https://doi.org/10.1080/00908310390142361

Chen, Y., Wang, L., Zhao, M., Ma, H., Chen, D., Zhang, Y., & Zhou, J. (2021). Comparative Study on the Pyrolysis Behaviors of Pine Cone and Pretreated Pine Cone by Using TGA-FTIR and Pyrolysis-GC/MS. *ACS Omega*, *6*(5), 3490–3498. https://doi.org/10.1021/acsomega.0c04456

Chhabra, V., Bhattacharya, S., & Shastri, Y. (2019). Pyrolysis of mixed municipal solid waste: Characterisation, interaction effect and kinetic modelling using the thermogravimetric approach. *Waste Management*, *90*, 152–167. https://doi.org/10.1016/j.wasman.2019.03.048

Cuixia, Y., Yingming, X., Lin, W., Xuefeng, L., Yuebing, S., & Hongtao, J. (2020). Effect of different pyrolysis temperatures on physico-chemical characteristics and lead(II) removal of biochar derived from chicken manure. *RSC Advances*, *10*(7), 3667–3674. https://doi.org/10.1039/c9ra08199b

Das, S., Lee, S. H., Kumar, P., Kim, K. H., Lee, S. S., & Bhattacharya, S. S. (2019). Solid waste management: Scope and the challenge of sustainability. *Journal of Cleaner Production*, *228*, 658–678. https://doi.org/10.1016/j.jclepro.2019.04.323

Demirbaş, A., & Arin, G. (2002). An overview of biomass pyrolysis. *Energy Sources*, *24*(5), 471–482. https://doi.org/10.1080/00908310252889979

El-Sayed, S. A., Khass, T. M., & Mostafa, M. E. (2023). Thermal degradation behaviour and chemical kinetic characteristics of biomass pyrolysis using TG/DTG/DTA techniques. *Biomass Conversion and Biorefinery*, *0123456789*, 20–

40. https://doi.org/10.1007/s13399-023-03926-2

Elnour, A. Y., Alghyamah, A. A., Shaikh, H. M., Poulose, A. M., Al-Zahrani, S. M., Anis, A., & Al-Wabel, M. I. (2019). Effect of pyrolysis temperature on biochar microstructural evolution, physicochemical characteristics, and its influence on biochar/polypropylene composites. *Applied Sciences (Switzerland)*, *9*(6), 7–9. https://doi.org/10.3390/app9061149

Encinar, J. M., Beltrán, F. J., Bernalte, A., Ramiro, A., & González, J. F. (1996). Pyrolysis of two agricultural residues: Olive and grape bagasse. Influence of particle size and temperature. *Biomass and Bioenergy*, *11*(5), 397–409. https://doi.org/10.1016/S0961-9534(96)00029-3

Environmental Protection Agency (EPA). (2023). *Non-hazardous Waste*. https://www.epa.gov/rcra/resource-conservation-and-recovery-act-rcra-regulations#nonhaz

Erdin, E. (2005). *Katı atıkların kompostlaştırılması*. http://web.deu.edu.tr/erdin/tr/ders/kati_atik/ders_not/katiatiklarinkompostlastirilmasi.pdf

European Union. (2008). Directive 2008/98/EC of the European Parliament and of the Council of 19 November 2008 on waste and repealing certain directives. *Official Journal of the European Union*, 3–30. https://doi.org/2008/98/EC.; 32008L0098

European Union. (2018). COUNCIL DIRECTIVE 1999/31/EC of 26 April 1999 on the landfill of waste. *The Official Journal of the European Union*, L 182, 1-30. https://doi.org/10.1017/CBO9781107415324.004

Fang, S., Yu, Z., Ma, X., Lin, Y., Lin, Y., Chen, L., Fan, Y., & Liao, Y. (2017). Co-pyrolysis characters between combustible solid waste and paper mill sludge by TG-FTIR and Py-GC/MS. *Energy Conversion and Management*, *144*, 114–122. https://doi.org/10.1016/j.enconman.2017.04.046

Fonts, I., Azuara, M., Gea, G., & Murillo, M. B. (2009). Study of the pyrolysis liquids obtained from different sewage sludge. *Journal of Analytical and Applied*

Pyrolysis, *85*(1–2), 184–191. https://doi.org/10.1016/j.jaap.2008.11.003

Ghorbel-Abid, I., Galai, K., & Trabelsi-Ayadi, M. (2010). Retention of chromium (III) and cadmium (II) from aqueous solution by illitic clay as a low-cost adsorbent. *Desalination*, *256*(1–3), 190–195. https://doi.org/10.1016/j.desal.2009.06.079

Global Methane Initiative. (2016). *Global Methane Initiative Overview of Anaerobic Digestion for Municipal Solid Waste* (Issue October).

Gopu, C., Gao, L., Volpe, M., Fiori, L., & Goldfarb, J. L. (2018). Valorizing municipal solid waste: Waste to energy and activated carbons for water treatment via pyrolysis. *Journal of Analytical and Applied Pyrolysis*, *133*(May), 48–58. https://doi.org/10.1016/j.jaap.2018.05.002

Greenough, S., Kurian, J. K., Gariépy, Y., Prasher, S., Khripin, C. Y., Mehlem, J. J., & Dumont, M. J. (2022). Protein-based biochars as potential renewable fillers in styrene-butadiene rubber composites. *Journal of Analytical and Applied Pyrolysis*, *167*(September). https://doi.org/10.1016/j.jaap.2022.105697

Grycová, B., Koutník, I., Pryszcz, A., & Kaloč, M. (2016). Application of pyrolysis process in processing of mixed food wastes. *Polish Journal of Chemical Technology*, *18*(1), 19–23. https://doi.org/10.1515/pjct-2016-0004

Gui, X., Liu, C., Li, F., & Wang, J. (2020). Effect of pyrolysis temperature on the composition of DOM in manure-derived biochar. *Ecotoxicology and Environmental Safety*, *197*(February), 110597. https://doi.org/10.1016/j.ecoenv.2020.110597

Guo, F., He, Y., Hassanpour, A., Gardy, J., & Zhong, Z. (2020). Thermogravimetric analysis on the co-combustion of biomass pellets with lignite and bituminous coal. *Energy*, *197*, 1–9. https://doi.org/10.1016/j.energy.2020.117147

Guo, S., Xiong, X., Che, D., Liu, H., & Sun, B. (2021). Effects of sludge pyrolysis temperature and atmosphere on characteristics of biochar and gaseous products. *Korean Journal of Chemical Engineering*, *38*(1), 55–63. https://doi.org/10.1007/s11814-020-0685-0

Halim, R., Danquah, M. K., & Webley, P. A. (2012). Extraction of oil from microalgae for biodiesel production : A review. *Biotechnology Advances*, *30*(3), 709–732. https://doi.org/10.1016/j.biotechadv.2012.01.001

Haykiri-Acma, H., Yaman, S., & Kucukbayrak, S. (2006). Effect of heating rate on the pyrolysis yields of rapeseed. *Renewable Energy*, *31*(6), 803–810. https://doi.org/10.1016/j.renene.2005.03.013

Iacovidou, E., Ohandja, D., & Voulvoulis, N. (2012). Food waste co-digestion with sewage sludge e Realising its potential in the UK. *Journal of Environmental Management*, *112*, 267–274. https://doi.org/10.1016/j.jenvman.2012.07.029

Inguanzo, M., Domı´nguez, A., Mene´ndez, J. A., Blanco, C. G., & Pis, J. J. (2002). On the pyrolysis of sewage sludge: The influence of pyrolysis temperature on biochar, liquid and gas fractions. *Journal of Analytical and Applied Pyrolysis*, *63*(1), 209–222. https://doi.org/10.4028/www.scientific.net/AMR.518-523.3412

Inyang, M. I., Gao, B., Yao, Y., Xue, Y., Zimmerman, A., Mosa, A., Pullammanappallil, P., Ok, Y. S., & Cao, X. (2016). A review of biochar as a low-cost adsorbent for aqueous heavy metal removal. *Critical Reviews in Environmental Science and Technology*, *46*(4), 406–433. https://doi.org/10.1080/10643389.2015.1096880

Islam, M. N., Islam, M. N., Beg, M. R. A., & Islam, M. R. (2005). Pyrolytic oil from fixed bed pyrolysis of municipal solid waste and its characterization. In *Renewable Energy* (Vol. 30, Issue 3, pp. 413–420). https://doi.org/10.1016/j.renene.2004.05.002

İSTAÇ. (n.d.). *İSTAÇ-Bizi Tanıyın*. Retrieved February 24, 2020, from https://www.istac.istanbul/tr/hakkimizda/bizi-taniyin

ITC. (n.d.). *Gazlaştırma / Yakma ve ATY Üretimi*. Retrieved February 7, 2020, from http://www.itcturkiye.com/tr/gazlastirma-yakma-ve-aty-uretimi/11927

Jaramillo-Arango, A., Fonts, I., Chejne, F., & Arauzo, J. (2016). Product compositions from sewage sludge pyrolysis in a fluidized bed and correlations with temperature.

Journal of Analytical and Applied Pyrolysis, *121*, 287–296. https://doi.org/10.1016/j.jaap.2016.08.008

Jenkins, B. M., Williams, R. B., Adams, L. S., Peace, C., Petersen, G., & Leary, M. (2008). *Current Anaerobic Digestion Technologies Used for Treatment of Municipal Organic Solid Waste* (Issue March).

Jerzak, W., Bieniek, A., & Magdziarz, A. (2021). Multifaceted analysis of products from the intermediate co-pyrolysis of biomass with Tetra Pak waste. *International Journal of Hydrogen Energy*, *xxxx*. https://doi.org/10.1016/j.ijhydene.2021.06.202

Jouiad, M., Al-Nofeli, N., Khalifa, N., Benyettou, F., & Yousef, L. F. (2015). Characteristics of slow pyrolysis biochars produced from rhodes grass and fronds of edible date palm. *Journal of Analytical and Applied Pyrolysis*, *111*(November), 183–190. https://doi.org/10.1016/j.jaap.2014.10.024

Junga, R., Yilmaz, E., & Bozhenko, B. (2021). Thermal Decomposition of Olive-Mill Byproducts : A TG-FTIR Approach. *Energies*.

Kanca, A. (2019). Comparison of Pyrolysis and Oxidation Behaviors of Cotton Waste, Hazelnut Shell, and Walnut Shell. *Kocaeli Üniversitesi Fen Bilimleri Dergisi*, *2*(2), 43–54. http://dergipark.gov.tr/koufbd

Kanca, A. (2020). Investigation on pyrolysis and combustion characteristics of low quality lignite, cotton waste, and their blends by TGA-FTIR. *Fuel*, *263*(August 2019), 116517. https://doi.org/10.1016/j.fuel.2019.116517

Khan, S. R., & Zeeshan, M. (2022). Catalytic potential of low-cost natural zeolite and influence of various pretreatments of biomass on pyro-oil up-gradation during co-pyrolysis with scrap rubber tires. *Energy*, *238*, 121820. https://doi.org/10.1016/j.energy.2021.121820

Kirubakaran, V., Sivaramakrishnan, V., Nalini, R., Sekar, T., Premalatha, M., & Subramanian, P. (2009). A review on gasification of biomass. *Renewable and Sustainable Energy Reviews*, *13*(1), 179–186. https://doi.org/10.1016/j.rser.2007.07.001

Kobayashi, I., Owada, H., Ishii, T., & Iizuka, A. (2017). Evaluation of specific surface area of bentonite-engineered barriers for Kozeny-Carman law Evaluation of specific surface area of bentonite-engineered barriers. *Soils and Foundations*, *57*(5), 683–697. https://doi.org/10.1016/j.sandf.2017.08.001

Kobayashi, T., Xu, K., Li, Y., & Inamori, Y. (2012). Evaluation of hydrogen and methane production from municipal solid wastes with different compositions of fat , protein , cellulosic materials and the other carbohydrates. *International Journal of Hydrogen Energy*, *37*(20), 15711–15718. https://doi.org/10.1016/j.ijhydene.2012.05.044

Kong, W., Shen, B., Ma, J., Kong, J., Feng, S., Wang, Z., & Xiong, L. (2022). Pyrolysis of Spirulina platensis, Tetradesmus obliquus and Chlorella vulgaris by TG-FTIR and Py-GC/MS: Kinetic analysis and pyrolysis behaviour. *Energy*, *244*, 123165. https://doi.org/10.1016/j.energy.2022.123165

Kostecki, P., Morrison, R., & Dragun, J. (2005). Hydrocarbons. In D. Hillel, C. Roszenweig, D. Powlson, K. Scow, M. Singer, & D. Sparks (Eds.), *Encyclopedia of soils in the enviorment - Vol1* (pp. 217–226).

Kumar, A., & Samadder, S. R. (2017). A review on technological options of waste to energy for effective management of municipal solid waste. *Waste Management*, *69*, 407–422. https://doi.org/10.1016/j.wasman.2017.08.046

Lahtela, V., & Kärki, T. (2018). Mechanical sorting processing of waste material before composite manufacturing - A review. *Journal of Engineering Science and Technology Review*, *11*(6), 35–46. https://doi.org/10.25103/jestr.116.06

Li, G., Zhu, W., Zhu, L., & Chai, X. (2016). Effect of pyrolytic temperature on the adsorptive removal of p-benzoquinone, tetracycline, and polyvinyl alcohol by the biochars from sugarcane bagasse. *Korean Journal of Chemical Engineering*, *33*(7), 2215–2221. https://doi.org/10.1007/s11814-016-0067-9

Li, J., Yao, X., Chen, S., Xu, K., Fan, B., Yang, D., Geng, L., & Qiao, H. (2022). Investigation on the co-pyrolysis of agricultural waste and high-density

polyethylene using TG-FTIR and artificial neural network modelling. *Process Safety and Environmental Protection*, *160*, 341–353. https://doi.org/10.1016/j.psep.2022.02.033

Li, Y., Zhao, H., Sui, X., Wang, X., & Ji, H. (2022a). Corrigendum to "Studies on individual pyrolysis and co-pyrolysis of peat–biomass blends: Thermal decomposition behavior, possible synergism, product characteristic evaluations and kinetics" [Fuel 310 (2021) 122280] (Fuel (2022) 310(PB), (S0016236121021542. *Fuel*, *323*(August 2021). https://doi.org/10.1016/j.fuel.2022.124426

Li, Y., Zhao, H., Sui, X., Wang, X., & Ji, H. (2022b). Studies on individual pyrolysis and co-pyrolysis of peat–biomass blends: Thermal decomposition behavior, possible synergism, product characteristic evaluations and kinetics. *Fuel*, *310*(Part B), 122280. https://doi.org/10.1016/j.fuel.2021.122280

Lisk, D. J. (1988). Environmental implications of incineration of municipal solid waste and ash disposal. *Science of the Total Environment, The*, *74*(C), 39–66. https://doi.org/10.1016/0048-9697(88)90128-3

Liu, R., Deng, C., Wang, J., Liu, R., Deng, C., & Wang, J. (2009). *Environmental Effects Fast Pyrolysis of Corn Straw for Bio-oil Production in a Bench-scale Fluidized Bed Reactor Fast Pyrolysis of Corn Straw for Bio-oil Production in a Bench-scale Fluidized Bed Reactor*. *7036*. https://doi.org/10.1080/15567030802094037

Lu, S., & Zong, Y. (2018). Pore structure and environmental serves of biochars derived from different feedstocks and pyrolysis conditions. *Environmental Science and Pollution Research*, *25*(30), 30401–30409. https://doi.org/10.1007/s11356-018-3018-7

Luo, J., Li, Q., Meng, A., Long, Y., & Zhang, Y. (2018). Combustion characteristics of typical model components in solid waste on a macro-TGA. *Journal of Thermal Analysis and Calorimetry*, *132*(1), 553–562. https://doi.org/10.1007/s10973-017-6909-9

Ma, J., Qi, J., Yao, C., Cui, B., Zhang, T., & Li, D. (2012). A novel bentonite-based adsorbent for anionic pollutant removal from water. *Chemical Engineering Journal*, *200–202*, 97–103. https://doi.org/10.1016/j.cej.2012.06.014

Ma, M., Wang, J., Song, X., Su, W., Bai, Y., & Yu, G. (2020). Co-gasification of cow manure and bituminous coal: A study on reactivity, synergistic effect, and char structure evolution. *ACS Omega*, *5*(27), 16779–16788. https://doi.org/10.1021/acsomega.0c01785

Ma, W., Rajput, G., Pan, M., Lin, F., Zhong, L., & Chen, G. (2019). Pyrolysis of typical MSW components by Py-GC/MS and TG-FTIR. *Fuel*, *251*(March), 693–708. https://doi.org/10.1016/j.fuel.2019.04.069

Ma, Z., Chen, D., Gu, J., Bao, B., & Zhang, Q. (2015). Determination of pyrolysis characteristics and kinetics of palm kernel shell using TGA-FTIR and model-free integral methods. *Energy Conversion and Management*, *89*, 251–259. https://doi.org/10.1016/j.enconman.2014.09.074

Meegoda, J. N., Li, B., Patel, K., & Wang, L. B. (2018). A review of the processes, parameters, and optimization of anaerobic digestion. *International Journal of Environmental Research and Public Health*, *15*(10). https://doi.org/10.3390/ijerph15102224

Miskolczi, N., & Ateş, F. (2016). Thermo-catalytic co-pyrolysis of recovered heavy oil and municipal plastic wastes. *Journal of Analytical and Applied Pyrolysis*, *117*, 273–281. https://doi.org/10.1016/j.jaap.2015.11.005

Mohammed, M., Ozbay, I., & Durmusoglu, E. (2017). Bio-drying of green waste with high moisture content. *Process Safety and Environmental Protection*, *111*, 420–427. https://doi.org/10.1016/j.psep.2017.08.002

Moneim, M. A., El Naggar, A. M. A., El Sayed, H. A., Mostafa, M. S., Khalil, N. M., & Hassan, M. E. D. (2018). Direct conversion of an agricultural solid waste to hydrocarbon gases via the pyrolysis technique. *Egyptian Journal of Petroleum*, *27*(4), 991–995. https://doi.org/10.1016/j.ejpe.2018.03.008

Morales-Polo, C., Cledera-Castro, M. del M., & Soria, B. Y. M. (2018). Reviewing the Anaerobic Digestion of Food Waste : From Waste Generation and Anaerobic Process to Its Perspectives. *Applied Sciences*, *8*(1804), 1–35. https://doi.org/10.3390/app8101804

Mu, J., & Lai, Z. (2017). Pyrolysis Characteristics of Wood-Based Panels and its Products. In M. Samer (Ed.), *Pyrolysis* (pp. 53–70). InTech. https://doi.org/10.5772/67506

Murray, R. S., & Quirk, J. P. (1990). Surface Area of Clays. *Langmuir*, *6*(1), 122–124. https://doi.org/10.1021/la00091a018

Mustapha, S., Ndamitso, M. M., Abdulkareem, A. S., Tijani, J. O., Mohammed, A. K., & Shuaib, D. T. (2019). Potential of using kaolin as a natural adsorbent for the removal of pollutants from tannery wastewater. *Heliyon*, *5*(11), e02923. https://doi.org/10.1016/j.heliyon.2019.e02923

Nanda, S., Mohanty, P., Pant, K. K., Naik, S., Kozinski, J. A., & Dalai, A. K. (2013). Characterization of North American Lignocellulosic Biomass and Biochars in Terms of their Candidacy for Alternate Renewable Fuels. *Bioenergy Research*, *6*(2), 663–677. https://doi.org/10.1007/s12155-012-9281-4

Naroznova, I., Møller, J., & Scheutz, C. (2016). Characterisation of the biochemical methane potential (BMP) of individual material fractions in Danish source-separated organic household waste. *Waste Management*, *50*, 39–48. https://doi.org/10.1016/j.wasman.2016.02.008

Naseem, R., & Tahir, S. S. (2001). Removal of Pb(II) from aqueous/acidic solutions by using bentonite as an adsorbent. *Water Research*, *35*(16), 3982–3986. https://doi.org/10.1016/S0043-1354(01)00130-0

Ni, B. J., Zhu, Z. R., Li, W. H., Yan, X., Wei, W., Xu, Q., Xia, Z., Dai, X., & Sun, J. (2020). Microplastics Mitigation in Sewage Sludge through Pyrolysis: The Role of Pyrolysis Temperature. *Environmental Science and Technology Letters*, *7*(12), 961–967. https://doi.org/10.1021/acs.estlett.0c00740

Niu, M., Sun, R., Ding, K., Gu, H., Cui, X., Wang, L., & Hu, J. (2022). Synergistic effect on thermal behavior and product characteristics during co-pyrolysis of biomass and waste tire: Influence of biomass species and waste blending ratios. *Energy*, *240*, 122808. https://doi.org/10.1016/j.energy.2021.122808

Nzioka, A. M., Kim, M. G., Hwang, H. U., & Kim, Y. J. (2019). Kinetic Study of the Thermal Decomposition Process of Municipal Solid Waste Using TGA. *Waste and Biomass Valorization*, *10*(6), 1679–1691. https://doi.org/10.1007/s12649-017-0183-8

Onay, O., & Koca, H. (2015). Determination of synergetic effect in co-pyrolysis of lignite and waste tyre. *Fuel*, *150*, 169–174. https://doi.org/10.1016/j.fuel.2015.02.041

Oyedun, A. O., Lam, K. L., & Hui, C. W. (2012). Charcoal production via multistage pyrolysis. *Chinese Journal of Chemical Engineering*, *20*(3), 455–460. https://doi.org/10.1016/S1004-9541(11)60206-1

Özçifçi, A., & Özbay, G. (2013). Mobilya endüstrisi atiklarindan katalitik piroliz yöntemi ile biyoyakit üretimi. *Journal of the Faculty of Engineering and Architecture of Gazi University*, *28*(3), 473–479.

Patel, A., Antonopoulou, I., Enman, J., Rova, U., Christakopoulos, P., & Matsakas, L. (2019). Lipids detection and quantification in oleaginous microorganisms : an overview of the current state of the art. *BMC Chemical Engineering*, *1*(13). https://doi.org/10.1186/s42480-019-0013-9

Pehlivan, E. (2017). Utilization of activated carbon produced from fruit juice industry solid waste for the adsorption of reactive red (procion red MX-5B) from aqueous solutions. *Pamukkale University Journal of Engineering Sciences*, *23*(7), 912–918. https://doi.org/10.5505/pajes.2017.33497

Pütün, A. E. (2002). Biomass to bio-oil via fast pyrolysis of cotton straw and stalk. *Energy Sources*, *24*(3), 275–285. https://doi.org/10.1080/009083102317243656

Rada, E. C., Franzinelli, A., Taiss, M., Ragazzi, M., Panaitescu, V., & Apostol, T.

(2007). Lower heating value dynamics during municipal solid waste bio-drying. *Environmental Technology*, *28*(4), 463–469. https://doi.org/10.1080/09593332808618807

Rada, E. C., Ragazzi, M., & Badea, A. (2012). MSW Bio-drying: Design criteria from A 10 years research. *UPB Scientific Bulletin, Series D: Mechanical Engineering*, *74*(3), 209–216.

Raveendran, K., Ganesh, A., & Khilar, K. C. (1996). Pyrolysis characteristics of biomass and biomass components. *Fuel*, *75*(8), 987–998. https://doi.org/10.1016/0016-2361(96)00030-0

Reza, M. S., Afroze, S., Bakar, M. S. A., Saidur, R., Aslfattahi, N., Taweekun, J., & Azad, A. K. (2020). Biochar characterization of invasive Pennisetum purpureum grass: effect of pyrolysis temperature. *Biochar*, *2*(2), 239–251. https://doi.org/10.1007/s42773-020-00048-0

Ronsse, F., van Hecke, S., Dickinson, D., & Prins, W. (2013). Production and characterization of slow pyrolysis biochar: Influence of feedstock type and pyrolysis conditions. *GCB Bioenergy*, *5*(2), 104–115. https://doi.org/10.1111/gcbb.12018

Ruiz-Gómez, N., Quispe, V., Ábrego, J., Atienza-Martínez, M., Murillo, M. B., & Gea, G. (2017). Co-pyrolysis of sewage sludge and manure. *Waste Management*, *59*, 211–221. https://doi.org/10.1016/j.wasman.2016.11.013

Saleem, W., Zulfiqar, A., Tahir, M., Asif, F., & Yaqub, G. (2016). Latest technologies of municipal solid waste management in developed and developing countries : A review. *International Journal of Advanced Science and Research*, *1*(10).

Sanlisoy, A., & Carpinlioglu, M. O. (2017). A review on plasma gasification for solid waste disposal. *International Journal of Hydrogen Energy*, *42*(2), 1361–1365. https://doi.org/10.1016/j.ijhydene.2016.06.008

Saravanan, A., Kumar, P. S., Nhung, T. C., Ramesh, B., Srinivasan, S., & Rangasamy, G. (2022). A review on biological methodologies in municipal solid waste

management and landfilling: Resource and energy recovery. *Chemosphere*, *309*(P1), 136630. https://doi.org/10.1016/j.chemosphere.2022.136630

Şenol, H., & Açikel, Ü. (2019). Araştırma Makalesi / Research Article Evsel Organik Atıklar ve Sığır Gübresi Karışımlarından Biyogaz Üretiminin İncelenmesi Investigation of Biogas Production from Domestic Organic Waste and Cattle Manure Mixtures. *BEU Journal of Science*, *8*(1), 132–142.

Shim, J. W., Pyo, S., Lam, S. S., Jae, J., Jeon, B. H., Khan, M. A., Lin, K. Y. A., Kim, Y. M., Jung, S. C., & Park, Y. K. (2022). Catalytic pyrolysis of chicken manure over various catalysts. *Fuel*, *322*(March), 124241. https://doi.org/10.1016/j.fuel.2022.124241

Siengchum, T., Isenberg, M., & Chuang, S. S. C. (2013). Fast pyrolysis of coconut biomass - An FTIR study. *Fuel*, *105*, 559–565. https://doi.org/10.1016/j.fuel.2012.09.039

Singh, R. K., Patil, T., Pandey, D., Tekade, S. P., & Sawarkar, A. N. (2022). Co-pyrolysis of petroleum coke and banana leaves biomass: Kinetics, reaction mechanism, and thermodynamic analysis. *Journal of Environmental Management*, *301*(September 2021), 113854. https://doi.org/10.1016/j.jenvman.2021.113854

Singh, S., Kumar, V., Dhanjal, D. S., Datta, S., Bhatia, D., Dhiman, J., Samuel, J., Prasad, R., & Singh, J. (2020). A sustainable paradigm of sewage sludge biochar: Valorization, opportunities, challenges and future prospects. *Journal of Cleaner Production*, *269*, 122259. https://doi.org/10.1016/j.jclepro.2020.122259

Sipra, A. T., Gao, N., & Sarwar, H. (2018). Municipal solid waste (MSW) pyrolysis for bio-fuel production A review ofeffects of MSW components and catalysts.pdf. *Fuel Processing Technology*, *175*, 131–147.

Sogancioglu, M., Yel, E., & Ahmetli, G. (2017). Pyrolysis of waste high density polyethylene (HDPE) and low density polyethylene (LDPE) plastics and production of epoxy composites with their pyrolysis chars. *Journal of Cleaner Production*, *165*, 369–381. https://doi.org/10.1016/j.jclepro.2017.07.157

Song, Q., Zhao, H. yu, Xing, W. long, Song, L. hua, Yang, L., Yang, D., & Shu, X. (2018). Effects of various additives on the pyrolysis characteristics of municipal solid waste. *Waste Management*, *78*, 621–629. https://doi.org/10.1016/j.wasman.2018.06.033

Song, W., & Guo, M. (2012). Quality variations of poultry litter biochar generated at different pyrolysis temperatures. *Journal of Analytical and Applied Pyrolysis*, *94*, 138–145. https://doi.org/10.1016/j.jaap.2011.11.018

Sørum, L., Grønli, M. ., & Hustad, J. . (2001). Pyrolysis characteristics and kinetics of municipal solid waste. *Fuel*, *80*(9), 1217–1227. https://doi.org/10.1016/S0016-2361(00)00218-0

Stantec. (2011). Waste to Energy: A Technical Review of Municipal Solid Waste Thermal Treatment Practices. In *Stantec Publications* (Issue March).

Stout, S. A., & Wang, Z. (2016). Standard Handbook Oil Spill Environmental Forensics: Fingerprinting and Source Identification: Second Edition. In *Standard Handbook Oil Spill Environmental Forensics: Fingerprinting and Source Identification: Second Edition*.

Stylianou, M., Christou, A., Dalias, P., Polycarpou, P., Michael, C., Agapiou, A., Papanastasiou, P., & Fatta-Kassinos, D. (2020). Physicochemical and structural characterization of biochar derived from the pyrolysis of biosolids, cattle manure and spent coffee grounds. *Journal of the Energy Institute*, *93*(5), 2063–2073. https://doi.org/10.1016/j.joei.2020.05.002

Sukarni, S., Yanuhar, U., Wardana, I. N. G., Sudjito, S., Hamidi, N., Wijayanti, W., Wibisono, Y., Sumarli, S., Nauri, I. M., & Suryanto, H. (2018). Combustion of microalgae nannochloropsis oculata biomass: Cellular macromolecular and mineralogical content changes during thermal decomposition. *Songklanakarin Journal of Science and Technology*, *40*(6), 1456–1463. https://doi.org/10.14456/sjst-psu.2018.178

Sun, H., Hockaday, W. C., Masiello, C. A., & Zygourakis, K. (2012). Multiple controls

on the chemical and physical structure of biochars. *Industrial and Engineering Chemistry Research*, *51*(9), 1587–1597. https://doi.org/10.1021/ie201309r

Suriapparao, D. V., & Vinu, R. (2015). Bio-oil production via catalytic microwave pyrolysis of model municipal solid waste component mixtures. *RSC Advances*, *5*(71), 57619–57631. https://doi.org/10.1039/c5ra08666c

Tabakaev, R., Kanipa, I., Astafev, A., Dubinin, Y., Yazykov, N., Zavorin, A., & Yakovlev, V. (2019). Thermal enrichment of different types of biomass by low-temperature pyrolysis. *Fuel*, *245*(August 2018), 29–38. https://doi.org/10.1016/j.fuel.2019.02.049

Tanguay-Rioux, F., Spreutels, L., Héroux, M., & Legros, R. (2022). Mixed modeling approach for mechanical sorting processes based on physical properties of municipal solid waste. *Waste Management*, *144*(April), 533–542. https://doi.org/10.1016/j.wasman.2022.04.025

Thangalazhy-Gopakumar, S., Adhikari, S., Ravindran, H., Gupta, R. B., Fasina, O., Tu, M., & Fernando, S. D. (2010). Physiochemical properties of bio-oil produced at various temperatures from pine wood using an auger reactor. *Bioresource Technology*, *101*(21), 8389–8395. https://doi.org/10.1016/j.biortech.2010.05.040

The Ministry of Environment and Urbanization. (2016). *Ulusal Atık Yönetimi Ve Eylem Planı 2023*. http://www.csb.gov.tr/db/cygm/editordosya/Ulusal_Atik_Yonetimi_ve_Eylem_Plani.pdf

Tozlu, A., Özahi, E., & Abuşoɨlu, A. (2016). Waste to energy technologies for municipal solid waste management in Gaziantep. *Renewable and Sustainable Energy Reviews*, *54*, 809–815. https://doi.org/10.1016/j.rser.2015.10.097

TurkStat. (2018). *Solid Waste Statistics of Municipalities*. Turkish Statistics Institute, Central Delivery System. https://biruni.tuik.gov.tr/medas/?kn=119&locale=tr

Velghe, I., Carleer, R., Yperman, J., & Schreurs, S. (2011). Study of the pyrolysis of municipal solid waste for the production of valuable products. *Journal of Analytical*

and Applied Pyrolysis, *92*(2), 366–375. https://doi.org/10.1016/j.jaap.2011.07.011

Vu, H., Kim, S., Hyung, J., Chul, H., & Kim, J. (2016). Fast pyrolysis of Saccharina japonica alga in a fixed-bed reactor for bio-oil production. *Energy Conversion and Management*, *122*, 526–534. https://doi.org/10.1016/j.enconman.2016.06.019

Wang, C., Bi, H., Lin, Q., Jiang, X., & Jiang, C. (2020). Co-pyrolysis of sewage sludge and rice husk by TG–FTIR–MS: Pyrolysis behavior, kinetics, and condensable/non-condensable gases characteristics. *Renewable Energy*, *160*, 1048–1066. https://doi.org/10.1016/j.renene.2020.07.046

Wang, F., Zhou, C., He, W., Zhu, H., Huang, J., & Li, G. (2016). The Content Variation of Fat, Protein and Starch in Kitchen Waste Under Microwave Radiation. *Procedia Environmental Sciences*, *31*, 530–534. https://doi.org/10.1016/j.proenv.2016.02.075

Wang, G., Wang, S., Sun, W., Sun, Z., & Zheng, S. (2017). Synthesis of a novel illite@carbon nanocomposite adsorbent for removal of Cr(VI) from wastewater. *Journal of Environmental Sciences (China)*, *57*(Vi), 62–71. https://doi.org/10.1016/j.jes.2016.10.017

Wang, T., Chen, Y., Li, J., Xue, Y., Liu, J., Mei, M., Hou, H., & Chen, S. (2020). Co-pyrolysis behavior of sewage sludge and rice husk by TG-MS and residue analysis. *Journal of Cleaner Production*, *250*, 119557. https://doi.org/10.1016/j.jclepro.2019.119557

Wang, X., Chang, V. W. C., Li, Z., Chen, Z., & Wang, Y. (2021). Co-pyrolysis of sewage sludge and organic fractions of municipal solid waste: Synergistic effects on biochar properties and the environmental risk of heavy metals. *Journal of Hazardous Materials*, *412*(September 2020), 125200. https://doi.org/10.1016/j.jhazmat.2021.125200

Wen, Y., Shi, Z., Wang, S., Mu, W., Jönsson, P. G., & Yang, W. (2021). Pyrolysis of raw and anaerobically digested organic fractions of municipal solid waste: Kinetics, thermodynamics, and product characterization. *Chemical Engineering Journal*,

415(February). https://doi.org/10.1016/j.cej.2021.129064

Wentrup, C. (2014). Flash (vacuum) pyrolysis apparatus and methods. *Australian Journal of Chemistry*, *67*(8–9), 1150–1165. https://doi.org/10.1071/CH14096

Wentrup, C. (2017). Flash Vacuum Pyrolysis: Techniques and Reactions. *Angewandte Chemie - International Edition*, *56*(47), 14808–14835. https://doi.org/10.1002/anie.201705118

Worrell, W. A., & Vesilind, P. A. (2012). *Solid Waste Engineering* (2nd ed.). Cengage Learning.

Wu, W., Yang, M., Feng, Q., McGrouther, K., Wang, H., Lu, H., & Chen, Y. (2012). Chemical characterization of rice straw-derived biochar for soil amendment. *Biomass and Bioenergy*, *47*, 268–276. https://doi.org/10.1016/j.biombioe.2012.09.034

Xu, Y., & Chen, B. (2013). Investigation of thermodynamic parameters in the pyrolysis conversion of biomass and manure to biochars using thermogravimetric analysis. *Bioresource Technology*, *146*, 485–493. https://doi.org/10.1016/j.biortech.2013.07.086

Yang, Y., Heaven, S., Venetsaneas, N., Banks, C. J., & Bridgwater, A. V. (2018). Slow pyrolysis of organic fraction of municipal solid waste (OFMSW): Characterisation of products and screening of the aqueous liquid product for anaerobic digestion. *Applied Energy*, *213*(January), 158–168. https://doi.org/10.1016/j.apenergy.2018.01.018

Yang, Y., Zhang, Y., Omairey, E., Cai, J., Gu, F., & Bridgwater, A. V. (2018). Intermediate pyrolysis of organic fraction of municipal solid waste and rheological study of the pyrolysis oil for potential use as bio-bitumen. *Journal of Cleaner Production*, *187*, 390–399. https://doi.org/10.1016/j.jclepro.2018.03.205

Yassin, L., Lettieri, P., Simons, S., & Germanà, A. (2005). Energy recovery from thermal processing of waste: A review. *Proceedings of the Institution of Civil Engineers: Engineering Sustainability*, *158*(2), 97–103.

https://doi.org/10.1680/ensu.2005.158.2.97

Yuan, J., Zhang, D., Li, Y., Li, J., Luo, W., Zhang, H., Wang, G., & Li, G. (2018). Effects of the aeration pattern, aeration rate, and turning frequency on municipal solid waste biodrying performance. *Journal of Environmental Management*, *218*, 416–424. https://doi.org/10.1016/j.jenvman.2018.04.089

Yuan, X., He, T., Cao, H., & Yuan, Q. (2017). Cattle manure pyrolysis process: Kinetic and thermodynamic analysis with isoconversional methods. *Renewable Energy*, *107*, 489–496. https://doi.org/10.1016/j.renene.2017.02.026

Yusuf, A. A., Inambao, F. L., Hassan, A. S., Nura, S. S., & Karthickeyan, V. (2020). Comparative study on pyrolysis and combustion behavior of untreated Matooke biomass wastes in East Africa via TGA, SEM, and EDXS. *International Journal of Energy and Environmental Engineering*, *11*(2), 265–273. https://doi.org/10.1007/s40095-019-00331-2

Zaker, A., Chen, Z., & Zaheer-Uddin, M. (2021). Catalytic pyrolysis of sewage sludge with HZSM5 and sludge-derived activated char: A comparative study using TGA-MS and artificial neural networks. *Journal of Environmental Chemical Engineering*, *9*(5), 105891. https://doi.org/10.1016/j.jece.2021.105891

Zhang, J., Lü, F., Zhang, H., Shao, L., Chen, D., & He, P. (2015). Multiscale visualization of the structural and characteristic changes of sewage sludge biochar oriented towards potential agronomic and environmental implication. *Scientific Reports*, *5*, 1–8. https://doi.org/10.1038/srep09406

Zhou, H., Meng, A., Long, Y., Li, Q., & Zhang, Y. (2014). Interactions of municipal solid waste components during pyrolysis: A TG-FTIR study. *Journal of Analytical and Applied Pyrolysis*, *108*, 19–25. https://doi.org/10.1016/j.jaap.2014.05.024

APPENDICES

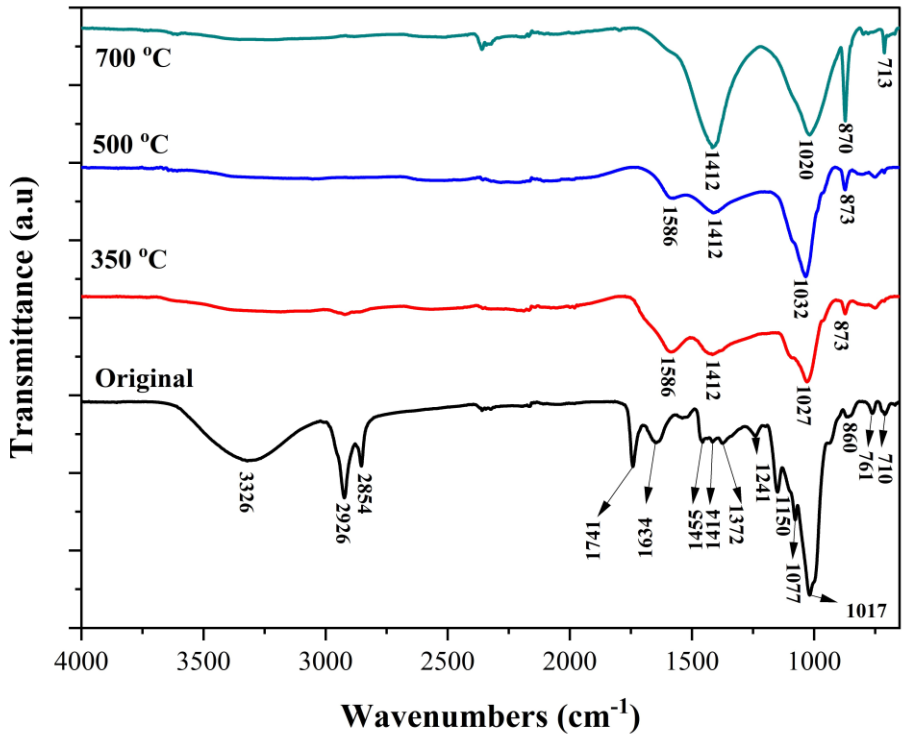

Figure-S 1 FT-IR graph of M18

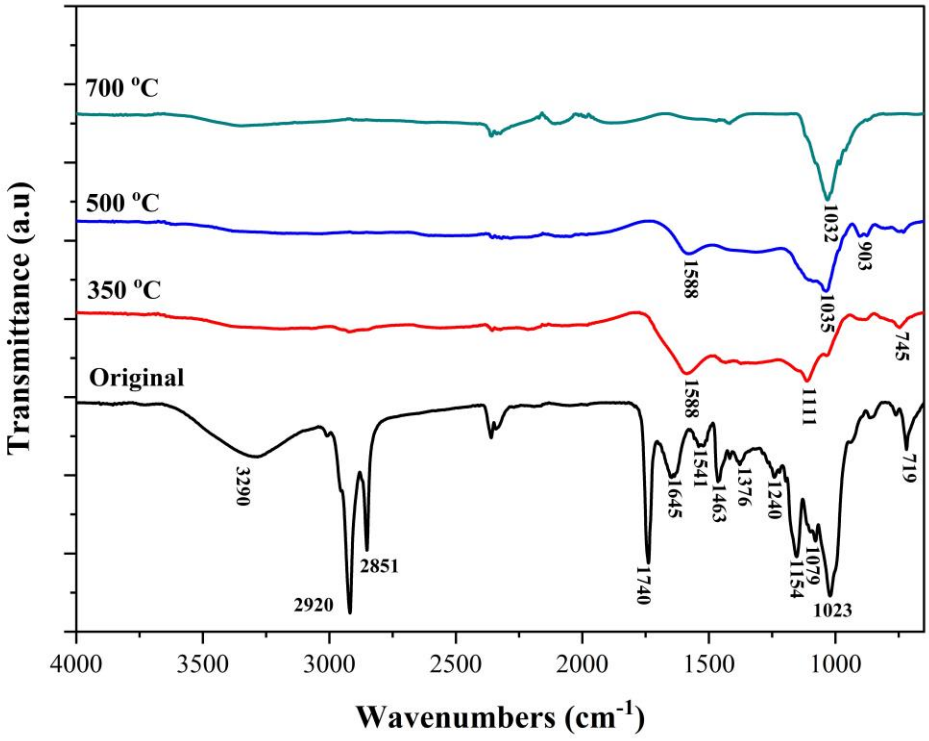

Figure-S 2 FT-IR graph of M21

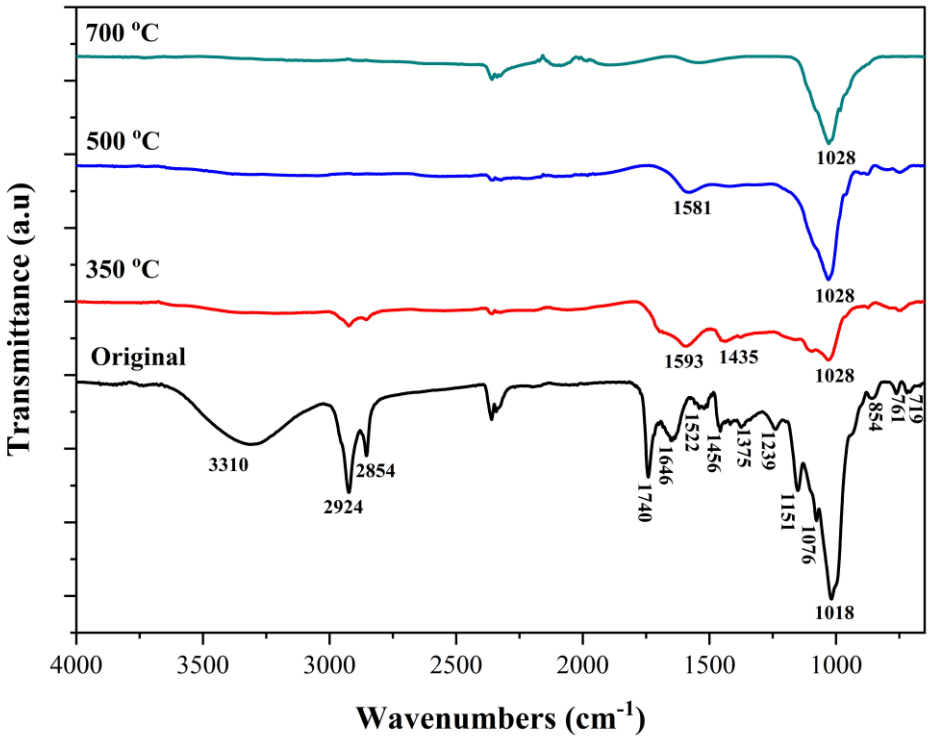

Figure-S 3 FT-IR graph of M27

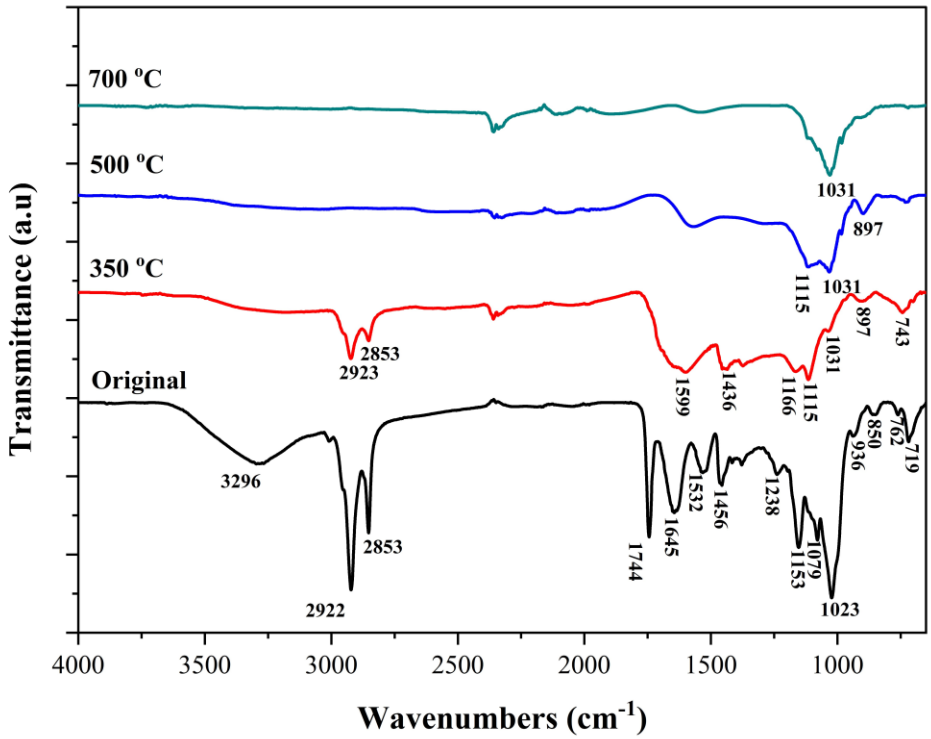

Figure-S 4 FT-IR graph of M28

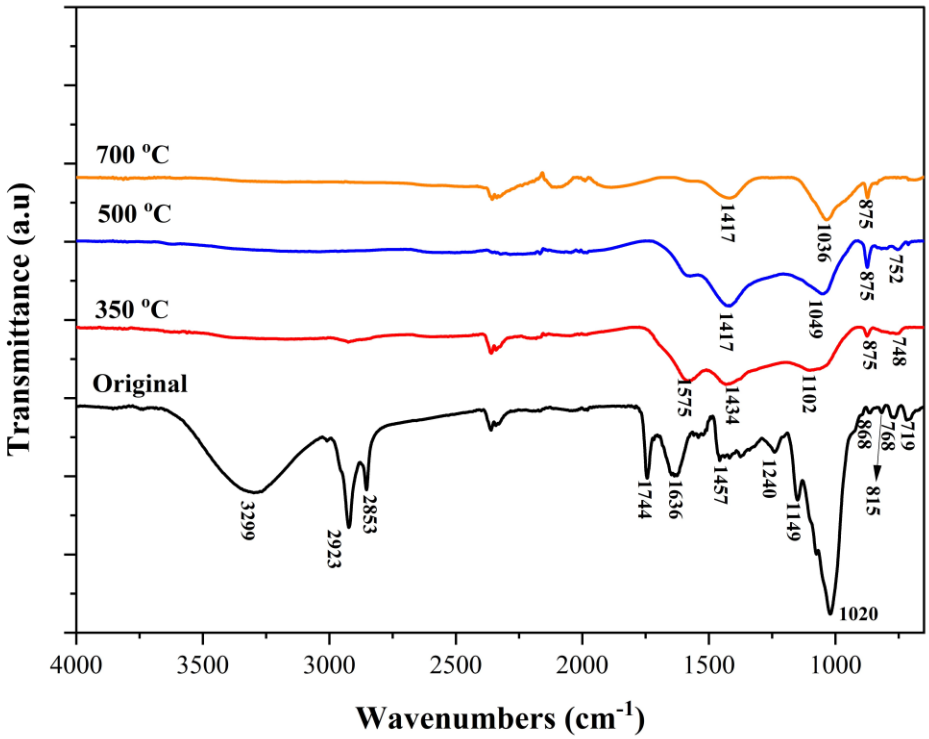

Figure-S 5 FT-IR graph of W1.2

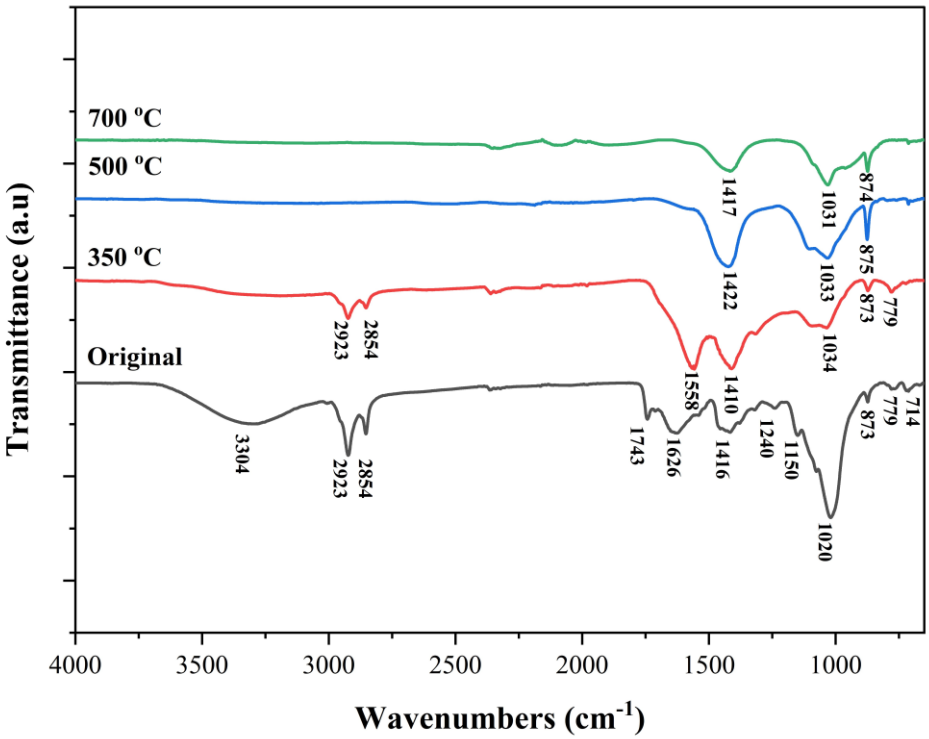

Figure-S 6 FT-IR graph of 2.1

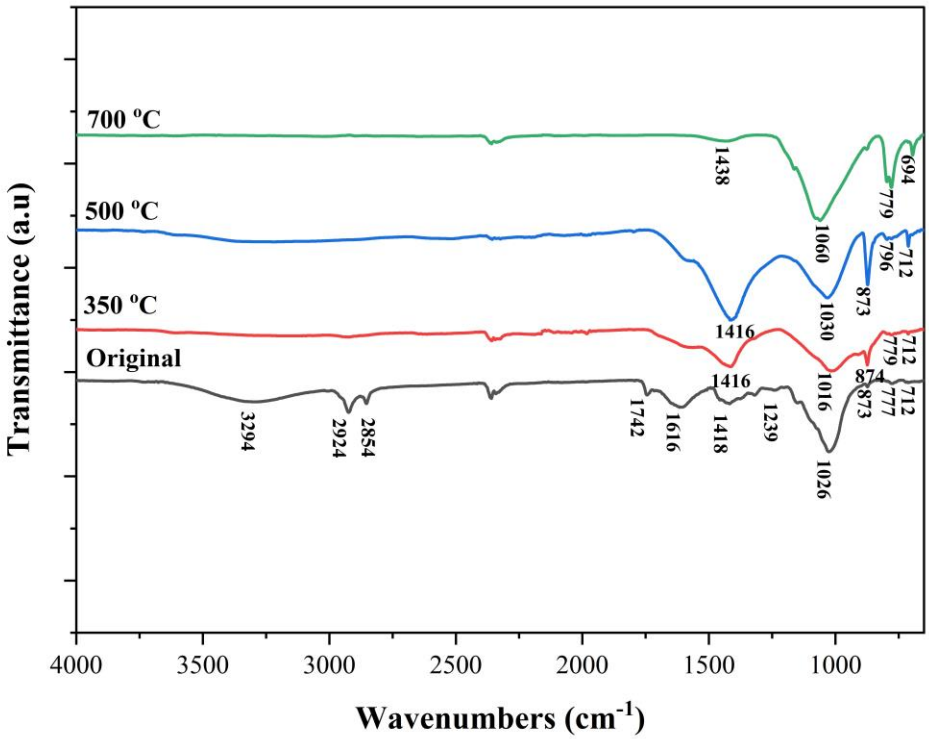

Figure-S 7 FT-IR graph of W2.2

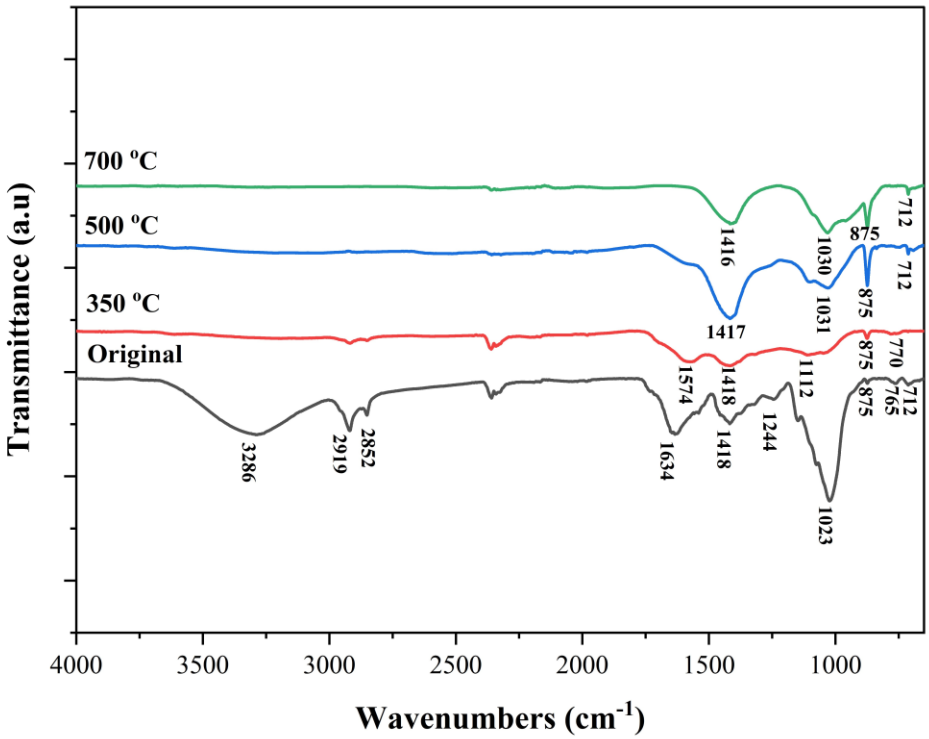

Figure-S 8 FT-IR graph of W3.1

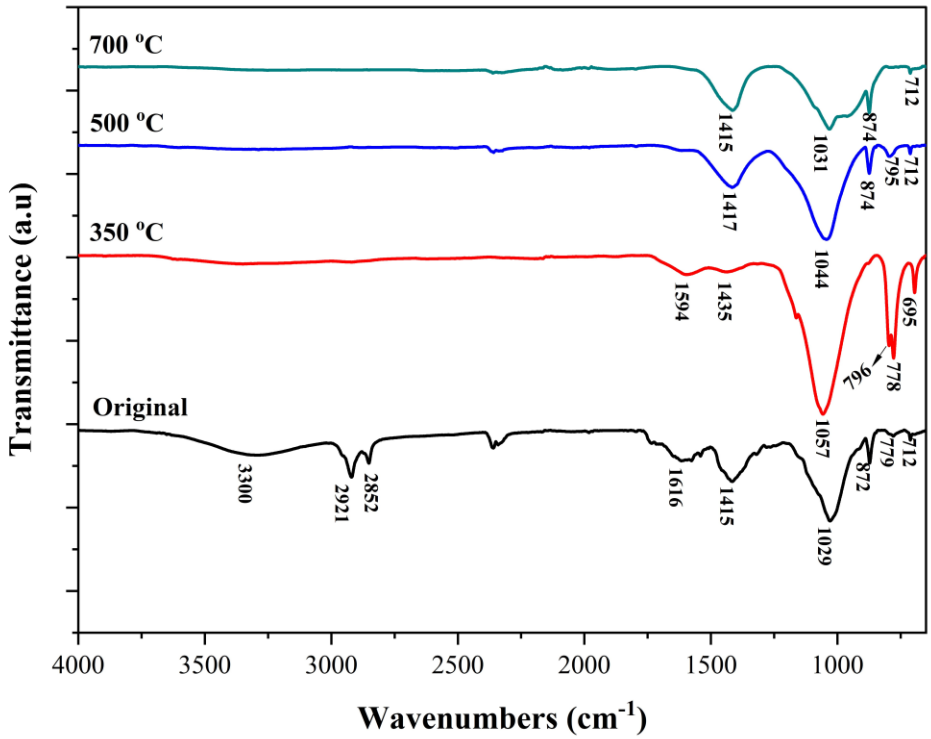

Figure-S 9 FT-IR graph of W3.2

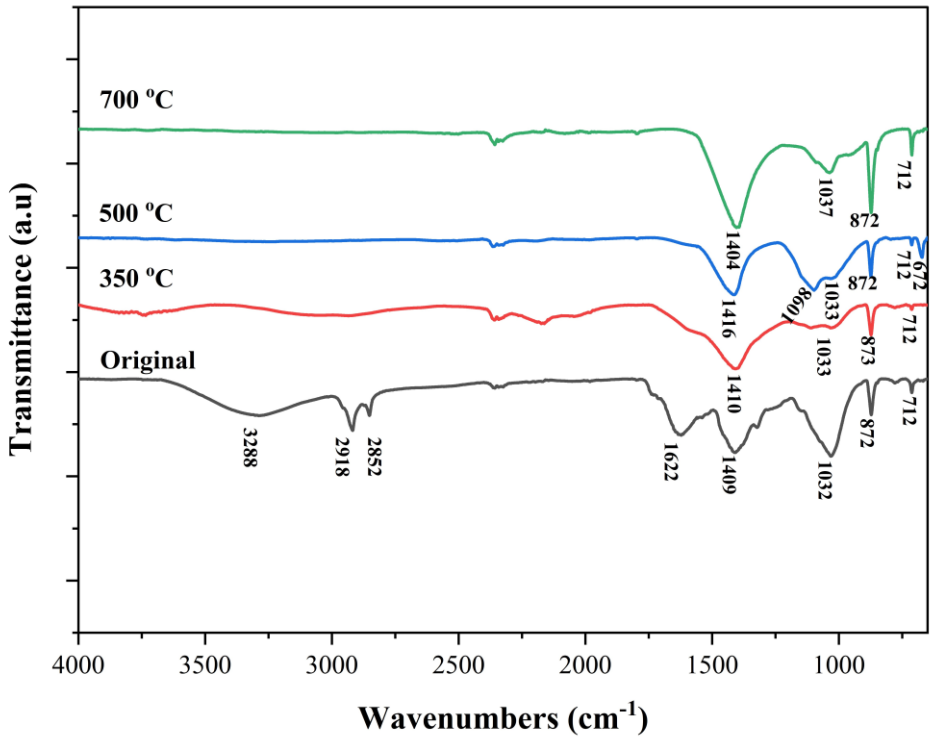

Figure-S 10 FT-IR graph of W4.1

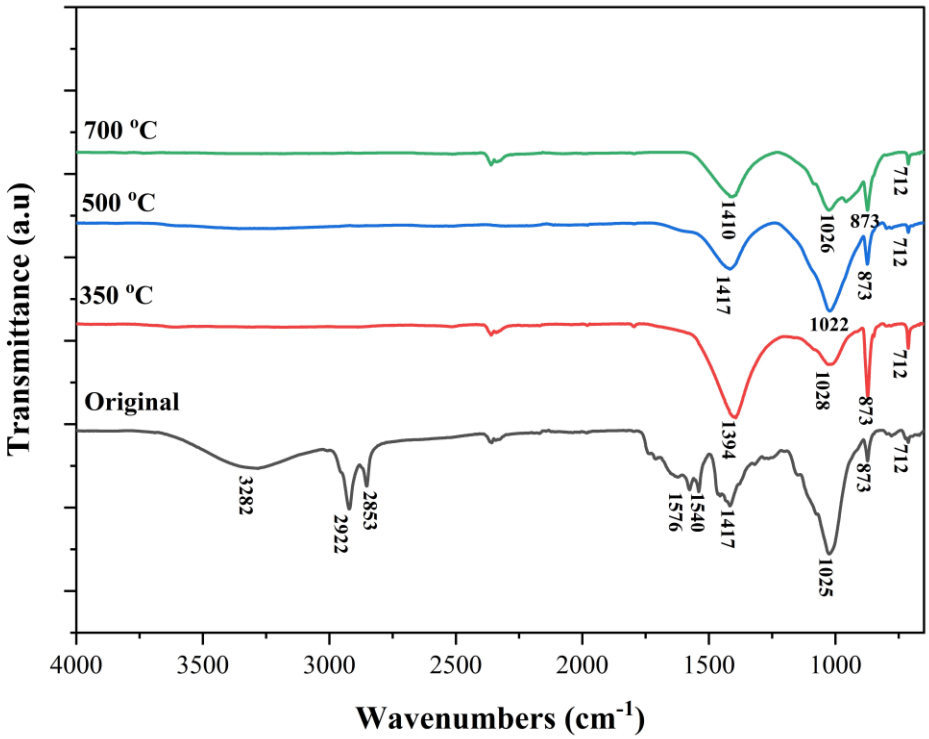

Figure-S 11 FT-IR graph of W4.2

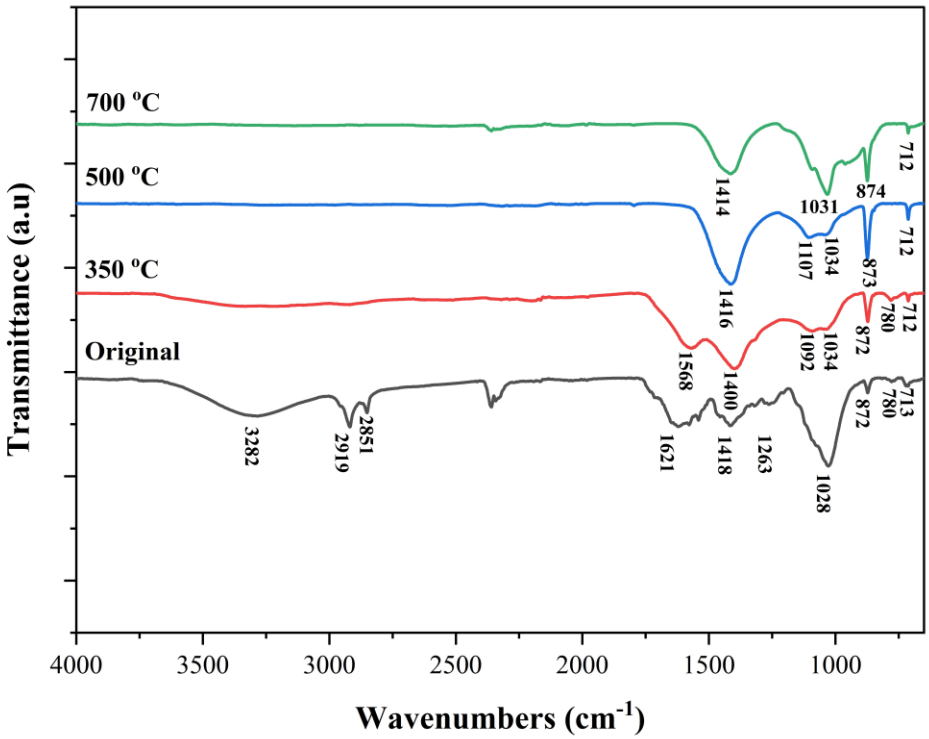

Figure-S 12 FT-IR graph of W5.1

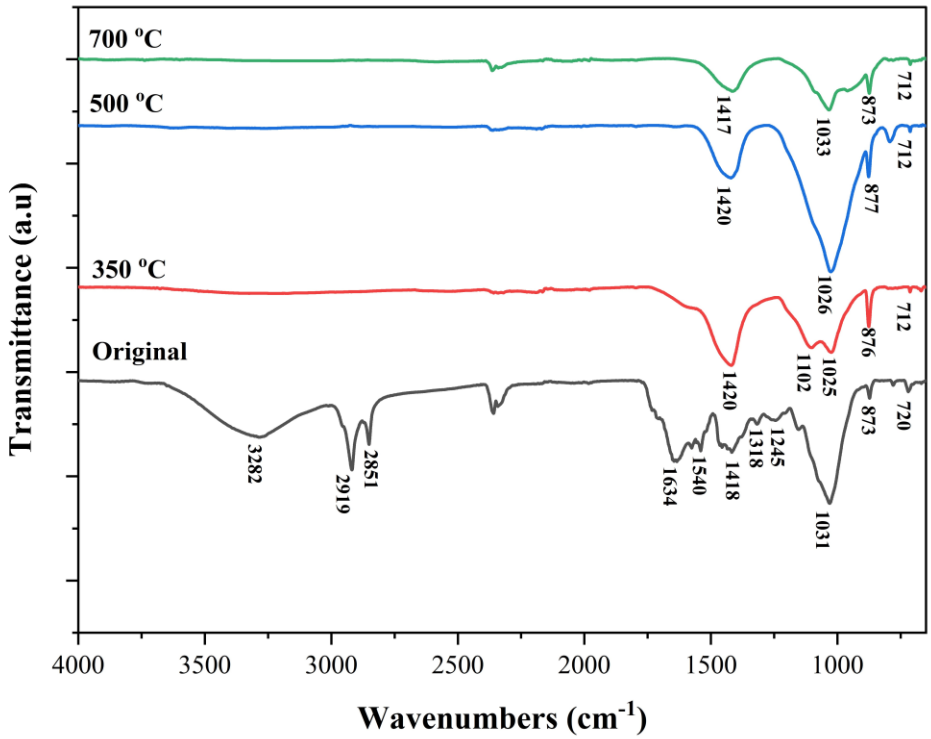

Figure-S 13 FT-IR graph of W5.2

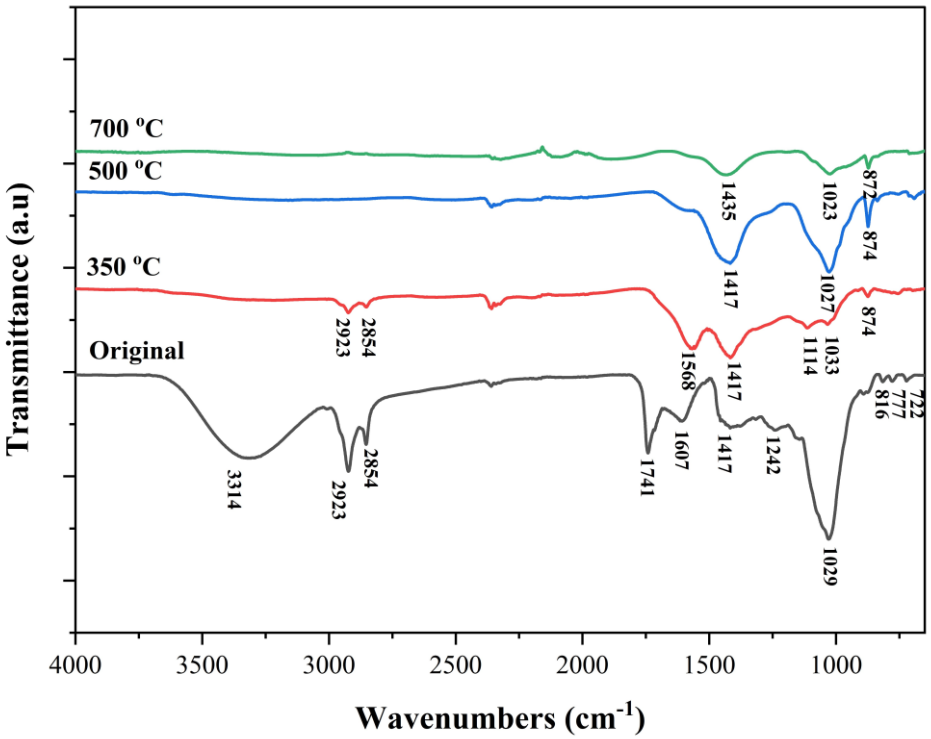

Figure-S 14 FT-IR graph of W6.1

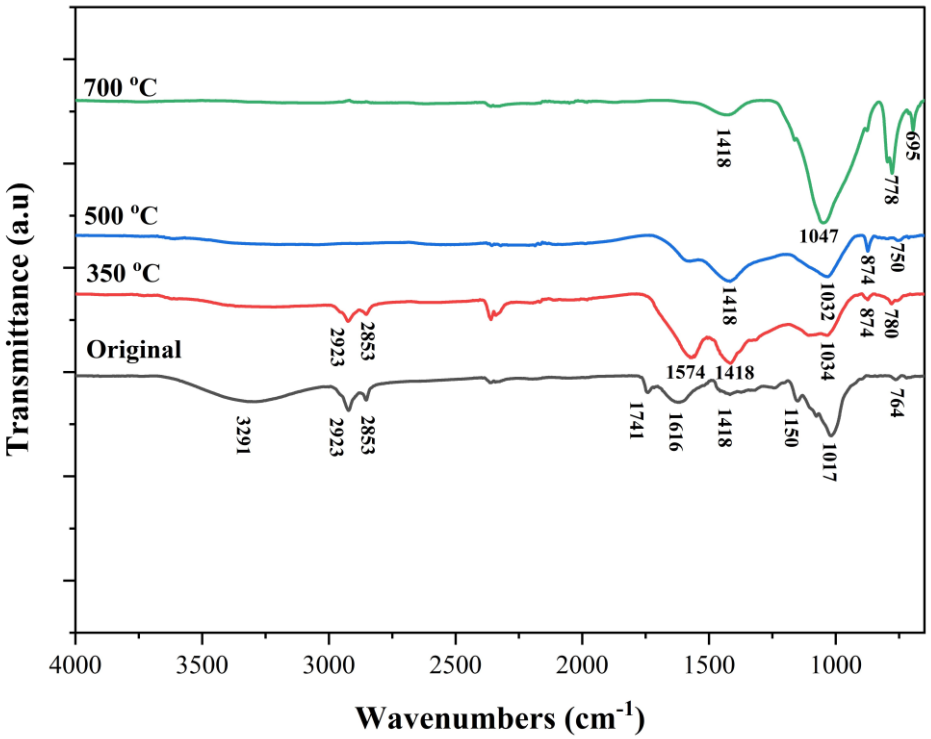

Figure-S 15 FT-IR graph of W6.2

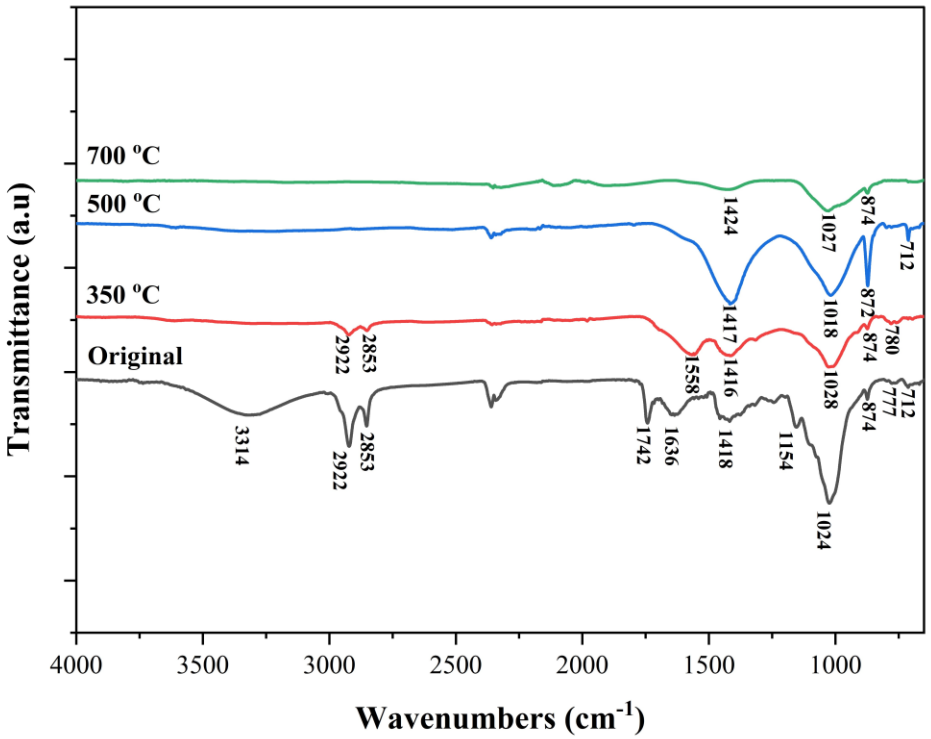

Figure-S 16 FT-IR graph of W7.2

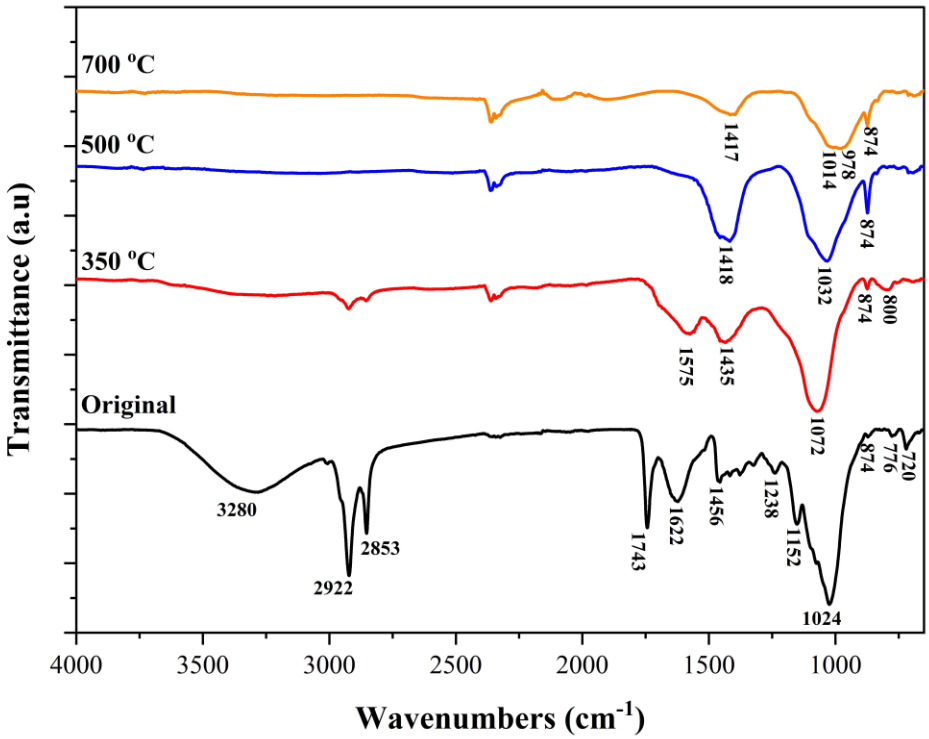

Figure-S 17 FT-IR graph of W8.2

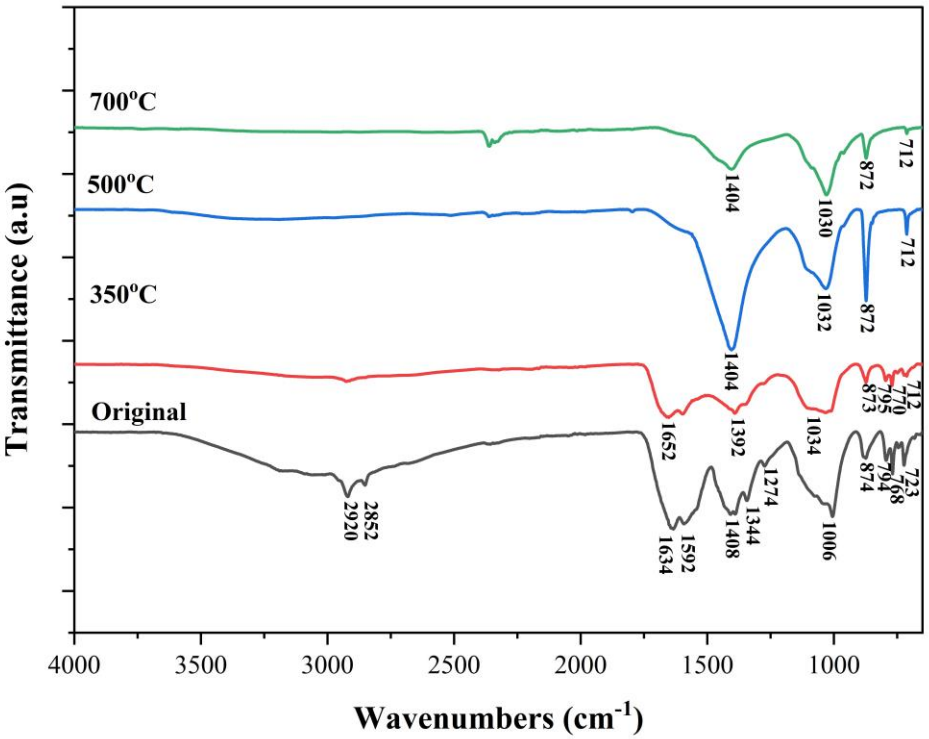

Figure-S 18 FT-IR graph of PM

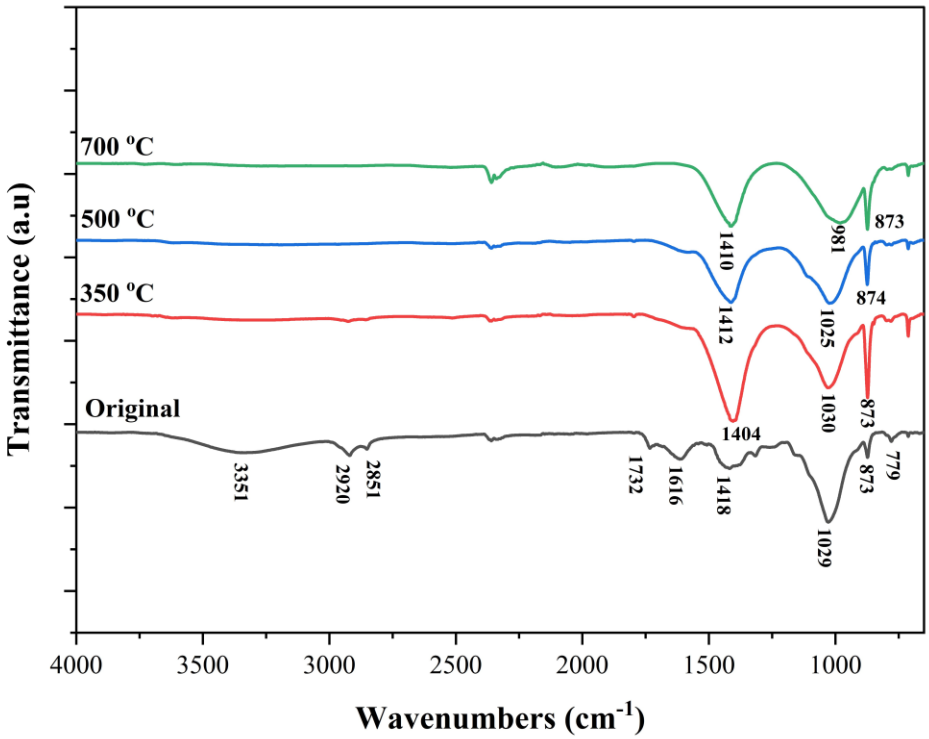

Figure-S 19 FT-IR graph of YW

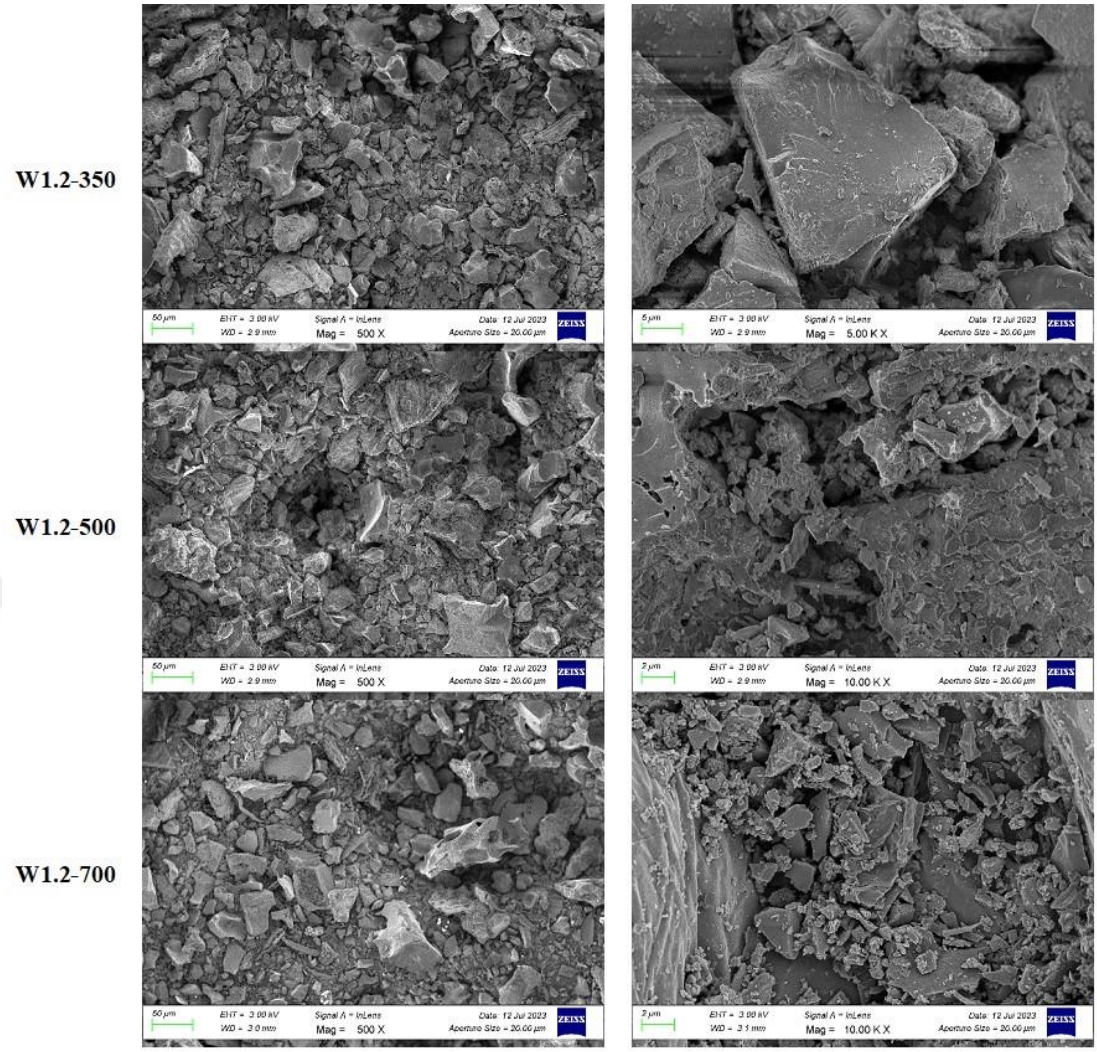

Figure-S 20 SEM images of W1.2

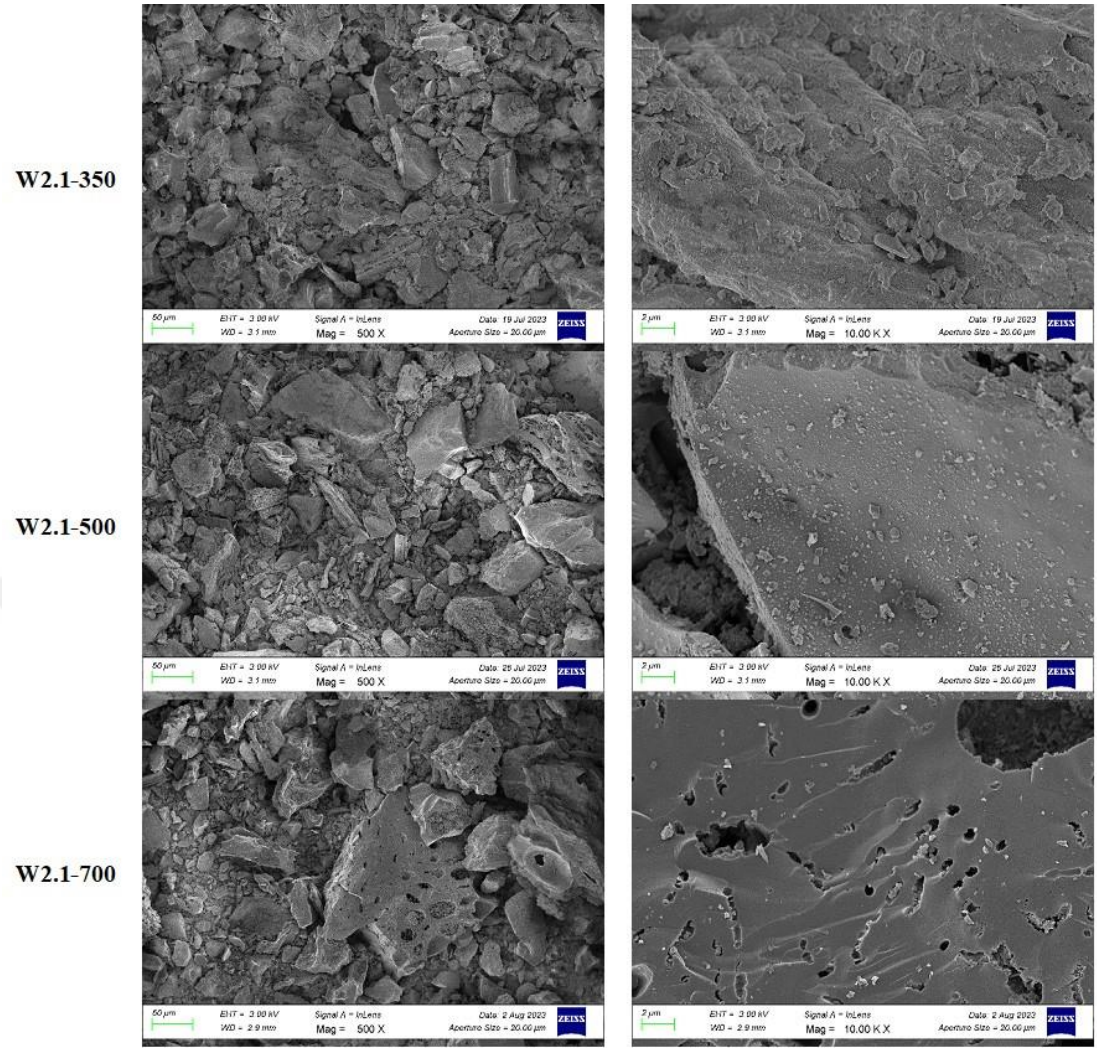

Figure-S 21 SEM images of W2.1

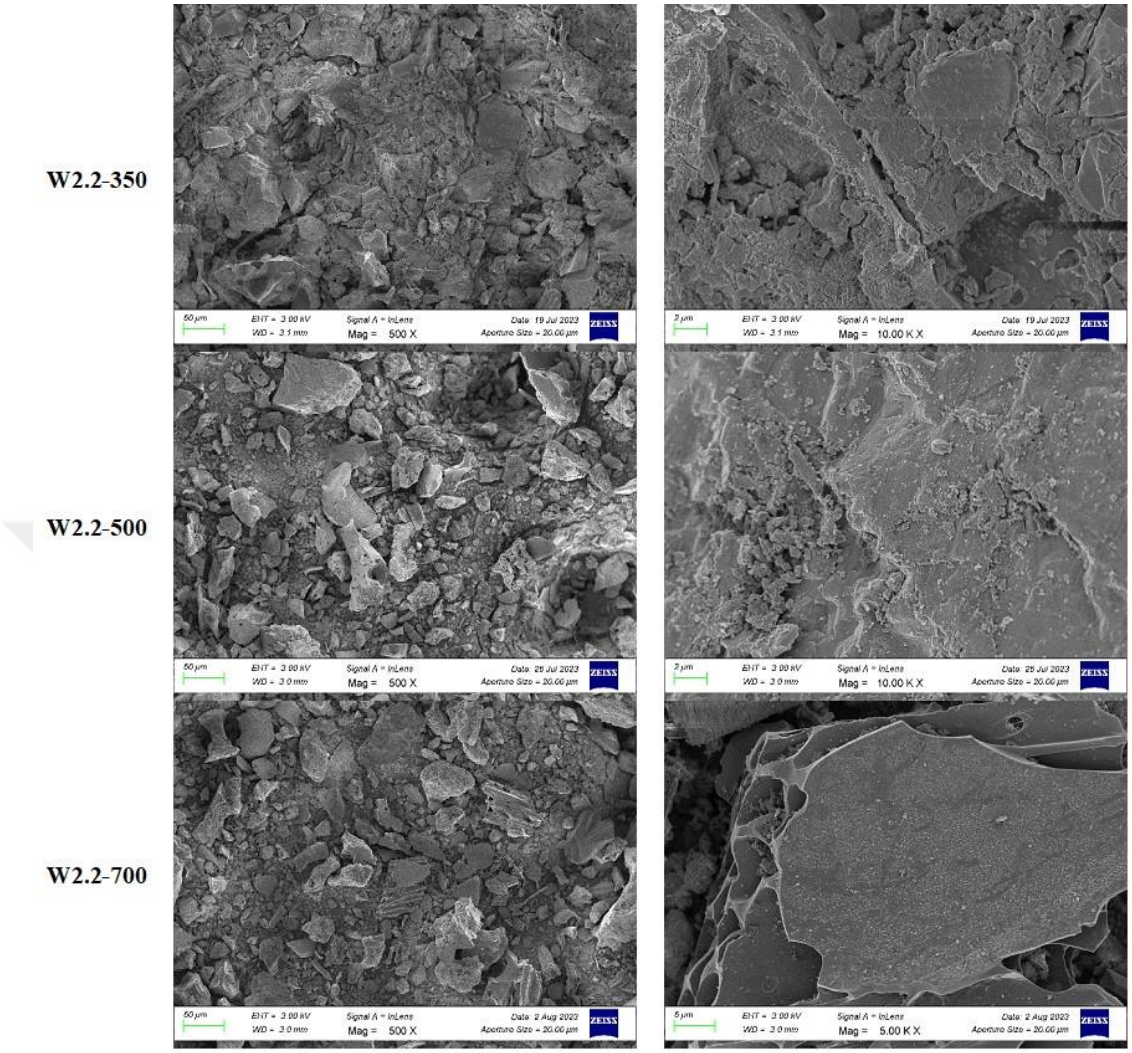

Figure-S 22 SEM images of W2.2

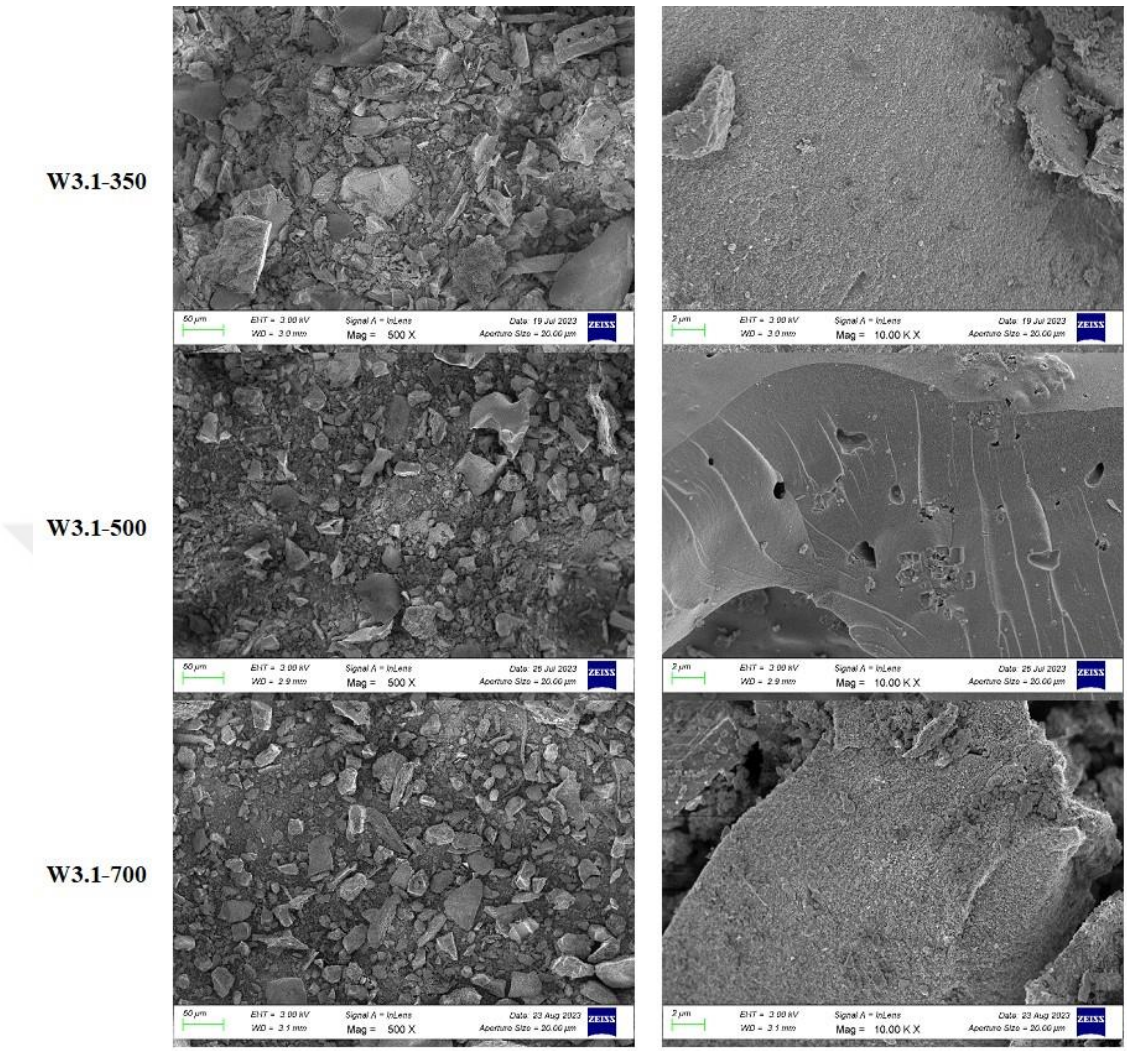

Figure-S 23 SEM images of W3.1

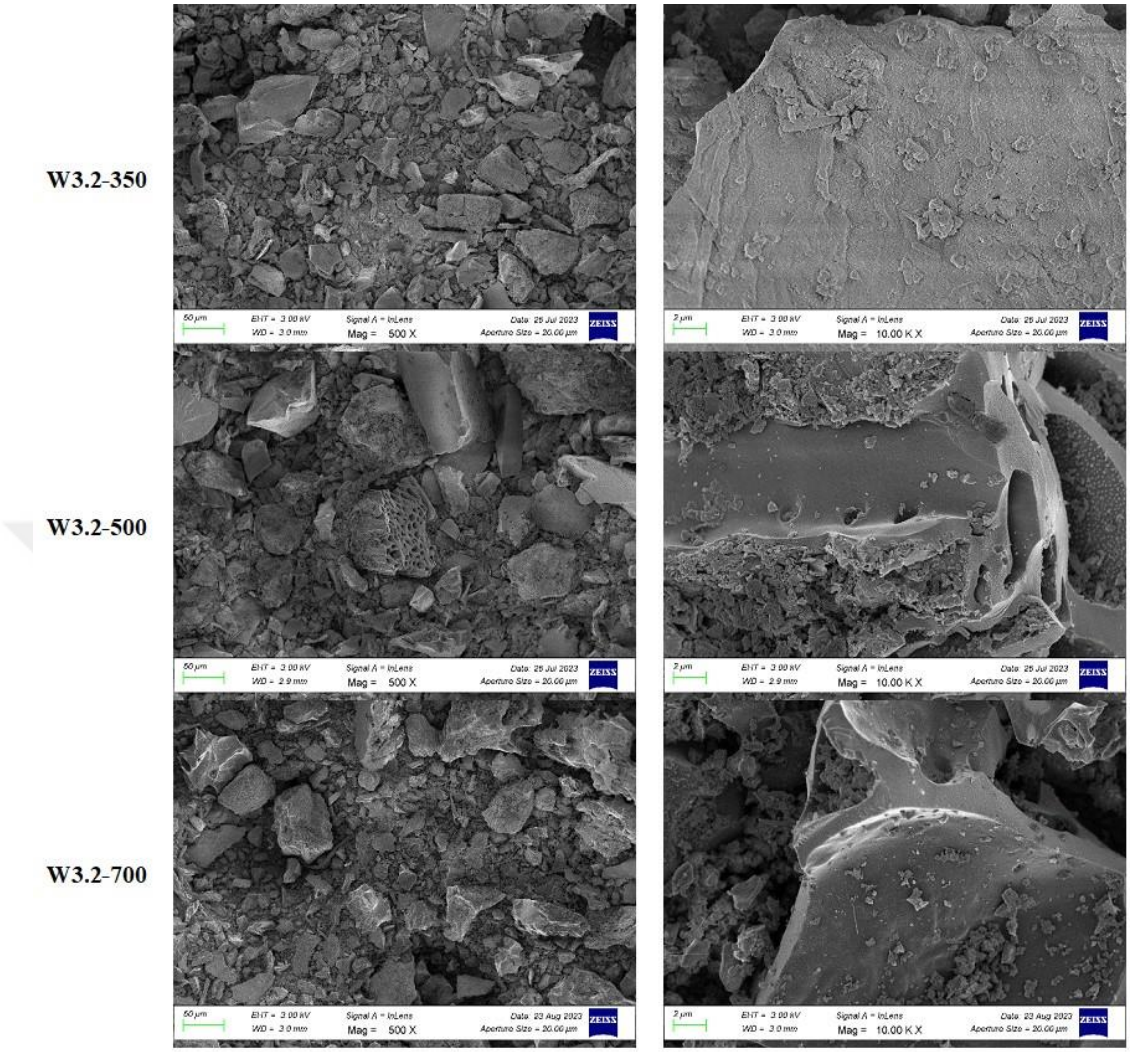

Figure-S 24 SEM images of W3.2

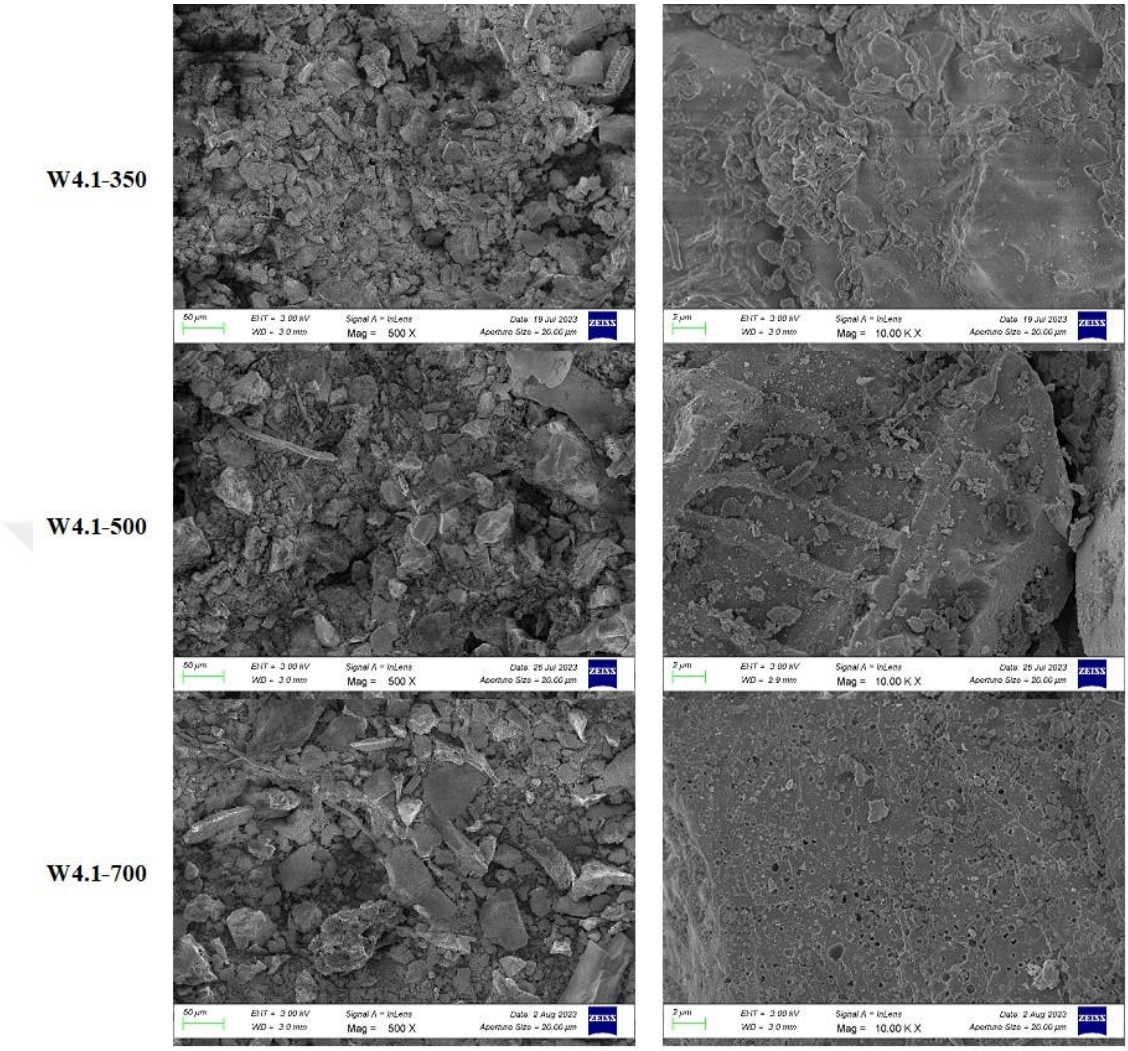

Figure-S 25 SEM images of W4.1

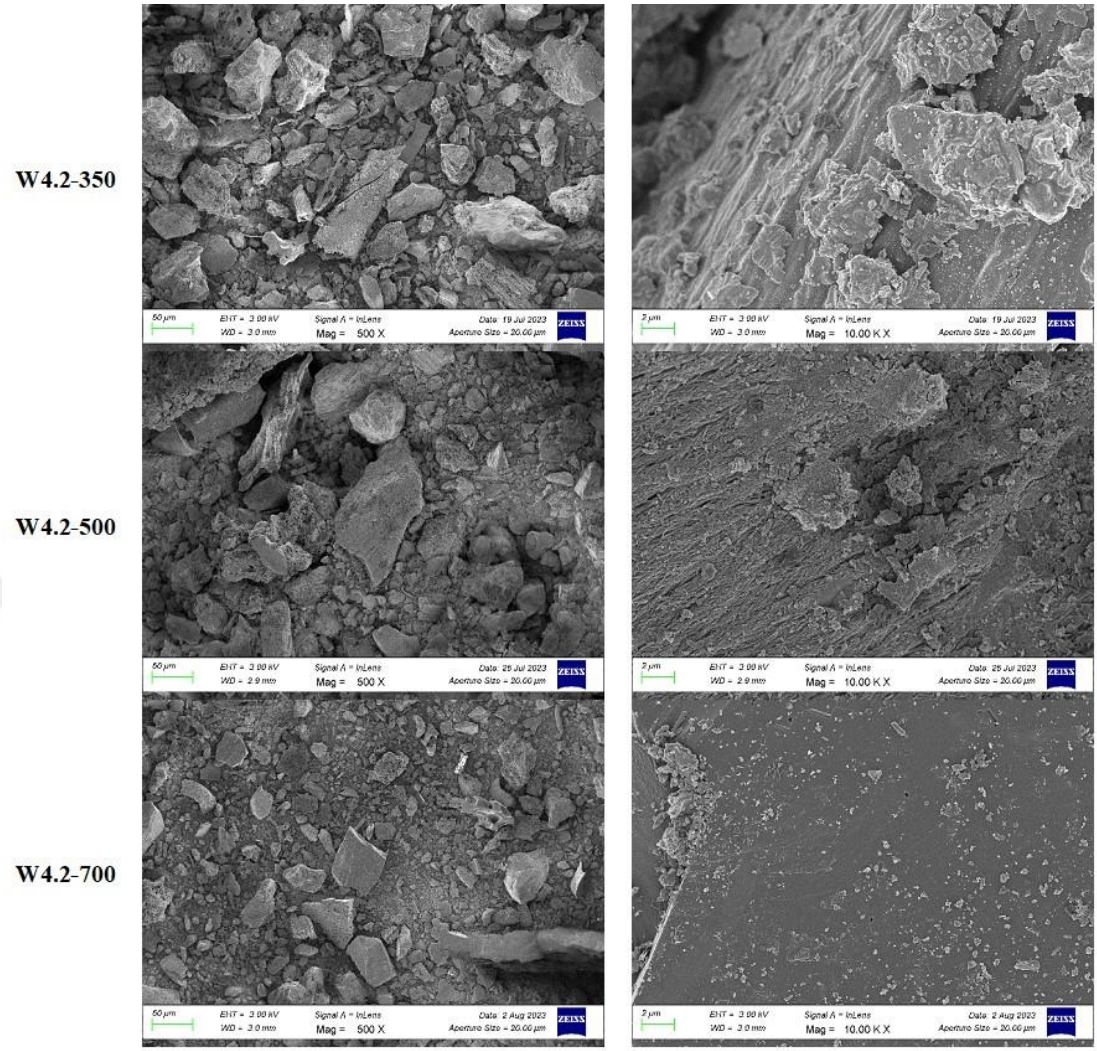

Figure-S 26 SEM images of W4.2

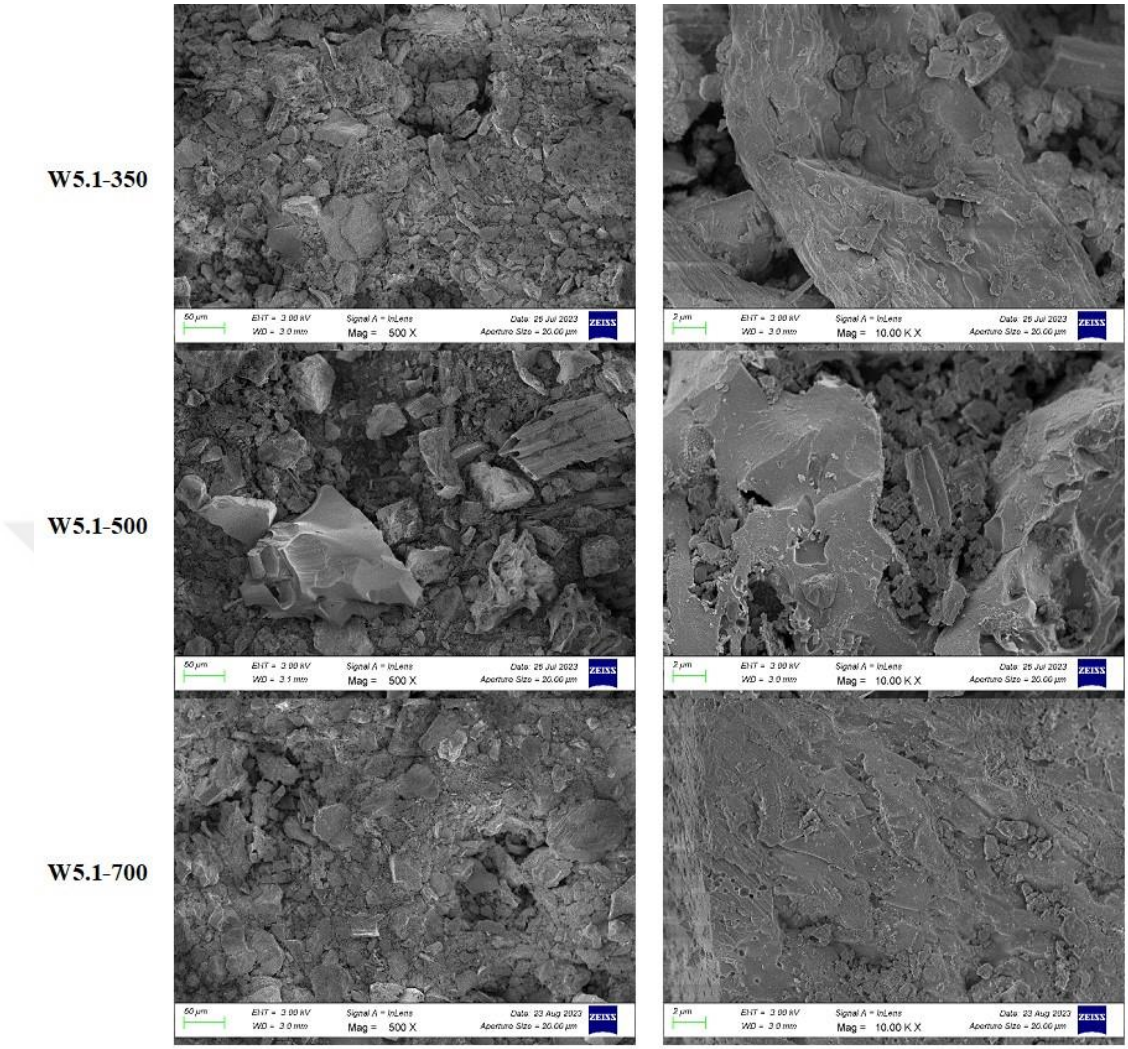

Figure-S 27 SEM images of W5.1

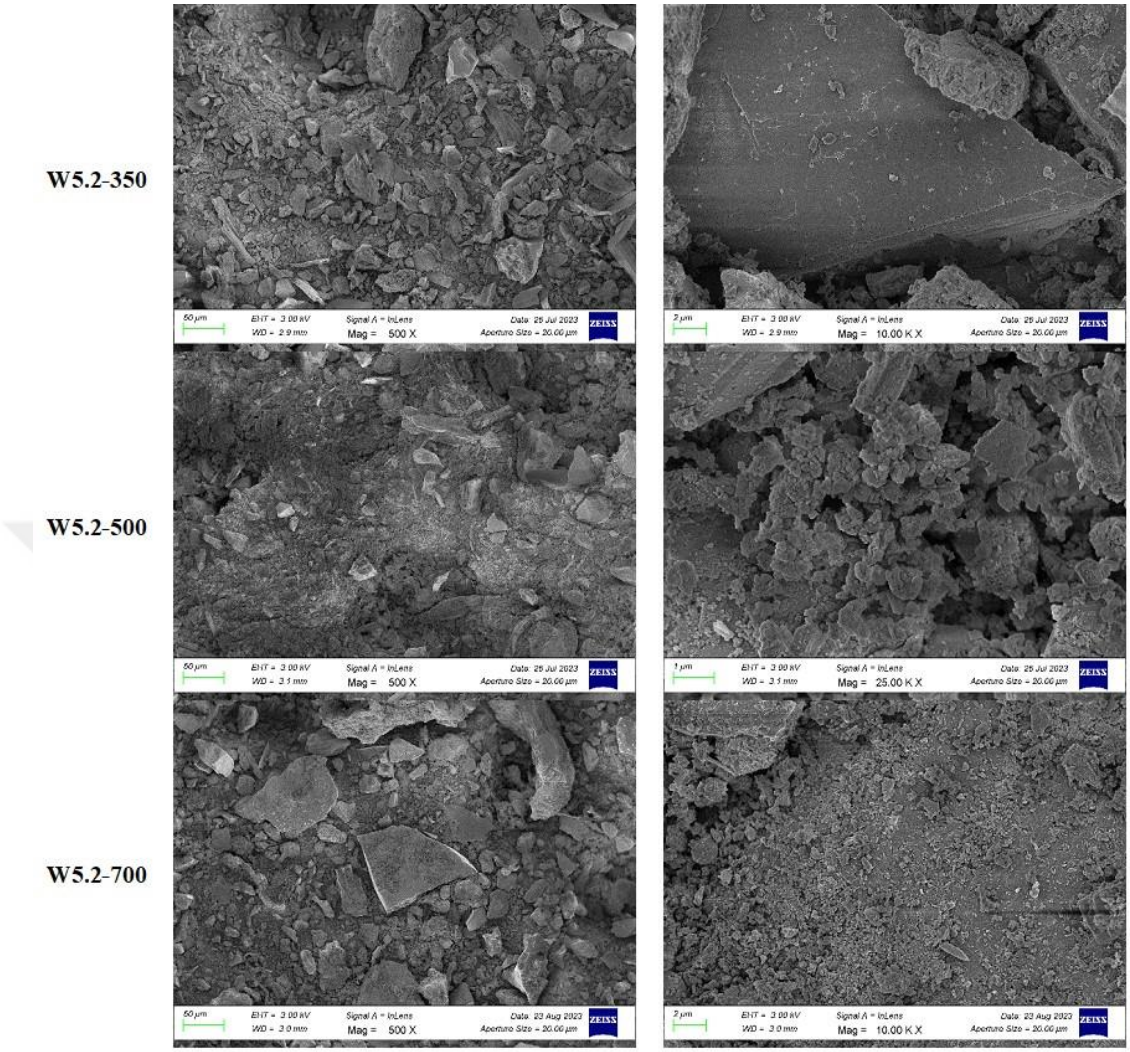

Figure-S 28 SEM images of W5.2

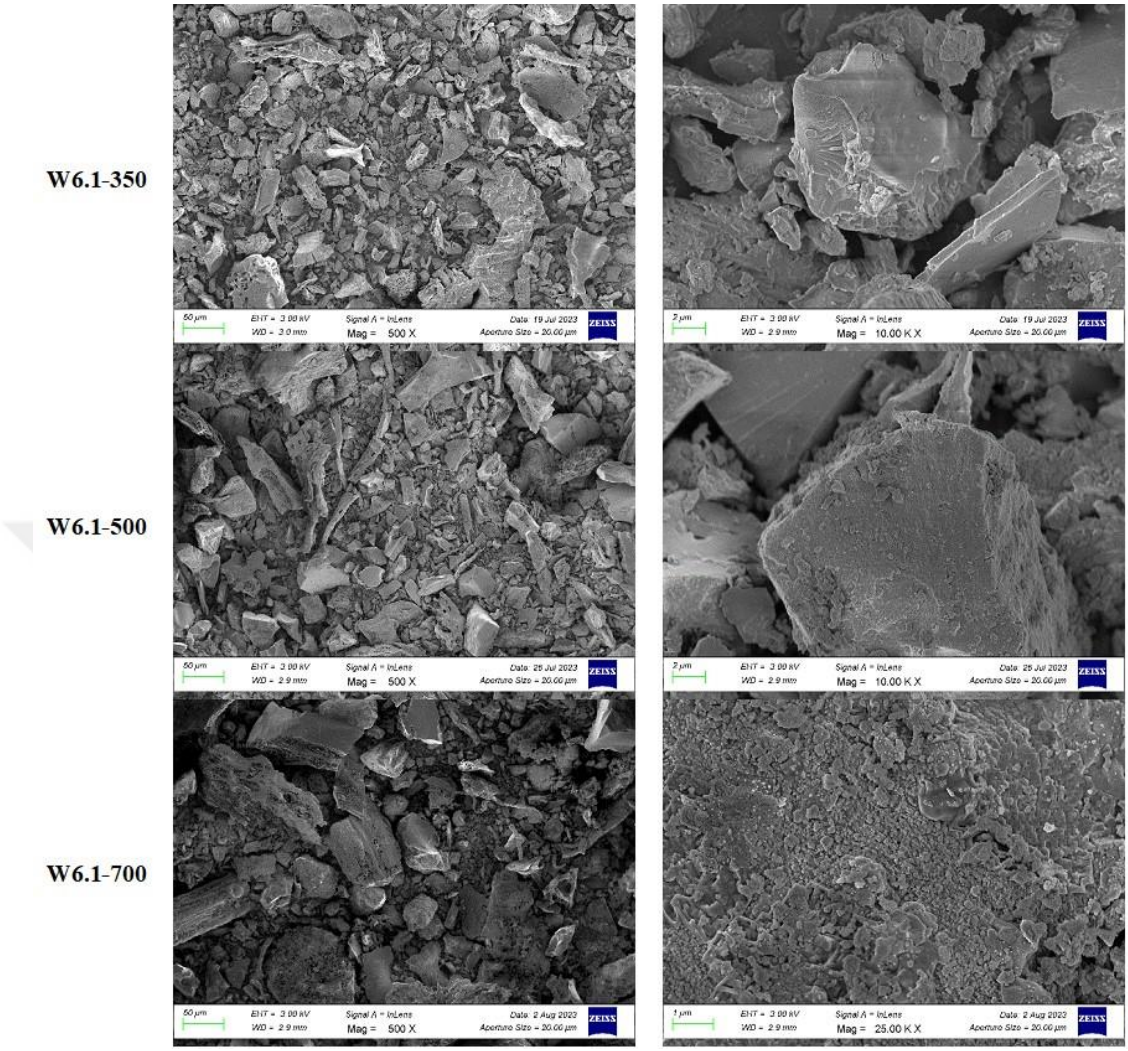

Figure-S 29 SEM images of W6.1

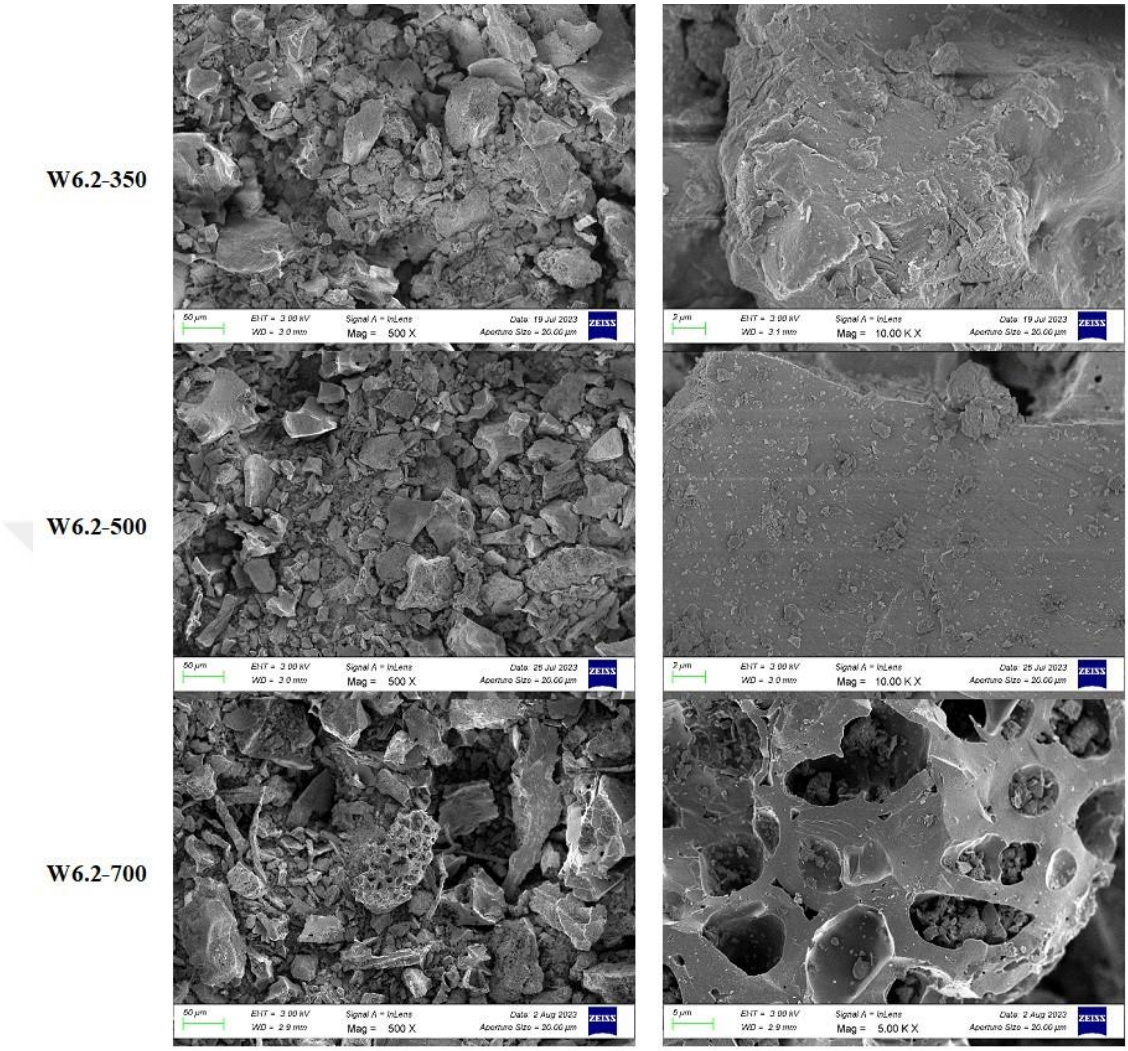

Figure-S 30 SEM images of W6.2

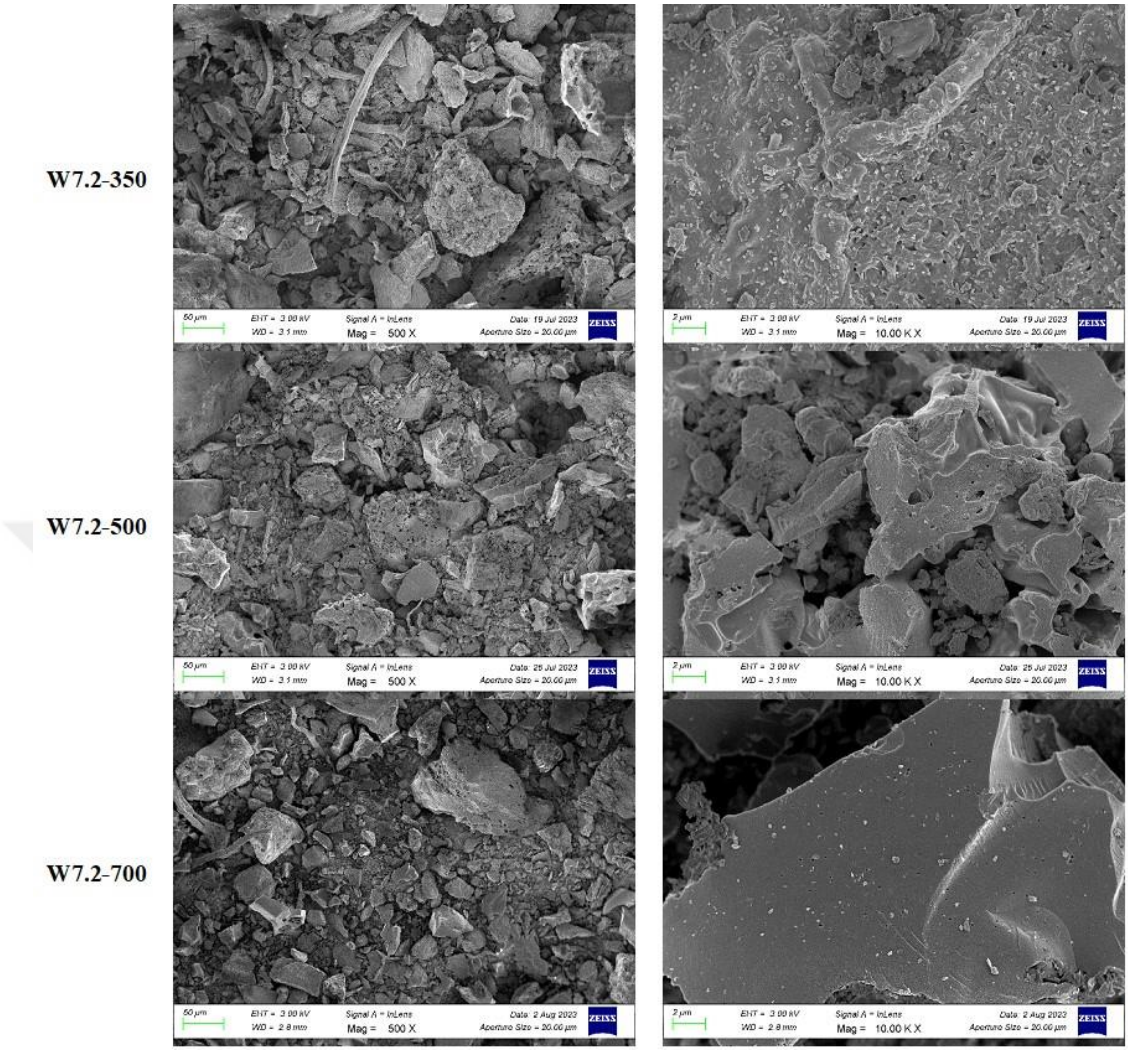

Figure-S 31 SEM images of W7.2

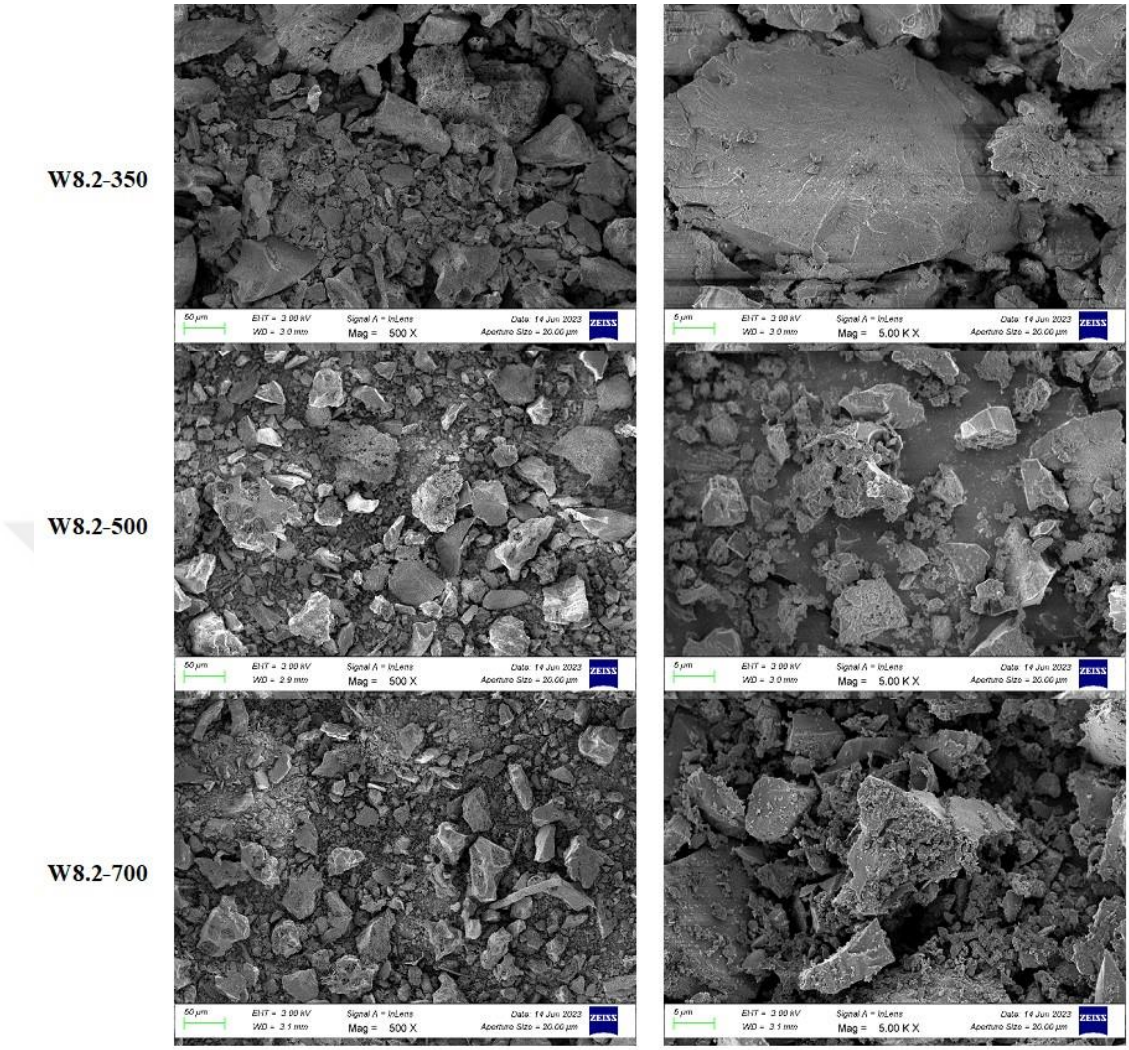

Figure-S 32 SEM images of W8.2

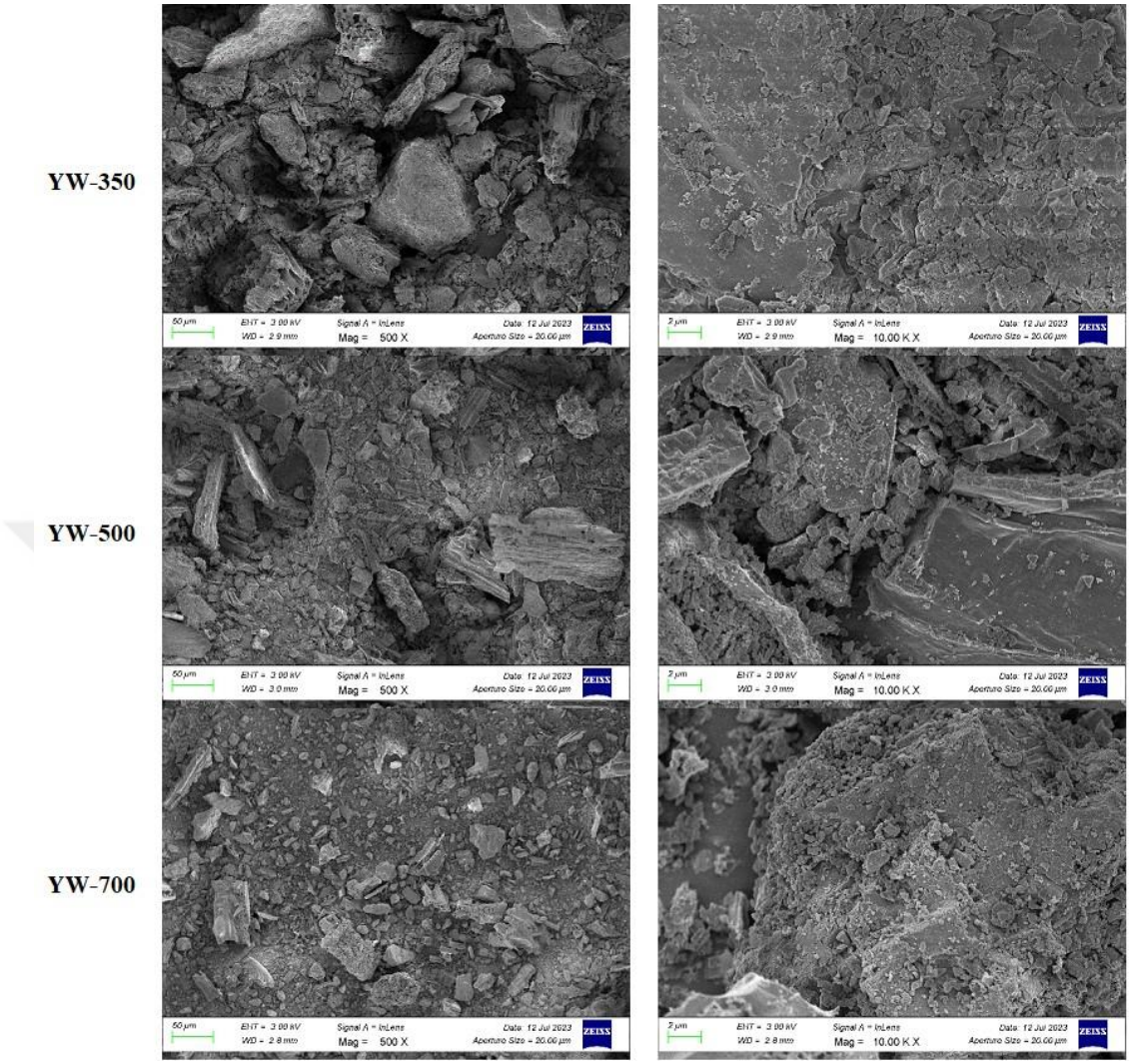

Figure-S 33 SEM images of YW

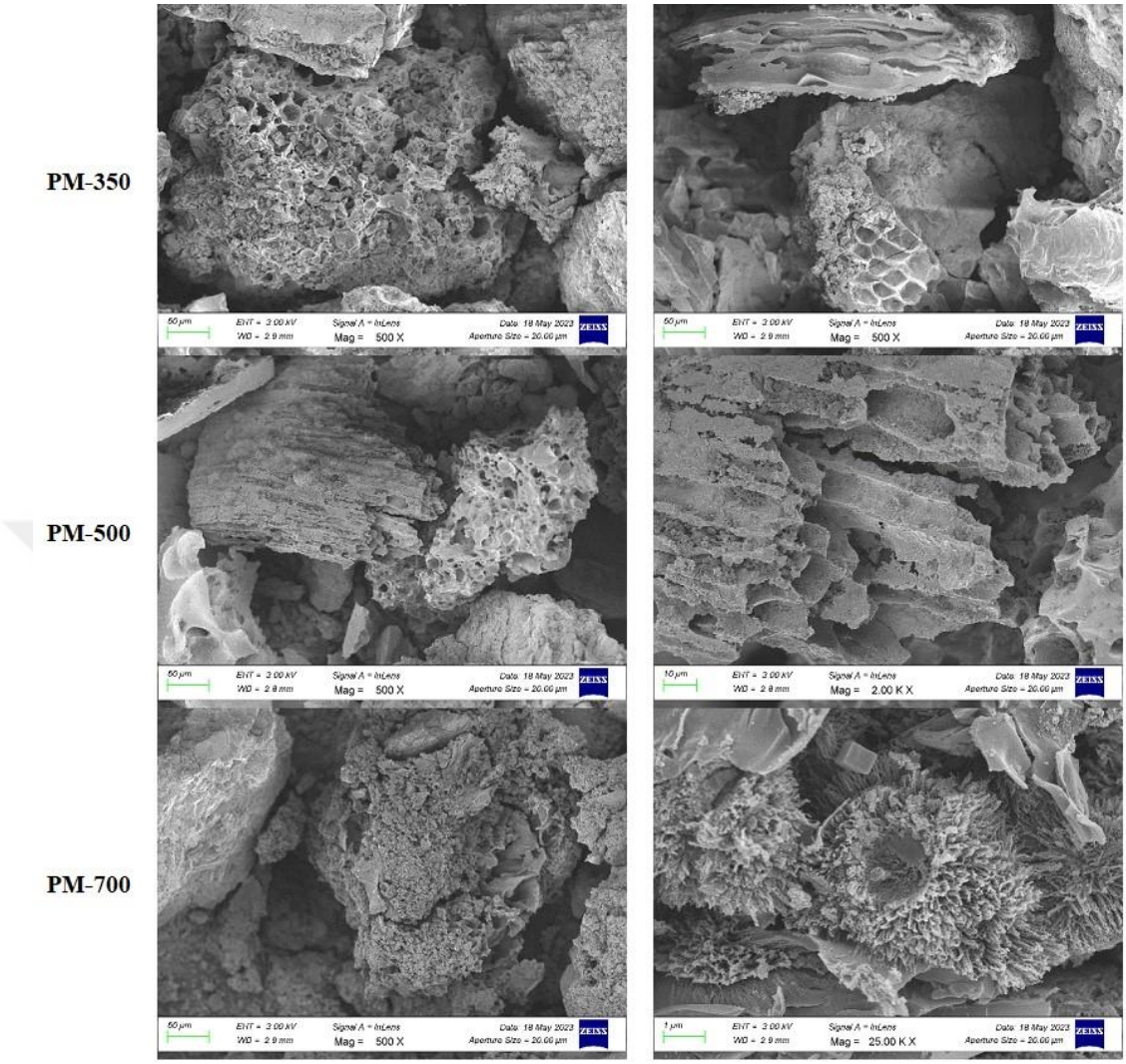

Figure-S 34 SEM images of PM

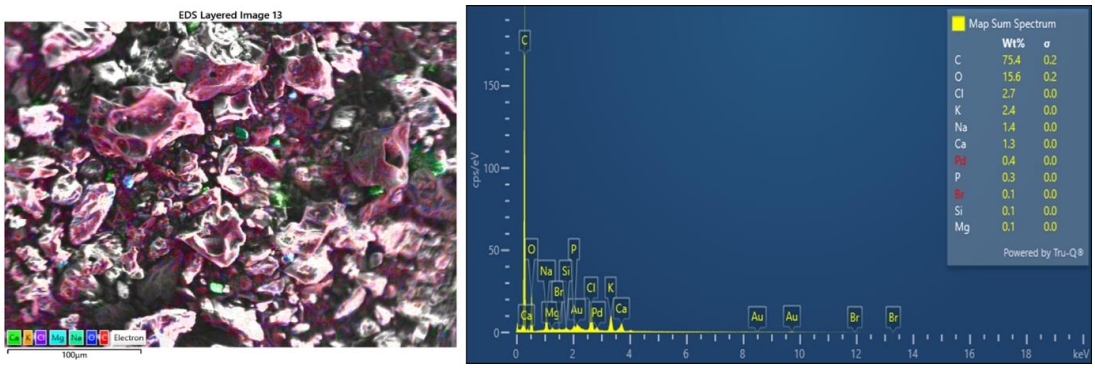

Figure-S 35 SEM-EDS result of W1.1-350

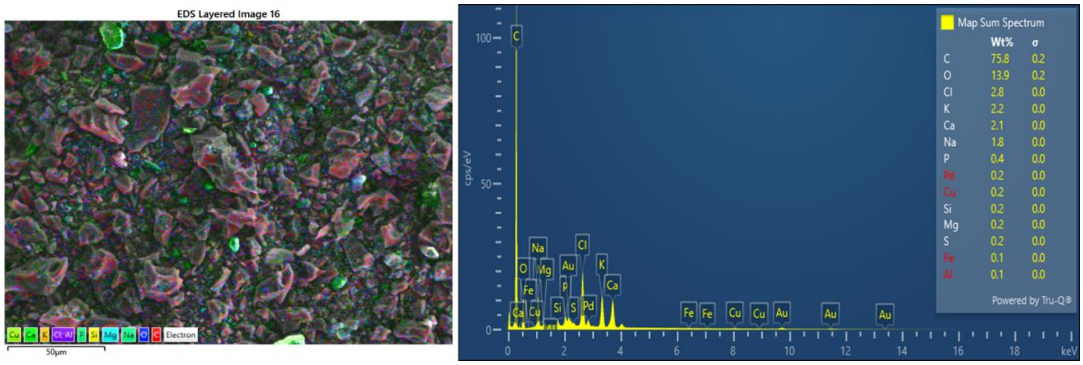

Figure-S 36 SEM-EDS result of W1.1-500

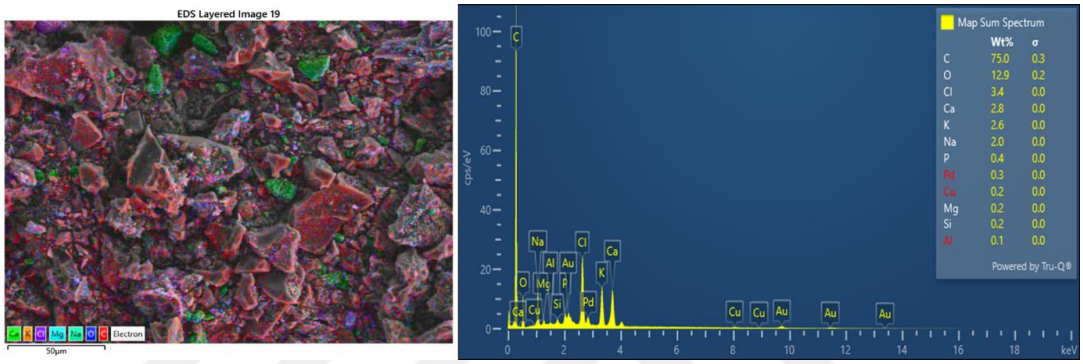

Figure-S 37 SEM-EDS result of W1.1-700

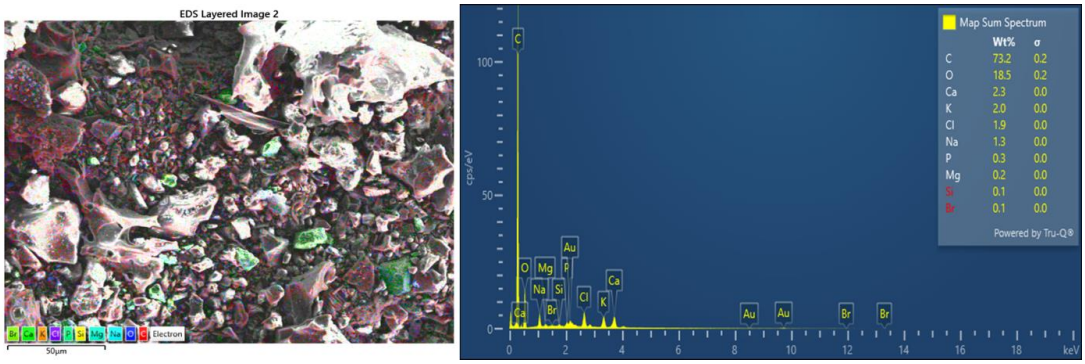

Figure-S 38 SEM-EDS result of W1.2-350

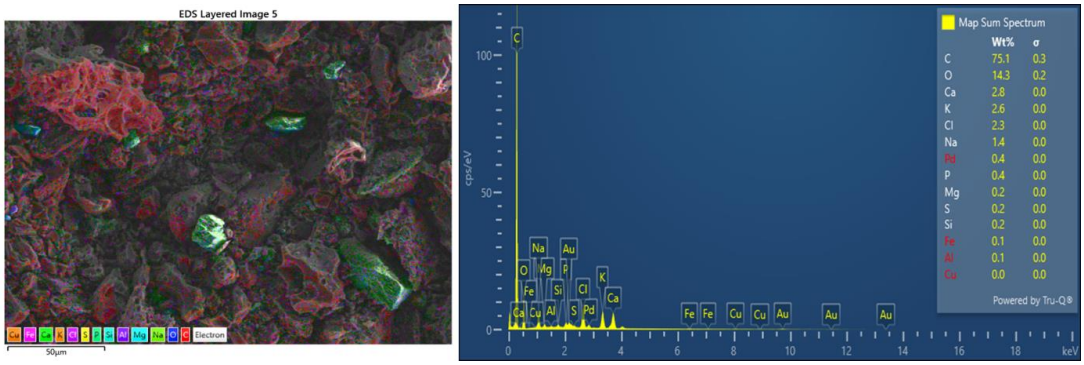

Figure-S 39 SEM-EDS result of W1.2-500

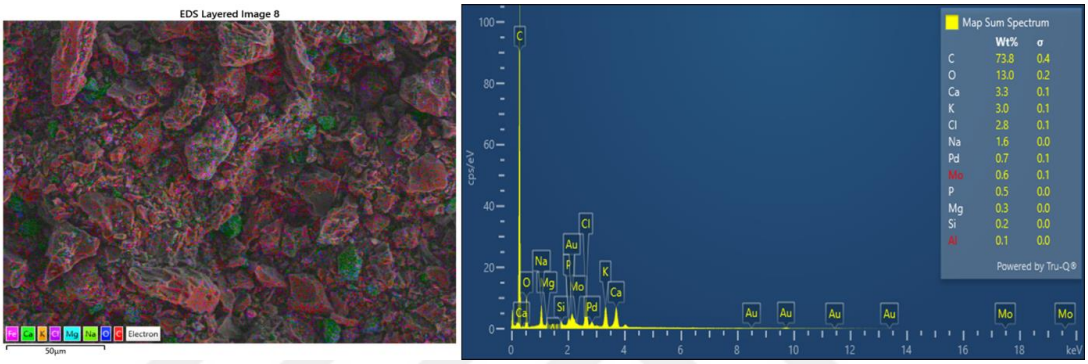

Figure-S 40 SEM-EDS result of W1.2-700

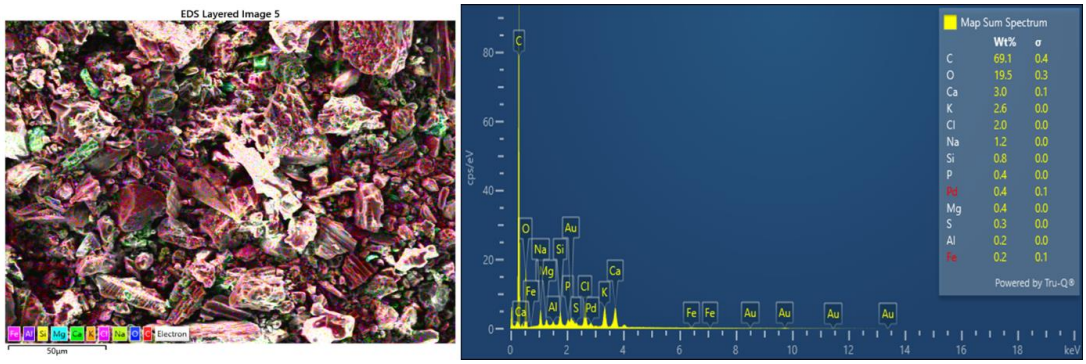

Figure-S 41 SEM-EDS result of W2.1-350

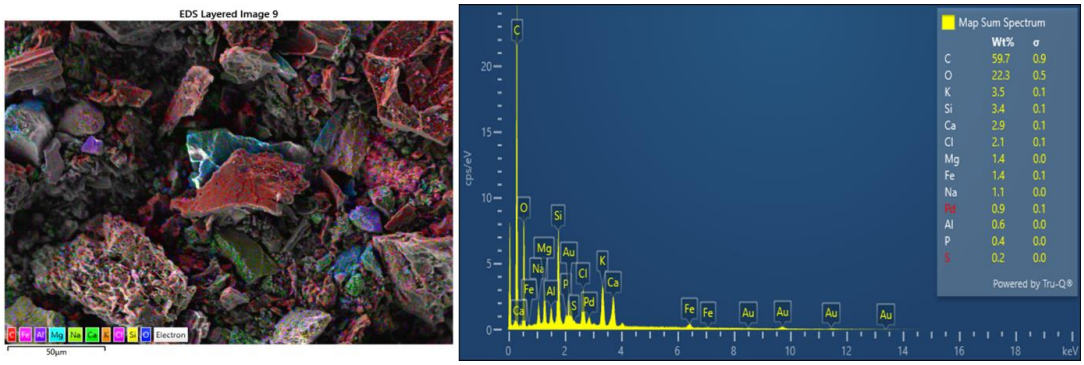

Figure-S 42 SEM-EDS result of W2.1-500

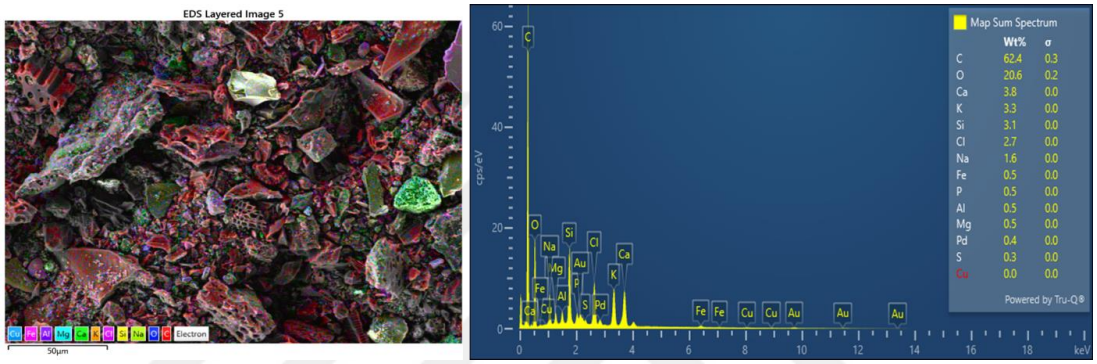

Figure-S 43 SEM-EDS result of W2.1-700

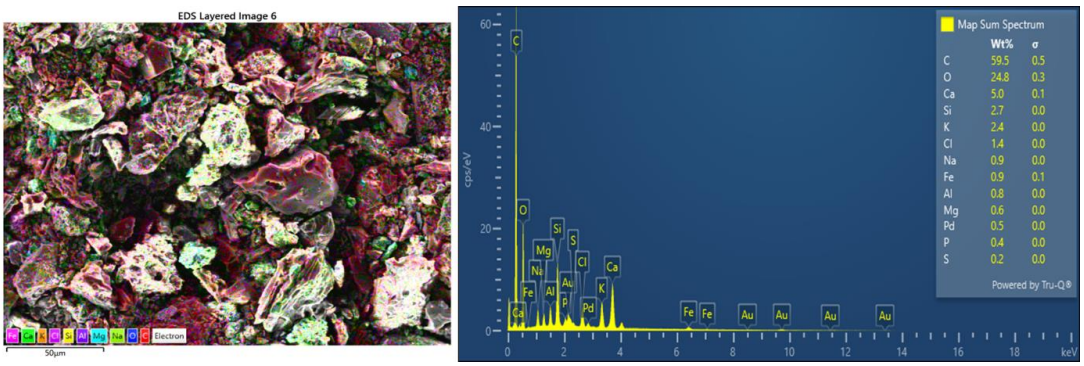

Figure-S 44 SEM-EDS result of W2.2-350

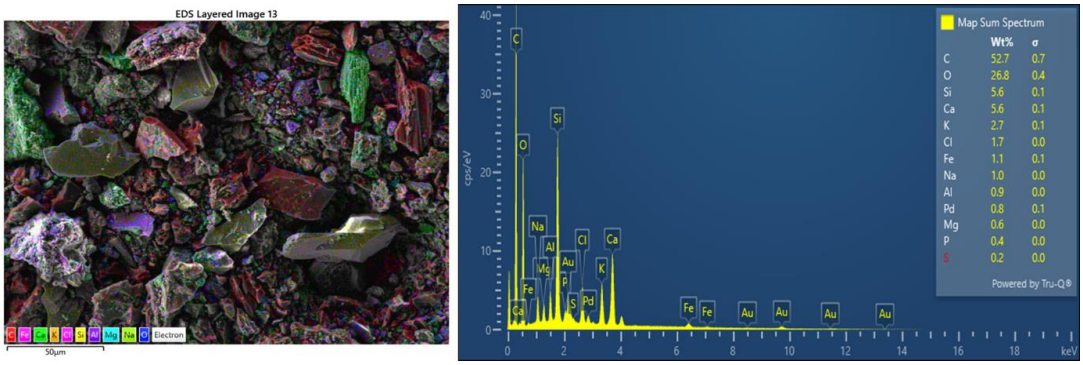

Figure-S 45 SEM-EDS result of W2.2-500

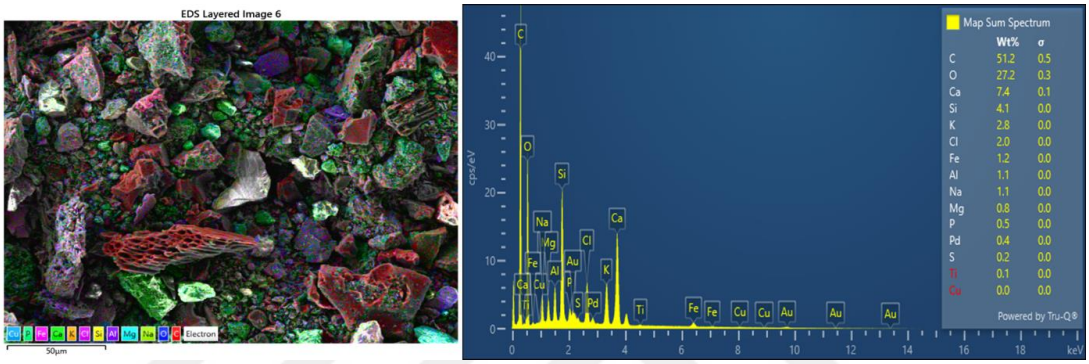

Figure-S 46 SEM-EDS result of W2.2-700

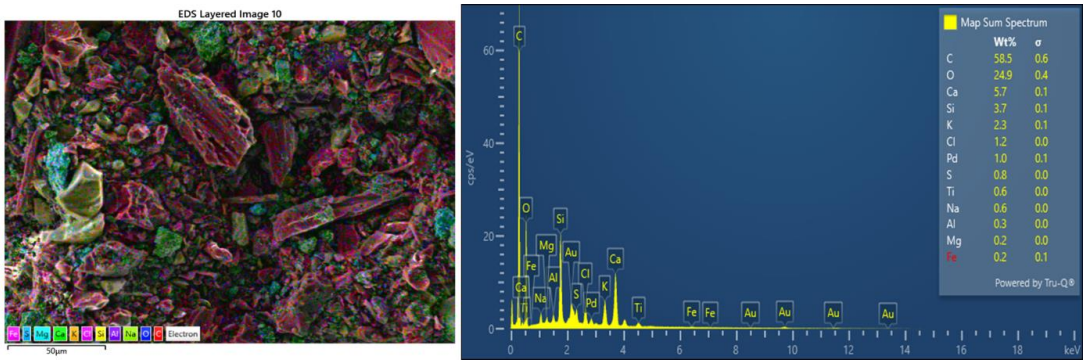

Figure-S 47 SEM-EDS result of W3.1-350

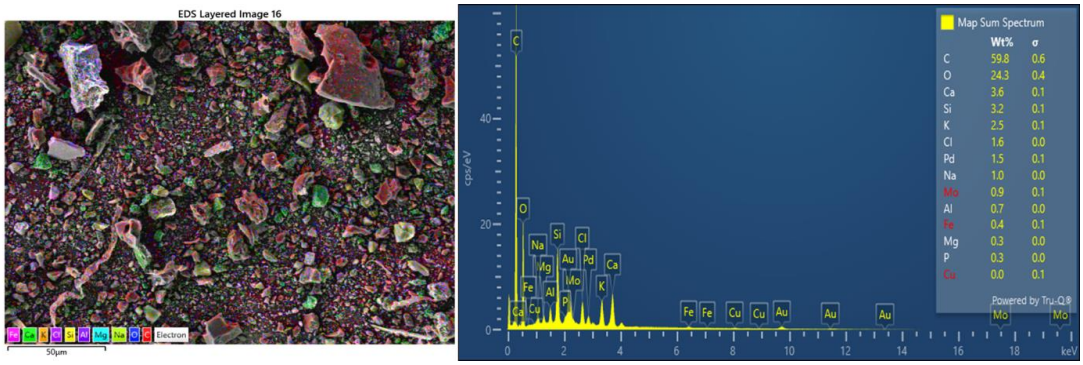

Figure-S 48 SEM-EDS result of W3.1-500

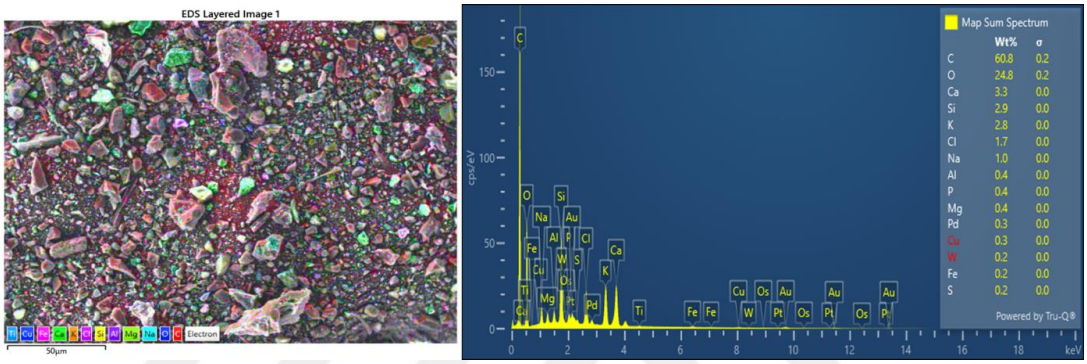

Figure-S 49 SEM-EDS result of W3.1-700

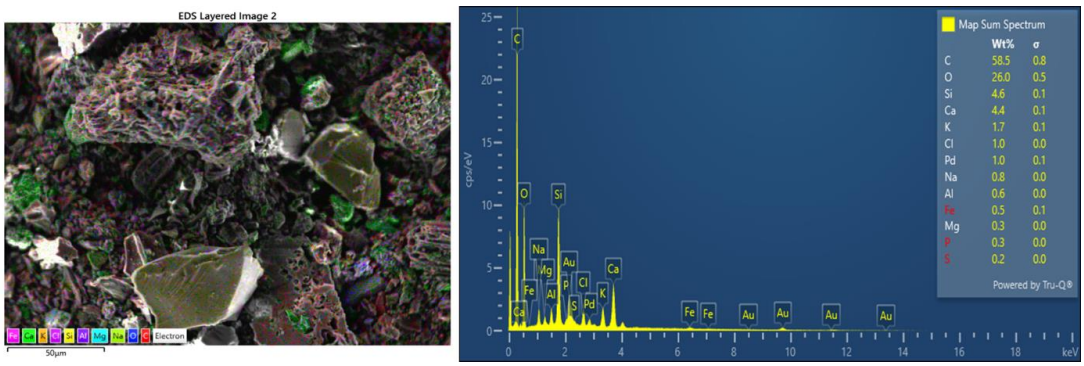

Figure-S 50 SEM-EDS result of W3.2-350

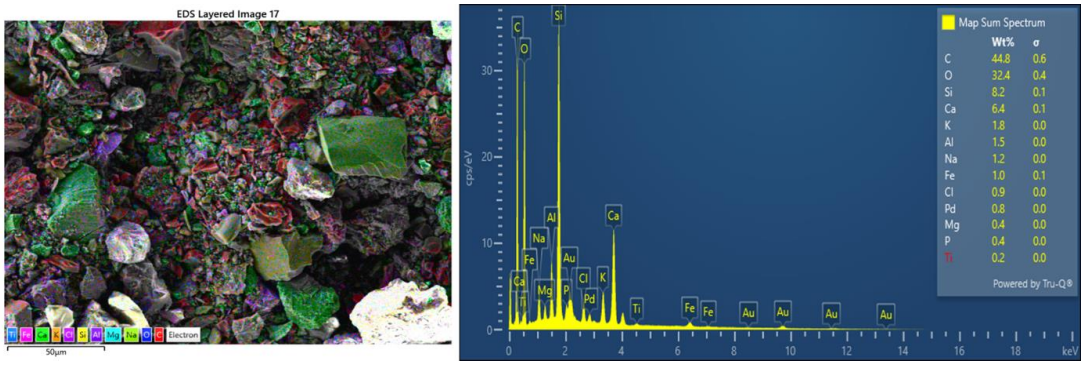

Figure-S 51 SEM-EDS result of W3.2-500

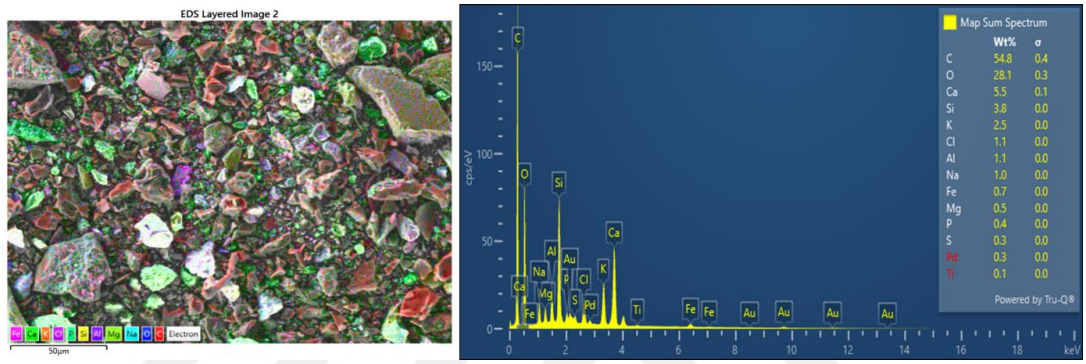

Figure-S 52 SEM-EDS result of W3.2-700

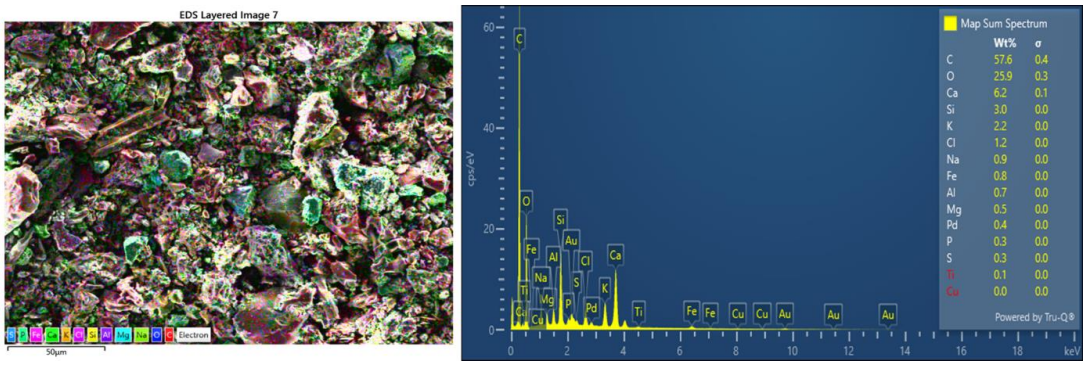

Figure-S 53 SEM-EDS result of W4.1-350

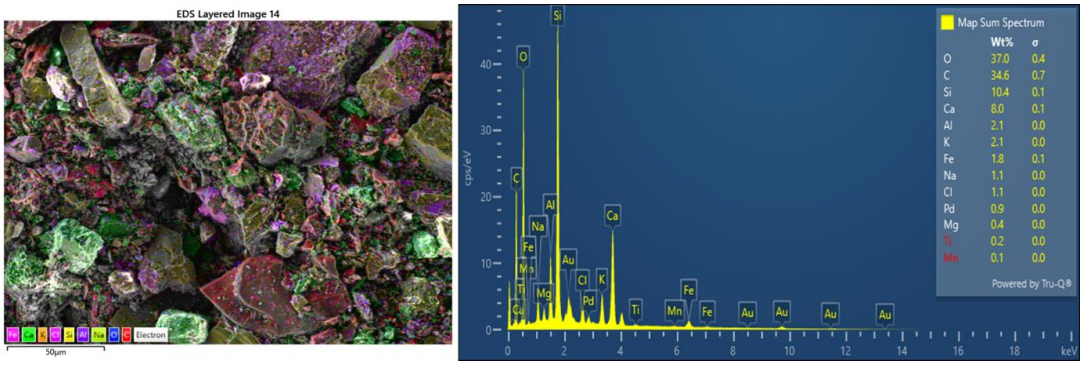

Figure-S 54 SEM-EDS result of W4.1-500

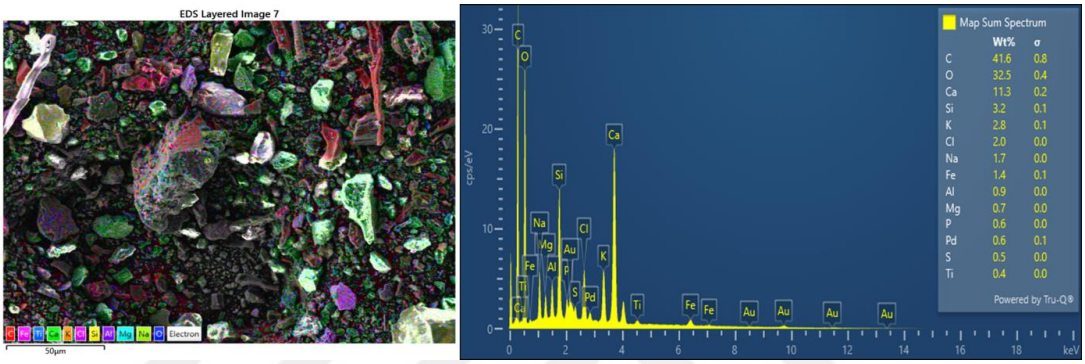

Figure-S 55 SEM-EDS result of W4.1-700

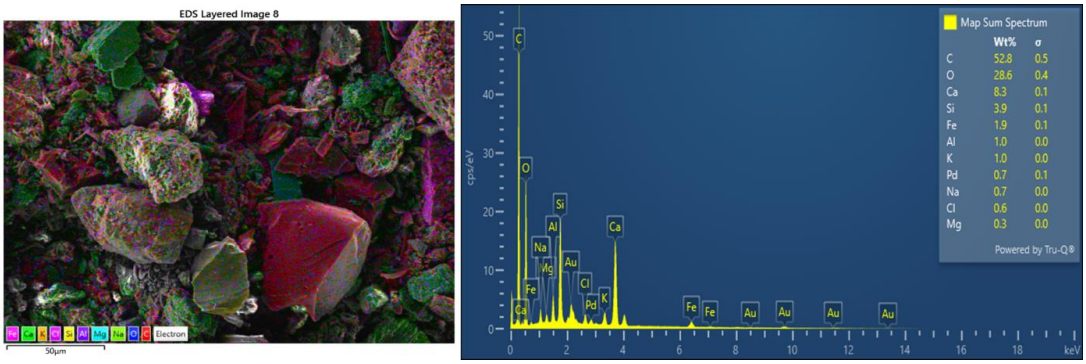

Figure-S 56 SEM-EDS result of W4.2-350

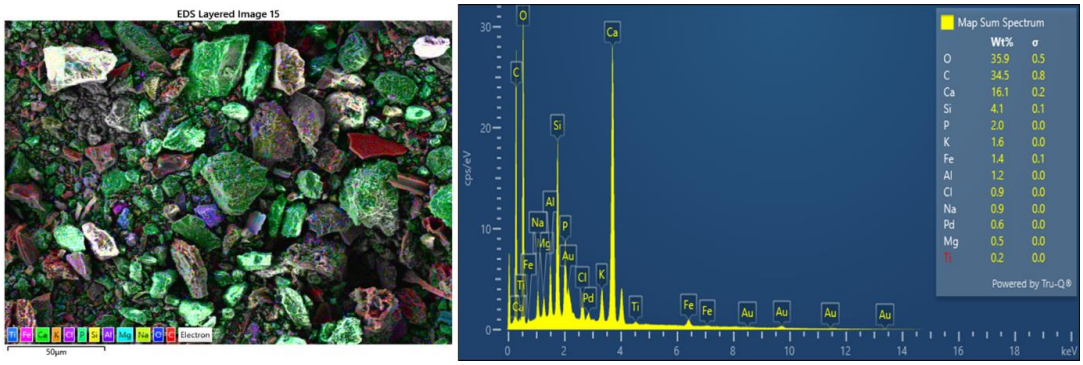

Figure-S 57 SEM-EDS result of W4.2-500

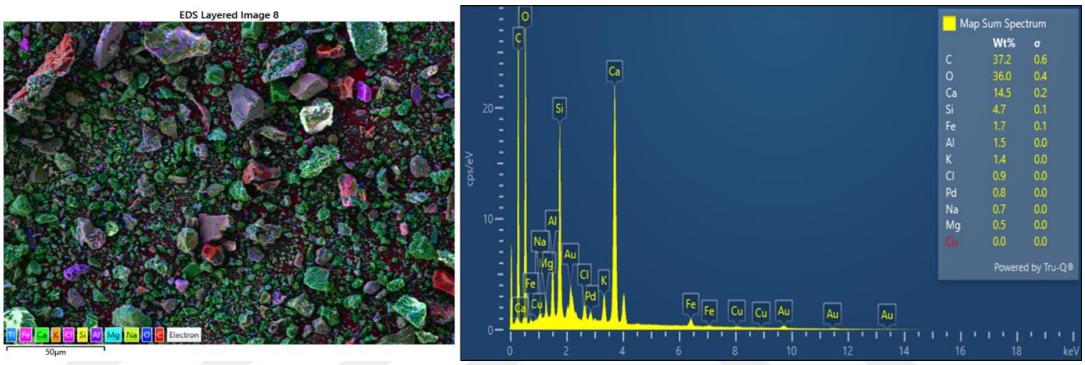

Figure-S 58 SEM-EDS result of W4.2-700

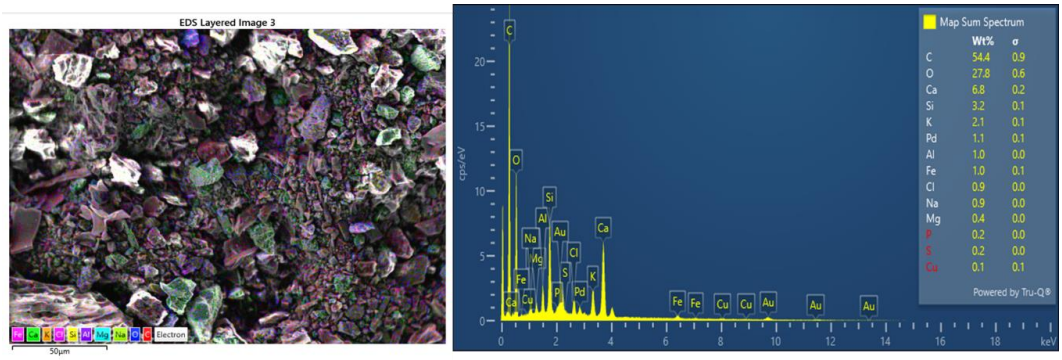

Figure-S 59 SEM-EDS result of W5.1-350

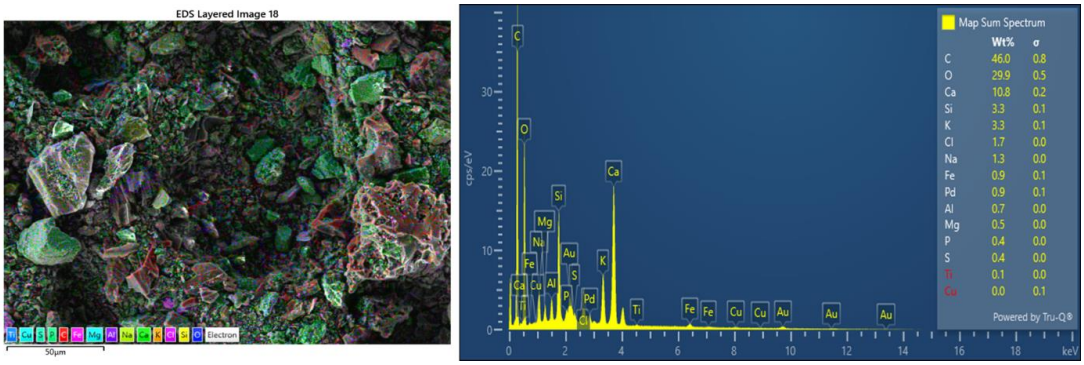

Figure-S 60 SEM-EDS result of W5.1-500

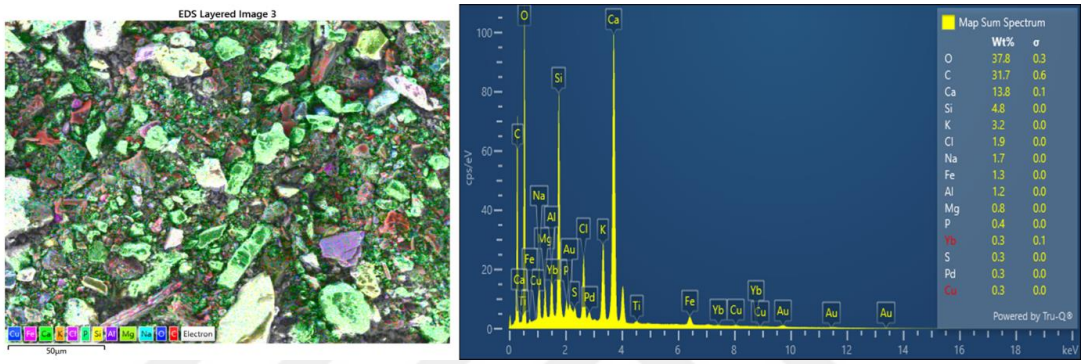

Figure-S 61 SEM-EDS result of W5.1-700

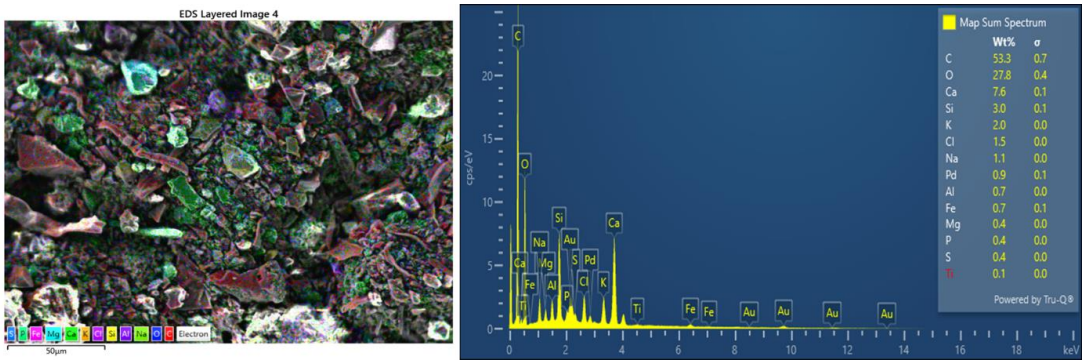

Figure-S 62 SEM-EDS result of W5.2-350

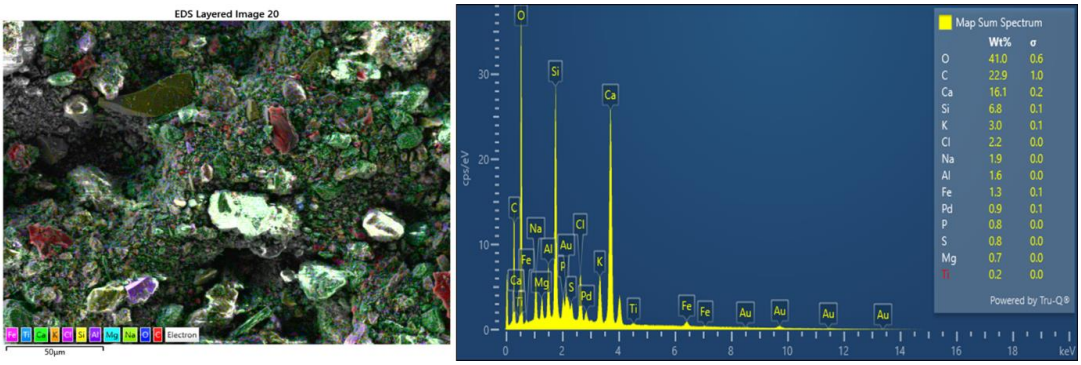

Figure-S 63 SEM-EDS result of W5.2-500

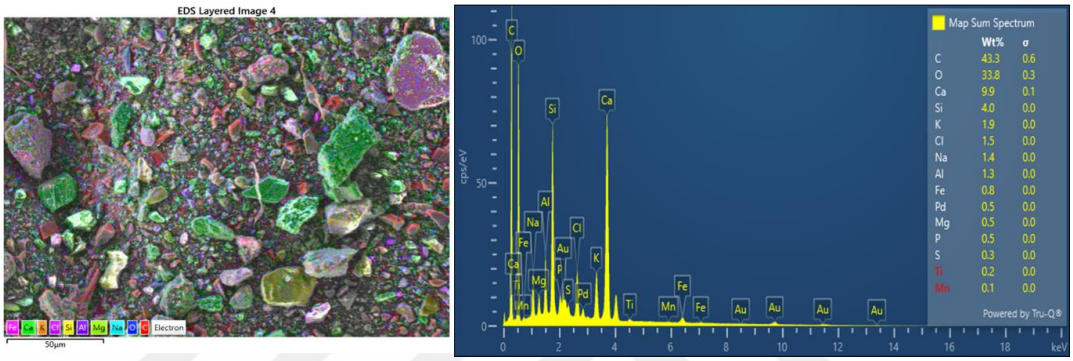

Figure-S 64 SEM-EDS result of W5.2-700

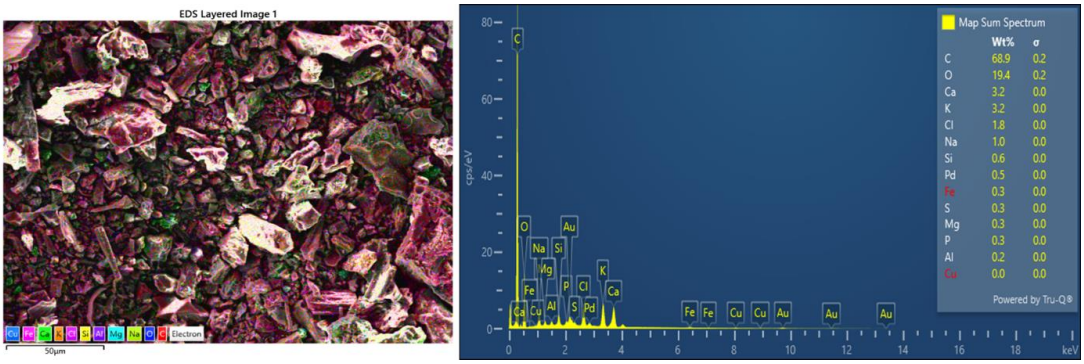

Figure-S 65 SEM-EDS result of W6.1-350

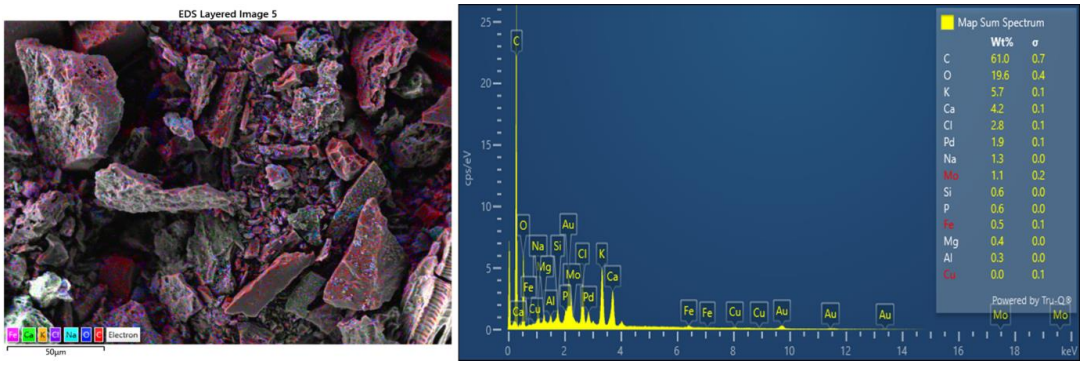

Figure-S 66 SEM-EDS result of W6.1-500

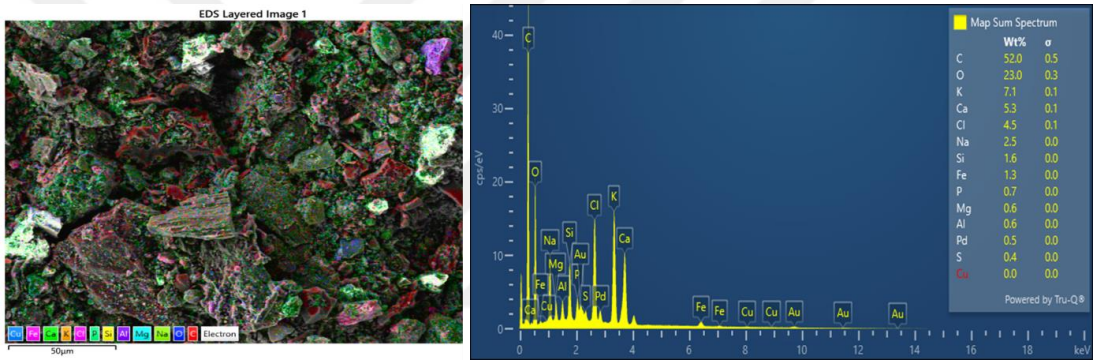

Figure-S 67 SEM-EDS result of W6.1-700

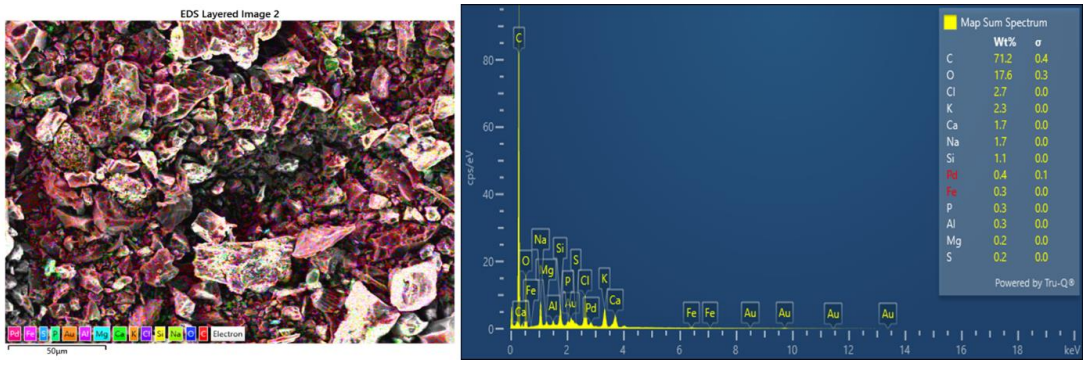

Figure-S 68 SEM-EDS result of W6.2-350

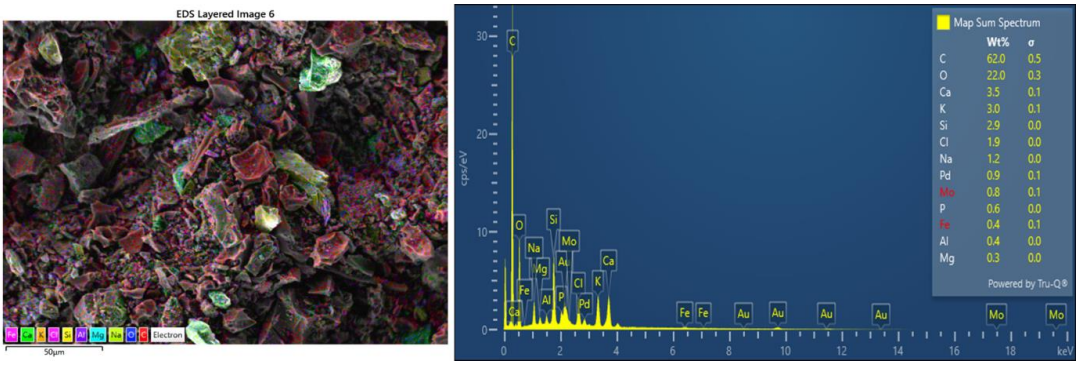

Figure-S 69 SEM-EDS result of W6.2-500

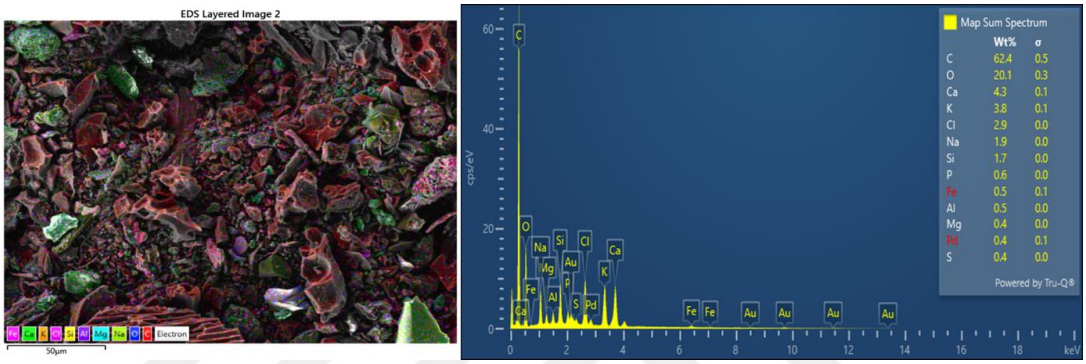

Figure-S 70 SEM-EDS result of W6.2-700

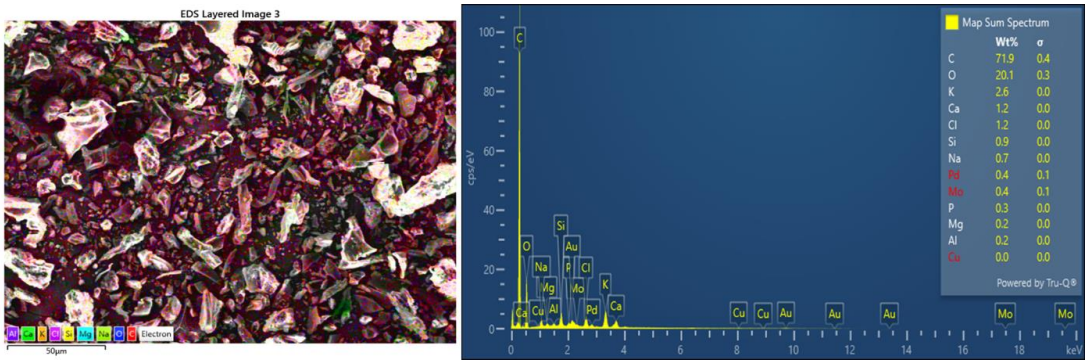

Figure-S 71 SEM-EDS result of W7.1-350

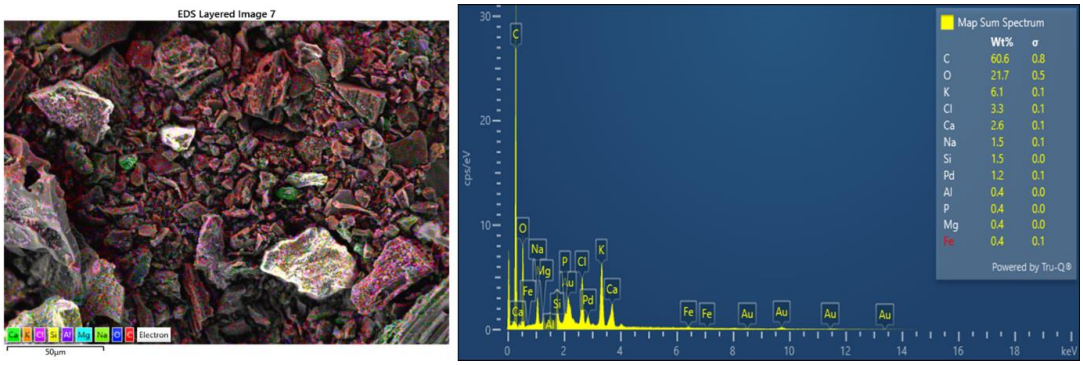

Figure-S 72 SEM-EDS result of W7.1-500

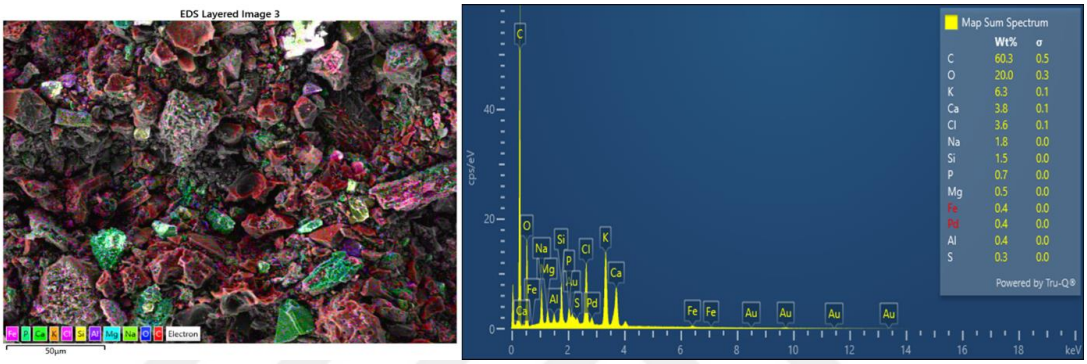

Figure-S 73 SEM-EDS result of W7.1-700

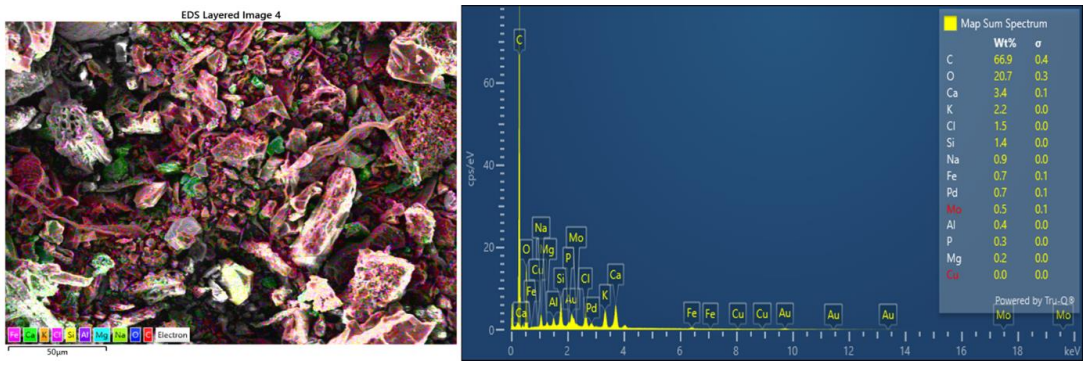

Figure-S 74 SEM-EDS result of W7.2-350

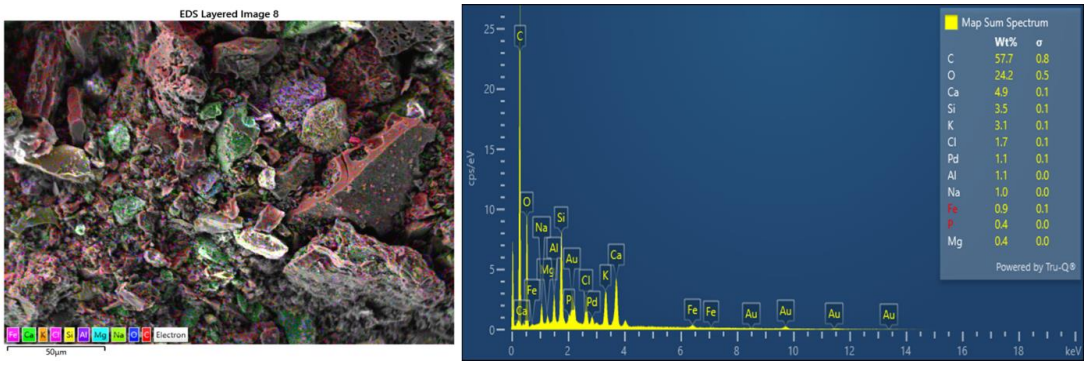

Figure-S 75 SEM-EDS result of W7.2-500

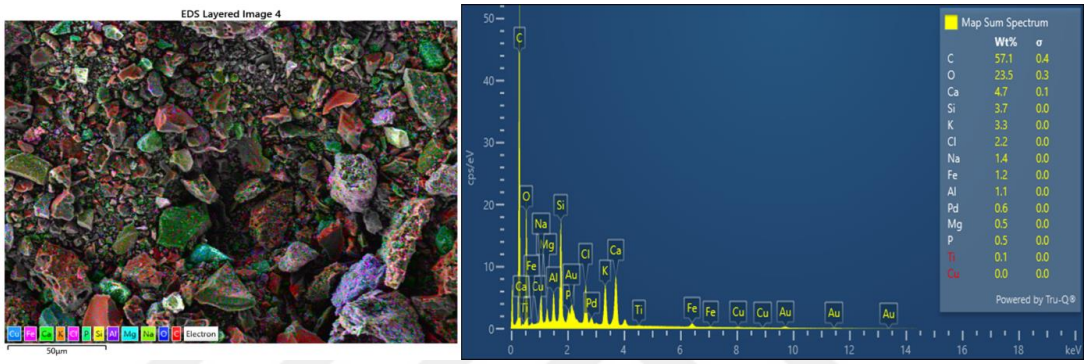

Figure-S 76 SEM-EDS result of W7.2-700

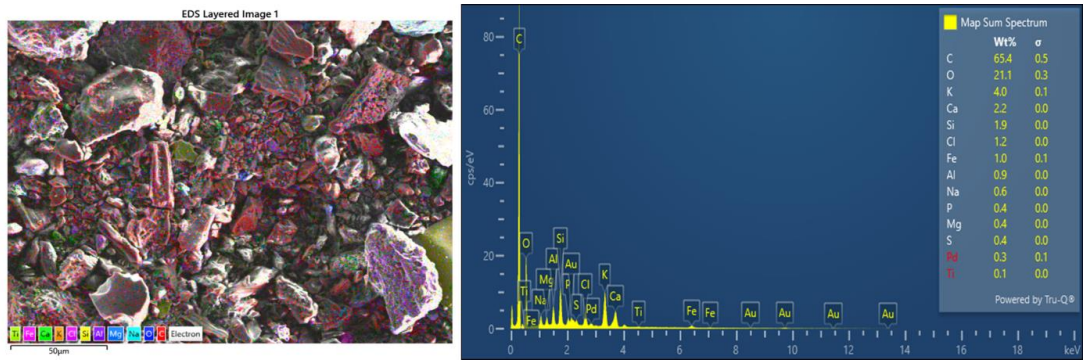

Figure-S 77 SEM-EDS result of W8.1-350

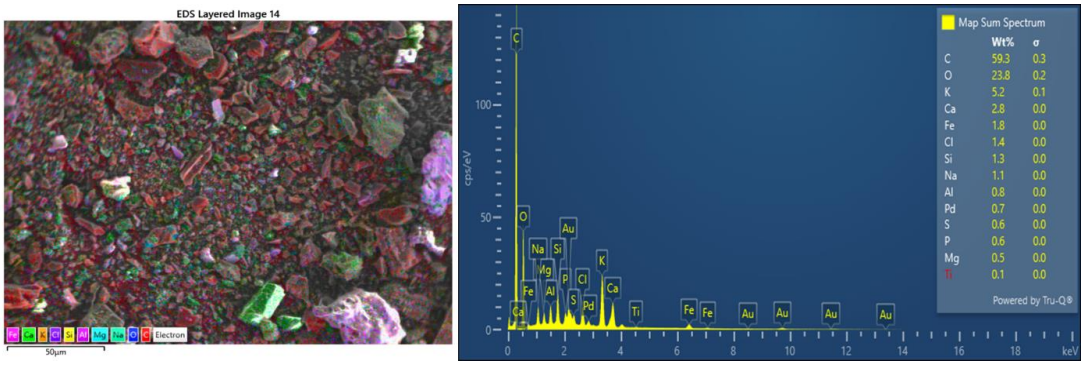

Figure-S 78 SEM-EDS result of W8.1-500

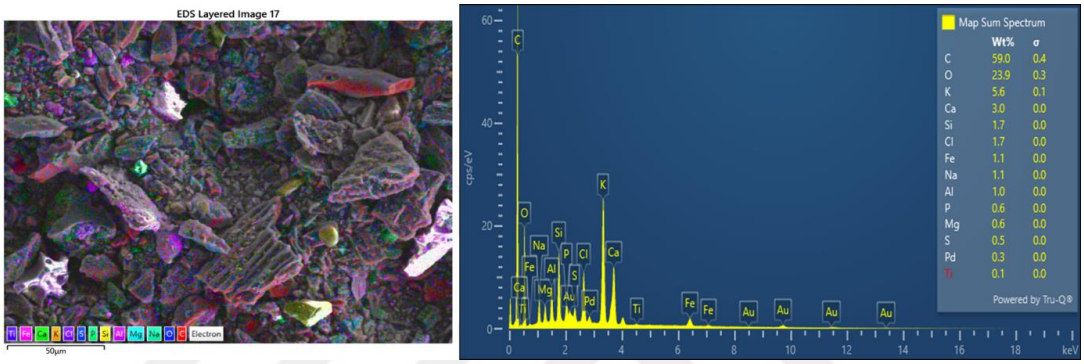

Figure-S 79 SEM-EDS result of W8.1-700

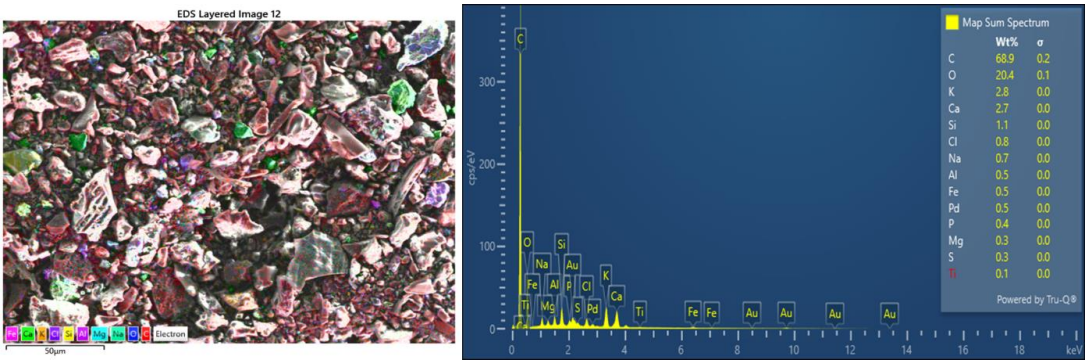

Figure-S 80 SEM-EDS result of W8.2-350

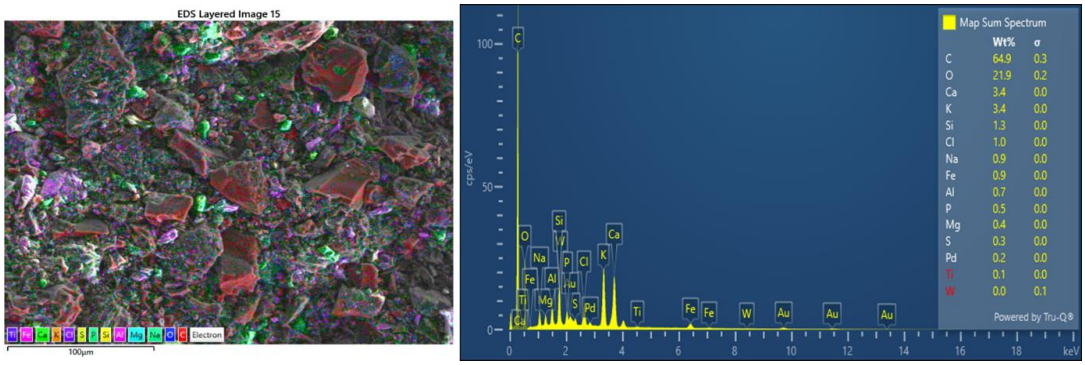

Figure-S 81 SEM-EDS result of W8.2-500

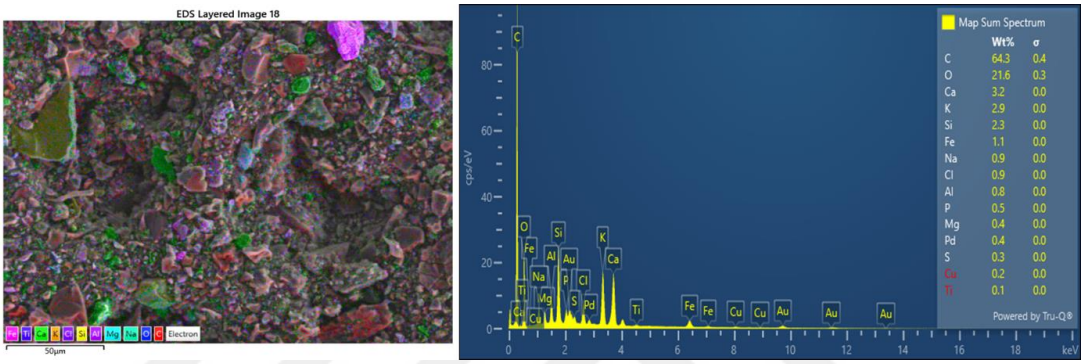

Figure-S 82 SEM-EDS result of W8.2-700

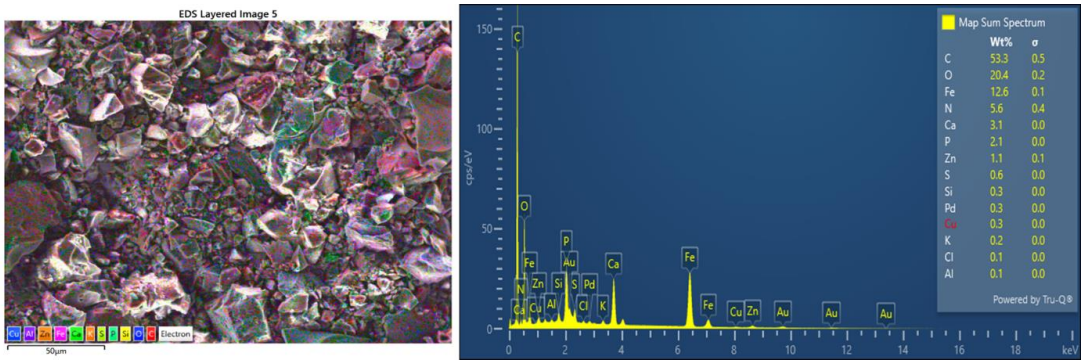

Figure-S 83 SEM-EDS result of CM-350

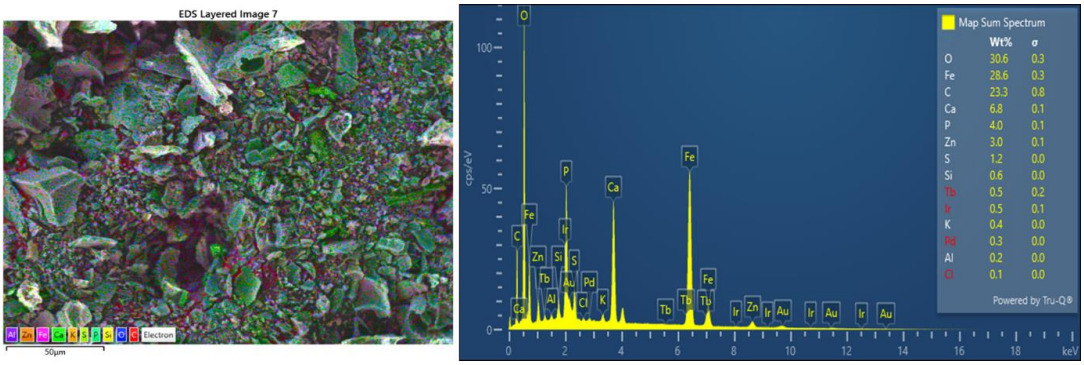

Figure-S 84 SEM-EDS result of CM-500

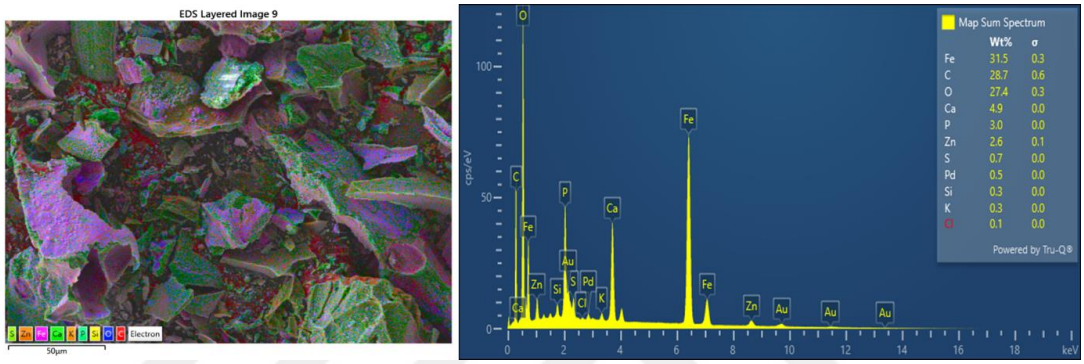

Figure-S 85 SEM-EDS result of CM-700

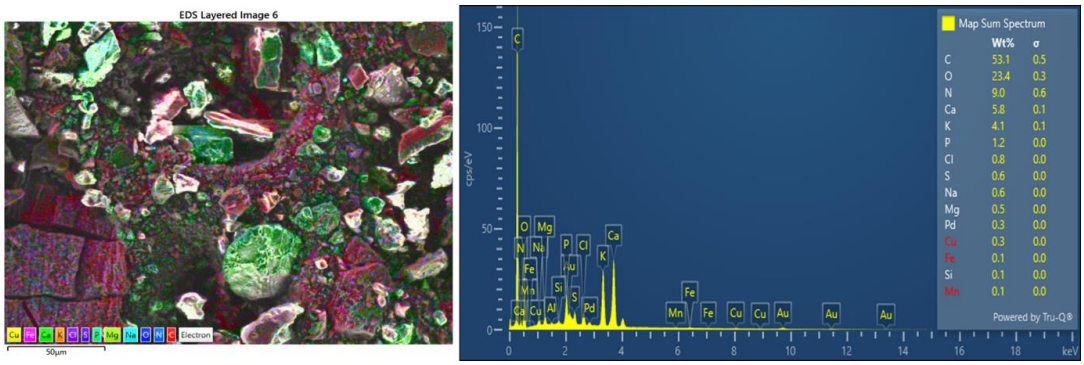

Figure-S 86 SEM-EDS result of PM-350

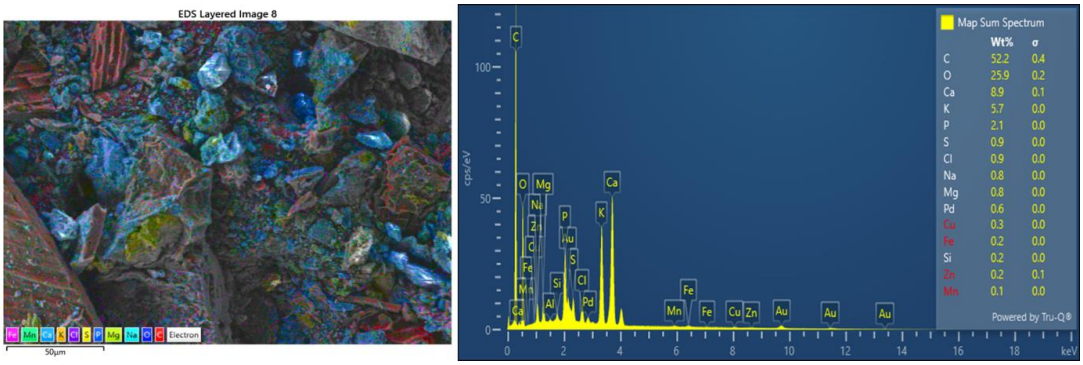

Figure-S 87 SEM-EDS result of PM-500

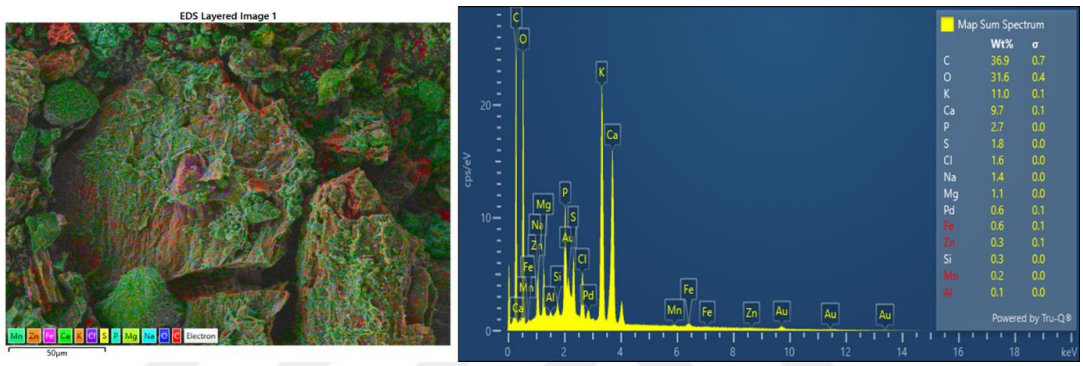

Figure-S 88 SEM-EDS result of PM-700

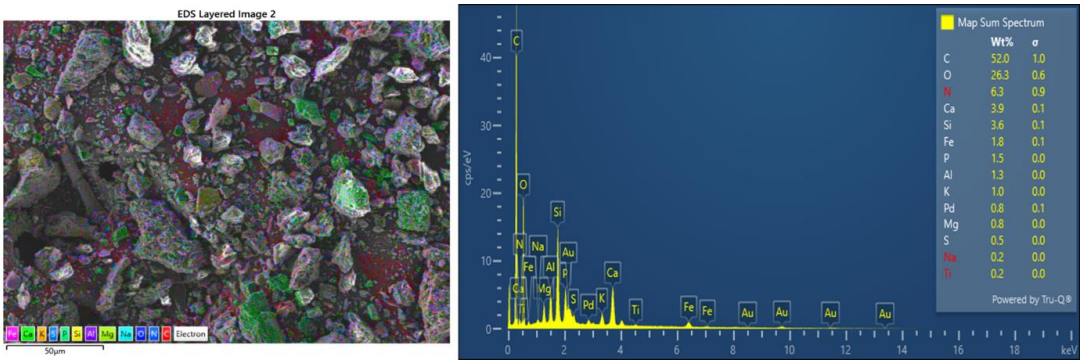

Figure-S 89 SEM-EDS result of SS-350

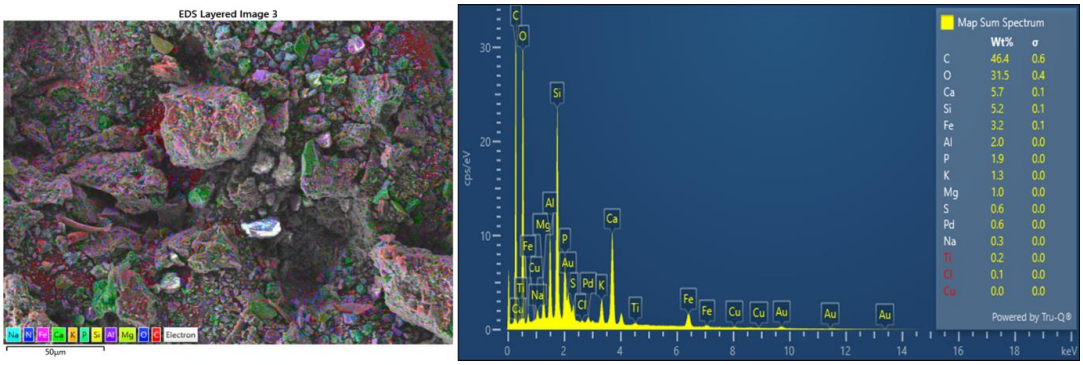

Figure-S 90 SEM-EDS result of SS-500

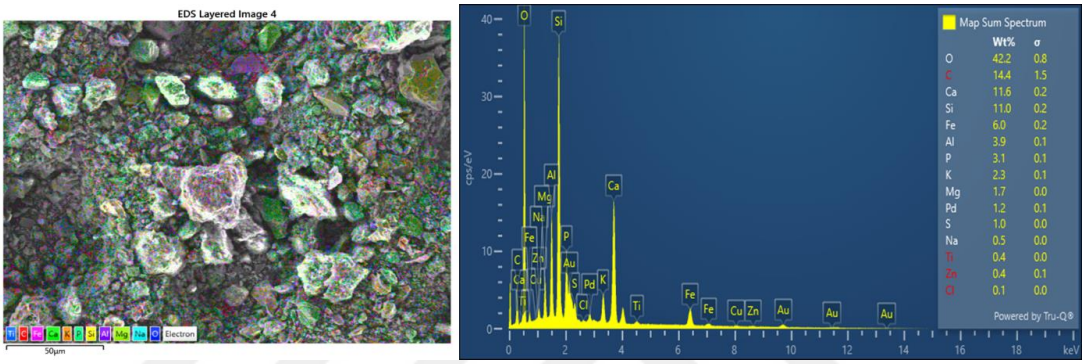

Figure-S 91 SEM-EDS result of SS-700

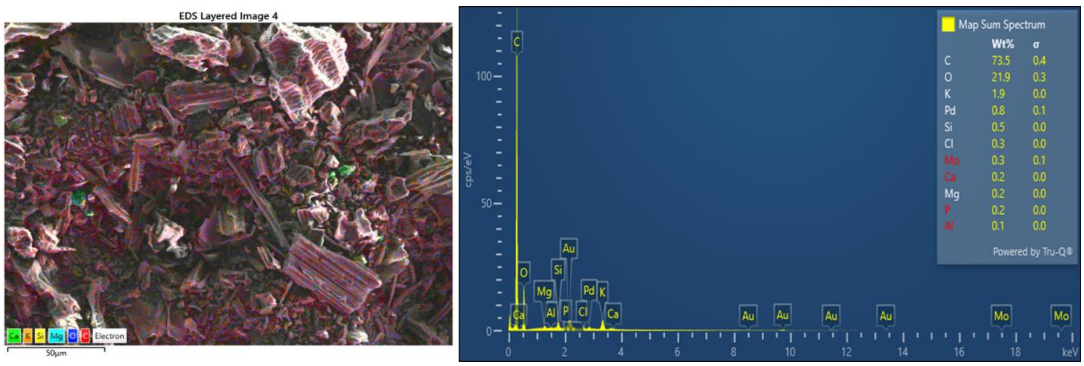

Figure-S 92 SEM-EDS result of CS-350

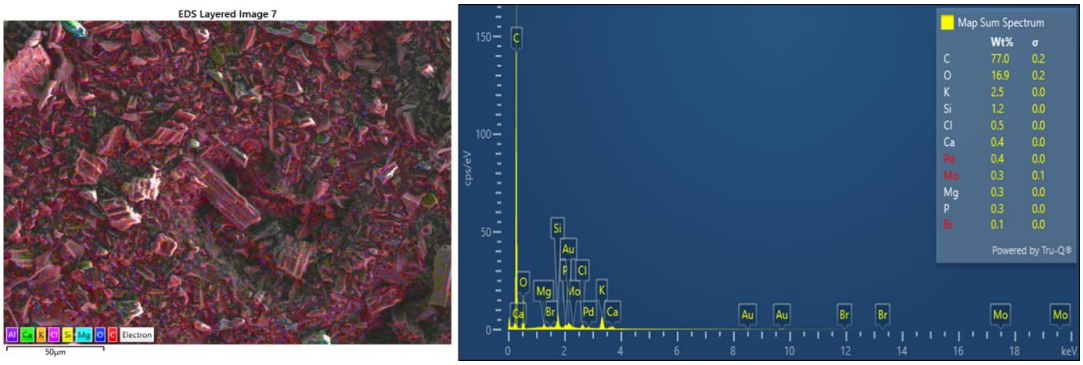

Figure-S 93 SEM-EDS result of CS-500

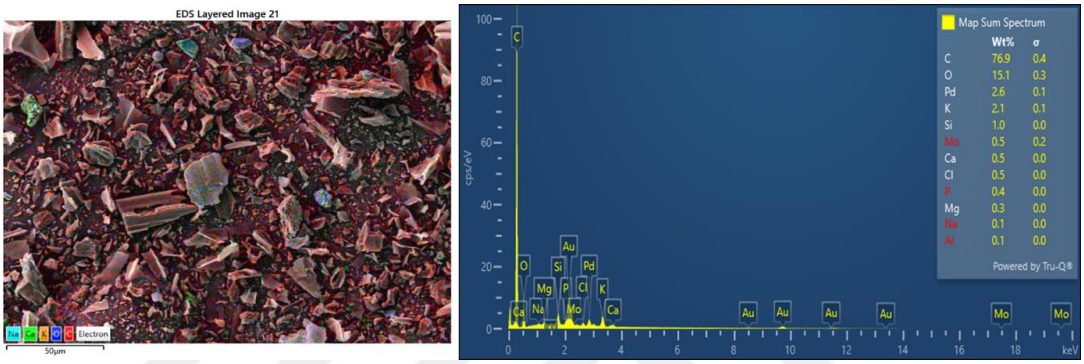

Figure-S 94 SEM-EDS result of CS-700

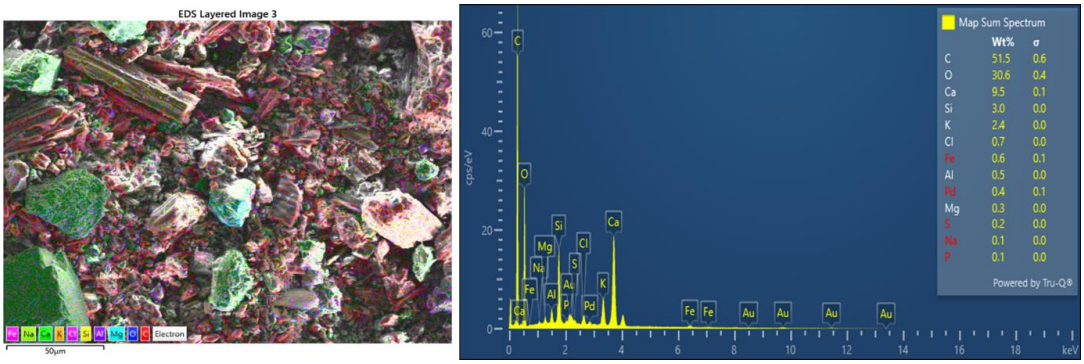

Figure-S 95 SEM-EDS result of YW-350

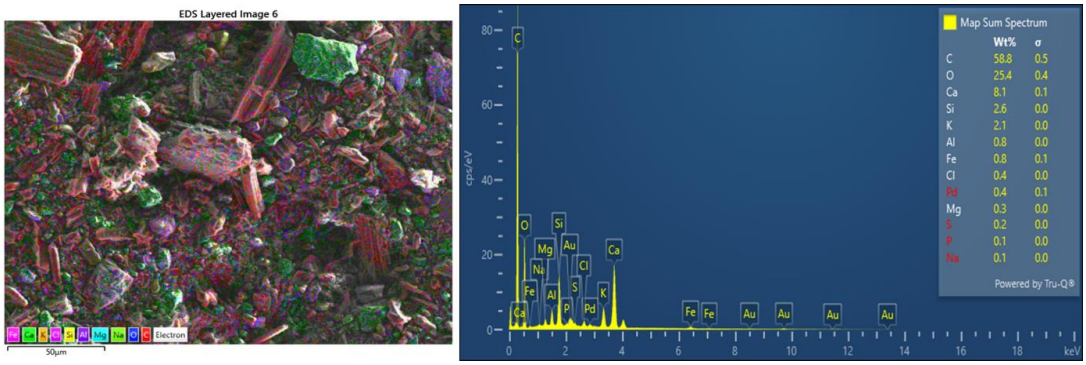

Figure-S 96 SEM-EDS result of YW-500

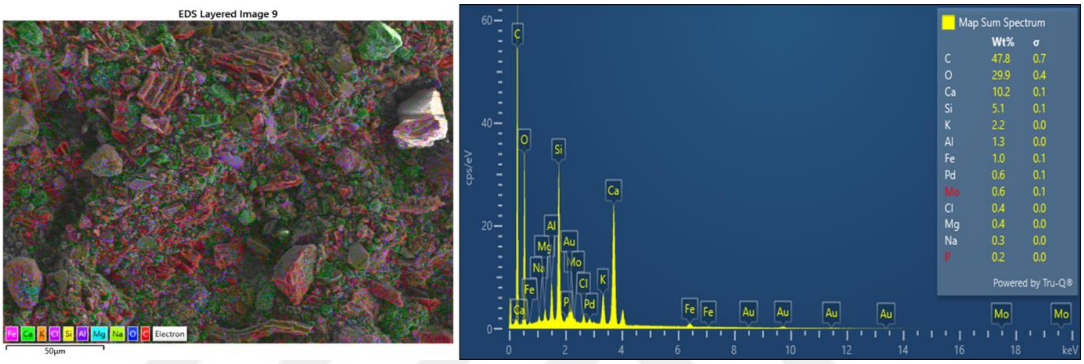

Figure-S 97 SEM-EDS result of YW-700

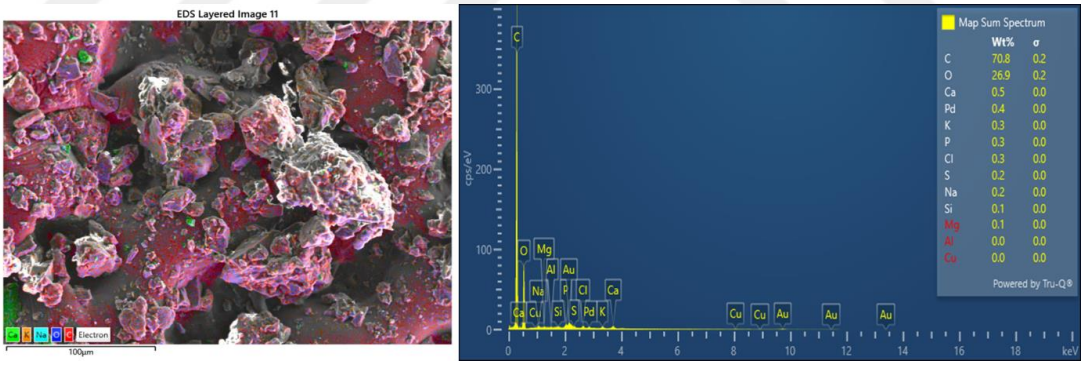

Figure-S 98 SEM-EDS result of feedstock (Dry dog/cat food)

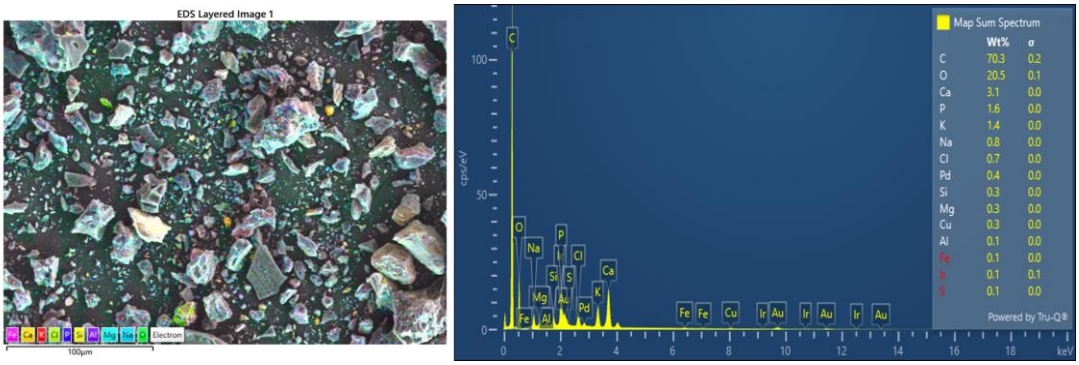

Figure-S 99 SEM-EDS result of BC1

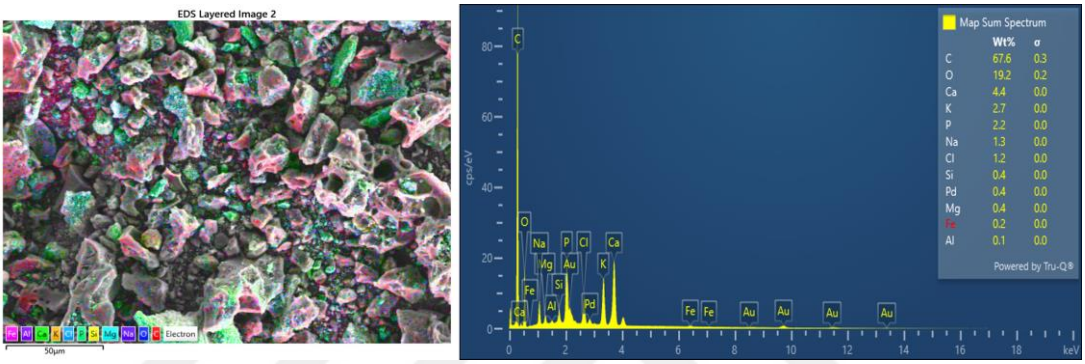

Figure-S 100 SEM-EDS result of BC2

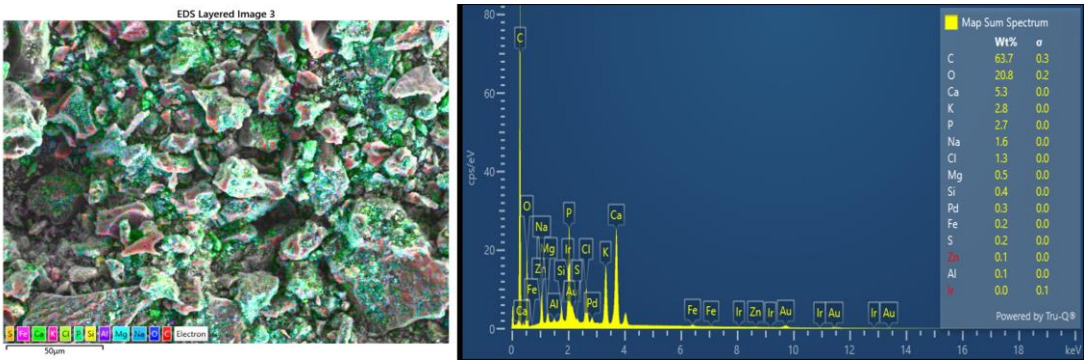

Figure-S 101 SEM-EDS result of BC3

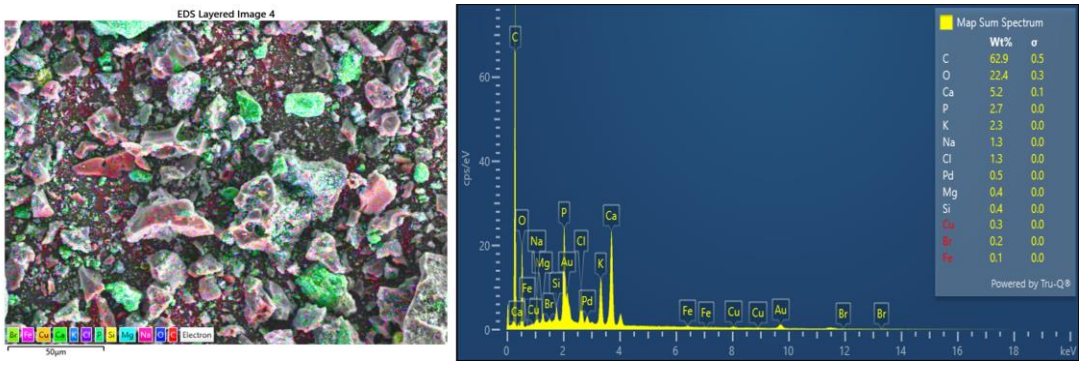

Figure-S 102 SEM-EDS result of BC4

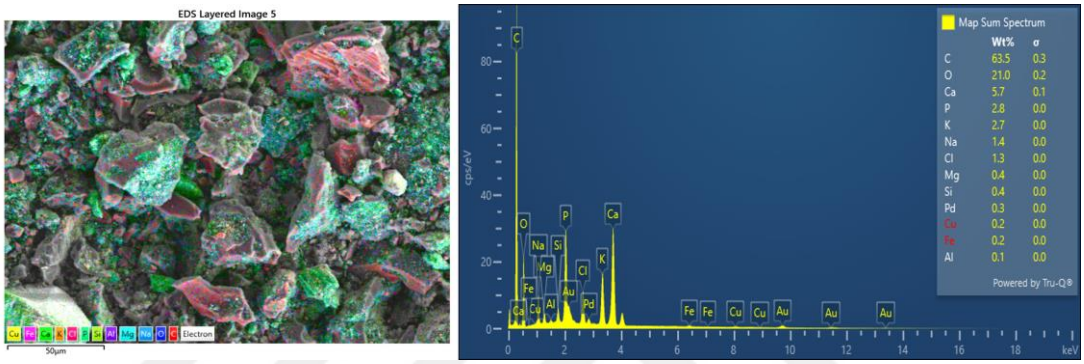

Figure-S 103 SEM-EDS result of BC5

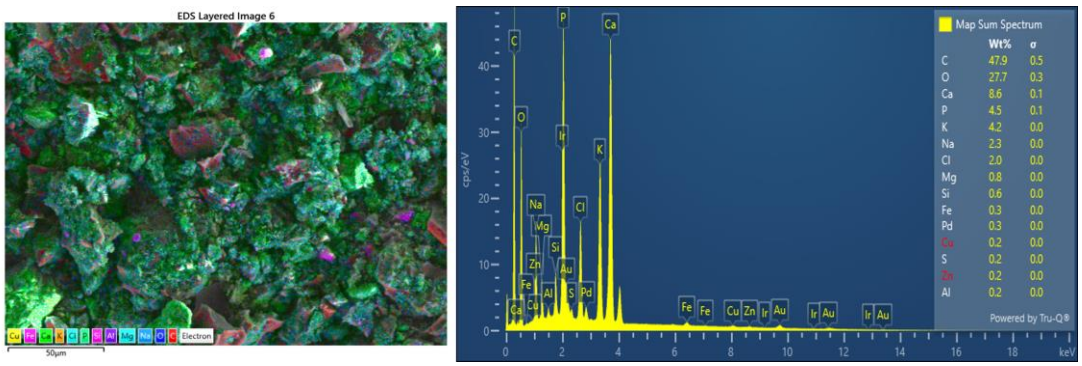

Figure-S 104 SEM-EDS result of BC6

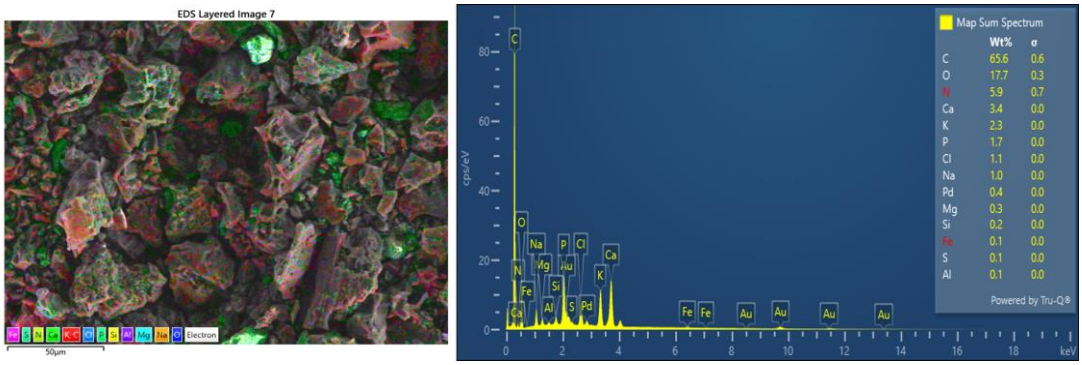

Figure-S 105 SEM-EDS result of BC7

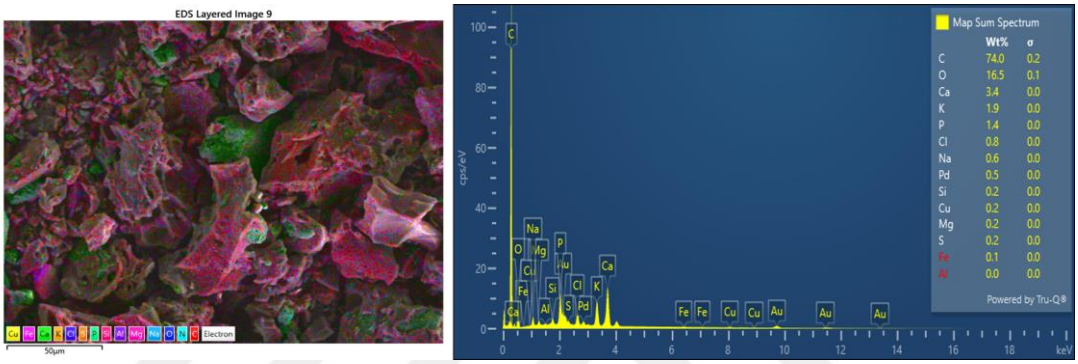

Figure-S 106 SEM-EDS result of BC8

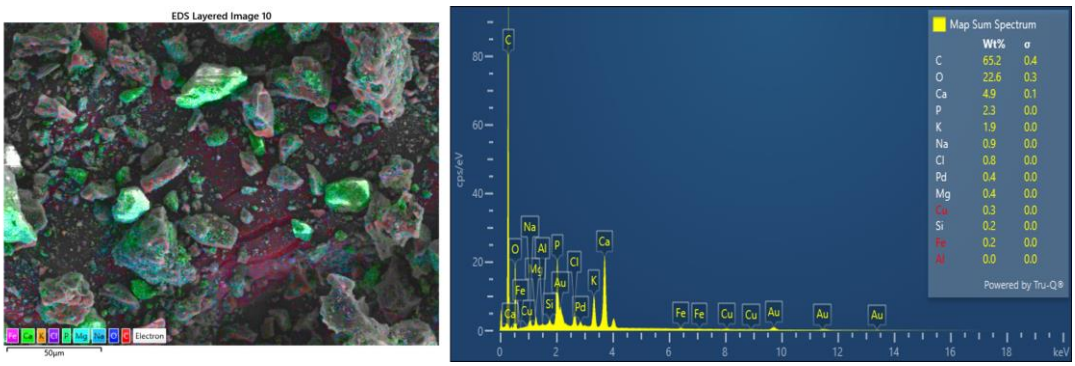

Figure-S 107 SEM-EDS result of BC9

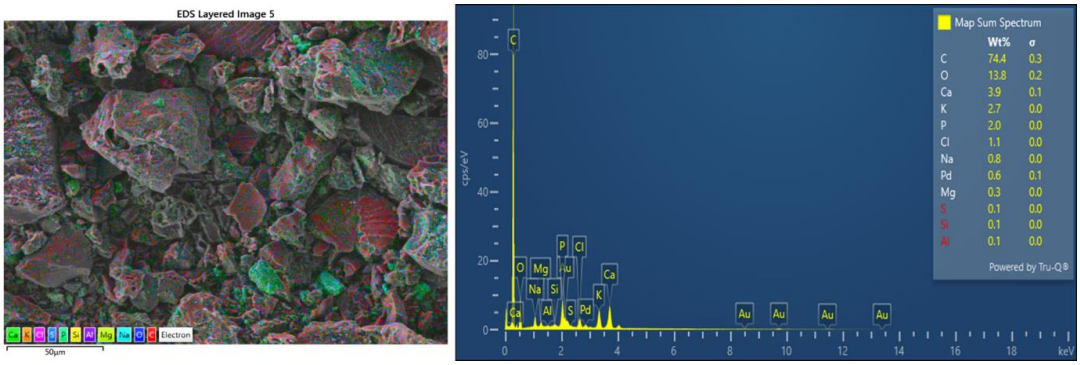

Figure-S 108 SEM-EDS result of BC10

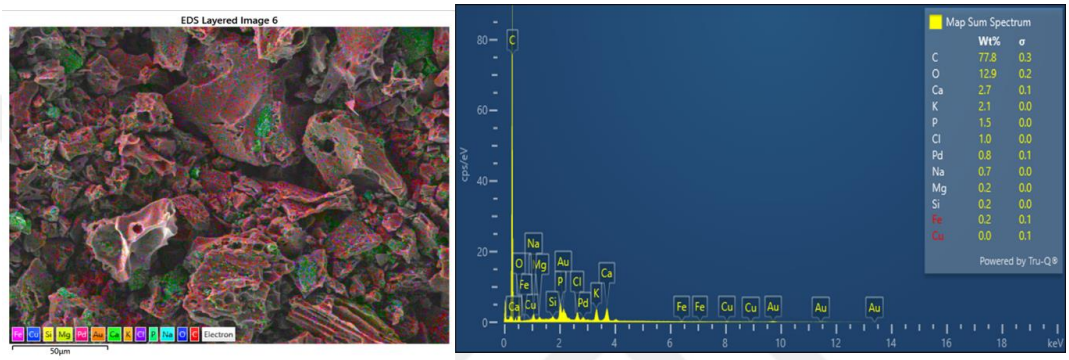

Figure-S 109 SEM-EDS result of BC11

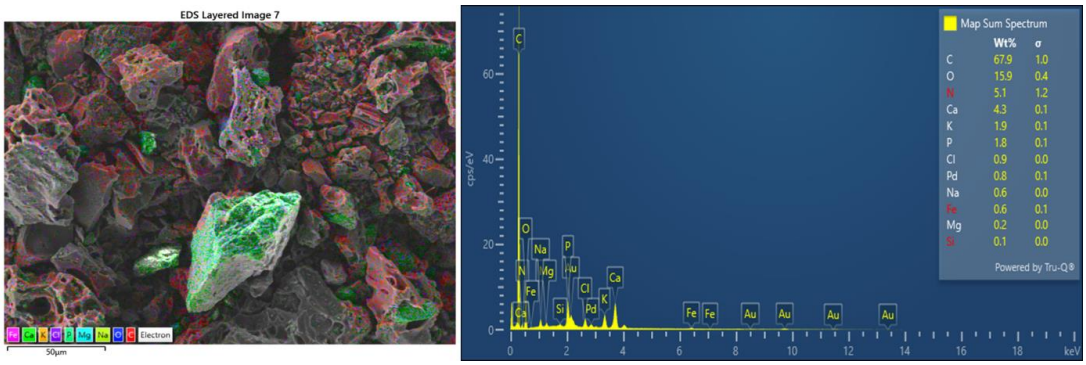

Figure-S 110 SEM-EDS result of BC12

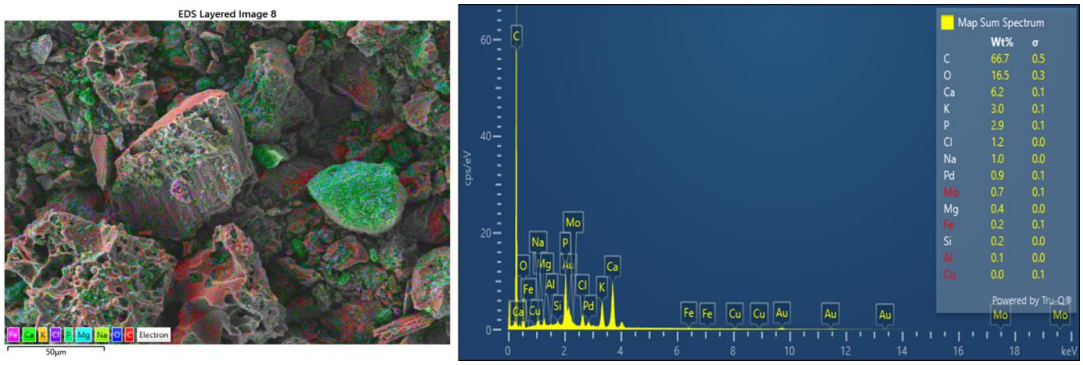

Figure-S 111 SEM-EDS result of BC13

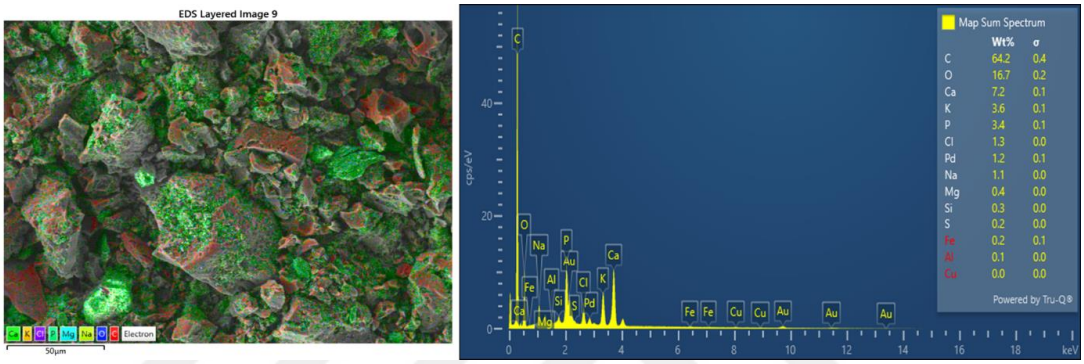

Figure-S 112 SEM-EDS result of BC14

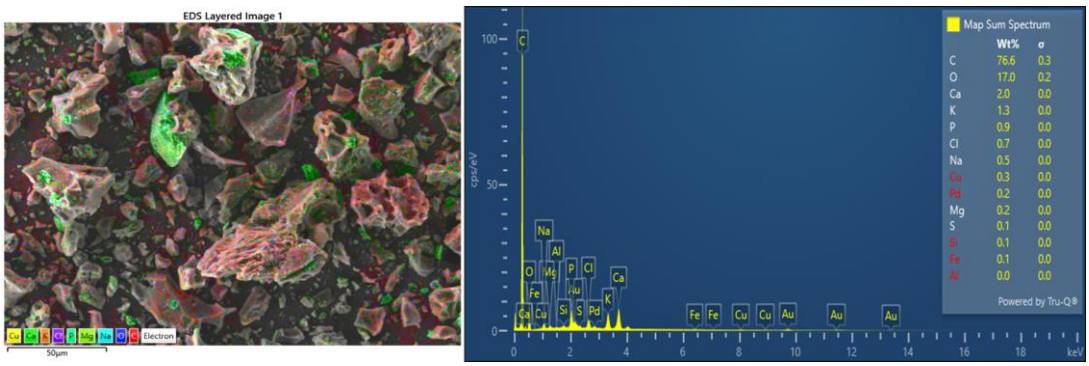

Figure-S 113 SEM-EDS result of BC15

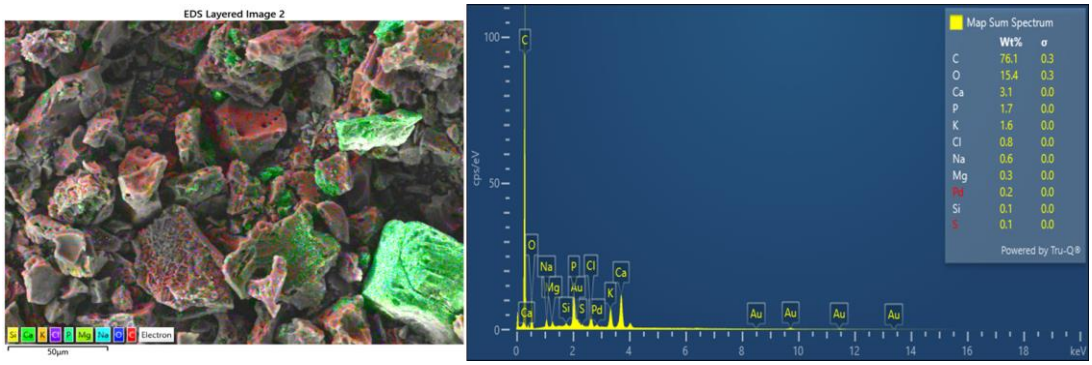

Figure-S 114 SEM-EDS result of BC16

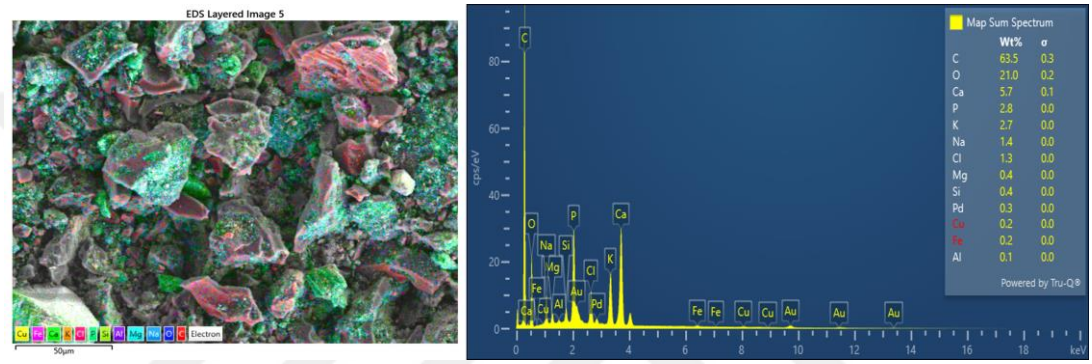

Figure-S 115 SEM-EDS result of BC17

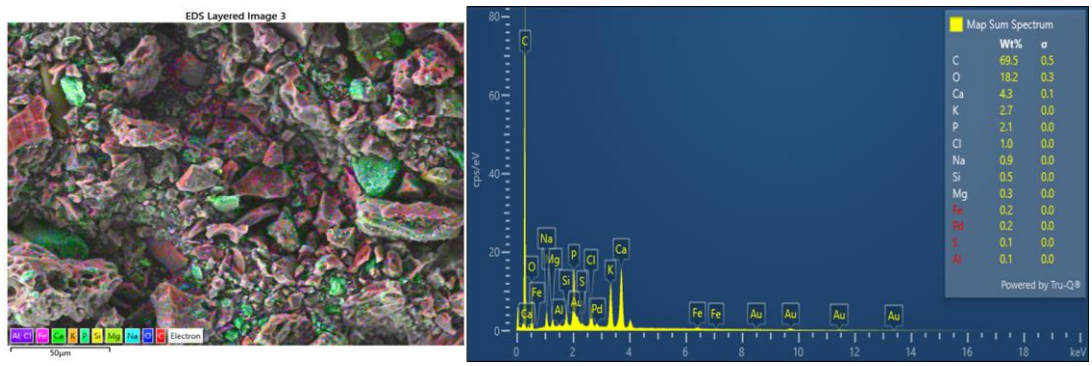

Figure-S 116 SEM-EDS result of BC18

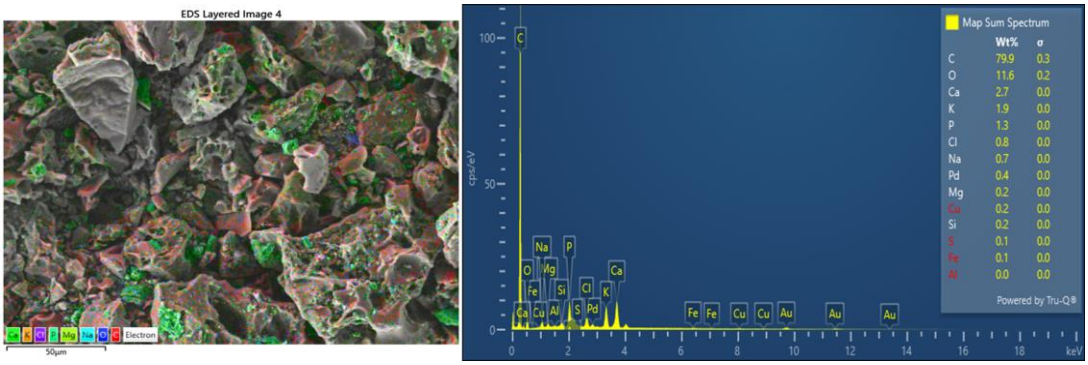

Figure-S 117 SEM-EDS result of BC19

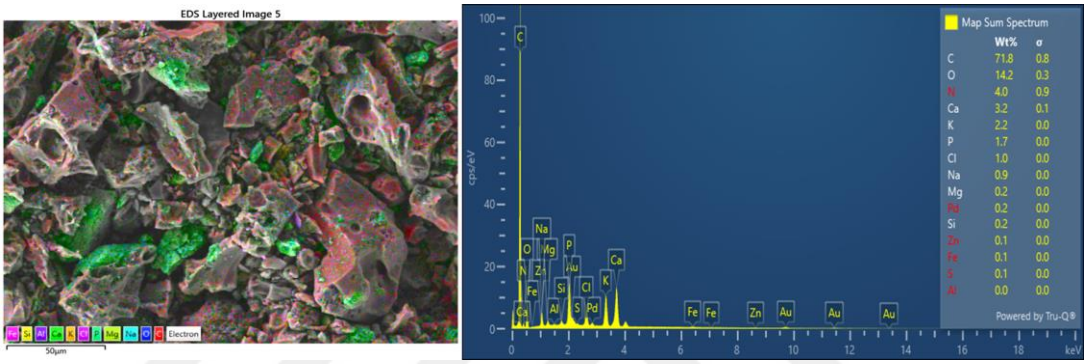

Figure-S 118 SEM-EDS result of BC20

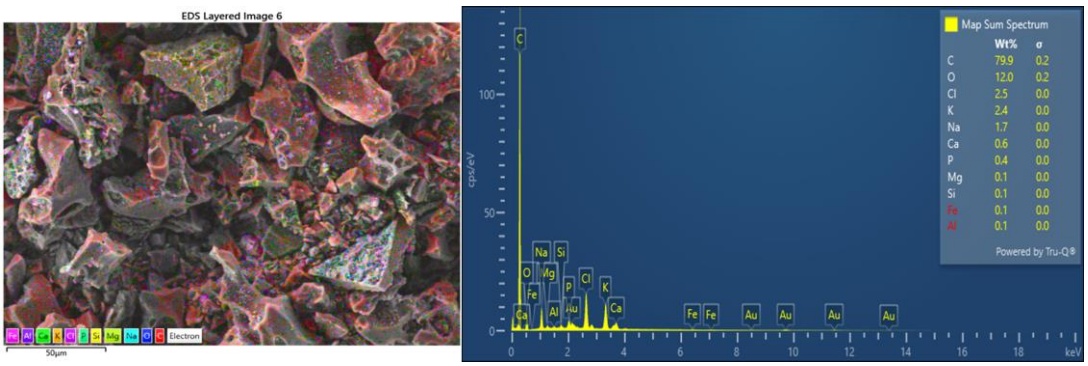

Figure-S 119 SEM-EDS result of BC21

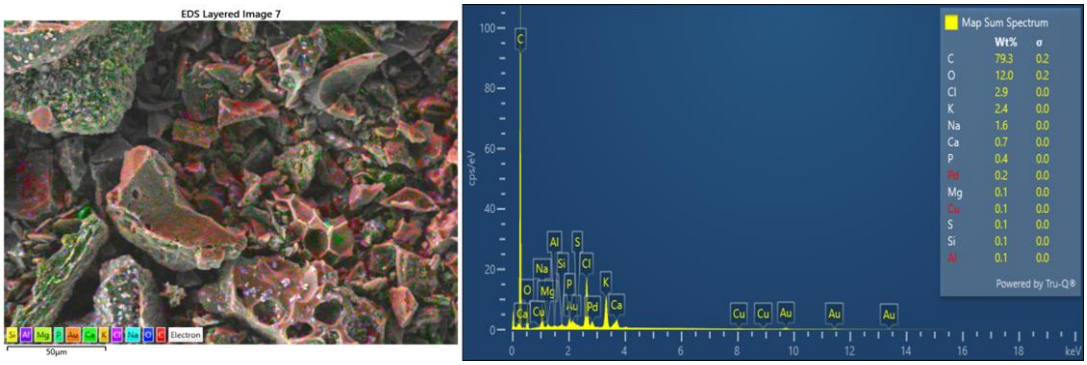

Figure-S 120 SEM-EDS result of BC22

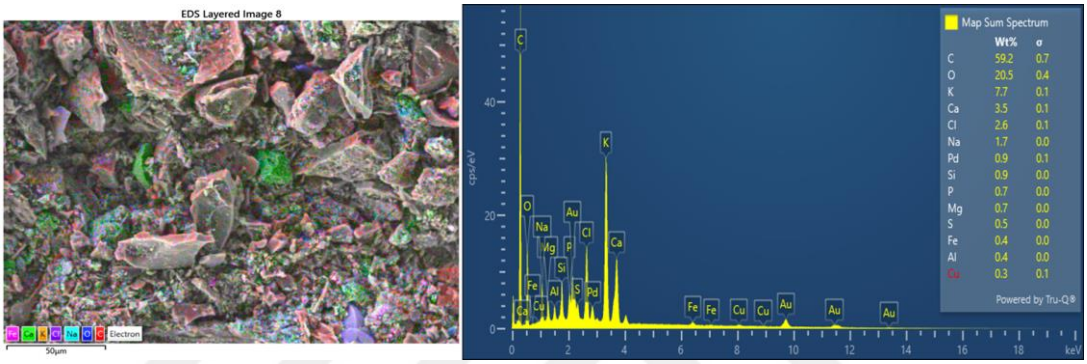

Figure-S 121 SEM-EDS result of BC23

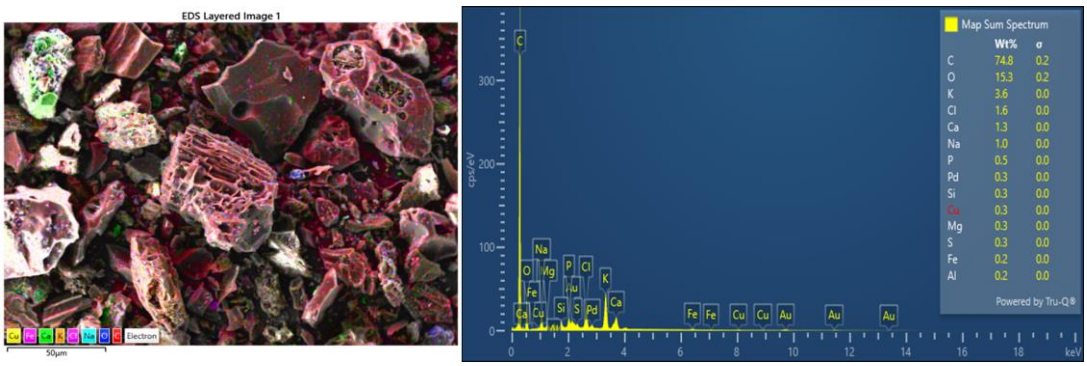

Figure-S 122 SEM-EDS result of BC24

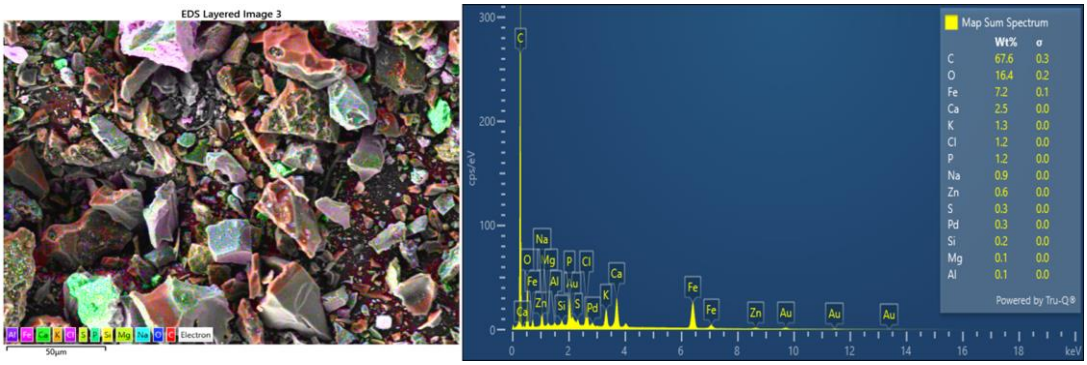

Figure-S 123 SEM-EDS result of BC25

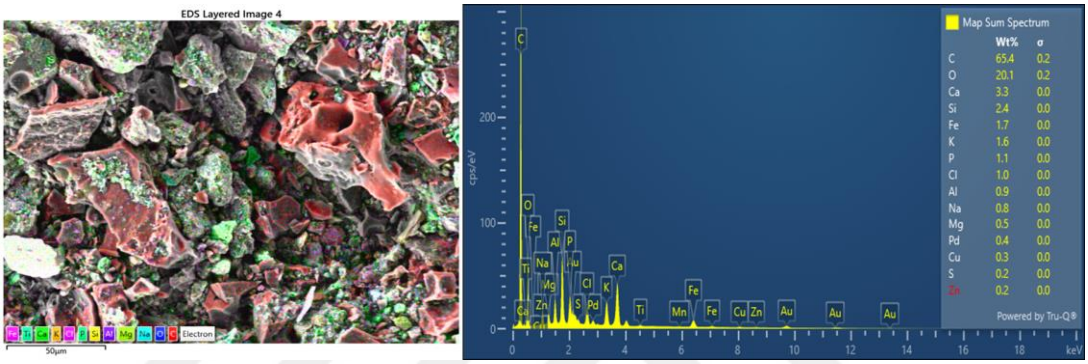

Figure-S 124 SEM-EDS result of BC26

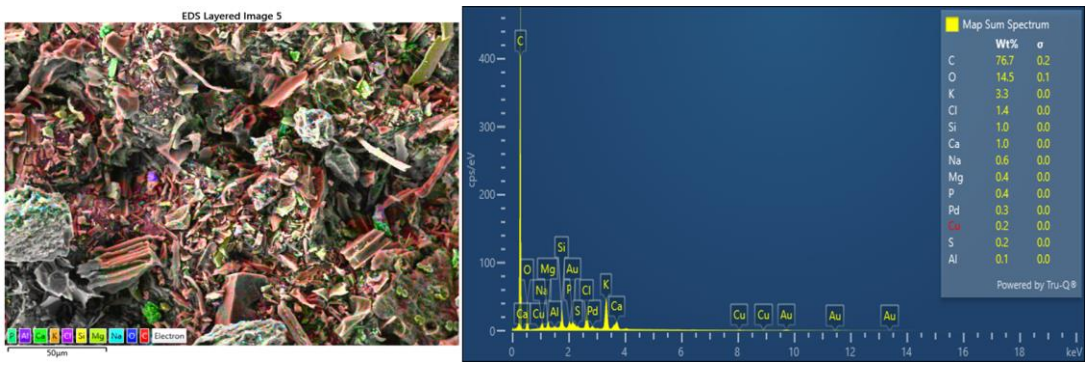

Figure-S 125 SEM-EDS result of BC27

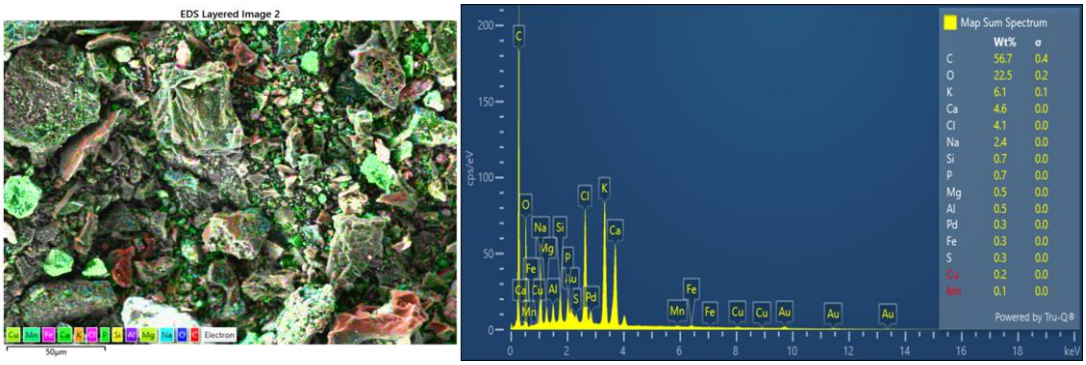

Figure-S 126 SEM-EDS result of BC28

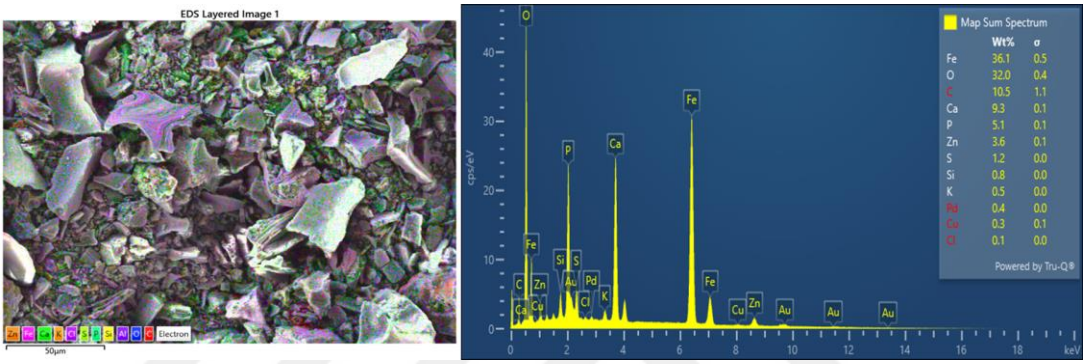

Figure-S 127 SEM-EDS result of BC29

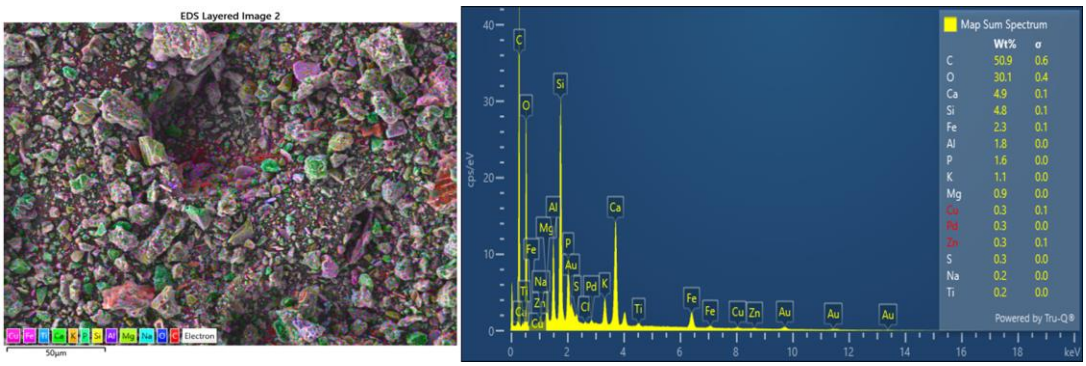

Figure-S 128 SEM-EDS result of BC30

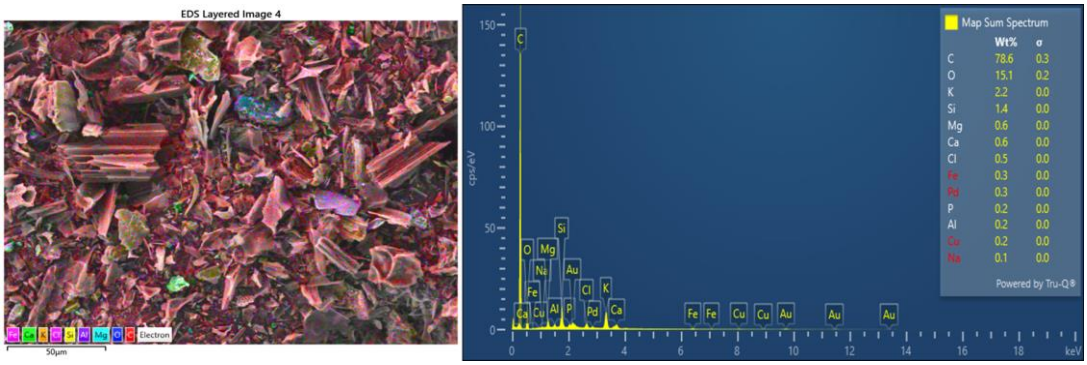

Figure-S 129 SEM-EDS result of BC31

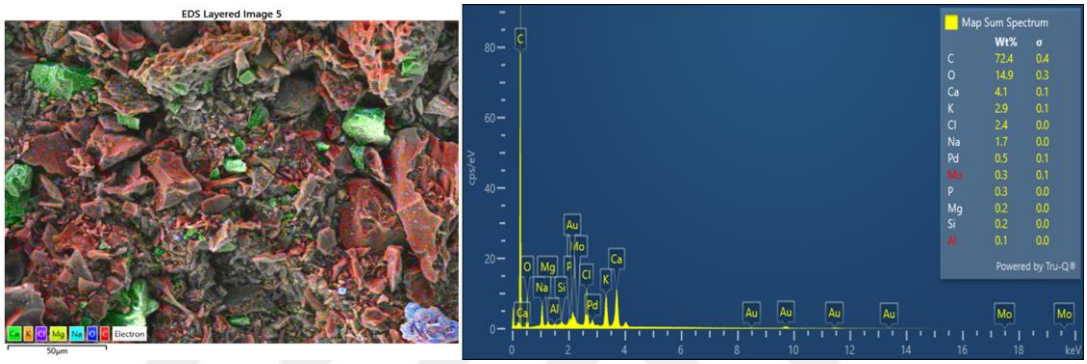

Figure-S 130 SEM-EDS result of BC32

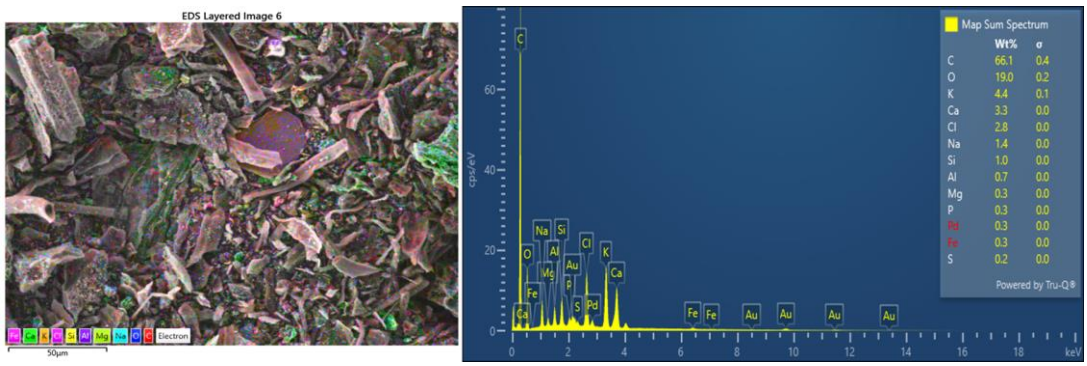

Figure-S 131 SEM-EDS result of BC33

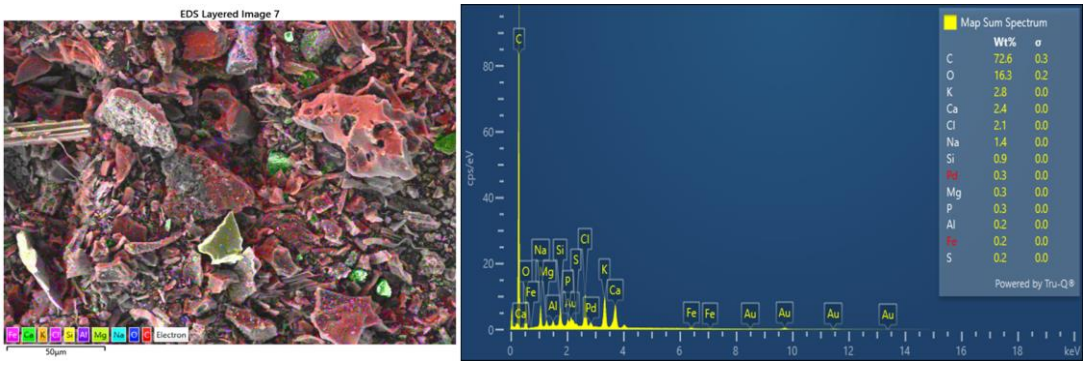

Figure-S 132 SEM-EDS result of BC34

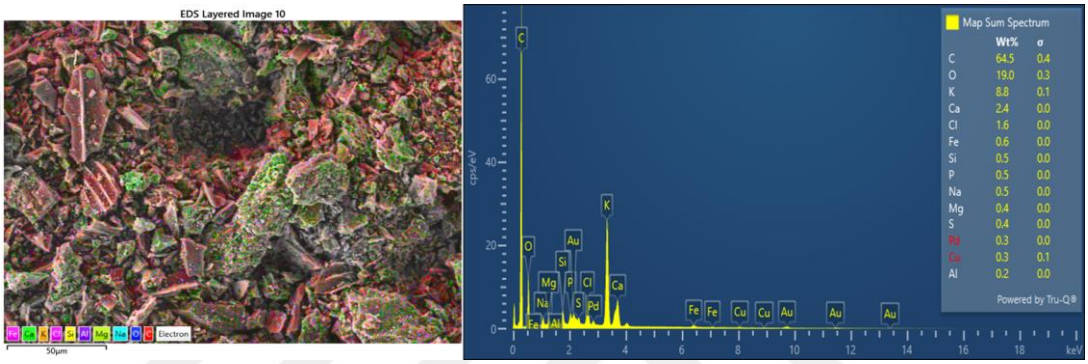

Figure-S 133 SEM-EDS result of BC35

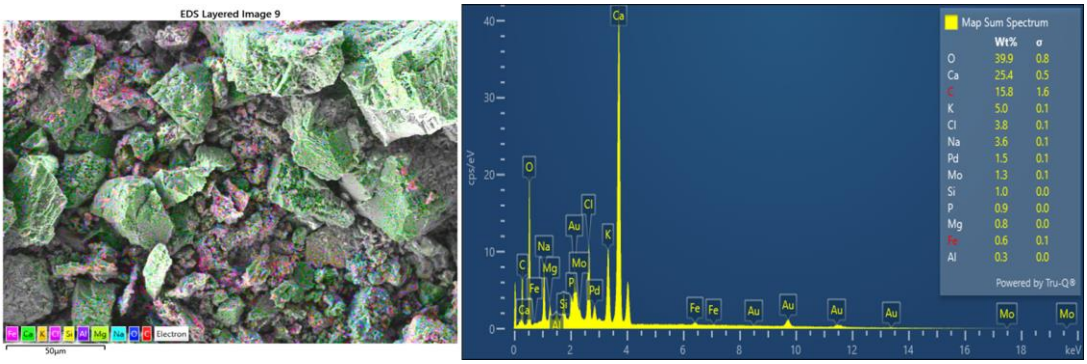

Figure-S 134 SEM-EDS result of ash

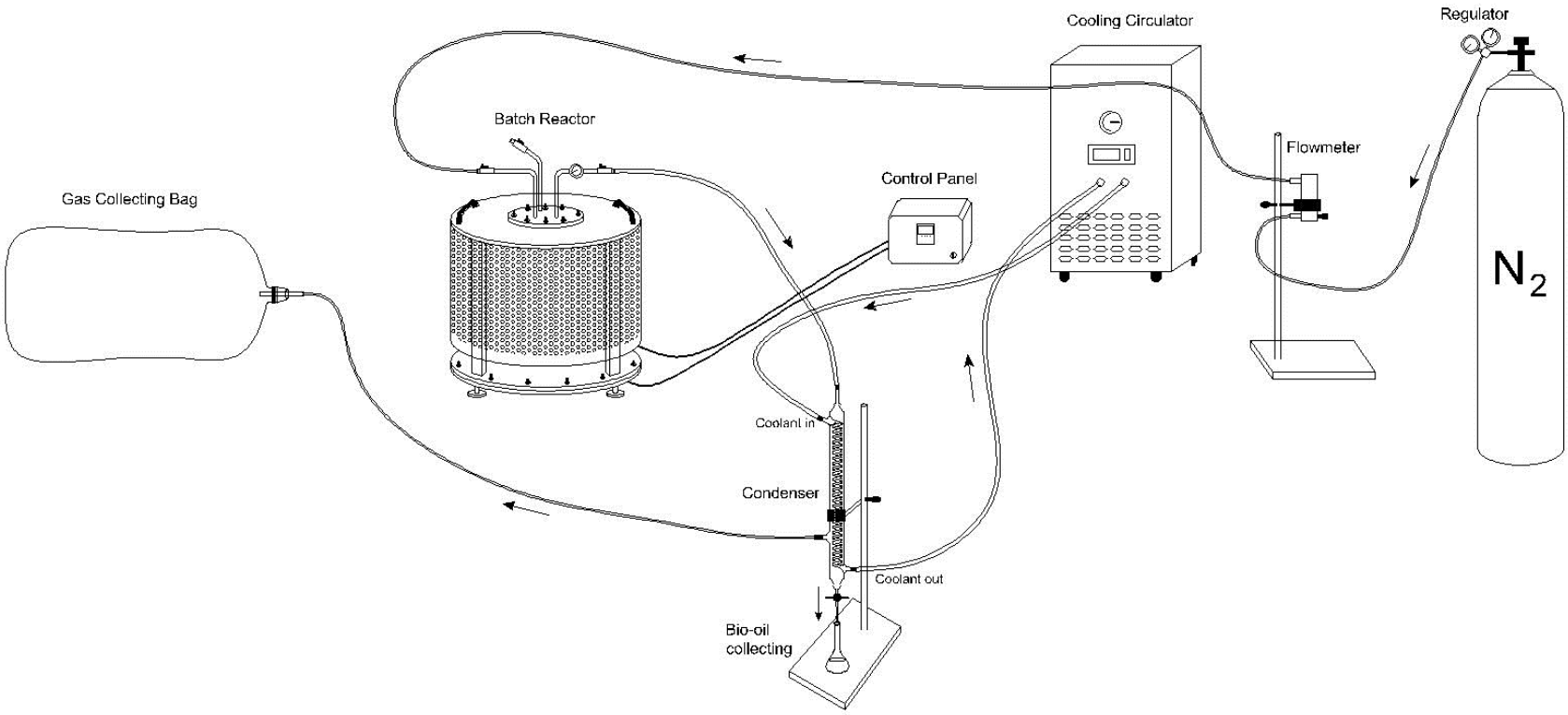

Figure-S 135 Pyrolysis system drawing